

STATUS OF THESIS

Title of thesis

REACTION LAYERS IN DIFFUSION BONDED OF SIALON
TO FERRITIC STEEL

I HUDIYO FIRMANTO

hereby allow my thesis to be placed at the Information Resource Center (IRC) of
Universiti Teknologi PETRONAS (UTP) with the following conditions:

1. The thesis becomes the property of UTP
2. The IRC of UTP may make copies of the thesis for academic purposes only.
3. This thesis is classified as

Confidential

Non-confidential

If this thesis is confidential, please state the reason:

The contents of the thesis will remain confidential for _____ years.

Remarks on disclosure:

Endorsed by

Signature of Author

Signature of Supervisor

Permanent address:
Jl. Nanas VI/582
Pondok Candra Indah
Sidoarjo – 61256
Jawa Timur – Indonesia

Assoc. Prof. Dr. Patthi Hussain

Date: _____

Date: _____

UNIVERSITI TEKNOLOGI PETRONAS
REACTION LAYERS IN DIFFUSION BONDED OF SIALON TO
FERRITIC STEEL

by

HUDIYO FIRMANTO

The undersigned certify that they have read, and recommend to the Postgraduate Studies Programme for acceptance this thesis for the fulfillment of the requirements for the degree stated.

Signature: _____

Main Supervisor: Assoc. Prof. Dr. Patthi Hussain

Signature: _____

Co-Supervisor: Assoc. Prof. Dr. Othman Mamat

Signature: _____

Head of Department: Assoc. Prof. Dr. Ahmad Majdi Abdul Rani

Date: _____

REACTION LAYERS IN DIFFUSION BONDED OF SIALON TO
FERRITIC STEEL

by

HUDIYO FIRMANTO

A Thesis

Submitted to the Postgraduate Studies Programme
as a Requirement for the Degree of

DOCTOR OF PHILOSOPHY

DEPARTMENT OF MECHANICAL ENGINEERING

UNIVERSITI TEKNOLOGI PETRONAS

BANDAR SERI ISKANDAR

PERAK

MARCH 2011

DECLARATION OF THESIS

Title of thesis

REACTION LAYERS IN DIFFUSION BONDED OF SIALON
TO FERRITIC STEEL

I HUDIYO FIRMANTO

hereby declare that the thesis is based on my original work except for quotations and citations which have been duly acknowledged. I also declare that it has not been previously or concurrently submitted for any other degree at UTP or other institutions.

Witnessed by

Signature of Author

Signature of Supervisor

Permanent address:
Jl. Nanas VI/582
Pondok Candra Indah
Sidoarjo – 61256
Jawa Timur – Indonesia

Assoc. Prof. Dr. Patthi Hussain

Date: _____

Date: _____

DEDICATION

I wish to dedicate this thesis for my lovely wife, Rita Febriana and my marvelous sons, Muhammad Rahudita Sofiansah and Muhammad Pramadita Wirawan.

ACKNOWLEDGEMENT

I would like to express my greatest appreciation to my supervisor, AP. Dr. Patthi Hussain for giving me a continuous support, supervision and assistance from finding the idea to completion of this work. He was always keen to share his knowledge and values of life with me during my life in UTP. He always genuinely tried very hard to help me every time I faced a difficult situation. Without his kindness, this journey might have been much tougher. Those will not be forgotten.

I am also grateful to my co-supervisor and former Head of Mechanical Engineering Department, UTP, AP. Dr. Othman Mamat for his support in a number of ways. Especially, for his help during set up time of my life in UTP; his support in reviewing my research plan for study evaluation and his feedback in preparing the Short Term Internal Research Fund (STIRF) proposal.

I am very much indebted to AP. Dr. Mohd Noh Karsiti, Post Graduate Director of UTP. His wise advice and decision has put me back on the line when I was about to hit the wall in this journey. Together with AP. Dr. Patthi Hussain, AP. Dr. Mohd Noh Karsiti has made a great effort for me to stay in the line to pursue this dream. This will always be remembered.

My great appreciation is also for UTP for providing financial support through Graduate Assistantship (GA) scheme and also the research fund through STIRF scheme. Those schemes make this work possible.

My sincere thanks are due to laboratory technologist in Materials Laboratory UTP, Mr. M Anuar A Muin, Mr. Faisal Ismail, Mr. Irwan Othman, Mr. Omar Ramli, and Mr. Shairul Harun, for helping me performing my research and always provide a warm friendly-environment.

The help from Mr. Jani Alang Ahmad, laboratory technologist of Manufacturing Group UTP, especially in preparing the tube-furnace accessories for gas nitriding experiment, is also highly appreciated.

The main experiments and several characterizations work for this research were conducted at AMREC, SIRIM Bhd. It is a pleasure for me to thank Mr. M Idrus Sidik (former AMREC staff), Mr. Eliassidi Abu Othman, Dr. Mazli Mustapha, and Mr Syahiddan from AMREC, SIRIM Bhd who have helped me in performing the experiments in their laboratory.

I am grateful to Mr. Nick Fecitt, Technical Manager, International Syalons (Newcastle) Limited, UK for providing the sialon samples for the research. I also deeply appreciate the help of FH-Prof. Dr. Reinhold S.E. Schneider and Mr. Christopher Schueller of Upper Austria University of Applied Sciences – Wels, Austria for their kindness in performing a separate investigation on my nitriding works.

My colleague of PG students at UTP did much favour for my work. My gratitude should be rewarded to them, *i.e.* Mr. Waskito, PG student at IT Department, UTP, for his help to fix the XPS software and Miss Chee Kai Ling, PG student at Chemical Engineering Department, UTP for her valuable discussion on XPS analysis. Great appreciation is due to Dr. Suwardo for helping to deal with excel software and also his valuable assistance in formatting the thesis manuscript. Many other colleagues have supported me in a number of ways, which I cannot mention all in this limited space. Those are all greatly appreciated.

Thanks are also due to the management of the University of Surabaya, for giving the permission for the study, also for their sympathy and attention.

Most essentially, I owe my deepest gratitude to my dearest wife, Rita Febriana, and my sons, Muhammad Rahudita Sofiansah and Muhammad Pramadita Wirawan, for they love, patience, and continuous encouragement. Being away from them for such a long period is one of the hardest parts of this odyssey. For them this achievement should be dedicated.

ABSTRACT

Besides dissimilar bonding nature that makes difficulties in joining ceramics with metals, different thermal expansion coefficient of the materials is another important issue. This can cause residual stress which may crack the ceramics. In diffusion bonding, ceramic-metal joint is attained by formation of reaction layers in the interface. Mechanical properties, thickness and morphology of the layers highly affect the joint strength. Thus, understanding the reaction layer is important. This work investigated reaction layers in sialon – AISI 430 FSS and sialon – 7.5%-Cr FS joints. The materials were diffusion bonded to produce the joint and grow the reaction layers. The sialon was also joined with nitrided steels. The reaction layers were studied using OM, FESEM, EDX, XRD, and XPS. Microstructure of the interface illustrated the interfacial joint. Sialon decomposed and liberated Si and N. EDX analyses found Si in the steel adjacent to the interface. Thus, Si diffused into the steel which had lower concentration of Si and created silicon-diffusion layer. Since Cr and Si are ferrite formers, Si dissolved in α -Fe(Cr, Si) in the layer. Similarly, the EDX analyses found more-dominant Fe and Cr and less Si in the interface layer in sialon side. This revealed the transfer of Fe and Cr from the steel into the sialon-decomposed part. XRD and XPS confirmed silicide and oxides precipitation in the interface layer. They also revealed α -Fe(Cr, Si) in the matrix which was same with the phase in diffusion layer. It depicted that the interface-layer matrix and the diffusion layer was one species that composed the joint. Hence, cohesive joint was formed through ferrite-solid-solution bridge. Pre-dissolved nitrogen in nitrided steel might have occupied the space in steel lattice; therefore it reduced the nitrogen solubility in the steel during the joining. This impeded sialon – nitrided steels reactivity and suppressed FeSi₂ formation as verified by XPS and XRD on the interface-layer surface. The sialon – steel joint could be potentially useful to serve high-temperature and abrasive environment such as agitator for abrasive slurry, turbine rotor, rocker arm or other automotive components.

ABSTRAK

Lain daripada sifat ikatan kimia yang berbeza yang membuat kesukaran untuk menghubungkan seramik dengan keluli, perbezaan nilai muatan haba tentu kedua-dua bahan adalah hal yang penting. Ini menghasilkan tegangan sisa yang boleh menyebabkan rekahan pada seramik. Di dalam penyambungan difusi, sambungan seramik-keluli didapati kerana lapisan reaksi yang terbentuk di ruang perhubungannya. Sifat mekanik, tebal, dan morfologi lapisan reaksi ini mempengaruhi kekuatan sambungan. Oleh itu, pemahaman tentang lapisan tersebut adalah penting. Kajian ini bertujuan menghubungkan sialon dengan keluli tahan karat gred AISI 430 dan 7.5%-Cr. Bahan-bahan tersebut dihubungkan untuk menghasilkan sambungan dan mendapatkan lapisan reaksi. Sialon juga disambungkan dengan keluli yang telah dinitridkan. Lapisan reaksi dikaji menggunakan OM, FESEM, EDX, XRD, and XPS. Mikrostruktur di ruang sambungan menunjukkan sambungan yang rapat. Sialon terurai dan membebaskan Si dan N. Kajian EDX mendapati Si menyerap masuk ke dalam keluli dan membentuk lapisan serapan. Kerana Si dan Cr adalah pembentuk ferrite, Si menyerap masuk ke dalam α -Fe(Cr, Si). Fe dan Cr yang lebih utama dengan Si yang sedikit ditemui di dalam lapisan perhubungan. Ini membuktikan perpindahan Fe dan Cr daripada keluli ke dalam bahagian sialon yang terurai. Kajian XPS membenarkan silisida dan oksida di dalam lapisan perhubungan dan α -Fe(Cr, Si) di dalam matriknya. Larutan ferrum padat ini sama dengan yang didapati pada lapisan serapan di dalam keluli. Ini menunjukkan bahawa matrik lapisan perhubungan dan lapisan serapan adalah bahagian yang sama yang membentuk sambungan yang rapat. Nitrogen yang diserapkan terlebih dahulu ke dalam keluli yang dinitridkan mengurangkan tindak balas sialon dengan keluli dan menghalang pembentukan FeSi₂. Sambungan sialon dengan keluli boleh bermanfaat untuk melayani pekerjaan pada suhu tinggi dan abrasive misalnya agitator for abrasive slurry, turbine rotor, rocker arm atau komponen enjin kereta yang lain.

In compliance with the terms of the Copyright Act 1987 and the IP Policy of the university, the copyright of this thesis has been reassigned by the author to the legal entity of the university,

Institute of Technology PETRONAS Sdn Bhd.

Due acknowledgement shall always be made of the use of any material contained in, or derived from, this thesis.

© Hudiyo Firmanto, 2011

Institute of Technology PETRONAS Sdn Bhd

All rights reserved.

TABLE OF CONTENTS

STATUS OF THESIS	
APPROVAL PAGE	
TITLE	
DECLARATION	iv
DEDICATION	v
ACKNOWLEDGEMENT	vi
ABSTRACT.....	viii
ABSTRAK.....	ix
COPY RIGHT.....	x
TABLE OF CONTENTS.....	xi
LIST OF TABLES	xiv
LIST OF FIGURES	xv
LIST OF ABBREVIATIONS AND NOMENCLATURE	xix
PREFACE.....	xxi
CHAPTER 1 INTRODUCTION	1
1.0 Overview.....	1
1.1 Background	1
1.2 Problem Statement.....	5
1.3 Objectives of the Study	5
1.4 Scope of the Study	6
1.5 Thesis organization	6
CHAPTER 2 LITERATURE REVIEW	8
2.0 Overview.....	8
2.1 Sialon	8
2.2 Stainless Steel	11
2.3 Nitriding of Stainless Steel	14
2.4 Diffusion Bonding Theory.....	18
2.4.1 Modeling joint formation.....	20
2.4.2 Diffusion of elements.....	22
2.5 Solid State Joining of Ceramics with Metals.....	24
2.6 Reaction of Silicon Nitride and Sialon with Steel	34
2.6.1 Decomposition of Silicon Nitride	36
2.6.2 Interdiffusion and Reaction of Elements	37
CHAPTER 3 METHODOLOGY	42
3.0 Overview.....	42
3.1 Methodology	42
3.2 Experimental Procedure.....	43
3.2.1 Materials	43

3.2.2 Experimental Procedure for Solution Nitriding.....	44
3.2.3 Experimental Procedure for Diffusion Bonding.....	46
3.2.4 Characterization and Hardness Test.....	48
3.2.4.1 Microstructural Characterization.....	48
3.2.4.2 Elemental Analysis.....	49
3.2.4.3 XRD Examination.....	50
3.2.4.4 XPS Examination.....	50
3.2.4.5 Hardness Test.....	51
CHAPTER 4 RESULTS AND DISCUSSION.....	53
4.0 Overview.....	53
4.1 Solution Nitriding of Stainless Steel Samples.....	53
4.1.1 Solution Nitriding of AISI 430 FSS.....	54
4.1.2 Solution Nitriding of 7.5%-Cr FS.....	60
4.2 Joining of Sialon to AISI 430 FSS.....	65
4.2.1 Joining of Sialon with As-received AISI 430 FSS.....	66
4.2.1.1 Microstructure of the Joint.....	66
4.2.1.2 Elemental Analysis.....	69
4.2.1.3 XRD.....	73
4.2.1.4 XPS.....	74
4.2.1.5 Hardness Test across the Joint.....	77
4.2.2 Joining of Sialon with One-hour-nitrided AISI 430 FSS.....	79
4.2.2.1 Microstructure of the Joint.....	79
4.2.2.2 Elemental Analysis.....	82
4.2.2.3 XRD.....	86
4.2.2.4 XPS.....	87
4.2.2.5 Hardness Test across the Joint.....	89
4.2.3 Joining of Sialon with Four-hours-nitrided AISI 430 FSS.....	90
4.2.3.1 Microstructure of the Joint.....	90
4.2.3.2 Elemental Analysis.....	92
4.2.3.3 XRD.....	96
4.2.3.4 XPS.....	97
4.2.3.5 Hardness Test across the Joint.....	98
4.2.4 Discussion.....	99
4.2.4.1 Joining of Sialon – As-received Steel.....	99
4.2.4.2 Joining of Sialon – Nitrided Steel.....	108
4.2.4.3 Hardness of the Joint Section.....	114
4.3 Joining of Sialon with 7.5%-Cr FS.....	115
4.3.1 Joining of Sialon with As-received 7.5%-Cr FS.....	116
4.3.1.1 Microstructure of the Joint.....	116
4.3.1.2 Elemental Analysis.....	119
4.3.1.3 XRD.....	123
4.3.1.4 XPS.....	123
4.3.1.5 Hardness Test across the Joint.....	125
4.3.2 Joining of Sialon with One-hour-nitrided 7.5%-Cr FS.....	126
4.3.2.1 Microstructure of the Joint.....	126
4.3.2.2 Elemental Analysis.....	129
4.3.2.3 XRD.....	132
4.3.2.4 XPS.....	133

4.3.2.5 Hardness Test across the Joint	135
4.3.3 Joining of Sialon with Four-hours-nitrided 7.5%-Cr FS	136
4.3.3.1 Microstructure of the Joint.....	136
4.3.3.2 Elemental analysis	138
4.3.3.3 XRD	142
4.3.3.4 XPS	143
4.3.3.5 Hardness Test across the Joint	145
4.3.4 Discussion on the Joining of Sialon with 7.5%-Cr FS.....	146
4.3.4.1 Joining of Sialon – As-received 7.5%-Cr FS.....	146
4.3.4.2 Joining of Sialon – Nitrided 7.5%-Cr FS.....	150
4.3.4.3 Hardness of the Joint Section.....	155
 CHAPTER 5 CONCLUSIONS AND RECOMMENDATIONS	 158
5.1 Conclusions.....	158
5.2 Contributions.....	160
5.3 Recommendations.....	161
 AWARDS AND PUBLICATIONS.....	 163
Conferences:	163
Journal Publications:.....	163
Awards:	164
Patent Filing:	164
 REFERENCES	 165

LIST OF TABLES

Table 2.1	Investigations on reaction of Si_3N_4 and sialon with iron and steel	35
Table 3.1	Chemical compositions of sialon	43
Table 3.2	Chemical composition of as-received AISI 430 FSS	44
Table 3.3	Chemical composition of as-received 7.5%-Cr FS	44
Table 4.1	Concentration of elements of the interface-layer matrix in sialon – as received AISI 430 FSS joint	71
Table 4.2	Concentration of elements of the precipitates at the interface layer in sialon – as-received AISI 430 FSS joint	71
Table 4.3	Concentration of elements of the interface-layer matrix in sialon – one-hour-nitrided 430 FSS joint	84
Table 4.4	Concentration of elements of the precipitates at the interface layer in sialon – one-hour-nitrided 430 FSS joint	84
Table 4.5	Concentration of elements of the interface-layer matrix in sialon – four-hours-nitrided AISI 430 FSS joint	94
Table 4.6	Concentration of elements of the precipitates at the interface layer in sialon – four-hours-nitrided AISI 430 FSS joint	95
Table 4.7	Concentration of elements of the interface-layer matrix in sialon – as-received 7.5%-Cr FS joint	121
Table 4.8	Concentration of elements of the precipitates at the interface layer in sialon – as-received 7.5%-Cr FS joint	121
Table 4.9	Concentration of elements of the interface-layer matrix in sialon – one-hour-nitrided 7.5%-Cr FS joint	131
Table 4.10	Concentration of elements of the precipitates at the interface layer in sialon – one-hour-nitrided 7.5%-Cr FS joint	131
Table 4.11	Concentration of elements of the interface-layer matrix in sialon – four-hours-nitrided 7.5%-Cr FS joint	140
Table 4.12	Concentration of elements of the precipitates at the interface layer in sialon – four-hours-nitrided 7.5%-Cr FS joint	141

LIST OF FIGURES

Figure 2.1	The Si-Al-O-N behaviour diagram at 1750°C	9
Figure 2.2	Fe-Cr equilibrium diagram	12
Figure 2.3	Fe-Ni equilibrium diagram	13
Figure 2.4	Influence of alloying elements on the activity coefficient of nitrogen in pure iron at 1200°C and 1 atm of N ₂ gas.....	15
Figure 2.5	Microhardness profiles of gas nitrided AISI 410	16
Figure 2.6	Calculated iso-thermal section phase diagrams of Fe-(0-30)%Cr- (0-3)%N system at 1473K	17
Figure 2.7	Calculated vertical section phase diagram of Fe-24%Cr – (0- 2.5)%N system	18
Figure 2.8	Stages in the growth of the contact area between asperities	20
Figure 2.9	Local material transport mechanism involved in the growth of a bonded neck.....	21
Figure 2.10	Concentration profiles for nonsteady-state diffusion taken at the different times t_1 , t_2 , and t_3	23
Figure 2.11	Phase diagram of Fe – Si	40
Figure 3.1	Setting of solution nitriding experiment.....	45
Figure 3.2	Setting of diffusion bonding experiment.....	47
Figure 4.1	Microstructure of as-received AISI 430 FSS	55
Figure 4.2	Microstructure of AISI 430 FSS nitrided for one hour	55
Figure 4.3	Microstructure of AISI 430 FSS nitrided for four hours	56
Figure 4.4	Microstructure of AISI 430 FSS nitrided for seven hours	56
Figure 4.5	X-ray diffractogramme of AISI 430 FSS nitrided for four hours	57
Figure 4.6	Hardness of nitrided AISI 430 FSS	59
Figure 4.7	Microstructure of as-received 7.5%-Cr FS.....	61
Figure 4.8	Microstructure of 7.5%-Cr FS nitrided for one hour.....	62
Figure 4.9	Microstructure of 7.5%-Cr FS nitrided for four hours	62
Figure 4.10	Microstructure of 7.5%-Cr FS nitrided for seven hours.....	63
Figure 4.11	X-ray diffractogramme of 7.5%-Cr FS after nitrided for four hours	63
Figure 4.12	Hardness of nitrided 7.5%-Cr FS	65
Figure 4.13	Optical micrograph of the cross section of sialon – as-received AISI 430 FSS joint	66
Figure 4.14	Scanning electron micrograph of the cross section of sialon – as- received AISI 430 FSS joint.....	67
Figure 4.15	Scanning electron micrograph of the cross section of the interface layer in sialon- as-received AISI 430 FSS joint.....	67
Figure 4.16	Concentration profile of elements across the sialon – as-received AISI 430 FSS joint	70

Figure 4.17 Map of EDX spot analysis at the interface layer of sialon – as-received 430 FSS joint	71
Figure 4.18 X-ray diffractogramme of the interface layer in sialon – as-received AISI 430 FSS joint	74
Figure 4.19 XPS spectra of Fe from the interface layer in sialon – as-received AISI 430 FSS joint	75
Figure 4.20 XPS spectra of silicon from the interface layer in sialon – as-received AISI 430 FSS joint.....	76
Figure 4.21 Hardness test across the joint of sialon – as-received AISI 430 FSS.....	78
Figure 4.22 Optical micrograph of the cross section of sialon – one-hour-nitrided AISI 430 FSS joint.....	80
Figure 4.23 Scanning electron micrograph of the cross section of sialon – one-hour-nitrided AISI 430 FSS joint	80
Figure 4.24 Scanning electron micrograph of the cross section of the interface layer in sialon – one-hour-nitrided AISI 430 FSS joint	81
Figure 4.25 Concentration profile of elements across the sialon – one-hour-nitrided AISI 430 FSS joint.....	83
Figure 4.26 Map of EDX spot analysis at the interface layer of sialon – one-hour-nitrided AISI 430 FSS joint	84
Figure 4.27 X-ray diffractogramme of the interface layer in sialon – one-hour-nitrided 430 FSS joint.....	87
Figure 4.28 XPS spectra of Fe from the interface layer in sialon – one-hour-nitrided AISI 430 FSS joint.....	88
Figure 4.29 XPS spectra of silicon from the interface layer in sialon – one-hour-nitrided AISI 430 FSS joint.....	88
Figure 4.30 Hardness test across the joint of sialon – one-hour-nitrided AISI 430 FSS joint.....	89
Figure 4.31 Optical micrograph of the cross section of sialon – four-hours-nitrided AISI 430 FSS joint.....	90
Figure 4.32 Scanning electron micrograph of the cross section of sialon – four-hours-nitrided AISI 430 FSS joint.....	91
Figure 4.33 Scanning electron micrograph of the cross section of the interface layer in sialon – four-hours-nitrided AISI 430 FSS joint.....	91
Figure 4.34 Concentration profile of elements across the sialon – four-hours-nitrided AISI 430 FSS joint.....	93
Figure 4.35 Map of EDX spot analysis at the interface layer of sialon – four-hours-nitrided AISI 430 FSS joint.....	94
Figure 4.36 X-ray diffractogramme of the interface layer in sialon – four-hours-nitrided AISI 430 FSS joint.....	96
Figure 4.37 XPS spectra of Fe from the interface layer in sialon – four-hours-nitrided AISI 430 FSS joint.....	97
Figure 4.38 XPS spectra of Si from the interface layer in sialon – four-hours-nitrided AISI 430 FSS joint.....	98
Figure 4.39 Hardness test across the sialon – four-hours-nitrided AISI 430 FSS joint.....	99
Figure 4.40 Average thickness of the interface layer and the diffusion layer in the sialon – AISI 430 FSS joint.....	113
Figure 4.41 Optical micrograph of the cross section of sialon – as-received 7.5%-Cr FS joint.....	117

Figure 4.42 Scanning electron micrograph of the cross section of sialon – as-received 7.5%-Cr FS joint	117
Figure 4.43 Scanning electron micrograph of the cross section of the interface layer in sialon – as-received 7.5%-Cr FS joint.....	118
Figure 4.44 Concentration profile of elements across the sialon – as-received 7.5%-Cr FS joint.....	119
Figure 4.45 Map of EDX spot analysis at the interface layer of sialon – as-received 7.5%-Cr FS joint	120
Figure 4.46 X-ray diffractogramme of the interface layer in sialon – as-received 7.5%-Cr FS joint.....	123
Figure 4.47 XPS spectra of Fe from the interface layer in sialon – as-received 7.5%-Cr FS joint.....	124
Figure 4.48 XPS spectra of Si from the interface layer in sialon – as-received 7.5%-Cr FS joint.....	124
Figure 4.49 Hardness across the sialon – as-received 7.5%-Cr FS joint	126
Figure 4.50 Optical micrograph of the cross section of sialon – one-hour-nitrided 7.5%-Cr FS joint	127
Figure 4.51 Scanning electron micrograph of the cross section of sialon – one-hour-nitrided 7.5%-Cr FS joint	127
Figure 4.52 Scanning electron micrograph of the cross section of the interface layer in the sialon – one-hour-nitrided 7.5%-Cr FS joint.....	128
Figure 4.53 Concentration of elements across the sialon – one-hour-nitrided 7.5%-Cr FS joint.....	129
Figure 4.54 Map of EDX spot analysis at the interface layer of sialon – one-hour-nitrided 7.5%-Cr FS joint	130
Figure 4.55 X-ray diffractogramme of the interface layer in sialon – one-hour-nitrided 7.5%-Cr FS joint	133
Figure 4.56 XPS spectra of Fe from the interface layer in sialon – one-hour-nitrided 7.5%-Cr FS joint	134
Figure 4.57 XPS spectra of Si from the interface layer in sialon – one-hour-nitrided 7.5%-Cr FS joint	134
Figure 4.58 Hardness test across the sialon – one-hour-nitrided 7.5%-Cr FS joint.....	135
Figure 4.59 Optical micrograph of the cross section of sialon – four-hours-nitrided 7.5%-Cr FS joint	136
Figure 4.60 Scanning electron micrograph of the cross section of sialon – four-hours-nitrided 7.5%-Cr FS joint.....	137
Figure 4.61 Scanning electron micrograph of the cross section of the interface layer in sialon – four-hours-nitrided 7.5%-Cr FS joint	137
Figure 4.62 Concentration of elements across the joint of sialon – four-hours-nitrided 7.5%-Cr FS joint	139
Figure 4.63 Map of EDX spot analysis at the interface layer of sialon – four-hours-nitrided 7.5%-Cr FS joint.....	140
Figure 4.64 X-ray diffractogramme of the interface layer in sialon – four-hours-nitrided 7.5%-Cr FS joint	143
Figure 4.65 XPS spectra of Fe from the interface layer in sialon – four-hours-nitrided 7.5%-Cr FS joint	144
Figure 4.66 XPS spectra of Si from the interface layer in sialon – four-hours-nitrided 7.5%-Cr FS joint	144

Figure 4.67 Hardness test across the sialon – four-hours-nitrided 7.5%-Cr FS joint.....	145
Figure 4.68 Average thickness of interface layer and diffusion layer in sialon – 7.5%-Cr FS joint.....	154

LIST OF ABBREVIATIONS AND NOMENCLATURE

AISI	american institute of steel and iron
FSS	ferritic stainless steel
FS	ferritic steel
SS	stainless steel
OM	optical microscope
FESEM	field emission scanning electron microscope
EDX	energy dispersive X-ray spectroscopy
XRD	X-ray diffraction
XPS	X-ray photoelectron spectroscopy
ASTM	american society for testing material
GIA XRD	glancing incidence angle X-ray diffraction
ICP-OES	inductively-coupled-plasma optical emission spectroscopy
M_s	martensite start
fxN	ratio of nitrogen solubility in pure iron and in binary Fe-X alloy concerned
T_m	melting temperature in degree Kelvin
P_{ext}	external pressure
S	spacing between the ridges
σ_y	yield stress of the material
A_B	width of a contact /interface area
σ	stress
E	elasticity modulus
N	power term
Q_v	activation energy
A	a constant related to fundamental deformation characteristics of the material such as Burgers vector
R	gas constant, 8.31 J/mol-K or 8.62×10^{-5} eV/atom-K

T	absolute temperature
ρ_G	density of the transported gaseous material
P_{vap}	equilibrium vapor pressure
P_0	constant
ΔH_g	evaporation enthalpy
D	diffusion coefficient
D_0	temperature-independent pre-exponential
Q_d	activation energy for diffusion

PREFACE

The title of this thesis is “Reaction Layers in Diffusion Bonded of Sialon to Ferritic Steel”. It is submitted as the requirement for the degree of Doctor of Philosophy in the Department of Mechanical Engineering, Universiti Teknologi PETRONAS, Malaysia. The thesis is written based on the results of an extensive experiments and investigations that were carried out in UTP and AMREC, SIRIM, Bhd., Malaysia.

The research is aimed to investigate the reaction layer in the diffusion bonded of sialon to AISI 430 FSS and 7.5%-Cr FS. Sialon has a good corrosion resistant. It is chemically and thermally stable. The ceramic is also very hard. Therefore it is suitable for high temperature, corrosive and abrasive environment. Nevertheless, the ceramic is extremely brittle. It invites difficulties in machining it into a complex component. Thus, combination of the ceramic with metal is required. The AISI 430 FSS and the 7.5%-Cr FS also own corrosion resistant and commonly applied for high-temperature application, therefore they are suitable for combining with sialon. Joining the sialon with the steels optimizes the properties of the materials. Diffusion bonding produces stronger joint than other joining methods. The joint attained by this process is highly influenced by the reaction layers produced in the interface. Therefore, understanding the reaction layer in the interface of the joined materials is meaningful for achieving the joint.

The investigation was carried out by performing diffusion bonding experiment using a hot press machine. The process was conducted in AMREC, SIRIM, Bhd., Malaysia. Joining of sialon with nitrided steel was also studied as earlier work indicated that it could improve the joint. Characterization was performed on the joint of the materials to study the reaction layers in the joint interface.

The results are presented in a structured presentation in this thesis. Motivation and objectives of the study are presented in Chapter 1 of the thesis. A review on the relevant previous work was reported in Chapter 2. The chapter describes the road map of the research and the current issue on this area. This part is aimed to identify the opportunity for producing a meaningful contribution in the joining of ceramic to stainless steel. Methodology to achieve the objectives of the research is written in Chapter 3. This chapter also provides information on the materials, experimental setting and characterization techniques employed in the study. The later chapter, *i.e.* Chapter 4, reports the results of the study. Analyses with theory on the results of the experiment were performed to draw the conclusions that are presented in Chapter 5. Chapter 5 also identifies and highlights potential issues for further study in this area.

Hudiyo Firmanto

Bandar Seri Iskandar, March 2011

CHAPTER 1

INTRODUCTION

1.0 Overview

This chapter provides an overview of the present research. Initially it explains the background that motivates to perform the study. Problem statements are derived based on brief observation on latest development of the concerned area. Subsequently, objectives and methodology to achieve them are described briefly. At the end of the chapter, organization of the thesis is explained. The section is aimed to help readers to go through the thesis more easily.

1.1 Background

Sialon is an engineering ceramic that owns good properties of high hardness and thermal resistance. Thus it is good in serving abrasive and corrosive, as well as high temperature environment. With regards to this benefit, it has been widely used for components that experience abrasive and high temperature conditions. However, it is mainly used for individual components such as mechanical clamp, extrusion dies, cutting tool, and sand blasting nozzle. This is due to its poor machinability and difficulties in joining it with metal. Therefore, joining it with metal is necessary to expand its utilization.

Joining ceramics with steels is required to optimize properties of the materials. The components would obtain benefits from high hardness and corrosion resistance of the ceramics, and toughness of the steel. With this idea, bulk part of components can be made of the steel, while the ceramics is employed for the part that was directly involved in corrosive and high-temperature environments. Turbocharger rotor, glow

plug head and rocker arm tip made of silicon nitride are the examples of the ceramics metals joining applications [1].

Despite the prospect in its application, joining ceramics with metals is difficult. There are two issues that relate to the joining difficulties [2-3]. The first is regarding the difference of chemical bonding between ceramics with metals. The difficulty to join ceramics with metal is due to the different chemical bonding of the materials. Ceramics own covalent and ionic bonds. It does not have metallic bonds where outer shell electrons of atoms in the structure become delocalised. Control of this ceramic/metal interface is highly responsible for the intrinsic strength of joint. The different of bonding nature between ceramics and metal may prevent formation of strong bonds. Another serious concern in ceramic – metal joining is the different thermal expansion coefficient of the materials, which is more important especially in designing components and joint. The different thermal expansion coefficient of the materials results in high thermal residual stress at the joint which is generated during cooling stage in the joining process. Excessive residual stress at the joint may crack the ceramics though the interfacial bonds can be attained. Thus, compensating for thermal expansion mismatches between the materials is important to prevent the crack.

Several techniques are commonly applied for joining ceramics to metal. Brazing is frequently employed, yet it uses filler metal that limits the service temperature of the joint. Alternatively, solid state joining is also often attempted. In this technique, problems that arise from the different thermal expansion coefficient of the joined materials become more critical as the process involves heating to and cooling from a high temperature. This may lead to a crack due to the high residual stress at the joint. This case was observed in joining of sialon with austenitic stainless steel [4-5] and also indicated in the case of silicon nitride with steel [6-7].

Reaction of metal with ceramics during the joining is another source of the problem. Thickness of reaction layer affects the joint strength, while brittle phase in the layer may weaken the joint [8-12]. The brittle phase can also produce microcrack. The works observed optimum condition that gives maximum joint strength. Although a joint is achieved by reaction of ceramics with metals, however excessive growth of

the reaction layer deteriorates the joint. Therefore, reaction layers are important for achieving the joint.

Joining of silicon nitride with stainless steel has been carried out [2, 10, 12-14]. Reactions of the materials are noticed. However, different reaction products in the joint are claimed. For a relatively-new-developed engineering ceramic, a few works were attempted to join sialon with steel. Joining of sialon with austenitic stainless steel was impossible since crack occurred in the ceramics due to the different coefficient of thermal expansion [4-5]. However, the ceramics was successfully joined with 9%-Cr FSS. The work claimed that ductile reaction layers at the interface contributed to the joint successfulness. Although the ductility of the layer was noted, nevertheless detailed phase identification on the layer was not carried out. Phases in the layer were analytically predicted based on the elements at the joint and no other characterization techniques were employed to investigate the phases. Hence, phases which appear in the reaction layer in sialon – 9%-Cr FSS joint remain unclear. Another investigation on reactivity of sialon with iron-based alloys observed that the ceramics could be joined with steel [15].

Since the reaction layers are important for attaining the joint, controlling the layers is essential. Hussain [5] proposed nitriding pre-treatment on the steel prior to joining to improve the joint of sialon-ferritic stainless steel. The treatment was aimed to diffuse nitrogen into the steel surface before joining. It was claimed that nitrogen in the steel could suppress the decomposition of sialon and improve the joint. Nonetheless, the effect of the treatment was not clearly explained. Furthermore, the work did not provide obvious evidence. However, nitrogen in titanium prior to joining with silicon nitride was found to suppress the growth of titanium silicide in the interface. This slightly improves the joint strength [8]. Adding nitrogen into the steel to counteract the nitrogen liberation from the decomposed sialon was in line with the idea of avoiding fast decomposition rate of ceramics to control the reaction layers [16].

The above brief reviews show that despite good prospect of sialon-steel joint application, not many works reported on the joining of the materials. The importance of reaction layer at ceramic-steel joint has also been revealed. However, for the

sialon-steel joint, phases at the joint were not clearly identified. It seems that complexity of elements interdiffusion at the interface and the thin layer at the joint has led to the difficulties in accomplishing the task. Hence, studying the reaction layers (*i.e.* thickness, properties and phases) and their relation to the joint in the interface of the sialon-steel joint is still such a challenging research.

It was also noted that nitriding pre-treatment improved the joint of sialon-ferritic stainless steel. Influence of nitrogen pre-solved metal on the joining with silicon nitride was known in the case of titanium-silicon nitride joining. However, its influence on the elements diffusion and the reaction layer formation was not scrutinized in the sialon-stainless steel joining [4-5].

In this work, joining of sialon with AISI 430 FSS and 7.5%-Cr FS were attempted. Since joining of sialon and austenitic stainless steel was not possible, AISI 430 FSS could be an alternate stainless steel to propose. AISI 430 FSS is suitable for corrosive environment and commonly used for high temperature application. Therefore it is appropriate to be combined with ceramics to serve corrosive and high temperature environments. Moreover, the steel is also commercially available in the market. The 7.5%-Cr FS was also joined with sialon to investigate the phases in the reaction layer that has not been completely identified in the previous works [5, 17]. In those works, characterization was performed on the cross section of the joint. They did not attempt to perform the characterization on the surface of the reaction layer. Applying the characterization on the reaction layer cross section was difficult since the reaction layer in the joint was too thin. Therefore, only elemental analysis was performed to analyze the phases of the reaction layers. Consequently, the works failed to identify the phases in the reaction layer of the sialon – stainless steel joint. Despite its lower Cr content, the 7.5%-Cr FS has a good corrosion resistance and frequently used in high temperature applications such as in power plant and nuclear industry. In the present research, the steels were joined in as-received and nitrided condition to study the influence of the pre-treatment on the joint as well as the reaction layer.

1.2 Problem Statement

The above discussions reveal up several problems that can be formulated. Those are as follows:

1. Difficulties in joining sialon with steel have limited the utilization of sialon to individual components. Few efforts in joining sialon with steel leads to the assumption that the materials cannot be joined, thus the success of the joining will expand the utilization of the sialon.
2. Decomposition of the joined materials and interdiffusion of elements at the interface of the joint may form the reaction layers that affect the joint; hence understanding the characteristics of the joint is valuable in joining the materials.
3. The works in sialon-ferritic stainless steel joining had identified a ductile layer at the joint interface. This has an important role on achieving the joint. Nevertheless, detail investigation on the phases at the layer was not carried out; hence distribution of phases at the interface was still unclear.
4. Nitriding pre-treatment on the steel prior to bonding with sialon has been claimed to improve the joint, however its influence on the reaction layers at the joint was not investigated [5, 17].

1.3 Objectives of the Study

With regards to the above problems, the present project was carried out with the following objectives:

1. To develop the solid state joining of sialon and AISI 430 FSS and 7.5%-Cr FS by using direct diffusion bonding process.
2. To study the interdiffusion of elements in the interface of the joint.
3. To investigate the reaction layers formed at the joint and their new phases.
4. To study the influence of the solution nitriding pre-treatment applied to the steel on the joint.

1.4 Scope of the Study

The research covers the investigation on solid state joining of sialon and AISI 430 FSS and 7.5%-Cr FS by using diffusion bonding process in a hot-press machine. The steels to be joined were in nitrated and unnitrated conditions. The study was focused on the interdiffusion of elements and the formation of the reaction layers at the interface. It was also aimed to identify the properties of the layers. Evaluation of the joint was carried out qualitatively from its microstructures. Comparison of the properties of the reaction layers at the interface for nitrated and unnitrated steel joined to sialon was performed. This was to study the influence of the pre-treatment on the diffusion bonding of the materials.

1.5 Thesis organization

The thesis is structured and organized as follows:

Chapter 1 presents the summary of the background and also the formulated problem in the area. It also describes the direction and objectives of the research. Brief description on the methodology to achieve the objectives is also presented.

Chapter 2 discusses the theoretical background of the study. It also provides literature review that was carried out in the research area. The discussion reflects the road map of work in the ceramic-metal joining and its related study.

Chapter 3 explains details of the steps of works that are performed to achieve the objectives of the research. Materials and procedure used in the experiments as well as characterization techniques utilized to gain the data are presented.

Chapter 4 presents the analysis and discussion on the results of the overall experiments. Initially, the results of solution nitriding of the AISI 430 FSS and the 7.5%-Cr FS are reported and discussed. The later part provides the analysis and the discussion of the diffusion bonding of the materials. The analysis and discussion of the diffusion bonding of sialon – AISI 430 FSS and sialon – 7.5%-Cr FS are presented separately.

Chapter 5 states the conclusions drawn from the research. This section also highlights the future work that can be explored further in this area.

CHAPTER 2

LITERATURE REVIEW

2.0 Overview

This chapter contains a review on theory and previous works which are relevant with the present research. The first two sections present brief discussions on the materials which are studied in this work. The later sections review previous works on solution nitriding of stainless steel and joining of ceramics with steel. The review is attempted to scrutinize the information which are useful either to plan the experiment or analyze the results. It is also focused on identifying the issues that is meaningful for further study.

2.1 Sialon

Sialon ceramics are engineering ceramics which consist of Si, Al, O and N in various compositions [18]. The materials are attractive for high temperature applications for their good properties, such as high hardness, anti oxidation, high fracture toughness, superior wear and corrosion resistance, and excellent thermal shock resistance [19-21]. These properties have led to application of the ceramics for materials in cutting tools, bearings, turbochargers, high temperature valves and other wear-resistant components [21-23].

Si_3N_4 has insufficient resistance to unpredictable brittle fracture, degradation of mechanical properties at elevated temperatures and insufficient oxidation resistance. These properties limit its application range [23]. Sialon ceramics are obtained by incorporating sintering additives (*e.g.* MgO or Y_2O_3) into the silicon nitride lattice. It reduces the amount of secondary phase and improves its high-temperature properties.

Based on the initial Si_3N_4 condition, sialon may be in the form of α and β sialon. β -sialon is a solid solution of β - Si_3N_4 with Al_2O_3 where Si and N were substituted with sufficient amount of Al and O [19]. It has a structure similar to hexagonal β - Si_3N_4 and softer than the α -sialon. Figure 2.1 presents the diagram of sialon behavior at 1750°C . The figure illustrates the β -sialon as a solid solution between Si_3N_4 and $\text{Al}_2\text{O}_3 - \text{AlN}$. The ceramics is represented by the formula of $\text{Si}_{6-z}\text{Al}_z\text{O}_z\text{N}_{8-z}$ ($0 < z < 4.2$). The sialons are produced according to the following reaction [24].

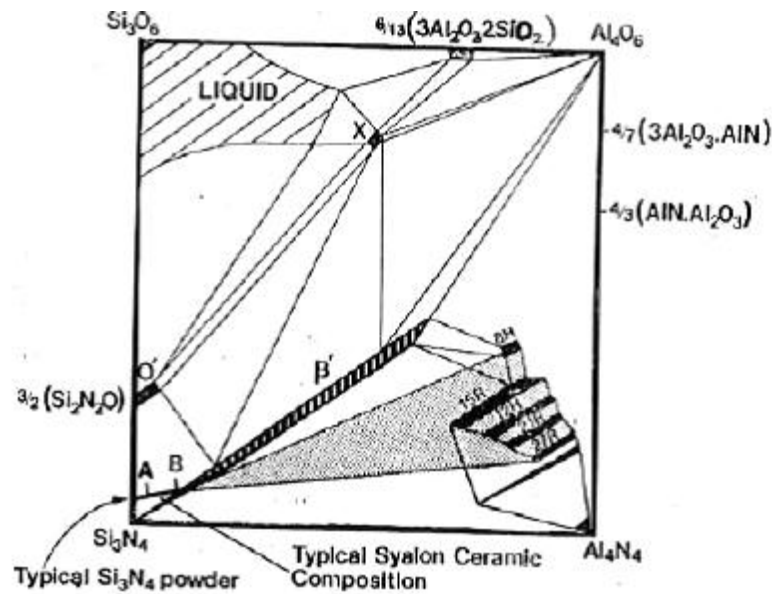
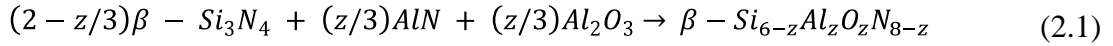


Figure 2.1 The Si-Al-O-N behaviour diagram at 1750°C [22]

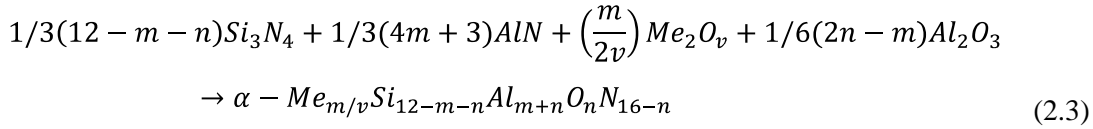
α -sialons have an expanded α structure. Their formation also involves the substitution of Si and N by Al and O respectively. Simultaneously, metal cations are incorporated into the interstices in the α - Si_3N_4 structure [25]. This can be obtained by reaction of lithium silicon nitride with alumina or of lithium aluminates with silicon nitride.

The sialons are found in Li-Si-Al-O-N system and also in Mg, Ca, Y-Si-Al-O-N systems. General formula of the ceramics is:



where $x \leq 2$, and $m(\text{Al-N})$, $n(\text{Al-O})$ replace $(m+n)(\text{Si-N})$ in each unit cell.

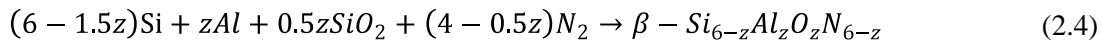
Chemical reaction for the formation of the solid solutions is:



The materials are harder than β - Si_3N_4 . They are also brittle and unstable at high temperatures. Therefore, the ceramics are less favorable for structural applications.

β -sialon was produced using ($Si_3N_4+Al_2O_3$); α - Al_2O_3 , β - Si_3N_4 , AlN powder as starting materials [19]. The powders were compacted into pellets in a die at 100 MPa using Y_2O_3 as sintering additives. The compacted samples were sintered by hot pressing in a graphite die at 1730°C for two hours under 0.1 MPa of nitrogen atmosphere with 30 MPa mechanical loads. Fully-densified pure β -sialon was obtained from the process.

Another work [21] used Si, Al and SiO_2 powder as starting material to prepare β -sialon. The powders were synthesized by combustion synthesis using β -sialon as the diluent under low nitrogen pressure (*i.e.* 1 MPa). The compacted powders were then sintered using a spark plasma sintering system under vacuum conditions of lower than 4 Pa at a compressive stress of 50 MPa. Sintering was carried out at 1600°C for 12 minutes without sintering additives. The ceramics is produced through the following reaction:



The process produced pure and dense β - $Si_{6-z}Al_zO_zN_{6-z}$ ($z=1-3$) with relative densities higher than 99% of the theoretical density.

Preparation of sialon using nano powder was investigated [26]. The powders were plasma-synthesized. Those were Si_3N_4 , mixture of 90% Si_3N_4 -10% AlN, 90% AlN-10% Y_2O_3 , Si_3N_4 -AlN- Al_2O_3 - Y_2O_3 and Y_2O_3 . Comparison was made with the sialon prepared from commercial powders, *i.e.* α - Si_3N_4 , AlN, Al_2O_3 and Y_2O_3 (nanophase) powders. The powders were compacted by die pressing to produce sialon sample. Sintering of the samples was performed under nitrogen atmosphere up to 1650°C for 2 hours. β sialon formation was started above 1400°C. Sintering improved the density

of the samples, *i.e.* from 40 – 48% to 95 – 98%. This was denser than the sialon prepared from commercial powder (maximum density of 87%). Compared to the sialon made from commercial μm -sized powder, dense material could be obtained from nano-sized powders at lower temperature (*i.e.* 1500 – 1600°C). Thus the work revealed that densification behavior of sialon was influenced by powder composition and size of particles used as starting powder.

Addition in excess of 2 or 5% yttrium produced fully-densified α -sialons after hot-isostatic pressing [27]. This was investigated on the α -sialons that were prepared from powders of Si_3N_4 , AlN , Al_2O_3 and Y_2O_3 . The compacted green pellets were hot-isostatic pressed at 1800°C for one hour under 1 MPa. Transformation of $\alpha - \beta$ phase was restrained by rapidly cooling the sample after densification. This also minimized crystallization of the glassy-grain boundary phase during cooling. Samples having same composition could not be densified without excessive Y_2O_3 incorporation. In this condition, density of the sample after sintering was only 70% as the treatment could not remove the closed porosity. Addition of excessive Y_2O_3 drove the formation of elongated α -sialon grain when the samples were heat-treated at relatively higher temperatures (1700° and 1900°C). This improved fracture toughness of the sialons.

2.2 Stainless Steel

Chromium is the main alloying element in stainless steel. The element creates a thin protective film that prevents oxidation of the steel. Minimum content of chromium in stainless steel is about 11% [28]. Other elements are added to improve its particular characteristics.

Stainless steel is classified based on its microstructure. Phase diagram given in Figure 2.2 can be used to explain the idea behind the stainless steel classification. The figure shows that solubility limit of Cr in γ phase is around 13% at 1050°C. Therefore in this condition the steel is in γ phase. At this composition, martensite start temperature (M_s) is sufficiently high to transform the austenite into martensite[29]. Thus, at room temperature, the steel is in martensitic structure.

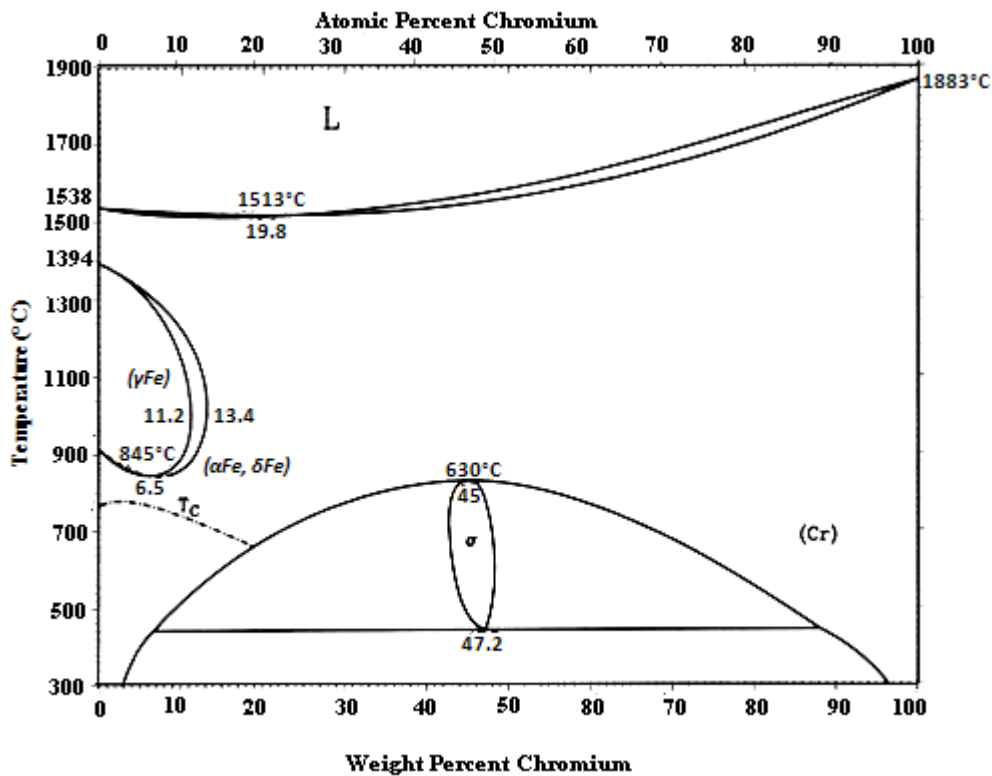


Figure 2.2 Fe-Cr equilibrium diagram [28]

Austenite transforms to ferrite when chromium is increased. This phase will remain in the steel upon cooling to room temperature and produce ferritic structure. With addition of nickel, austenite phase is stabilized even at high Cr content. This is due to the strong austenite-former characteristics of the element. Figure 2.3 illustrates that nickel stabilizes the austenite. Thus, even at higher Cr content, addition of 9% nickel makes the steel to be in austenite phase. The overall alloy decreases martensite-start and martensite-finish temperature down to sub-zero [29]. Therefore, the steel is in austenitic structure when it is cooled to room temperature.

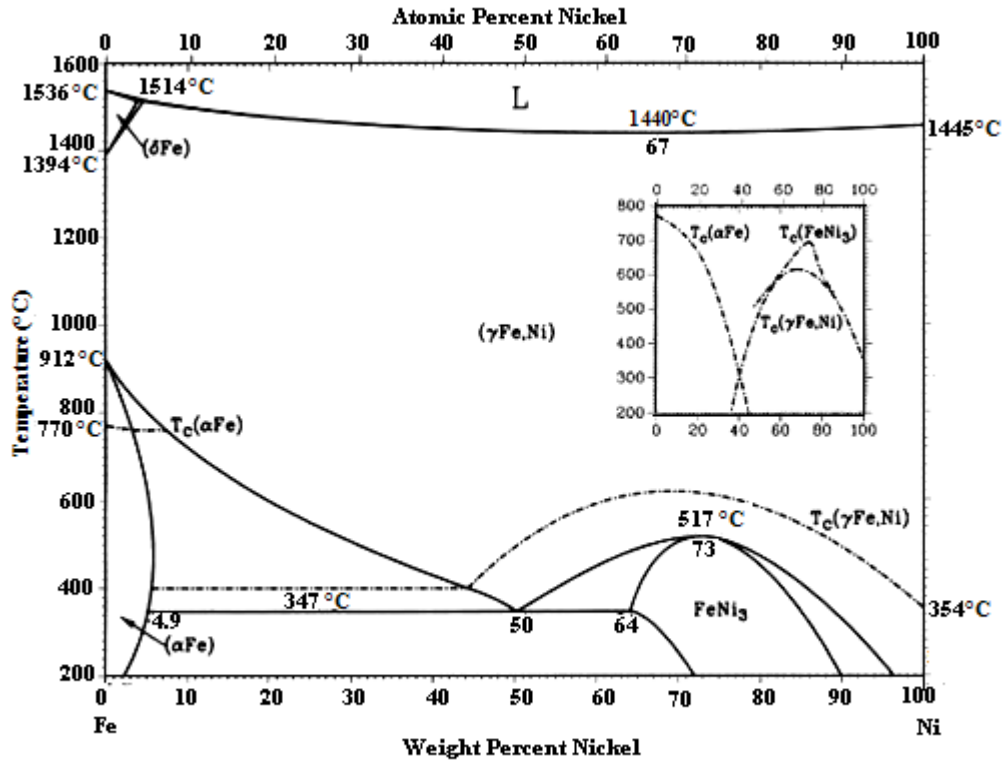


Figure 2.3 Fe-Ni equilibrium diagram [30]

Based on microstructure and alloy composition, five categories of stainless steel is derived, namely [31]:

1. Martensitic (11.5–18% Cr, 0.08–0.20% C); the standard martensitic grades are types 403, 410, 414, 416, 416Se, 420, 422, 431, 440A, 440B, and 440C
2. Ferritic (10.5–30% Cr); the standard ferrite stainless steels are types 405, 409, 429, 430, 430F, 430F–Se, 434, 436, 439, 444, and 446
3. Austenitic (16–26% Cr, 0.75–19.0% Mn, 1–40% Ni, 0.03–0.35% C, and sufficient N); 2xx and 3xx series are groups of this steel
4. Duplex (18–29% Cr, 2.5–8.5% Ni, and 1–4% Mo, up to 2.5% Mn, up to 2% Si, and up to 0.35% N); 329
5. Precipitation hardening (PH) stainless steel (austenitic and martensitic with alloy added to form precipitates; those are: Mo, Cu, Al, Ti, Nb, and N); essential alloys in this grade are 17-7PH (UNS S17700) and PH15-7Mo (UNS S15700)

2.3 Nitriding of Stainless Steel

Nitriding is an established technique to strengthen steel. In this method, nitrogen is diffused into the steel. The nitrogen may dissolve in the steel or precipitates in the form of nitride. Interstitial diffusion of the element in the steel or its precipitation improves hardness of the steel.

In gas nitriding technique, the steel is exposed in nitrogenous atmosphere at elevated temperature. Gas nitriding at 400 – 700°C is considered as low-temperature gas nitriding. During the process, nitrogen diffuses into the steel and forms a nitrogen solid solution or nitrides. A white compound is formed in the steel's surface. It consists of nitrogen solid solution and nitrides (Fe_xN or Cr_xN). This produces a hardened case in the steel [20, 32-38]. However, formation of the compound reduces its corrosion resistance [39-40].

Gas nitriding at high temperature (*i.e.* 1000 – 1200°C) is also known as solution nitriding. This is a relatively-new technique of heat treatment to harden stainless steel [39, 41]. The technique is carried out by heating the sample in nitrogenous atmosphere at high temperatures where austenite is the stable phase [39-42]. After being held for a certain time and quenching, a hardened case is normally obtained. In this method, nitrogen is added and diffused interstitially into the steel. The nitrogen forms a solid solution in the steel. The diffusion of nitrogen strengthens the steel. This treatment is widely employed in improving the hardness of martensitic [40], austenitic [39, 41-46], ferritic [47-50], and duplex [51-52] stainless steels. The works recognized that compared to low-temperature gas nitriding, the solution nitriding can diffuse nitrogen deeper into the steel.

Permeation of nitrogen in steel occurred through dissolution in austenite up to its solubility limit. This takes place according to the following reaction [40]:



Nitrogen can also precipitate in chromium nitrides through the reaction below:





Solubility of nitrogen in iron is affected by alloying elements. Figure 2.4 illustrates the influence of alloying elements on nitrogen solubility calculated by Vleugels *et al.* [15]. fxN is ratio of nitrogen solubility in pure iron and in binary Fe–X alloy concerned. Log fxN greater than 0 means that the element improves activity coefficient of nitrogen and reduces the nitrogen solubility, while element with fxN less than 0 enhances the nitrogen solubility. The figure shows that C, Ni and Si in the metal decreased reactivity of the sialon – iron-alloy since the elements reduced solubility of nitrogen. On the other hand, Cr, Mn and Mo increase the nitrogen solubility, thus they enhance the reactivity.

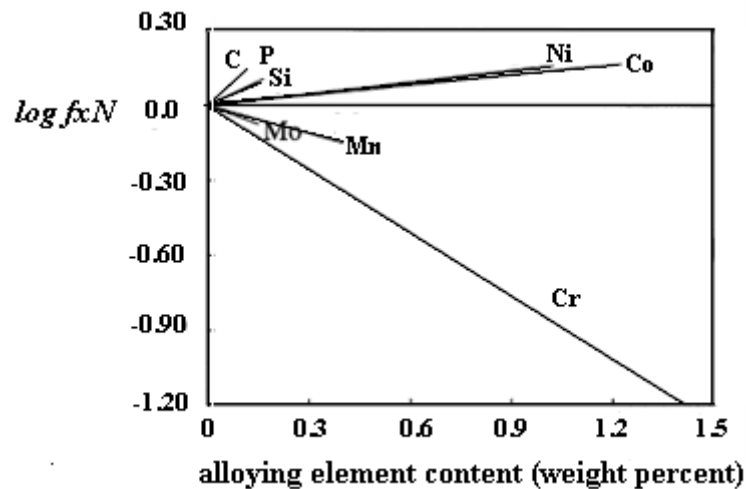


Figure 2.4 Influence of alloying elements on the activity coefficient of nitrogen in pure iron at 1200°C and 1 atm of N₂ gas [15]

Solution nitriding of duplex stainless steel at 1150°C for 15 hour produces nitrides (M₂N) at the sample surface [41]. However, the solution nitriding does not change microstructure of austenitic stainless steel [42-43]. In this kind of steel, absorption of nitrogen is increased with increasing N₂ partial pressure. Longer solution nitriding enlarges grain size of the steel. This implies that nitrogen is fully absorbed by the steel. Solution nitriding for 4.8 ks hardens overall cross section of 0.3 mm sheet thickness of the steel. It improves hardness of the steel from 1.7 GPa to

approximately 2.7 GPa. Tensile strength of the steel is also increased; *i.e.* from 400 MPa to 850 MPa.

Correlation of nitrogen and hardness of nitrided stainless steel was proven for austenitic stainless steel [41, 46]. For the nitriding of martensitic stainless steel, Nitrogen content in the steel correlated well with the martensite layer and also the steel hardness [47]. Nitriding the martensitic stainless steel produced martensite layer in steel surface and dual phase of ferrite and martensite at the sample core. It was also shown in nitriding AISI 410 SS at 1200°C under 0.25 MPa N₂ pressure for six hours which formed 2.2 mm martensite case in the surface [53]. Below the martensite layer, microstructure of the steel was dual phase; *i.e.* ferrite and martensite. However, nitrides were formed when nitriding was performed at 1000°C. Maximum nitrogen content of 0.7 weight percent was diffused into the steel. Figure 2.5 shows microhardness and nitrogen content profiles of gas nitrided AISI 410 SS.

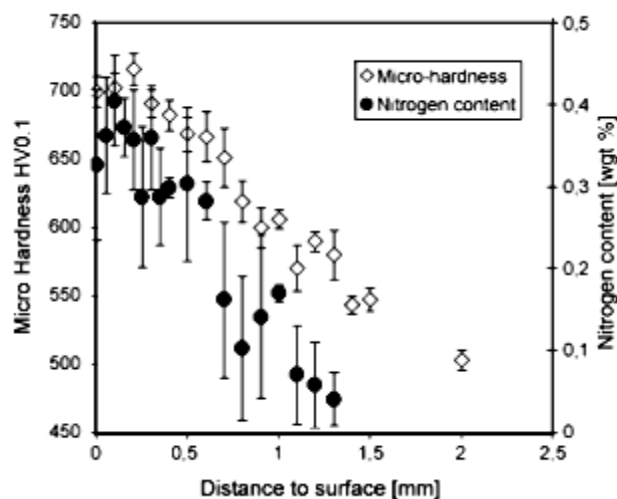


Figure 2.5 Microhardness profiles of gas nitrided AISI 410 stainless steel [53]

Nitrogen diffusion was estimated based on surface hardness since nitrogen content in steel correlates well with its hardness [17]. Martensite-case thickness was also utilized for this purpose. In this work, solution nitriding was employed to diffuse nitrogen into 9%-Cr FSS.

Solution nitriding of AISI 430 FSS at 1100°C for 15 minutes produced 130 μm martensite layer at the steel surface [50]. The whole 1.2 mm thickness of the steel was transformed to martensite when nitriding was lengthened for 10 hours. In the former setting, nitrogen was diffused with the content of 1 weight percent at the steel surface and diminished at approximately 160 μm below the surface. Maximum nitrogen content was found in the surface of the steel nitrided for 10 hours. It decreased to 0.43 weight percent in the core of the sample.

Separate investigation on the materials also gained martensite phase throughout the steel after nitriding for 1200°C under 0.1 MPa for 10 hours [49]. The steel absorbed 0.43 weight percent of nitrogen. Iso-thermal section phase diagrams of Fe–(0–30)%Cr–(0–3)%N system at 1473 K calculated by the worker is displayed in Figure 2.6. With composition of 16.21% Cr and 0.43% N, the steel is in γ phase. Subsequently the austenite transformed to martensite during cooling to martensite-start temperature.

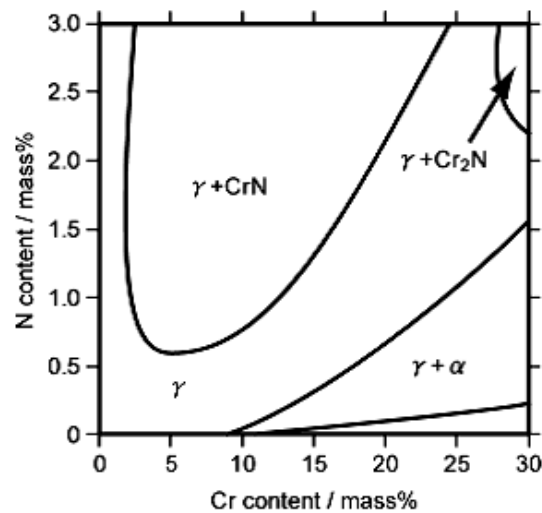


Figure 2.6 Calculated iso-thermal section phase diagrams of Fe–(0–30)%Cr–(0–3)%N system at 1473K [49]

At higher Cr and N content (*i.e.* 24% and 1.82% respectively), nitrogen pearlite which consists of α and Cr_2N was observed. Phase diagram of Fe–24%Cr – (0–2.5)%N system given in Figure 2.7 shows the possibility of $\alpha + \text{Cr}_2\text{N}$ at nitrogen content of 1 – 2.5%. The diagram also reveals that Cr_2N may be formed at lower temperature (*i.e.* up to 1300K or 1023°C).

Reviews on solution nitriding works in this section reveal the role of the treatment in strengthening stainless steel by diffusing nitrogen. It improves the hardness of austenitic, ferritic, martensitic and also duplex stainless steels. Nitrogen diffusion does not change the microstructure of the austenitic stainless steel due to its high solubility [42-43, 54]. However, the ferritic structure in the ferritic stainless steel underwent transformation to martensitic due to the nitrogen diffusion [47, 49-50]. Nitrogen content correlates well with hardness of nitrided steel. Therefore, thickness of martensite and hardened-case in nitrided-steel surface can be used to estimate depth of nitrogen diffusion in the steel [17]. Hence, this estimation technique was also employed in the present work.

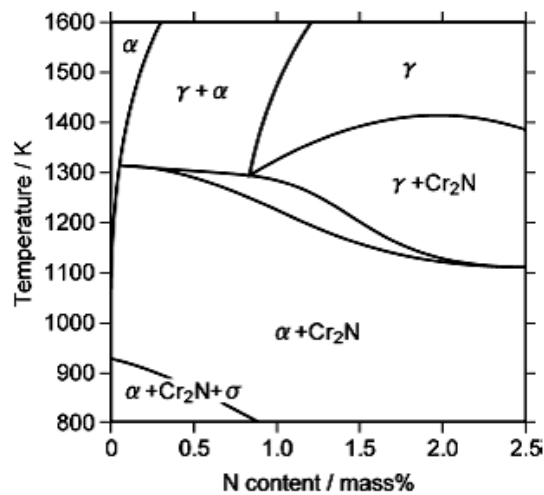


Figure 2.7 Calculated vertical section phase diagram of Fe-24%Cr – (0–2.5)%N system [49]

Besides dissolution in the steel, nitrogen may also precipitate in the form of nitrides. This occurs when nitriding is conducted at lower temperature. Nitrides were formed in nitriding of ferritic or martensitic stainless steel at 1000°C. Nitrogen pearlite is also produced when the nitrogen content exceeds its solubility in austenite.

2.4 Diffusion Bonding Theory

Diffusion bonding is a solid-state joining process to join similar or dissimilar materials. The joint was attained by reaction of the joined materials.

To grow the reaction, intimate contact between the joined materials has to be attempted. The interfacial reaction was achieved by the elements interdiffusion. To stimulate the elements interdiffusion, intimate contact was maintained for a sufficient time with an appropriate uniaxial pressure. Simultaneously, heating is applied at the temperature of at least $0.75T_m$, where T_m is the melting temperature of the less-refractory material in degree Kelvin. Heating cannot be applied at too high temperature as it will melt the less-refractory materials. However, it should be high enough to facilitate the diffusion process that will produce reaction between the joined materials.

Diffusion bonding pressure is needed to bring the mating surface into intimate contact. This should not be too high to prevent macroscopic deformation. Nevertheless, it should be sufficient to produce proper mating throughout the joined surface. The pressure can be applied by employing a dead load or utilizing a low-expansion-material jig to put the materials under pressure while heated. It can also be generated using hydraulically-operated rams in the chamber walls. Such technique is employed when the diffusion bonding is conducted in a hot-press machine.

Joining of ceramics with metal could be difficult due to the refractoriness of the material. Low plasticity of the material also results in difficulties to attain conformity of mating surfaces. To overcome this problem, interlayer is frequently utilized. The interlayer is placed in between the joined surfaces. It must be ductile so that it can deform easily to provide intimate contact between the mating surfaces under diffusion bonding temperature without yielding any macroscopic deformation. The interlayer may also absorb residual stress at the joint during cooling in the bonding process. The residual stress normally takes place when there is a big difference of the joined-materials' expansion.

Production of the ceramic – metal joint depends on the formation of interfacial reaction layer. The reaction layer acts as a bridging compound between the joined materials. Excessive growth of the layer may produce brittle reaction products which are harmful to the joint.

2.4.1 Modeling joint formation

Achieving the joint in diffusion bonding process is initiated with the formation of contact areas and the joint formation by the growth of bonded interfaces. Modeling of the joint is proposed [55] by assuming the bonding as two blocks of pure ductile material without any contaminants. This model is illustrated in Figure 2.8. The block is assumed as uniform shape of dome or pyramids whose peaks make the initial contact (Figure 2.8a). The contact flattens the peaks, yields neck formation (Figure 2.8b) and subsequently closes the voids (Figure 2.8c).

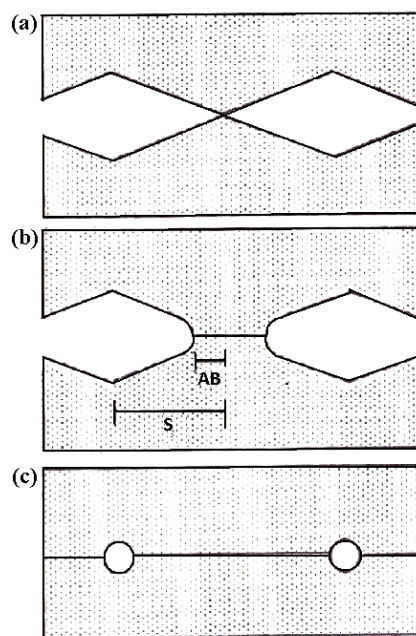


Figure 2.8 Stages in the growth of the contact area between asperities [55]

The initial contact is attained by the deformation on the contact points which generates a contact /interface area of width A_B . The contact area is expressed as:

$$A_B = P_{ext} \cdot \frac{S}{Constant \cdot \sigma_y} \quad (2.1)$$

where P_{ext} is the external pressure, S is spacing between the ridges, σ_y is the yield stress of the material.

Several processes are involved in closing the voids and developing the interface (Figure 2.9). It was started with creep to drive the flattening (Figure 2.9a), while vapor phase transport and diffusion takes place to make them spheroidize (Figure 2.9b) and shrink (Figure 2.9c).

The steady state creep is derived from the expression:

$$d\varepsilon_{SS}/dt = A(\sigma/E)^n \exp[-Q_v/RT] \quad (2.2)$$

where σ is the stress, E is the elasticity modulus, n is a power term (*i.e.* a value of typically between 4 and 5), Q_v is the activation energy and A is a constant related to fundamental deformation characteristics of the material such as Burgers vector.

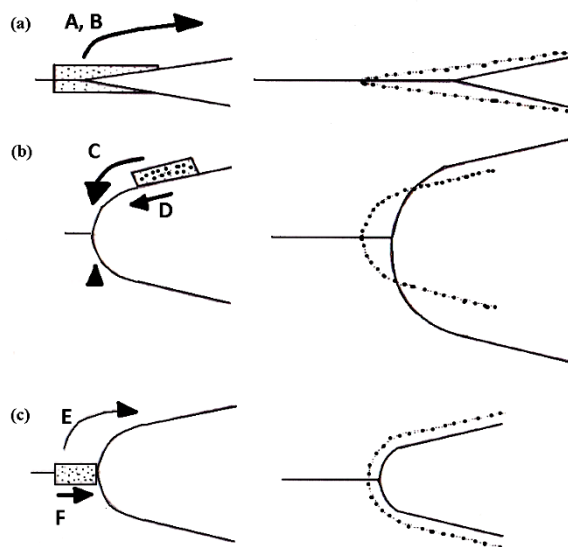


Figure 2.9 Local material transport mechanism involved in the growth of a bonded neck [55]

The maximum rate of vapor phase transport, dm^*/dt is given by the Langmuir evaporation equation

$$dm^*/dt = (3P_{vap} \cdot \rho_G)^{1/2} \quad (2.3)$$

where ρ_G is density of the transported gaseous material and P_{vap} is equilibrium vapor pressure. The equilibrium vapour pressure can be related to the temperature through the following equation:

$$P_{vap} = P_0 \cdot \exp(-\Delta H_g/RT) \quad (2.4)$$

where P_0 is a constant and ΔH_g is the evaporation enthalpy.

2.4.2 Diffusion of elements

Diffusion bonding involves materials transport in term of atomic migration through the lattice of a crystalline solid [56]. The process is a thermally-activated process and time dependent. Diffusion is defined as atomic movement from the higher-concentration to the lower-concentration. It is the only possible significant transport in solids [57]. Rate of diffusion with respect to the concentration gradient is expressed in a mathematical equation by Fick's first law as [58]:

$$J_x = -D \left(\frac{\partial C}{\partial x} \right) \quad (2.5)$$

where, J_x is the flux of the diffusing elements in the x direction, $\partial c/\partial x$ is concentration gradient which can be changeable with time, and D is the diffusion coefficient which is expressed in m^2/sec . The diffusion coefficient also means as the element's diffusivity.

The above equation is applied when the flux does not change with time. This condition is also called as steady-state diffusion. Nonetheless, in many cases, the diffusion runs in non-steady state condition, that is the diffusion flux and the concentration gradient vary with time. For this situation, concentration of the diffused elements continuously decreases with the increasing of time. This is illustrated in Figure 2.10.

Nonsteady-state diffusion is expressed in a mathematical equation which is known as Fick's second law. The equation for the Fick's second law is as follows:

$$\frac{\partial C}{\partial t} = \partial/\partial x \left(D \frac{\partial^2 C}{\partial x^2} \right) \quad (2.6)$$

When the diffusion coefficient is independent of composition, the equation can be simplified to:

$$\frac{\partial C}{\partial t} = D \frac{\partial^2 C}{\partial x^2} \quad (2.7)$$

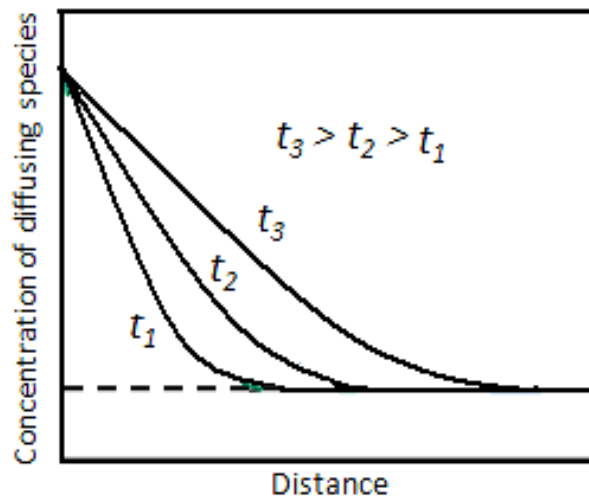


Figure 2.10 Concentration profiles for nonsteady-state diffusion taken at the different times t_1 , t_2 , and t_3 [58]

In a semi-infinite solid, in which the surface concentration is held constant, error function is the solution for equation 2.7. The solution was proposed with the assumption: for $t = 0$, $C = C_0$ at $0 \leq x \leq \infty$. For $t > 0$, $C = C_s$ (the constant surface concentration) at $x = 0$, $C = C_0$ at $x = \infty$. Application of the boundary produces the following equation:

$$\frac{C_x - C_0}{C_s - C_0} = 1 - \text{erf} \left(\frac{x}{2\sqrt{Dt}} \right) \quad (2.8)$$

where C_x corresponds to concentration at depth x after time t .

The error function $erf\left(\frac{x}{2\sqrt{Dt}}\right)$ is the Gaussian error function which is defined as:

$$erf(z) = \frac{2}{\sqrt{\pi}} \int_0^z e^{-y^2} dy \quad (2.9)$$

where $x/2\sqrt{Dt}$ is replaced by the variable z .

The diffusion coefficient is expressed as:

$$D = D_0 \exp\left(-\frac{Q_d}{RT}\right) \quad (2.10)$$

where

D_0 = a temperature-independent preexponential (m^2/s)

Q_d = the activation energy for diffusion (J/mol or eV/atom)

R = the gas constant, 8.31 J/mol-K or 8.62×10^{-5} eV/atom-K

T = absolute temperature (K)

2.5 Solid State Joining of Ceramics with Metals

The joining of ceramics to metals currently has become an important manufacturing step. Despite its benefit for utilization at high temperature and corrosive environment, ceramics possess low toughness and brittle. This makes it difficult to machine into complex part. Therefore, the combination of ceramics with metal is required [59]. The joining is also required since it is impractical to fabricate large-complex ceramic material. Furthermore, frequently only a certain part of equipment that requires the specific properties where ceramics can fulfill [60]. Machining ceramics is difficult as it is very hard and brittle. Thus, only diamond grinder normally used to machine the ceramics [61]. This will lead to high manufacturing cost and also limitation of shape. In this situation, the equipment can be made of metals for the main structure, while the ceramics is utilized for the particular component which needs corrosive or high temperature resistant. Therefore, success of ceramics application often requires utilization of the techniques. This was employed to produce an electric light bulb which was invented in the 1800s. The technique was then improved between 1950

and 1970 and currently is widely utilized in electronic industry, medical equipment and weaponry [62]. As established in section 1.1, metal – ceramic joining is also utilized for turbocharger rotor, glow plug head and rocker arm tip.

Many joining techniques were utilized to combine ceramics with metals; *i.e.* ranging from mechanical joining to solid state joining and liquid phase bonding [59]. In their review, Nascimento *et al.* [62] classified the ceramics – metal joining techniques into three categories, namely: mechanical joining, indirect joining and direct joining. Mechanical joining is the simplest and the most efficient. Examples of this process are screwing, fastening, clamping, and shrink fitting. In indirect joining, the joint is achieved by employing intermediate material such as filler metal. Adhesive bonding and brazing are grouped into this classification. In direct joining method, the additive material to achieve the bonding is not needed. Solid-state diffusion bonding is joining technique which is in the group of direct-joining method. However, intermetallic layer is commonly employed in the diffusion bonding process. This was applied for self-joining of ceramics [12] as well as joining ceramics to metals [4, 10]. Direct diffusion bonding without interlayer requires very high process temperature and a proper surface preparation [63]. The material is required to relieve the thermal residual stress at the joint. Ductile interlayer is also needed to create proper contact with the harder and more-brittle joined materials.

Diffusion bonding is a solid-state joining process to join similar or dissimilar materials. The process is carried out by applying the pressure to maintain intimate contact between the joined materials while heating them at temperature minimum of $0.75 T_m$, where T_m is melting temperature of less-refractory material [55]. Throughout the process, atomic diffusion occurred and bonding was produced. This technique can produce very stable joint that can operate at high temperature [64].

Although homogeneous structure of the joint interface is expected, however, it is hard to achieve, especially in joining dissimilar materials. Interface layer is often developed. Brittle layer is the interface product that should be avoided. This layer is difficult to accommodate residual stress that is generated during the cooling process. The residual stress is occurred due to the different coefficients of thermal expansion of the bonded materials. All of these have brought the interface layer to be the most-

critical part on the bonded material. This section reviewed several works on solid-state diffusion bonding of ceramics with metals. Important characteristics and parameters related to the joint achieved in the process will be highlighted and summarized at the end of the overall review.

Alumina was joined using Pt foil as interlayer [60]. The Pt foil was placed in between two alumina discs. The samples were then heated to 1450°C under argon atmosphere with uniaxial pressure of 1 MPa. The thickness of the foil was 25 – 250 µm. Microstructure of inherent voids was observed in the ceramics side. A thin layer of glass covered the ceramics and caused the defect. The interfacial failure was sensitive to the foil thickness. Thinner metal layer produced the joint strength which is comparable to the inherent strength of the ceramics.

Strength of ceramic metal joint can be examined using several techniques. Since machining ceramics is difficult, producing the joint that is suitable for standard mechanical test was not easy. Therefore, frequently the test should be customized based on the shape of the sample. Four-point flexure bending test of the joint was applied when the sample has sufficient length [60, 65]. Mechanical shearing test was often performed for examining the strength of cylindrical shape of joined sample [8, 66-67]. The method is normally employed when for point bending test was impossible due to the minimum length of the sample. Tensile test was carried out to examine the strength of alumina – kovar joint [68]. It was possible since the kovar was in the tube form. Groove was provided at the outer wall surface to allow gripping the sample. Another work attempted tensile test complying with the standard of ASTM E-338 to test the strength of aluminum – silicon carbide joint [69].

Travessa *et al.* [67] joined aluminum oxide with AISI 304 steel using Ti, Cu or Mo as interlayer materials. Diffusion bonding technique was employed. It was performed with 15 MPa uniaxial pressures under vacuum condition in the hot furnace. Joints were achieved with Ti interlayer. It produced average shear strength of 20 MPa. The diffusion bonding was feasible under process temperature of 700 – 900°C. However, the joining was unsuccessful with Cu or Mo. Diffusion bonding with Mo was failed since the metal is highly stable. This failure indicated poor reactivity of the materials at the employed diffusion bonding conditions. Reaction of the ceramics with

Cu also failed to produce joint. Best joint was given in the diffusion bonding setting of 800°C for 60 minutes. The joint was produced by the dissociation of the ceramics and diffusion of O₂ into Ti. Intermetallic compound of Ti₃Al was formed in the interface. Increasing diffusion bonding temperature and lengthening the time built brittle phase that endangered the joint.

Das *et al.* [68] performed the joining of alumina ceramics with Kovar tube using 20 µm-thickness aluminum interlayer. The materials were hot-pressed at around 600°C under vacuum condition. Three types of alumina ceramics were utilized for the experiments, namely: 90, 96, and 99% alumina ceramics. The materials were joined using 75 MPa uniaxial pressure for 10 minutes in temperatures range of 450 – 600°C. Maximum joint strength was obtained at the optimum temperatures of 550, 512, and 575°C for 90, 96, and 99% alumina ceramics respectively. The strength was enhanced when the bonding was carried out up to 90 minutes. Higher diffusion bonding temperatures stimulated the joint. However, they formed excessive thickness of reaction layer in the joint. This decreased the joint strength. Increasing bonding pressure improved the strength of the joint. Nonetheless, a limit of the maximum pressure was noted. This was limited by the deformation of the interlayer. Elemental diffusion took place between Al foil and alumina; whereas, reaction occurred between the Al foil with Kovar. The reaction products were identified as Ni₂Al₁₈O₂₉ and NiAl₃.

Shen *et al.* [70] diffusion bonded Al₂O₃-TiC composite ceramic and W18Cr4V, high speed steel. The diffusion bonding utilized a Ti-Cu-Ti (20 µm Ti + 60 µm Cu + 20 µm Ti) multi interlayers to deal with thermal residual stress. Uniaxial pressure of 10 – 15 MPa was applied while heating the samples at 1100 – 1130°C for 45 – 60 minutes in a vacuum chamber. The interlayer fully melted and reacted with the substrates to form the transition zone in the joint. Cu-Ti solid solution and Fe-Ti compound were predicted in the transition zone. Hardness of the transition zone was in between the hardness of the substrates.

Study on the solid-state reaction of SiC and Fe was attempted by Tang *et al.* [71]. The samples (SiC and iron) having 10mm × 10mm × 2mm dimensions were in contact with a load of 20 kgf in a tube furnace at temperatures of 1073 – 1373K for

0.5 – 40 h. The atmosphere of the furnace was gas mixture of Ar–20 vol.% H₂. Reaction of the materials produced Fe₃Si and Fe (Si) and carbon precipitation. Higher carbon precipitated in the layer produced brittle phase in the joint. Therefore, despite the reaction of the materials, crack at the ceramics side was demonstrated in the experiment.

Solid-state joining of SiC with Ni-based super alloy (HAYNES[®]214[™]) was studied by Hattali *et al.* [66]. The alloy was applied for high temperatures and severe chemical atmosphere. Ag metallic interlayer was employed to reduce residual stress at the joint. The joined materials were prepared in 15mm × 5mm × 5mm. The foil having same size with 200 μm thickness was located in between ceramic blocks. Joining was carried out under vacuum condition. It employed 6 MPa uniaxial pressures at 910°C for 1 hour. Utilization of the Ag foil hindered the formation of brittle reaction product of Si and N. Diffusion bonding of the materials using Ag interlayer achieved the joint strength up to 45±9 MPa. This could fulfill industrial applications at 700°C for more than 10,000 hours.

Aluminum was diffusion bonded with SiC at various temperatures (700, 750, 800, 850 and 900°C) and dwelling time of 10, 20 and 30 minutes [69]. Segregation of SiC occurred and reaction of Si and C with Al took place in the interface. Harder interface layer was observed in the diffusion bonding at higher temperature. Increasing the bonding temperatures improved the bond strength. This was recognized as joining at lower temperature produced poor wetting of the ceramics. At constant temperature the strength increased at holding time of 10 – 20 minutes. It subsequently decreased when the diffusion bonding was lengthened. This was caused by the presence of the reaction product in the interface.

Paulasto *et al.* [72] investigated the interfacial reactions in Ti/ Si₃N₄ and TiN/Si diffusion couples. The experiment was conducted under vacuum. It employed 200 N/cm² contact pressure and heated the materials at 950 and 1100°C. The materials reacted well. Precipitation of Ti₅Si₃, TiSi₂ and TiN_x and α-Ti(Si,N) solid solution was formed in the layer. Sintering additives, Y₂O₃ was also observed. Fracture in the joint occurred at the reaction products layer. This revealed the brittleness of the silicide. The work noted that the maximum solubility of N into TiN_x was influenced by the

nitrogen external pressure. Therefore the gas phase possessed strong effect on the reaction

Si_3N_4 -TiN composite joint with Ni, INVAR (Fe-Ni alloy), and IN600 (Ni-Cr-Fe alloy) interlayers was achieved using as diffusion bonding process [73]. The process was carried out in a hot furnace under argon or nitrogen atmosphere. Joining was performed at temperatures of 1100 – 1350°C with holding time of 1 – 4 hours. The joint of the composite with Ni interlayer was obtained at temperature above 1100°C. Reaction layer was formed in the interface. The layer consisted of the un-dissociated TiN surrounded by light particles. The particles were predicted to be solid solution of Si in Ni or nickel silicide. Diffusion of Si in the interlayer side was also discovered. The depth of the diffusion depended on the diffusion bonding temperatures and time.

Si_3N_4 with Ti foil interlayer was diffusion bonded in a hot press at temperatures ranging from 1250 – 1550°C [1]. A titanium foil with the thickness of 0.89 μm was sandwiched with two ceramics discs. The materials were positioned in a graphite furnace room and pressed with 20 MPa uniaxial pressures. Maximum joint strength of 145 MPa was attained in the diffusion bonding at 1500°C for two hours. Below 1400°C, the joint could not be produced. The joints were formed due to a reactive interface on the Ti side. Diffusion of Si and N into the Ti created Ti-N compound and titanium silicides precipitation on the reaction layer. Thermal micro crack occurred in the layer. The interface was generally brittle. Joint strength initially increased when the thickness of the layer increased. It reached its maximum at a certain layer-thickness and subsequently decreased when the layer grew thicker. Therefore the layer must be controlled to improve the joint strength.

Self diffusion of Si_3N_4 was attempted [74]. The diffusion bonding employed Ti and Cu-foil/Ti as the interlayer. The thickness of the Ti and the Cu-foils were 0.89 and 0.1 mm. These were utilized to reduce the generation of the residual thermal stress. The process was performed on the hydraulic press combined with a graphite resistance furnace at the temperature of 1400 – 1550°C for $\text{Si}_3\text{N}_4/\text{Ti}/\text{Si}_3\text{N}_4$ and 900 – 1100°C for $\text{Si}_3\text{N}_4/\text{Cu}/\text{Ti}/\text{Cu}/\text{Si}_3\text{N}_4/$ with several holding times. The reaction formed Ti_5Si_3 and TiN in the interface. These reaction products were known to be brittle. The work found that temperature is the most significant parameters that affected the joint.

The strength of the joint increased as the reaction-layer thickness increased to a certain value. This subsequently decreased after it reached a maximum strength (*i.e.* 147 MPa). This was achieved at a certain thickness of the reaction layer. The decrease of the strength was due to the excessive reaction-layer thickness. Therefore, the authors recommended controlling the reaction layer to obtain good joint.

Si₃N₄ was diffusion bonded with Ni interlayer [9]. The process was accomplished in a hot press at temperatures of 1050°C and 1150°C for one hour. It was carried out under vacuum condition with uniaxial pressure of 40 MPa. Highest shear strength was achieved in the diffusion bonding at 1050°C; while the strongest joint (*i.e.* 235 MPa) in bending test was obtained at diffusion bonding temperature of 1150°C with 0.26 mm Ni thickness. Diffusion of Si into Ni was at greater distance than the diffusion of Ni into the ceramics. Thin Ni produced weak joint due to its non-uniform distribution of pressure or by the degree of deformation of the interlayer. Nickel silicides and precipitates were found in the interface for diffusion bonding at 1150°C. In the joining process at 1050°C, these species were not identified.

Diffusion bonding of silicon nitride with molybdenum was studied by Martinelli *et al.* [75]. Direct diffusion bonding of 9mm × 9mm × 6mm of silicon nitrided with 9mm × 9mm × 2.5mm of molybdenum sheet was performed in a hot press furnace under vacuum and nitrogen atmosphere. The diffusion bonding was accomplished at temperatures range of 1100°C to 1800°C and the holding time of fifteen minutes to four hours. The uniaxial pressure of 10 MPa was applied at 10°C before it reached the diffusion-bonding temperature. The pressure was released at the end of the dwelling time. Bonding was not achieved at temperature below 1200°C. However, above this temperature, the joints could be achieved for all conditions. Layers of molybdenum silicides (Mo₃Si and Mo₅Si₃) were formed in the interface of the joint. Nitrogen atmosphere postponed the formation of the silicides, yet, it did not change the reaction products. Porous layer and precipitations of sintering additives were found in the joint. The overall thickness of the layers increased along with increase of the temperature. The joint strength increased to a maximum value (57 MPa of optimum condition) at certain diffusion bonding time and temperature. The strength was reduced when the parameters increased further. This was due to the substantial growth of the layer.

Silicon nitride and 253MA wear-resistant steel was diffusion bonded in a hot press at temperatures of 1200°C under vacuum condition [2]. Variable pressures (*i.e.* 1 – 10 MPa) were applied during cooling. Twenty percent improvement of the joint strength (from 75 MPa to 87 MPa) was achieved when the proper change of the pressure was employed. The joint strength was also improved by the smaller surface roughness of the joined materials.

Direct diffusion bonding of silicon nitride with austenitic stainless steel was attempted by Stoop *et al.* [14]. It was performed in a high-frequency induction furnace under vacuum condition. Diffusion bonding experiments were carried out under various bonding pressure (0 – 15 MPa), time (up to 1440 minutes) and temperatures (1000 – 1225°C). In the interface of the joint, the diffusion layer was formed in the steel side, while the porous zone was produced in the ceramics part. At a constant temperature, the joint strength was increased to a maximum at a certain holding time and decreased when the process was lengthened. Similarly, a definite temperature giving a maximum joint strength was also identified at a constant time. Subsequently, increasing the temperature decreased the strength. This was due to the growth of the diffusion and the porous layer. Maximum joint strength of 37 MPa was obtained at 1100°C, for three hours under 7 MPa uniaxial pressures.

Joining of the silicon nitride with austenitic stainless steel was also carried out by using metallic interlayer [12]. Fe, Ni, invar and kovar were employed for the interlayer. Among the materials, invar interlayer gave best joint. Diffusion bonding setting was the same as his previous work reviewed in the former paragraph. At the ceramics-invar interface, reaction layers comprised a porous zone in the ceramics and a diffusion area in the interlayer. In the other interface (*i.e.* invar – stainless steel), diffusion zones were formed in both materials. A certain value of bonding time and temperature (at constant temperature and time, respectively) that gave maximum joint strength was identified. The highest joint strength of higher than 70 MPa was achieved.

Three types of austenitic stainless steels (AISI 304, 316 and 321) were employed as interlayer in diffusion bonding of silicon nitride [10]. Thickness of the interlayer was 50 µm. Diffusion bonding in a hot press machine was executed at 1100°C for 120

minutes. The process took place in vacuum condition and employed 4 – 5 MPa uniaxial pressures. Joint strength produced by the interface layer was relatively the same as the self-joining of the Si_3N_4 (*i.e.* without interlayer) which was attained at much higher temperature. However, the joint of the ceramics using AISI 321 steel was stronger than the joint without interlayer. Metallic silicide in the interface was believed to decrease the strength of the joint.

Jadoon *et al.* [76] joined silicon nitride with high-temperature and corrosion resistant iron–chromium–aluminium alloy (federalloy). Joining was performed in a high-temperature vacuum furnace. The experiments were carried out at temperatures 850 – 1140°C under uniaxial pressure between 0 – 9.5 MPa for holding time between 0 – 60 minutes. Cu foil interlayer or Ti/Cu/Ti multilayer was placed in between the ceramics and the alloy for the joining. Good joint was obtained at 1100°C without remaining Cu or formation of reaction layer in the joint. At slightly higher temperature, precipitations of chromium nitrides and iron silicides were produced. A thin aluminum nitride was also developed at the interface in the ceramics side. The diffusion of elements occurred at higher pressure. The joint produced modest joint strength but well comparable with other metal-ceramic joints possessing high difference of coefficient of thermal expansion. The modest strength of the joint was believed due to the formation of brittle phase in the joint. Joining the materials using Ti/Cu/Ti was attempted to improve the joint. Nevertheless, the joining failed due to the formation of Ti–Cu–Si–N brittle compound.

Austenitic stainless steel was utilized as interlayer in joining sialon ceramics by Abed *et al.* [4]. Cookson Syalon 201 was joined using 316L stainless steel for the interlayer. The samples were pressed in a hot press machine with about 20 MPa compressive pressures at 1250°C. Reaction layer in the joint indicated the penetration of the steel into the sialon. Re-precipitation of the dissociated silicon nitride was also estimated at the steel side in the interface. The critical thickness of the interlayer was 1 mm. Thicker interlayer caused crack at the ceramics despite its good bonding.

Austenitic and ferritic stainless steels were diffusion bonded with sialon [5]. The joining was carried out by hot-pressing at 1250°C with uniaxial pressure of 15 MPa. Nitrogen was added into the steel prior to the joining by nitriding it under nitrogenous

atmosphere at 1200°C for four hours. The nitrogen in the steel was expected to counteract the liberation of the nitrogen from the sialon during the joining. Good joint was achieved for the joining with both steels. However, ceramics cracked in the joining with austenitic stainless steel. Better joint was attained in sialon – ferritic stainless steel joining. This was due to the formation of the ductile layer in the joint. The layer was presumed to absorb the residual stress generated during the process. Hence, good bonding was contributed.

The above works were presented in summary to identify important characteristics in ceramic – metal joining using diffusion bonding process. The summary describes that joining of ceramics to metal is possible. It was demonstrated by alumina, silicon carbide, silicon nitride, and sialon. The process was initiated with the dissociation of ceramics which liberated its elements. Diffusion of the elements occurred between the joined materials. It built a diffusion zone of the ceramics' elements in the metal side. Reaction between the elements also occurred and produced reactive interface in the joint. All of the works disclosed that diffusion and reaction of elements from the joined materials produced the joint.

All above works noticed that the joint strength correlated with thickness and phases of the reaction layer. A certain thickness of the layer was identified giving maximum joint strength. However excessive growth of the layer subsequently decreased the strength. Diffusion bonding temperatures increased the thickness of the reaction layer. Similarly, holding time employed in the diffusion bonding process also stimulated the growth of the layer. This was well known as diffusion was time and temperature dependent. Thus, for a certain level, these parameters improved the joint strength. However, excessive layer-thickness may weaken the joint. Therefore, too high temperature or too long dwelling time reduced the strength of the joint.

Structure of the joint affects the joint strength. Brittle phase such as nitrides or silicide decreases the strength Other than brittle phases, voids or porosities also deteriorate the joint. Thermal microcrack may also be formed. Controlling the phases in the layer was also recommended to improve the joint. Formation of ductile layer contributed the joint [5, 17]. The works also observed that nitrogen in steel prior to joining with sialon improved the joint. The use of Ag interlayer hindered formation of

Si-Ni brittle compound in the joint of SiC with Ni-based super alloy and thus enhanced the joint strength [66].

Problems due to difference coefficient of thermal expansion can be highlighted in several works. This caused crack in the joint of austenitic stainless steel – sialon [4-5, 17]. Thickness and materials of interlayer influence the results of joining ceramic-metal using interlayer. Too thick layer hinders the joint and may also cause excessive thermal residual stress and crack the ceramics [60]. Stable material hampers reaction with the substrates [67]. Thus, it is difficult to achieve the joint. Employing proper interlayer material and thickness effectively relieves the thermal residual stress in the joint [12, 66-68, 70].

Review of some works on the ceramic – metal joining clearly depicts the importance role of the ceramic – metal reaction on the joint. To attain the joint, reaction of the ceramics with the metal must be stimulated. However, excessive growth of the layer tends to weaken the joint. Brittle reaction products also deteriorate the joint. Discontinuity of the microstructure in the joint could also be in a form of voids, porosities or thermal micro crack. These may also endanger the bonding. Therefore, controlling the interfacial layer (*i.e.* phases and thickness) is recommended to improve the joint. Unfortunately, controlling the reaction layers in the joint seems not easy. The aforementioned review showed that an optimum condition was given by combinations of diffusion bonding parameters. It was also suggested that controlling the phases on the layer can be performed by selecting the suitable metallic interlayer. In direct diffusion bonding, nitrogen added into the steel was also claimed to improve the joint. With regard to the critical role for achieving the joint, understanding the reaction layers in the joint is important.

2.6 Reaction of Silicon Nitride and Sialon with Steel

Evaluation on the works in solid state diffusion bonding of ceramic – metal disclosed the importance of reaction layers in the joint. Formation of the reaction layers illustrates reactivity of the joined materials. Reaction of silicon nitride or sialon with

various kinds of steels or iron alloys has been studied in the last decade. Summary of the works is tabulated in Table 2.1.

Table 2.1 Investigations on reaction of Si_3N_4 and sialon with iron and steel

Materials	Setting	Reaction products		Ref.
		Ceramics side	Metal side	
Si_3N_4 -316 SS	T=1000-1150°C 7MPa; 120-200 min	Unknown	α and γ solid solution	[12, 14, 16]
Si_3N_4 -253MA	T=1200°C P=110MPa (variable) 30 minutes	Cr_3Si , Cr_2N $\text{Cr}_3\text{Ni}_5\text{Si}_2$, Fe_3Si , Cr_7C_3	Unknown	[2]
Sialon-AISI 420 Sialon-Fe Sialon-Cast iron	T=1100;1200°C P=2.5MPa vacuum	Al_2O_3 and α matrix	α (Fe,Si)	[15]
Si_3N_4 -Fe-Cr alloy	T=1100-1300°C	Fe_3Si and CrN	Fe_3Si , Cr_2N ; Fe_4N ; Fe solid solution	[13]
Si_3N_4 -St 37 Si_3N_4 -CK 45 Si_3N_4 -X20Cr13 Si_3N_4 -X210Cr13	T = 1050-1250°C P = 5-7.5 MPa; 0.5h-80h	Oxides	α -Fe pearlite α -Fe γ -Fe, $(\text{Cr,Fe})_7\text{C}_3$	[77-78]
Si_3N_4 -Fe	T = 1100°C – 1150°C P = 5 MPa	Enriched sintering additives	α -Fe (Si)	[6]
Si_3N_4 - 100Cr6 (oxidized) Si_3N_4 -Pristine 100Cr6	T = 500 – 1200°C	SiO_2 Enriched sintering additives, α -Fe (Cr,Si) matrix	SiO_2 , $\text{Fe}_{0.97}\text{Cr}_{2.03}\text{O}_4$ α -Fe (Cr,Si)	[7]
Si_3N_4 -AISI52100	T=500-1200°C Elastic & plastic region	Enriched sintering additives, α -Fe	α -Fe (Cr,Si)	[79]
Sialon-316 SS (nitrided) Sialon-9%Cr FSS (nitrided)	T=1200-1300°C P=15MPa; 1hr	Silicides, nitrides	α -Fe (Cr,Si), nitrogen pearlite α -Fe (Cr,Si)	[5, 17]
Sialon-sialon (316 interlayer)	T=1250°C P=20MPa	Unknown	α -Fe (silicon nitride)	[4]
Si_3N_4 (different sintering additives) – St 37	T = 1050-1250°C P = 5-7.5 MPa; 0.5h-80h	New oxides or intermetallic	α -Fe (Cr,Si)	[80]
Si_3N_4 -304,316,321 SS	T=1100°C P=4-5MPa; 120 minutes	Silicides, nitrides	α -Fe (Cr,Si)	[10]
Si_3N_4 -austenitic SS	T=1100°C P=4MPa; 2hrs	$\text{Cr}_3\text{Ni}_5\text{Si}_2$, $\text{Y}_2\text{Si}_2\text{O}_7$, silicides, nitrides	α -Fe (Cr,Si)	[81]
Sialon-316 SS; composite interlayer	T=1200-1300°C P=15MPa; 1hr	Unknown	α -Fe; nitrogen-pearlite	[82]

Some of the works listed in the table focused on investigating the reaction between the materials [6-7, 15, 77-78]. Thus, those were not intended to obtain the joint. However, the studies found good bonding in silicon nitride – iron interface, as well as in the interaction of the ceramics with steel. Despite crack at the ceramics, it indicates that joining the materials was actually possible. Several works focused on achieving the joint [2, 5, 10, 12, 81]. As part of the concerns, the studies also provide information on reactivity of the materials.

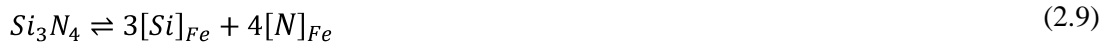
Table 2.1 illustrates that generally reaction products are formed in the interface of the materials. The reaction zone is created in both ceramics and metal parts. Several reaction products were identified in the interaction of silicon nitride or sialon with the metal. Silicides and nitrides were found by several workers [2, 5, 10, 17, 81]. However, the other researchers claimed that no new phase or compound was produced by the interaction of the materials [6-7, 15, 77-78].

A silicon-enriched sintering additives precipitation occurred in the interaction of silicon nitride with pure iron [6]. Vleugels *et al.* [15] suggested that elements released from ceramics recombined and formed the oxides. There are few works which even failed to identify the phases in the reaction layer [5, 12, 14, 16-17]. Instead of silicides or nitrides, several works claimed that decomposition of ceramics produced insoluble oxides in the reaction zone [77-78]. More complex compound of elements from the materials was also discovered [81].

2.6.1 Decomposition of Silicon Nitride

Reaction of ceramic – metal at high temperature is initiated with the dissociation of the ceramics. Silicon nitride decomposes when in contact with steel at high temperature. It releases its elements. The liberated elements are consumed for the reaction with steel [13, 77].

Decomposition and dissolution of silicon nitride in steel occur according to the following reactions [15]:



in which $[Si]_{Fe}$ and $[N]_{Fe}$ are the dissolved silicon and nitrogen in the steel. Reaction 2.8 started at temperature above 636°C; whereas, reaction 2.9 began at 1033°C.

The decomposition of silicon nitride creates a reaction layer in the ceramics side. The aforementioned discussions have established that the ceramics decomposition may produce insoluble oxides or precipitations of sintering additives. However, reaction of elements from the materials may also be formed in this area. When the work attempts to achieve a silicon nitride – steel joint, thickness of the layer strongly influences the joint strength [14]. Too thin reaction layer cannot produce the joint. Conversely, excessive growth of the layer also deteriorates the bonding [16]. For this reason, avoiding fast decomposition of the ceramics was suggested. Nevertheless, the worker did not provide a manner to do that. Adding nitrogen [17] into the steel prior to joining with sialon was proposed to hinder the sialon decomposition. It was claimed that it worked successfully; however, no clear evidence was given.

2.6.2 Interdiffusion and Reaction of Elements

Silicon and nitrogen released from the decomposition of silicon nitride or sialon diffused into the metal. Reaction 2.8 shows that the decomposition of silicon nitride occurs through gas phase. Heikinheimo *et al.* [6] suggested that the nitrogen gas would be removed from the ceramic-metal interface through open crack in the interface or along the interface. It may diffuse into the metal or be trapped and create pores in the interface. The nitrogen gas can also be freed into the atmosphere through the edge of the ceramic-metal contact zone [7, 15]. All works listed in Table 2.1 revealed porous zone in reaction front of silicon nitride or sialon with iron or steels. This was believed due to the trapped nitrogen in the interface.

Investigations on reactivity of silicon nitride with steel reviewed in this work were not able to detect nitrogen in joint interface. However, they all believed that the element dissolved in the metal side during the interaction. Peteves *et al.* [13] found the precipitations of CrN in the steel side close to the silicon-diffusion zone.

Martensite formation driven by nitrogen diffusion was recognized in the parent steel of 9.5%-Cr when it was joined with sialon [5, 17]; whereas nitrogen pearlite was identified in the steel-composite site [82]. Those proved that nitrogen also diffused into the steel. It may dissolve in the steel and stimulated martensite formation, or precipitated in the form of CrN or Cr₂N.

Kalin *et al.* [7] and Vleugels *et al.* [15] claimed that solution rate of nitrogen controlled the reactivity of silicon nitride and sialon with iron-based alloys. Thus, increasing solubility of nitrogen enhanced the reactivity. The solubility of nitrogen is influenced by the alloying elements. This was illustrated in Figure 2.4. The figure clearly shows that the increasing Cr, Mn and Mo increased the solubility of nitrogen, and thus improved the reactivity with ceramics.

Better reactivity of the materials could be reflected from the thicker reaction layer in the interface. Therefore, thickness of reaction front in sialon side was used for a measure of reactivity of the materials concerned. Kalin *et al.* [79] added the diffusion zone as a sign of the reactivity. Hence, other than reaction front in ceramics, they also proposed silicon-diffusion extent in steel to be used for estimating the reactivity.

Fe diffuses into the decomposed part of the silicon nitride or sialon in its interface. Si dissolves in the iron in this part to form an iron solid solution matrix. Table 2.1 reveals that in all works, iron solid solution was produced at the reaction area in the ceramics.

Diffusion of silicon is extended into the metal side and creates a silicon-diffusion zone. In an alloy containing high C, the reaction produces γ solid solution. However, with higher Cr content in the alloy, ferrite iron with dissolved Fe (α -Fe (Cr, Si)) is produced and stabilized since Cr and Si are both ferrite formers [77-78].

In addition to solid solution in layer matrix, the other reaction products are also found in the reaction front. Taking into account the diffusion of Fe and Cr from metal alloy into silicon nitride, one may expect the formation of silicides and nitrides in the joint. This was observed in interface of silicon nitride – Fe-Cr alloy system [2, 10, 13, 81]. An earlier work in joining silicon nitride with austenitic stainless steel found no new compound was made in the joined-materials interface [14]. XRD examination on the surface of reaction front in ceramics side could not detect any compound. However, another work on joining similar materials identified several silicides and nitrides using glancing incidence angle (GIA) XRD [10]. The later work predicted that the difference might be due to different materials used in the experiment. It also proved that characterization technique is essential to scrutinize the phases in the reaction front.

The findings discussed in previous paragraph reveals that dissociation of Si from silicon nitride in silicon nitride – steel interaction leads to opportunity of silicides formation. Similarly, nitrogen may form nitrides when it meets metallic-nitride formers. The possibility of the iron silicide formation can be learnt from the Fe – Si system (Figure 2.11) which shows the presence of Fe_2Si , Fe_5Si_3 , Fe_2Si and $\beta\text{-FeSi}_2$ (high temperature) and $\alpha\text{-FeSi}_2$ (low temperature). Maximum solubility of Si in γ is 1.9 weight percent. This is in temperature of around 1100°C . Slightly below 1300°C , 10.9 weight percent of Si would dissolve in iron.

Although silicides and nitrides were confirmed by several researchers in the interaction of silicon nitride – steel; however, Heikinheimo *et al.* [6] claimed that no silicides or nitrides were formed in silicon nitride – Fe interaction. Several other works found the same conditions [7, 77-79]. Instead of silicides or nitrides, the works claimed that the decomposition of silicon nitride produce insoluble oxides, precipitation of sintering additives or silicon-enriched sintering additives in interface of silicon nitride – steel.

In sialon – steel interface, Vleugels *et al.* [15] found that Al_2O_3 was produced from recombination of dissociated sialon elements. EDX analysis performed on precipitations in the interface found that the species were rich of Al and O. The alumina was confirmed using Raman spectroscopy. Characterizations on the interface

of sialon – 9.5% Cr failed to clarify any formation of compound [5, 17]. Nevertheless, chemical composition of the area indicated that silicides and nitrides might be present. Two other studies in joining sialon with austenitic stainless steel and steel composite also failed to ascertain the phases [4, 82].

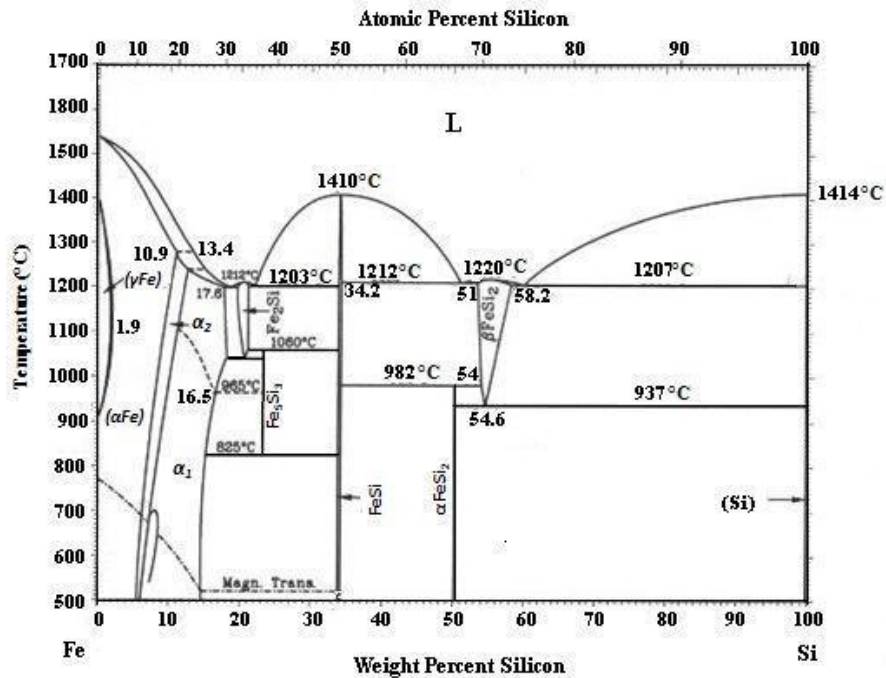


Figure 2.11 Phase diagram of Fe – Si [30]

Review of investigations on reaction of silicon nitride – steel in this section reveals that reaction of ceramic – metal occurs in the interface. The interaction produces reaction front in ceramics side and silicon-diffusion in steel side. While the works agree on the silicon-diffusion in steel, different reaction products are claimed in interface of the materials concerned.

Fewer studies were carried out on accessing sialon – steel interaction. Crack in sialon side was found in joining the ceramics with austenitic stainless steel [4]. However, the ceramics was successfully joined with 9%-Cr ferritic stainless steel [5]. Ductile layer formed in the interface was believed to relieve residual thermal stress and contributed the joint. Yet, despite its success in achieving the joint, phases in interface of the materials remain unclear since its characterization failed to identify them. Another study on reactivity of sialon with steel implied that the materials can be

joined [15] It was established that fast decomposition rate of ceramics in joining with metal should be avoided (section 2.5.1). Brittle phase, such as silicides and nitrides in the interface should also be prevented. To suppress decomposition of sialon, nitrogen addition through solution nitriding on the steel prior to joining was proposed [5, 17]. This was claimed successfully hindered the decomposition of sialon and thus qualitatively enhanced the joint. Nonetheless, the work did not provide any evidence on the reduction of the decomposition. Hence, phenomenon of the nitriding on the steel to improve the joint remains unclear.

CHAPTER 3

METHODOLOGY

3.0 Overview

To attain the objectives of the research, several experiments, characterizations and analytical works were carried out. This chapter describes the methods of investigation taken to accomplish the mission. The chapter is divided into two sections. In the first section, methodology of the research will be presented. It discusses general steps that were accomplished to study the joining of sialon and steel. Subsequently, detail of the experimental procedure is presented in the later part. The section discusses the materials used in the experiments as well as the techniques and equipments utilized in the experiment. Procedures and settings as well as the considerations in executing the experiments are presented.

3.1 Methodology

Reaction layer in the interface of sialon – ferritic steel was obtained by attempting the joining of the materials. The joining was performed by diffusion bonding process as the process produces the joint by stimulating reaction between the joined materials. Therefore, it would produce reaction layers that were going to be explored in this study.

Diffusion bonding of sialon was attempted with AISI 430 FSS and 7.5%-Cr FS in as-received and nitrided conditions. Joining of the sialon with nitrided steels was performed to study the influence of nitrided steel on the reaction layers of its joint with sialon. Solution nitriding was applied on the steel before the joining. The solution-nitriding treatment was intended to diffuse nitrogen into the steel. Thus, the steel would be diffusion bonded with sialon in nitrogen-pre-dissolved condition.

Reaction layers in the joint were studied in term of their thickness, phases, as well as the mechanical properties. Characterizations were carried out on the cross section of the joint. Metallographic study was performed using OM and FESEM. Elemental analysis was conducted using EDX across the joint. The analysis aimed to study elements interdiffusion across the joint. Analysis of the elements was also accomplished on a particular phase as indicated by the optical or scanning electron micrographs. This was conducted to identify phases in the reaction layers of the joint.

Further characterizations were undertaken using XRD and XPS to identify phases in the reaction layers. At the end, the results of the investigation on the reaction layers of the joint were analyzed. Characteristics of the reaction layers in sialon – as-received steel and sialon – nitrided steel joints would be compared. Comparison was also accomplished for the sialon – AISI 430 FSS and the sialon – 7.5%-Cr FS joints.

3.2 Experimental Procedure

This section presents the procedures of experiment that were conducted to attain the objective of the research. This covers the nitriding and the diffusion bonding experiments. Materials, equipments and the experimental setting employed in the study are reported.

3.2.1 Materials

The Sialon that would be joined with steels was β -sialon provided by Syalon Int. Ltd., UK with the trade name of Syalon 101[®]. The material was supplied in the form of discs of 20 mm diameter and 4 mm thickness. Chemical compositions of the as-received sample were analyzed using inductively-coupled-plasma optical emission spectroscopy (ICP-OES) of Sirim Bhd., Shah Alam, Malaysia. Table 3.1 presents the chemical compositions of the sialon.

Table 3.1 Chemical compositions of sialon (weight percent)

Al	O	N	Si
3.57	2.87	1.58	Balance

The AISI 430 FSS was in the form of 1.2mm-thickness sheet of Thainox Stainless Steel Co. Ltd., Thailand. The chemical composition of the steel is given in Table 3.2.

Table 3.2 Chemical composition of as-received AISI 430 FSS (weight percent)

C	Cr	Mn	Mo	Ni	S	Si	P	Ti	Fe
0.062	15.72	0.31	0.13	0.12	0.003	0.23	0.03	0.002	Balance

The second steel used in the experiment was 7.5 %-Cr FS. The material was supplied in the form of 16mm-diameter round bar. Chemical compositions of the steel are presented in Table 3.3.

Table 3.3 Chemical composition of as-received 7.5%-Cr FS (weight percent)

C	Cr	Mo	Ni	S	Si	Mn	V	Fe
0.06	7.51	0.69	0.87	0.002	0.32	0.64	0.29	Balance

3.2.2 Experimental Procedure for Solution Nitriding

Solution nitriding was employed to prepare the nitrided steel for joining with sialon. Nitrogen diffusion into the steel was expected from the nitriding treatment. The nitriding treatment was applied for the AISI 430 FSS and the 7.5%-Cr FS.

The solution nitriding was carried out in a Carbolite STF horizontal tube furnace. N₂ gas was used as it was commonly utilized in the treatment [41-42, 46-51, 83]. A gas flow meter was attached to the tube furnace to adjust the flow rate. It was also to maintain constant flow rate during the treatment. The gas outlet tube was connected to a Drechsel bottle. Five millimeters of the outlet tube length was inserted into the water to slightly increase the gas pressure flown in the furnace. Details of the equipments for the experiment were illustrated in Figure 3.1.

Samples of AISI 430 FSS were prepared in 20mm × 30mm dimension for the treatment, while the 7.5%-Cr FS was cut into 1.5mm thickness. The samples were washed with acetone before each experiment was carried out. For the nitriding of AISI 430 FSS; two samples were placed in alumina boat and inserted into the heating zone. After the nitriding, a small piece of the nitrided steel was cut for

characterization works, while the rest of the samples were then used for diffusion bonding with sialon.

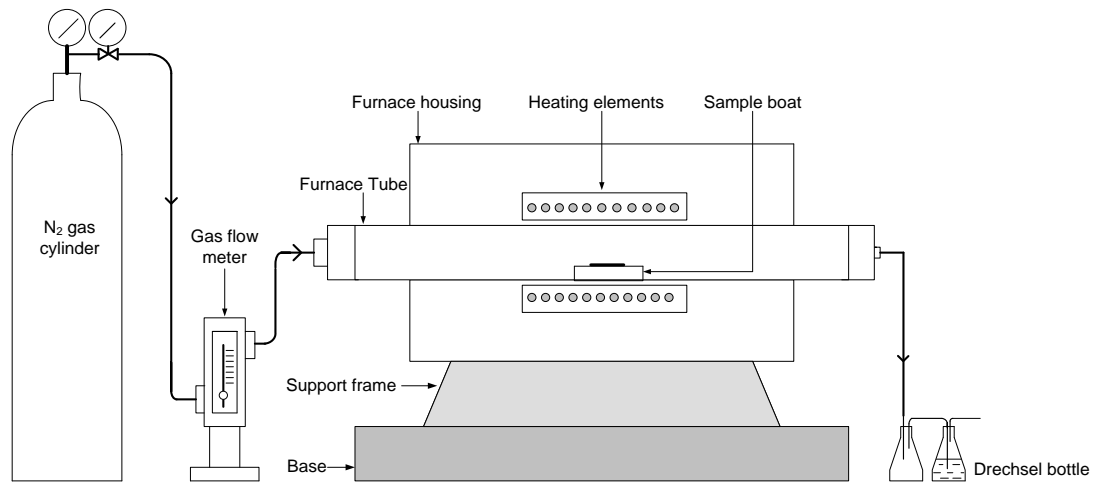


Figure 3.1 Setting of solution nitriding experiment

For the 7.5%-Cr steel, three samples were inserted into alumina boat for the nitriding treatment. One sample was used for the characterization and hardness test. Two other samples were prepared for the diffusion bonding. Putting three samples in one nitriding treatment was possible since the size of the 7.5%-Cr steel sample was smaller than the sample of AISI 430 FSS (*i.e.* 16mm-diameter disc with approximately 1.5mm thickness) and could be loaded into the alumina boat. Before heating, the air in the furnace was purged with nitrogen for 15 minutes at a flow rate of 1000cm³/min to prevent oxidation of the sample. Heating at 5°C/minute was started immediately after the purging completed. Nitrogen was flown into the furnace with the flow rate of 1000cm³/min when the temperature reached 1200°C. At the end of the process, the nitrogen flow was stopped and the samples were removed from the furnace and quenched into water.

Nitriding was conducted for one, four and seven hours. It was observed that solution nitriding AISI 430 FSS as short as ten minutes could diffuse nitrogen into 0.13 mm below the surface and created martensite formation [50]. It was also noted that nitriding for ten hours diffused nitrogen throughout the cross section of 1.2mm-thickness steel. Therefore nitriding for one hour could be expected to diffuse nitrogen into the steel. Nitriding for one hour should have been able to diffuse nitrogen into the

steel significantly. Three-hour interval was determined to produce different level of nitrogen diffusion into the steel.

For comparison purpose, the steel was also solution annealed. This aimed to normalize microstructure of the steel after the manufacturing processes. The solution annealed was accomplished by heating the steel at 1200°C under air atmosphere for one hour and quenched into water. Hardness of the solution-annealed sample would be used for the reference of the hardness improvement on the steel after nitriding treatment.

3.2.3 Experimental Procedure for Diffusion Bonding

Solid-state joining of the sialon and the steels was performed by using diffusion bonding technique. The process was carried out using Korea Vac hot press machine of Advance Materials Research Centre (AMREC), Sirim Bhd., Kulim, Kedah, Malaysia.

The steels to be joined were in three conditions, namely: as received and nitrided for one and four hours. Before joining, the AISI 430 FSS samples were cut into same dimension of the sialon discs. However, the sample of 7.5%-Cr FS was provided with 16mm-diameter rod which was smaller than the sialon diameter (*i.e.* 19 mm). This was cut into 1.5 mm thickness. The steel samples were ground and polished with 1µm diamond paste. Subsequently the sialon and the steels were washed with acetone in an ultrasonic cleaner and dried with a hot-air dryer.

Joining was performed in sandwich form where a steel sample was placed in between two sialon discs. To avoid reaction between the steels and graphite dies set, the joined materials were embedded in boron-nitride powder. Thus, there was no contact between the samples with the graphite dies in the hot press machine. Diffusion-bonding setting in the hot-press machine was illustrated in Figure 3.2.

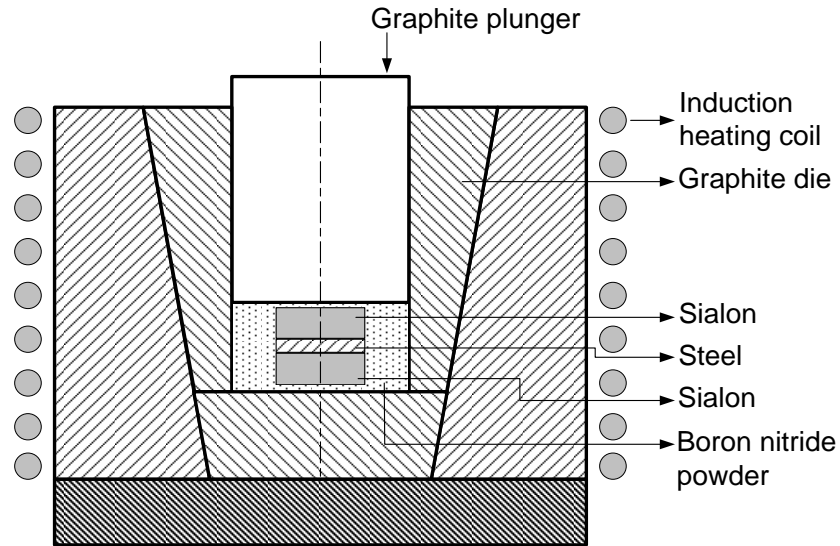


Figure 3.2 Setting of diffusion bonding experiment

Diffusion bonding parameters (*i.e.* temperature, time and diffusion bonding pressure) were determined before the diffusion bonding of the materials was undertaken. The diffusion bonding is generally carried out at high temperature to allow interdiffusion of elements and reaction of the materials. The process is performed at the temperature of at least $0.75T_M$, where T_M is a melting temperature in degrees Kelvin [55]. Phase diagram of Fe – Cr alloy given in Figure 2.2 (section 2.2) illustrates that melting temperature of the alloy with 7 – 15% Cr is around 1520°C . Therefore minimum diffusion bonding temperature for the AISI 430 FSS (15.7% Cr) and 7.5%-Cr FS is about 1072°C . Solid-state reaction for joining of sialon – 9%-Cr FS was attempted at $1200 - 1300^\circ\text{C}$ for one hour under about 15MPa [5]. It was in accordance with the suggestion that reaction of sialon and iron alloy occurred at 1100°C and 1200°C [15]. The diffusion bonding at 1200°C for one hour successfully produced the joint. Reaction of sialon with stainless steel interlayer was growth at 1200°C for one hour diffusion bonding under intimate contact pressure of 20 MPa. Based on the calculated minimum diffusion bonding temperature (*i.e.* 1072°C), and the experience provided by the previous works, diffusion bonding experiment in the present work was undertaken at 1200°C for one hour with uniaxial pressure of 20 MPa.

Diffusion bonding was performed by putting the samples into the furnace and pressing them with the graphite plunger. Those were then heated to 1200°C . Heating

and cooling rate of the furnace were set at 5°C/minute to avoid high thermal shock. The samples were held at 1200°C for one hour. Vacuum condition of about 2×10^{-5} Torr was simultaneously applied during the diffusion bonding. The diffusion bonding pressure was released when cooling started. The hot-press furnace was switched off and cooled to room temperature when it reached 500°C. Two diffusion bonded samples were prepared for each joining condition.

3.2.4 Characterization and Hardness Test

Characterization and hardness test were carried for the nitrated and the diffusion bonded samples. Metallographic study and hardness test for the nitrated samples were conducted to scrutinize the outcome of the treatment; *i.e.* phase changes and hardness improvement. For the joining samples, characterizations of the joint were accomplished to investigate the elements diffusion and the reaction layers. This was also to identify the phases in the reaction layers of the joint. Several techniques were utilized to accomplish the characterization. Whenever possible, the characterizations were executed on the joint cross section. However, assessing the thin interface layer in the joint might be difficult. In this case, the examinations were also conducted on the surface of the interface layer.

3.2.4.1 Microstructural Characterization

Microstructure of the nitrated steels was observed using optical microscope. Phase changes at the steel after the nitriding was studied through its optical micrograph. For the diffusion bonding sample, microstructural characterization was performed across the joint using OM and FESEM. Morphology of the joint cross section was initially investigated through its microstructure. More-detail assessment was executed on a particular area using the FESEM.

To enable the examination, the samples were cross sectioned. Abrasive disc cutter was used to cross-section the nitrated samples. Subsequently, the samples were ground with emery paper and polished with 1- μ m diamond paste.

The diffusion bonded was cross-sectioned using precision diamond cutter. The samples were ground using diamond grinding disc. Diamond grinding disc was employed to grind the sialon which is very hard. Subsequently, cross section of the samples was ground using 600-grade emery paper. The samples were then polished with 6- μm , 3- μm and 1- μm -polycrystalline diamond paste. To enable the microstructural observation in OM and FESEM, the nitrided and the diffusion bonded samples were etched using Glyceregia reagent, *i.e.* a mixture of three parts of glycerol, two parts of hydrochloric acid and one part of nitric acid [84]. Observation of the microstructure was conducted on Olympus optical microscope. The scanning electron micrograph was captured by using Zeiss Supra 55 VP FESEM.

The OM was employed to observe the overall joint as well as the phase distribution at the joined material. In some cases, optical micrograph could present better information on the phase distribution than the scanning electron micrograph. Exploring larger area of the microstructure can be performed by using smaller magnification. This is undertaken to identify the phases existed in the observed area. In this case, OM could present the image of phases with better contrast difference. Therefore, early phase identification can be performed. Further detail-observation on a particular region could be then accomplished using SEM or FESEM.

3.2.4.2 Elemental Analysis

Elemental analysis was carried out on the cross section of the diffusion bonded sample. The analysis employed EDX attached to the FESEM. It was required to study the decomposition of the sialon and also the interdiffusion of the elements from the sialon to the steel and *vice versa*. For these purposes, spot EDX analysis was carried out across the joint.

The elemental examination was started at the original sialon; *i.e.* around 30 μm from the border of the reaction layer at the sialon side. The analysis was continued approximately every 10 μm across the joint towards the parent steel. The analysis was stopped at the parent steel (around 20 μm away from the reaction layer at the steel) as diffusion was expected to diminish in this region. The results of the elemental analysis

across the joint were subsequently used to generate a concentration profile of elements across the joint.

Besides studying the sialon decomposition and elements interdiffusion, EDX analysis was also utilized to investigate phases in the reaction layer. For this aim, analysis was focused on particular area that was indicated as a different phase by the scanning electron micrograph. Assessment of the elements in the interface layer was performed on the precipitates and the interface-layer matrix. Ten spots were determined randomly to perform EDX analyses on the precipitates and the interface layer matrix. The spots were determined in such a way that covers the precipitates and the matrix throughout the observed area. The spots selection was attempted in direction of along and across the interface layer simultaneously. For the analyses of each joint, figure of the EDX-spot map was provided.

3.2.4.3 XRD Examination

Phase identifications of the joint were conducted using Bruker D8 XRD equipment. It was suggested that performing XRD right on the cross section of the joint was difficult due to the several thin layers that were available at the joint [5, 17]. Other efforts were successful in identifying the phases at the joint by applying the XRD examination at the fractured surface of the joined samples [8, 10-11]. Hence, in this research, XRD examinations were attempted on the fractured surface of the joined samples. To perform the examinations, the joined samples were broken down. The sialon was removed from the steel to expose the steel's surface. Subsequently, XRD examination was performed on the surface.

3.2.4.4 XPS Examination

To ascertain the phases identified by the XRD, surface of the reaction layer was analyzed using XPS. Thermo Scientific XPS equipment was employed to perform the investigation. XPS is a very sensitive characterization technique for thin surface [85]. Therefore, it could be suitable for examining the chemical state of the elements in the surface of the reaction layer.

To identify elements at the surface, a survey scan of XPS examination was performed on the surface of the fractured surface. Subsequently narrow scan was carried out for the elements that formed the compound identified by the XRD examination. This aimed to study their chemical states and estimate the compound.

3.2.4.5 Hardness Test

Hardness test was conducted for the nitrided samples to study the hardness improvement on the steel surface after nitriding. It was also performed on the solution-annealed sample.

Enhancement of the hardness caused by the nitriding treatment indicated the diffusion of nitrogen into the steel. Micro Vickers Hardness with 300 g load scale (HV 300) was attempted on the cross section of the sample. LECO LM247 AT micro hardness tester was employed to conduct the test. The hardness assessment was carried out from the surface of the steel and moved towards the core of the sample. Indentation was applied on the steel every 10 μm .

Hardness test was also undertaken for the diffusion bonded samples. The test was purposed to study the mechanical properties of the reaction layers in the joint. It was conducted across the joint and started from the original sialon side. The indentation was initiated around 50 μm from the border of the joint interface at the sialon side. Subsequently, the indentation was performed approximately every 10 μm across the joint. The hardness test was ended at the parent steel; *i.e.* around 30 μm from the reaction layer at the steel. Since the parent steel of AISI 430 FSS after the joining consisted two phases, namely: martensite and pearlite, the hardness test was carried out separately across each phase in the region.

The examination was performed using the same equipment that was previously used for the hardness test of the nitrided sample. However, the interface layer at the joint might be too thin, therefore Micro Vickers hardness test will leave an indentation that is larger than the thickness of the layer. For this reason, Knoop hardness test with

low load scale of 10g force was employed for the test. This technique allows small indentation at the surface. Thus, it enables to obtain the hardness value of the thin interface layer.

CHAPTER 4

RESULTS AND DISCUSSION

4.0 Overview

In this work, joining of sialon with AISI 430 FSS and 7.5%-Cr FS was investigated. It was reported that nitriding on the steel could produce more sound joint of ferritic stainless steel and sialon [5]. Thus, joining of sialon was also performed with the steels in nitrided condition. The influence of the steel pre-treatment on the joint was studied. This chapter reports and discusses the overall results of the experiment and the analyses. At the beginning, solution-nitriding experiments on the steel will be presented. The subsequent sections discuss separately the joining of the sialon with the AISI 430 FSS and the 7.5%-Cr FS. Each section will discuss the joining of the sialon with the steels in as-received, nitrided-for-one-hour, and nitrided-for-four-hours conditions. At the end of the results and the analyses presentation, one section is provided for the discussion and the wrap-up of the overall outcome of the joining.

4.1 Solution Nitriding of Stainless Steel Samples

Ceramics decomposed in the joining process with metal. It released their elements and produced the reaction layers in the joint. It was suggested that fast decomposition of the ceramics and formation of brittle phase in the joint should be avoided [14, 16]. In this case, nitrogen in the steel was believed to suppress the decomposition of the sialon [5, 17]. The later work added nitrogen into the steel by high-temperature gas nitriding (solution nitriding) technique before the joining. In the present study, the nitriding technique was applied on the AISI 430 FSS and the 7.5%-Cr FS before they were joined with sialon. The results would be compared with the joining of the sialon and the as-received steels. For this purpose, experiments on the solution nitriding of

the AISI 430 FSS and 7.5%-Cr FS were carried out. The objective was to ascertain the sufficient nitriding time for the steel before the joining.

Gas-nitriding technique has been discussed in section 2.3. Solution nitriding is a gas-nitriding technique that is performed at high temperature (*i.e.* 1000 – 1200°C). In this method, nitrogen is added and diffused interstitially into the steel. The nitrogen forms a solid solution in the steel. The technique is carried out by heating the sample at high temperature under nitrogenous atmosphere. Detail of the treatment setting in this work has been explained in Chapter 3. The diffusion of nitrogen leads to strengthening of the steel. It was established in section 2.3 that compared to low-temperature gas nitriding, the solution nitriding could diffuse nitrogen deeper into the steel [39, 43, 48, 51].

4.1.1 Solution Nitriding of AISI 430 FSS

Microstructure of the as-received AISI 430 FSS is shown in Figure 4.1. The microstructure is presented in this section for comparison purpose with microstructure of the nitrided steel. The original microstructure of AISI 430 FSS is typically ferritic stainless steel microstructure (Figure 4.1). The grain is elongated along the rolling direction.

Phase changes on the steel after the nitriding can be observed from the microstructures of the nitrided samples presented in Figure 4.2 to Figure 4.4. Martensite layer of approximately 0.3-mm thickness was observed from the surface of the sample nitrided for one hour (Figure 4.2). In the sample core, the phase was ferrite with coarse grain. When the nitriding time was extended, the martensite became denser and more phase transformation occurred in the deeper zone (Figure 4.3 and Figure 4.4). Martensite transformation occurred throughout the steel when the nitriding was carried out for four hours (Figure 4.3).

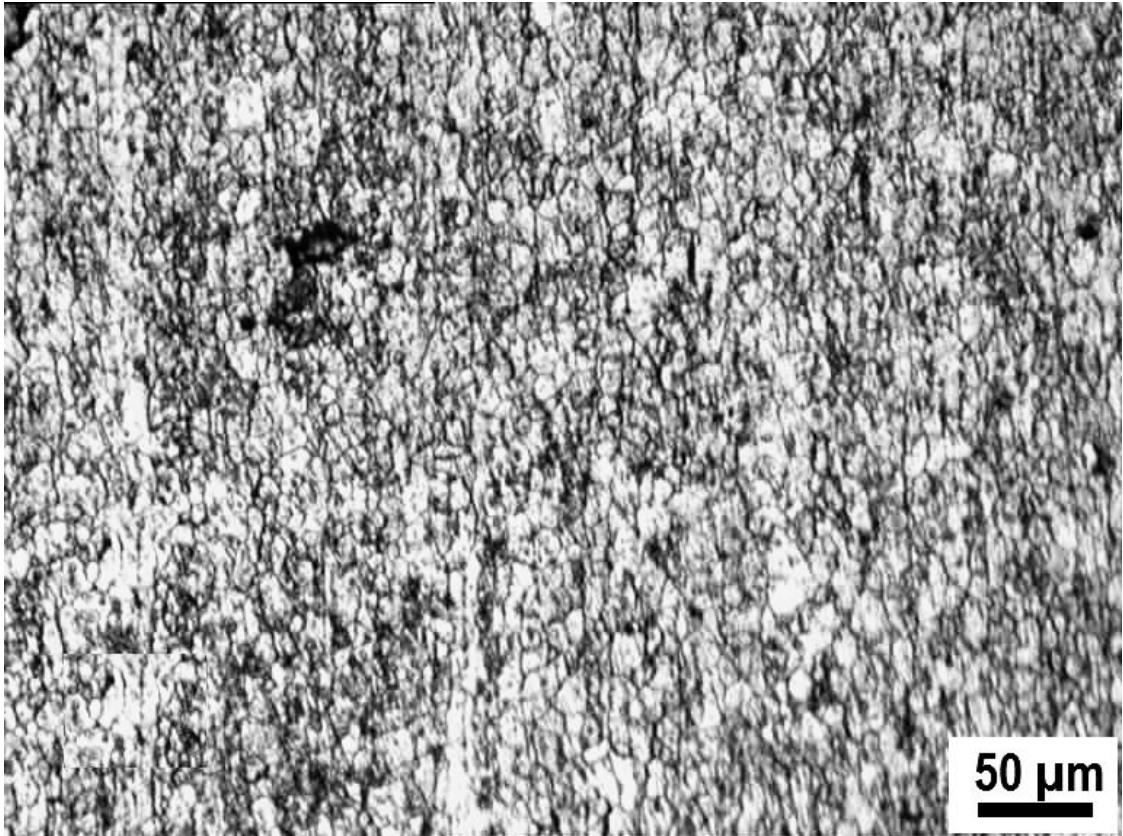


Figure 4.1 Microstructure of as-received AISI 430 FSS

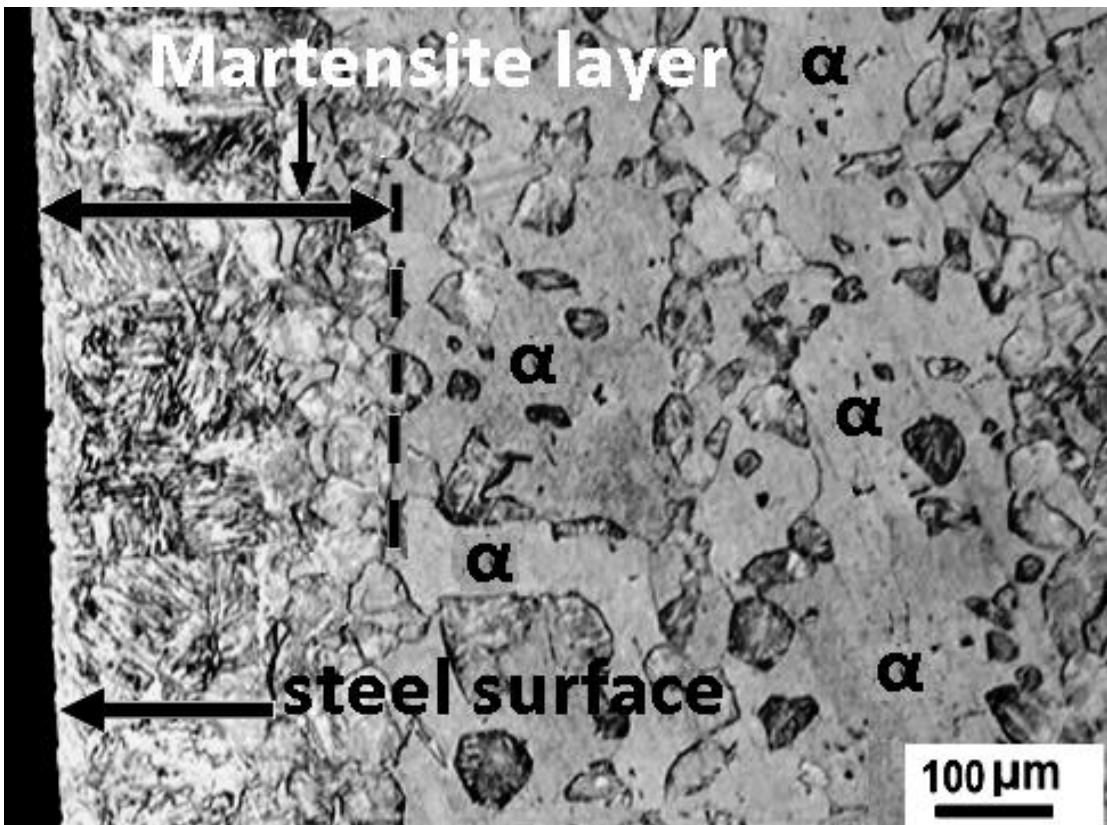


Figure 4.2 Microstructure of AISI 430 FSS nitrided for one hour

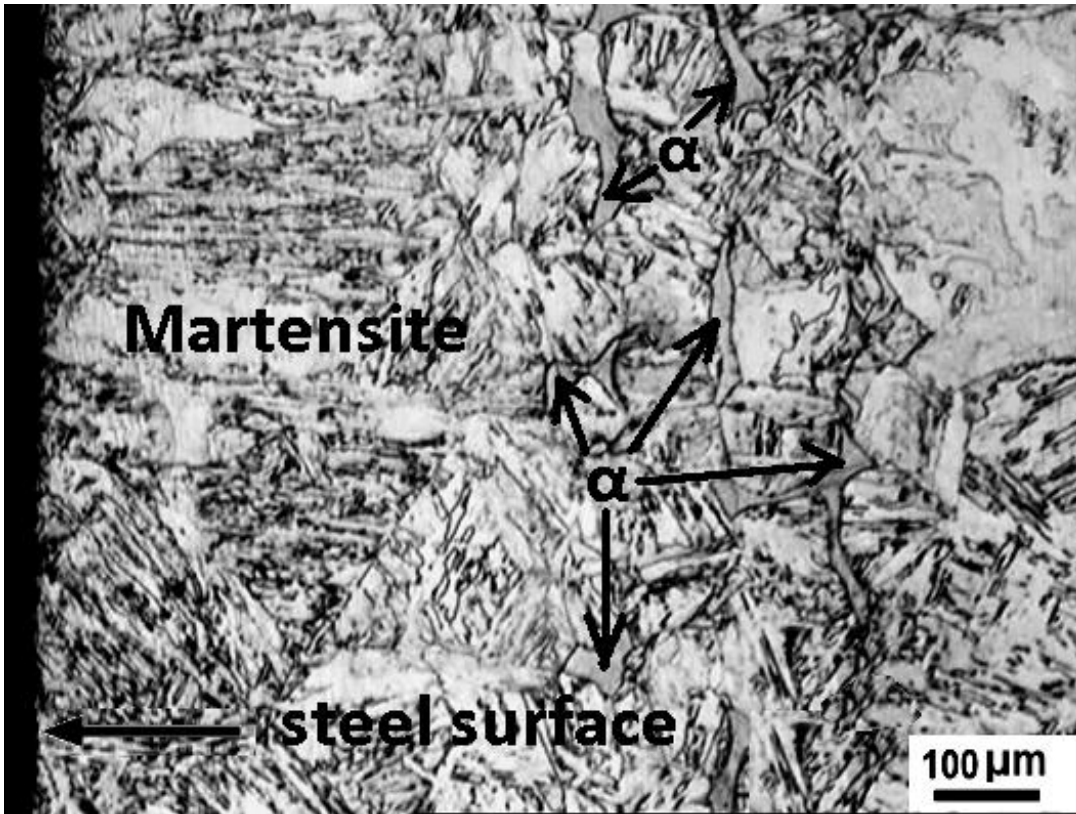


Figure 4.3 Microstructure of AISI 430 FSS nitrided for four hours

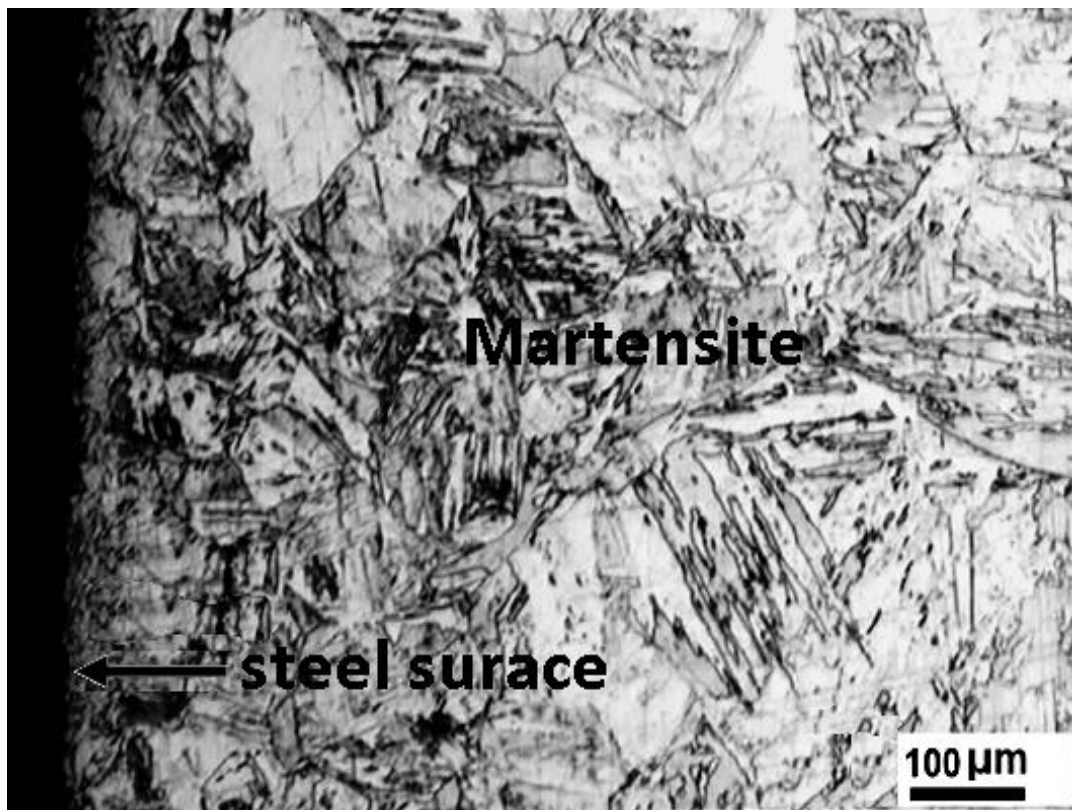


Figure 4.4 Microstructure of AISI 430 FSS nitrided for seven hours

Figure 4.2 to Figure 4.4 show that the thickness of the martensite layer was affected by the nitriding time, *i.e.* longer nitriding results in thicker martensite layer in the surface. In this case, four hours nitriding was sufficient to form martensite throughout the cross section of the steel (Figure 4.3). Nevertheless, small ferrite islands can still be observed in the interior part of the sample. The ferrite phase disappeared from the steel when it was nitrided for seven hours (Figure 4.4). The whole steel changed to martensite after nitriding for seven hours.

XRD pattern from the sample nitrided for four hours shows α peaks (Figure 4.5). This was considered as mixed phases of ferrite and martensite [49]. No retained austenite or nitrides were found. Retained austenite was found in AISI 430 FSS when it was nitrided at 1100°C [50]. At lower temperature, precipitation of Cr_2N was also detected. However, in the present work, microstructure of the nitrided samples (Figure 4.2 to Figure 4.4) did not indicate the existence of austenite or Cr_2N precipitations. It is also revealed by the XRD pattern of the sample (Figure 4.5) which shows only the existence of α phase.

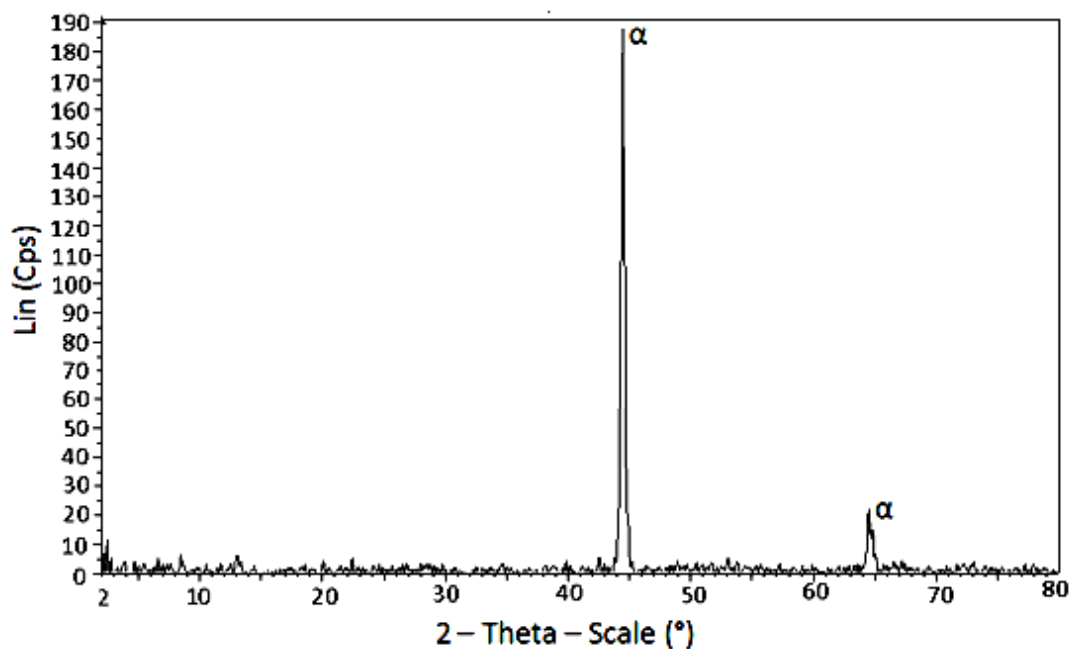


Figure 4.5 X-ray diffractogramme of AISI 430 FSS nitrided for four hours

In solution-nitriding treatment, Tschiptschin *et al.* [40] suggested that nitrogen could dissolve into the steel through reaction 2.5 or precipitated in the form of nitrides according to reaction 2.6 or 2.7. The reactions were given in section 2.3. The

nitrogen austenite transformed into martensite when it was cooled and reached the martensite-start temperature. Figure 2.6 given in section 2.3 illustrates the stabilized γ phase with respect to N content in the calculated isothermal phase diagram of the Fe–Cr–N ternary system at 1200°C. The chromium content of the AISI 430 FSS used in this experiment was 15.71 weight percent. Based on the diagram, with low nitrogen content, the steel was in γ and α phase. Therefore, martensite might be formed during cooling; while the ferrite remains unchanged at the room temperature. Hence, the phase of the steel at the room temperature would be a mixture of martensite and ferrite. The γ phase increased with the increasing nitrogen. This would produce more martensite when the material was cooled. Longer nitriding at 1200°C made the steel to be in fully austenitic condition and brought to fully martensitic phase when it was cooled to room temperature.

Figure 4.6 shows that up to 0.3 mm from the surface, hardness of the sample nitrided for one hour was significantly higher than the hardness of the as-received sample. The hardened-case depth was approximately same as the thickness of the martensite layer, *i.e.* approximately 0.3 mm (Figure 4.2). This divulged that thickness of the martensite layer was in accordance with hardness of the steel. Therefore, the effect of the treatment in improving the hardness of AISI 430 FSS was also evident. Deeper into the core, the hardness decreased. In this part, the hardness of the steel was about equal to the hardness of the solution-annealed steel. On the other side, hardness at the core of the steel nitrided for four and seven hours remained as high as the hardness of the surface. This was in line with the martensite phase that dominated the entire cross section of the sample (Figure 4.3 and Figure 4.4).

Based on the thickness of the martensite and the hardened case, nitrogen diffusion as deep as 0.3 mm from the surface was achieved by nitriding for one hour (see Figure 4.6); whereas nitriding for four hours diffused the nitrogen throughout the steel. It could be expected that further increase of the nitriding time would lead to the nitrogen saturation in the steel.

In solution nitriding treatment, nitrogen uptake occurs at the nitriding temperature. Fast cooling, *e.g.* quenching with water or oil is required to maintain the dissolution of the nitrogen that dissolves into the steel [39]. Ferrite transforms into

austenite when the nitrogen uptake into the ferritic-martensitic steel takes place [47]. Fast cooling applied in the nitriding treatment leads to martensite formation when it reaches the martensite-start temperature.

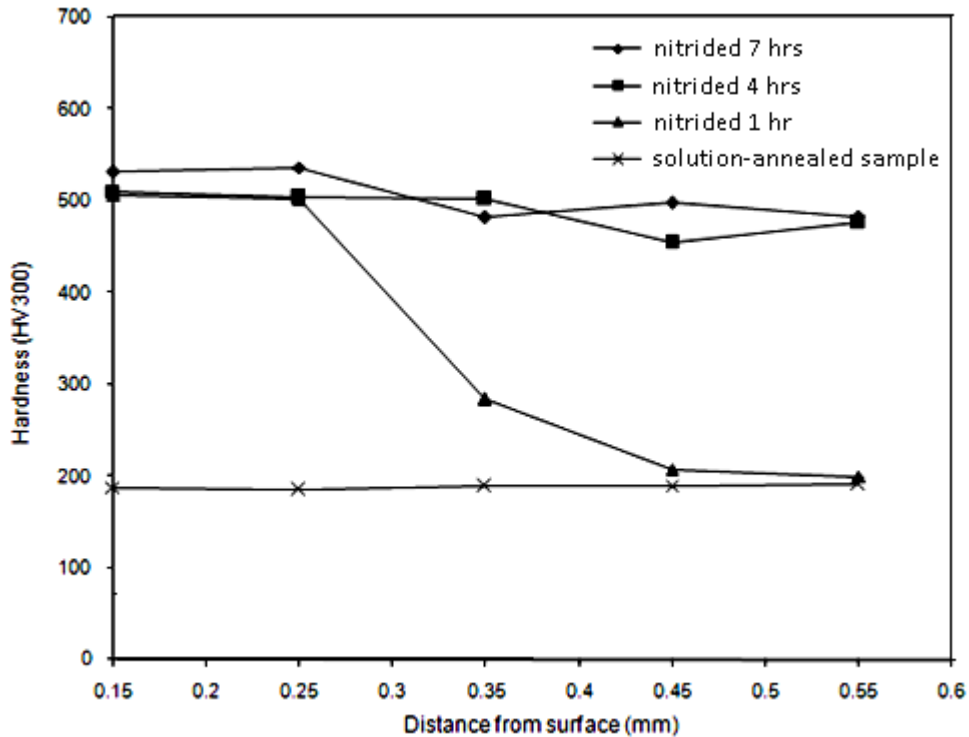


Figure 4.6 Hardness of nitrided AISI 430 FSS

Diffusion of nitrogen induced strong elastic distortion in the crystal lattice and increases the internal friction. This causes the movement of dislocation become more difficult. This is the reason for the nitrogen-solid-solution strengthening effect [48]. Thus, more nitrogen in the steel can be expected to produce higher hardness.

In term of kinetics diffusivity, diffusion of nitrogen obeys the 2nd Fick's Law of diffusion discussed in section 2.4.2. Therefore, the nitrogen diffusion is affected by time and temperature. This makes the nitrogen concentration decrease continuously with increasing distance from surface. Increasing the nitriding time diffused nitrogen in higher amount and also into deeper part of the steel [50]. This will lead to thicker and harder martensite layer when fast cooling applied. For this reason, the hardened-case depth is in accordance with the martensite layer thickness at the nitrided steel.

In the present work, martensite was formed in the steel after the nitriding. This was shown in Figure 4.2 to Figure 4.4. Thus, it indicates that nitrogen has diffused

into the steel. The results of the present work demonstrated that thickness of the martensite layer and the hardened-case depth was about equal. In one-hour-nitrided steel, the martensite layer thickness and the hardened case depth was about 0.3 mm. These were estimated from Figure 4.2 and Figure 4.6, respectively. The equal thickness of the martensite-layer and the hardened-case was caused by the nitrogen that stimulates the martensite formation and also enhances the hardness of the steel. This can be explained from the mechanism of nitrogen diffusion and nitrogen-solid-solution hardening discussed in the former paragraph. Based on this mechanism, nitrogen was presumed to diffuse 0.3 mm into the steel when the steel was nitrided for one hour.

Nitrogen diffusion was affected by time, *i.e.* longer nitriding may results in higher-amount and deeper nitrogen diffusion. This made thicker martensite when the nitriding was extended into four hours (Figure 4.3). Figure 4.3 shows that martensite occupies the overall cross section of the steel. Nevertheless, very-small ferrite islands were also observed at the core of the sample. This was ferrite that remained in the steel after the quenching. The hardness enhancement into the core of the sample was also exhibited by the four-hours-nitriding (Figure 4.6). Considering that thickness of the steel is 1.2 mm, the four-hours-nitriding was sufficient to diffuse nitrogen throughout cross section of the steel.

The influence of nitriding time on the nitrogen diffusion was also shown by the nitriding for seven hours which also attempted in this work. Microstructure of the steel nitrided for seven hours displayed fully martensitic phase (Figure 4.4). Ferrite phase was no longer observed in the microstructure. Hardness test across the steel also depicted the hardness improvement in the overall cross section (Figure 4.6). Therefore, nitrogen fully diffused into the steel. This condition may indicate that seven-hours nitriding has brought to nitrogen saturation in the steel.

4.1.2 Solution Nitriding of 7.5%-Cr FS

Microstructure of the as-received 7.5%-Cr FS is presented in Figure 4.7. The microstructure of the steel consisted of ferrite (white or light phase) with martensite

(black or dark phase). The rolled structure that indicates rolling direction in the manufacturing process of the steel was also obvious. Change of the microstructure after nitriding is shown in Figure 4.8 to Figure 4.10.

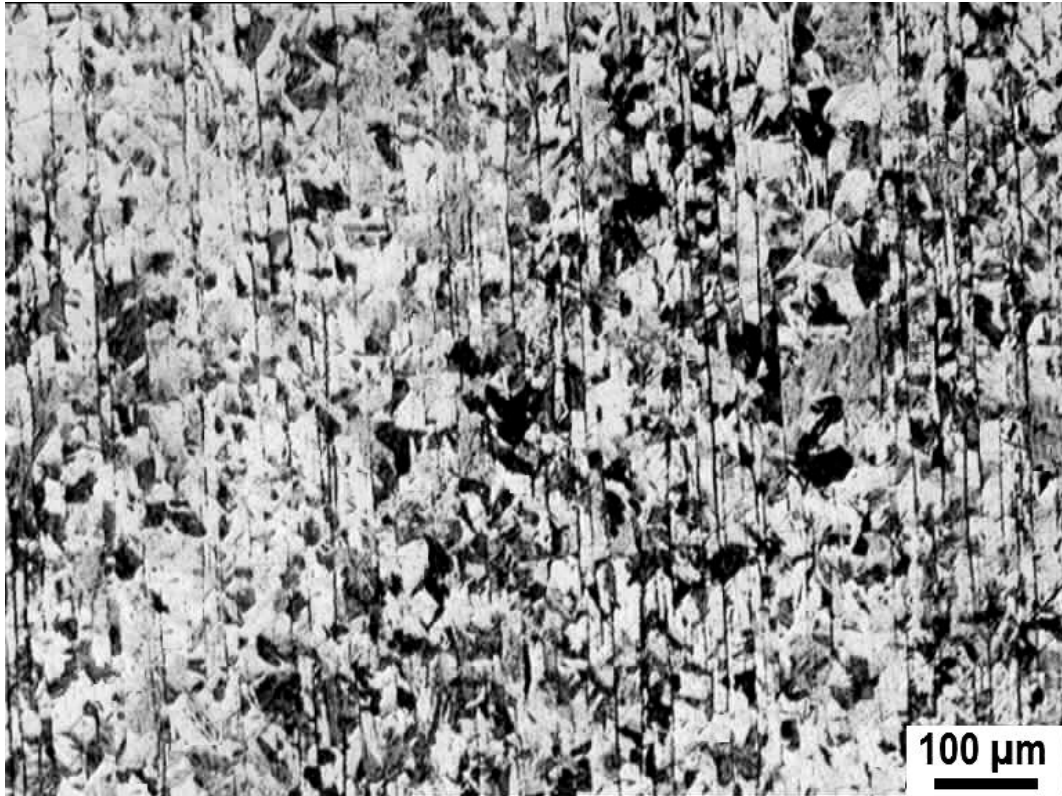


Figure 4.7 Microstructure of as-received 7.5%-Cr FS

Figure 4.8 to Figure 4.10 illustrate the existence of martensite phase in the microstructure. This suggested that nitrogen had diffused into the steel after the treatment. Nitrides or retained austenite were not indicated in the XRD pattern obtained from the seven-hour-nitrided sample (Figure 4.11). The XRD gave α peak which could represent the mixed phase of martensite and the un-transformed ferrite.

In the present work, the border of the martensite layer was hard to be determined as no clear boundary was observed. Microstructure of the as-received 7.5%-Cr FS consisted of martensite and ferrite. After the nitriding, nitrogen diffusion stimulated the transformation of ferrite to martensite. However, since the original microstructure of the steel consisted also martensite, after the nitriding the martensite phase was found not only in the area close to the steel surface. The phase seemed to be distributed throughout the cross section of the sample. Therefore it is difficult to

precisely determine the martensite layer thickness produced by the nitriding treatment from microstructure of the sample.

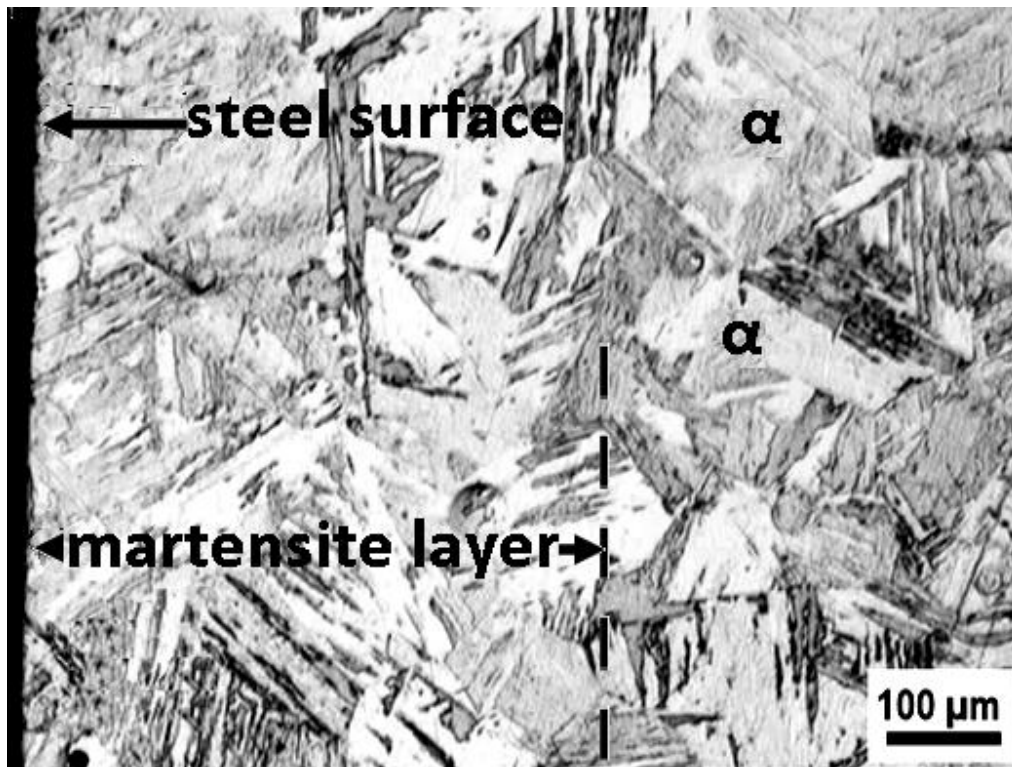


Figure 4.8 Microstructure of 7.5%-Cr FS nitrided for one hour

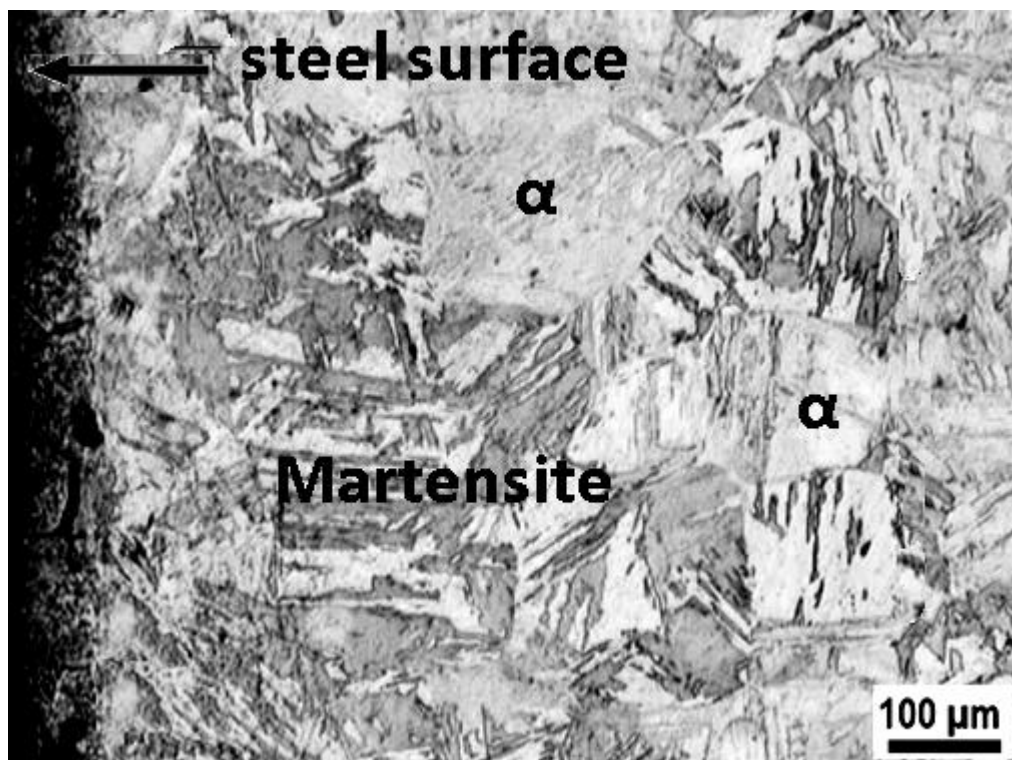


Figure 4.9 Microstructure of 7.5%-Cr FS nitrided for four hours



Figure 4.10 Microstructure of 7.5%-Cr FS nitrided for seven hours

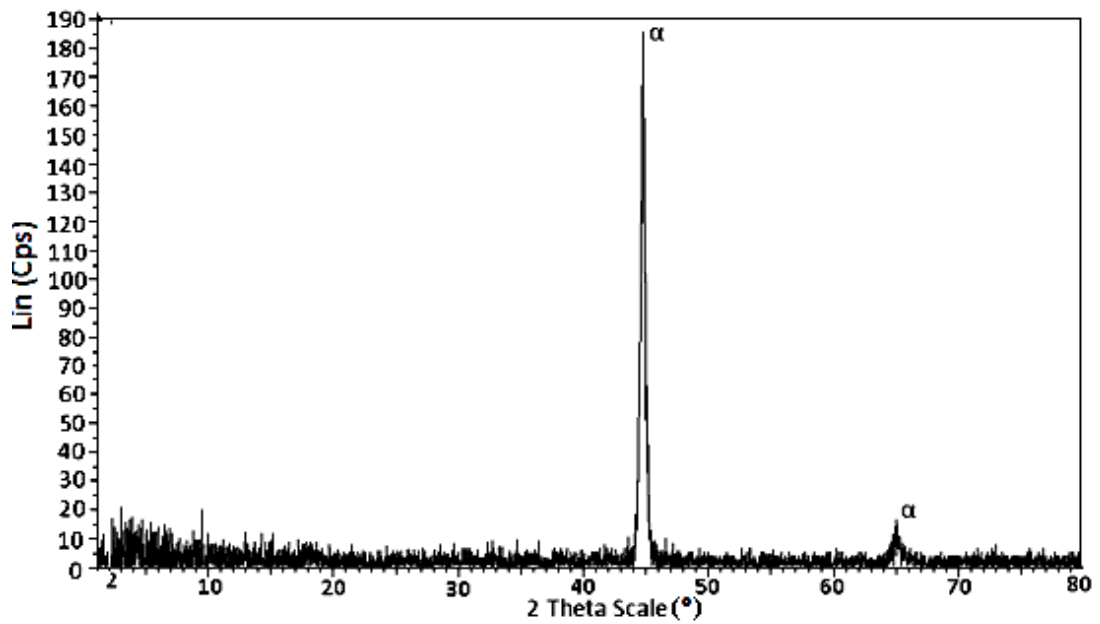


Figure 4.11 X-ray diffractogramme of 7.5%-Cr FS after nitrided for four hours

Nitriding enhanced the hardness of the surface of the 7.5%-Cr FS sample. This was shown in Figure 4.12. For the sample nitrided for one hour, the extent of the hardened part was around 0.75 mm. Longer nitriding produced higher hardness at the surface. This was shown by the hardness of the samples nitrided for four and seven hours. For these samples, the high-hardness area was maintained up to approximately 1 mm from the surface before it continuously decreased. At the distance of 1.5 mm from the surface, the seven-hours-nitrided steel was still harder than the other nitrided steels. However, the difference of the hardness in this depth was not significant. Based on the hardened-case depth, nitriding for one hour was observed to diffuse nitrogen around 0.75 mm from the surface. Extending the nitriding duration to four hours seemed likely to diffuse the nitrogen into 1 mm below the surface.

The influence of nitrogen in the hardness of the steel was discussed formerly in section 4.1.1. It was established that more nitrogen content led to hardness enhancement in the steel. The section also explained that nitrogen diffusion was influenced by time; *i.e.* longer nitriding diffuse more nitrogen into deeper part of the steel [50]. For this reason, longer nitriding may yield higher hardness of the steel as more nitrogen dissolved in the steel. This was also exhibited in the nitriding of the 7.5%-Cr FS attempted in this work. Figure 4.12 illustrates that nitriding of the 7.5%-Cr FS for four hours produced harder steel than the nitriding for one hour; while nitriding for seven hours results in higher hardness than nitriding for four hours. This was due to more nitrogen which dissolved in the longer-nitrided-steel. Since the thickness of the steel to be joined with the sialon was approximately 1.5 mm, nitriding for four hours should be sufficient to add the nitrogen throughout the steel.

Besides showing the higher hardness for the longer-nitrided steel, Figure 4.12 also illustrates that the hardness decreases with the increasing distance from surface. This was exhibited by the steels nitrided for one, four and seven hours. Explanation on this trend can be based on the discussion on the nitrogen diffusion mechanism written in section 4.1.1.

The diffusion of nitrogen obeys 2nd Fick's Law of diffusion [39]. Thus, nitrogen diffusion decreases with the increasing distance from the surface of the steel. Since nitrogen in the steel increases the hardness of the steel, the decrease of the nitrogen

with respect to the distance from surface leads to the inclination of its hardness trend. Hence, it can be disclosed that the reduction of the hardness with respect to the distance from surface (Figure 4.12) was due to the decreasing nitrogen content in the steel.

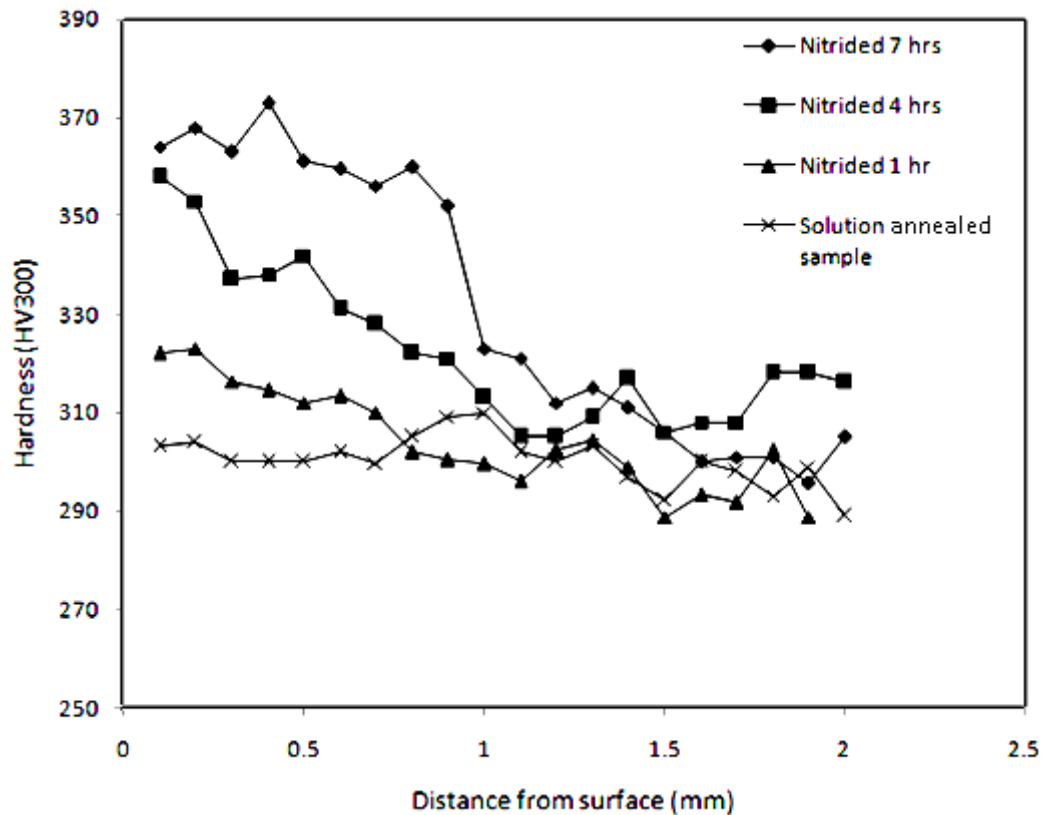


Figure 4.12 Hardness of nitrided 7.5%-Cr FS

4.2 Joining of Sialon to AISI 430 FSS

AISI 430 FSS is joined to sialon for several reasons. These have been mentioned in section 1.1. The steel could be an option since joining sialon with austenitic stainless steel was failed [5, 17]. It contains 15.72 % Cr and is a common grade of ferritic stainless steel which is available in the market. The material is ductile and commonly applied to high temperature environment. Thus it is suitable to be combined with the sialon. Reactivity of the sialon with Fe-Cr alloy [15] also suggested that the materials could be joined.

4.2.1 Joining of Sialon with As-received AISI 430 FSS

This section discusses joining of sialon with as-received AISI 430 FSS. This will be compared later with the joining of the sialon with the steel in nitrided condition. The as-received condition of the steel was given in Chapter 3. Sample preparation and joining procedure as well as characterization of the joint were also as explained in the chapter.

4.2.1.1 Microstructure of the Joint

Microstructure of the overall joint is presented in the optical and scanning electron micrographs given in Figure 4.13 and Figure 4.14, respectively. Scanning electron micrograph in Figure 4.14 depicted clearer morphology of the joint cross section, whereas detail of the sialon – steel interface is shown in Figure 4.15. Figure 4.15 shows that interfacial joint occurred between the sialon and the steel.

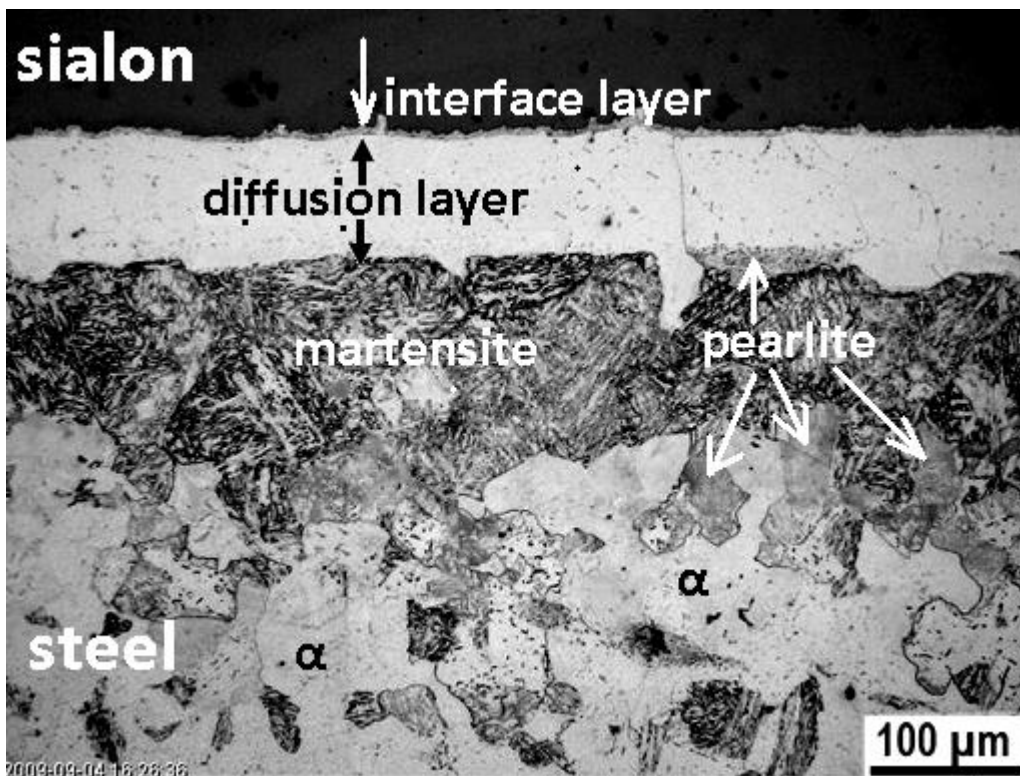


Figure 4.13 Optical micrograph of the cross section of sialon – as-received AISI 430 FSS joint

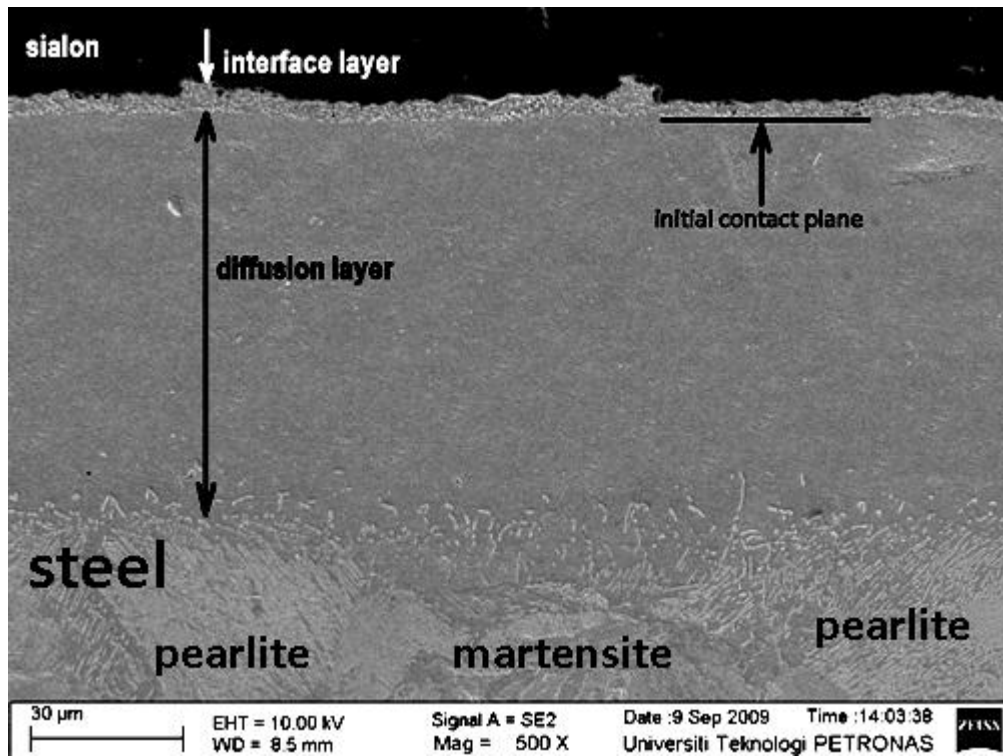


Figure 4.14 Scanning electron micrograph of the cross section of sialon – as-received
AISI 430 FSS joint

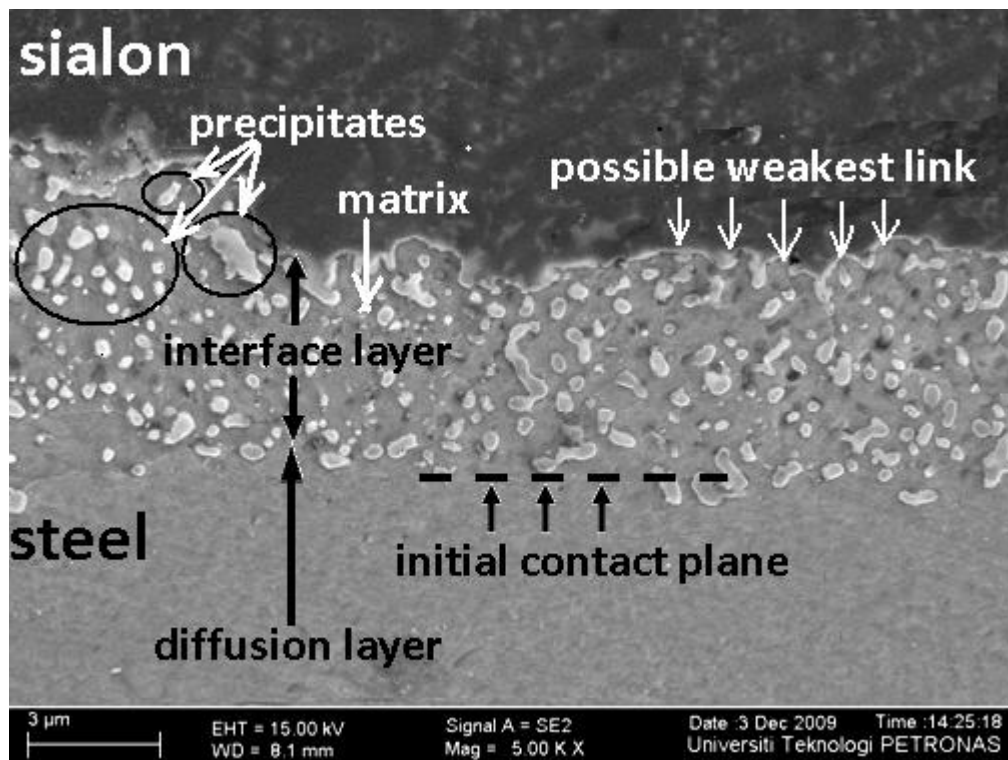


Figure 4.15 Scanning electron micrograph of the cross section of the interface layer in
sialon- as-received AISI 430 FSS joint

Scanning electron micrograph in Figure 4.14 depicted clearer morphology of the overall joint cross section. Reaction layers were indicated in the interface of the sialon and the steel. Thin and rough reaction layer was seen adjacent to the sialon; while the second layer was significantly thicker and extended into the steel. The interface of the first and the second layer was the initial contact plane of the joined materials. This was recognized in the previous works [7, 77-78]. Therefore, this was the border between the sialon and the steel part before the joining. This revealed that the thin-rough layer near the sialon was actually the sialon's part, while the thicker layer was the steel's part.

Rough-surface layer near the sialon was due to the porosities and the precipitates as shown in the exaggeration of the layer (Figure 4.15). Voids were observed in the interface of the layer with sialon. Precipitates in the reaction layer were the reaction products of the sialon and the steel. It was observed from Figure 4.15 that matrix of the layer owned the same contrast with the second layer that extended into the steel. This characteristic indicated that those parts might have the same phase. In other words, both parts might be the same species that composed the joint of the sialon with the steel. This made the initial sialon – steel contact plane was no longer obvious. Same species was observed across this contact plane. Based on this reason, it could be disclosed that cohesive joint was formed in the sialon – steel interface.

There were no other species at the reaction layer in the steel side. Thus, it seemed that the layer contained a single phase. Elemental study on this layer disclosed that this area was the diffusion zone of the silicon into the steel. This will be reported in the later section of this chapter. Subsequently, throughout the discussion, the reaction layer in the sialon was called interface layer; whereas, the layer in the steel side will be called as the diffusion layer. The thickness of the layers was obtained by measuring them on the microstructure of the joint. The average thickness of the diffusion layer was 78.57 μm ; while the average thickness of the interface layer was 4.45 μm . These were the average value of 10 measurements.

Microstructure of the interface layer given in Figure 4.15 displays the same contrast in diffusion layer and interface layer matrix. Therefore, it could be expected that the interface layer matrix and the diffusion layer might have the same phase. It

looked that material transfer occurred from the steel into the sialon across the initial contact plane. The steel-like phase penetrated into the interface layer in the sialon side and formed irregular boundary with the original sialon. The transfer of the steel phase into the sialon side has shifted the interface of sialon – steel slightly deeper into the sialon part. The boundary of the original sialon with the interface layer has become the new sialon – steel interface. Consequently this may turn into the weakest part of the joint since this area is the border of extreme different properties of the sialon and the steel.

4.2.1.2 Elemental Analysis

Interdiffusion of elements across the joint was analyzed using FESEM-EDX. Initially the analysis was attempted on the overall joint. This was carried out across the interface and the diffusion layers. Further analysis was also accomplished separately on the interface layer. This was aimed to investigate the elements in the precipitates as well as in the matrix of the layer.

The results of the analysis for the overall joint are presented in Figure 4.16. Silicon was detected in the steel at the distance of around 80 μm from the joint interface. This showed the silicon diffusion into the steel. It was difficult to determine the exact length of the diffusion distance from the figure. The more realistic way was to refer to the thickness of the diffusion layer measured from the microstructure. For this joint, the average thickness of the diffusion layer was 78.57 μm . Maximum concentration of the silicon in this layer was 1.57 weight percent (3.53 atomic percent). No other sialon's element was found; *i.e.* only silicon diffused from the sialon into the steel.

The interface layer was the reaction layer in the sialon side. This was revealed by the existence of the elements from both materials in this layer. As established in the previous section, the average thickness of this layer was 4.45 μm .

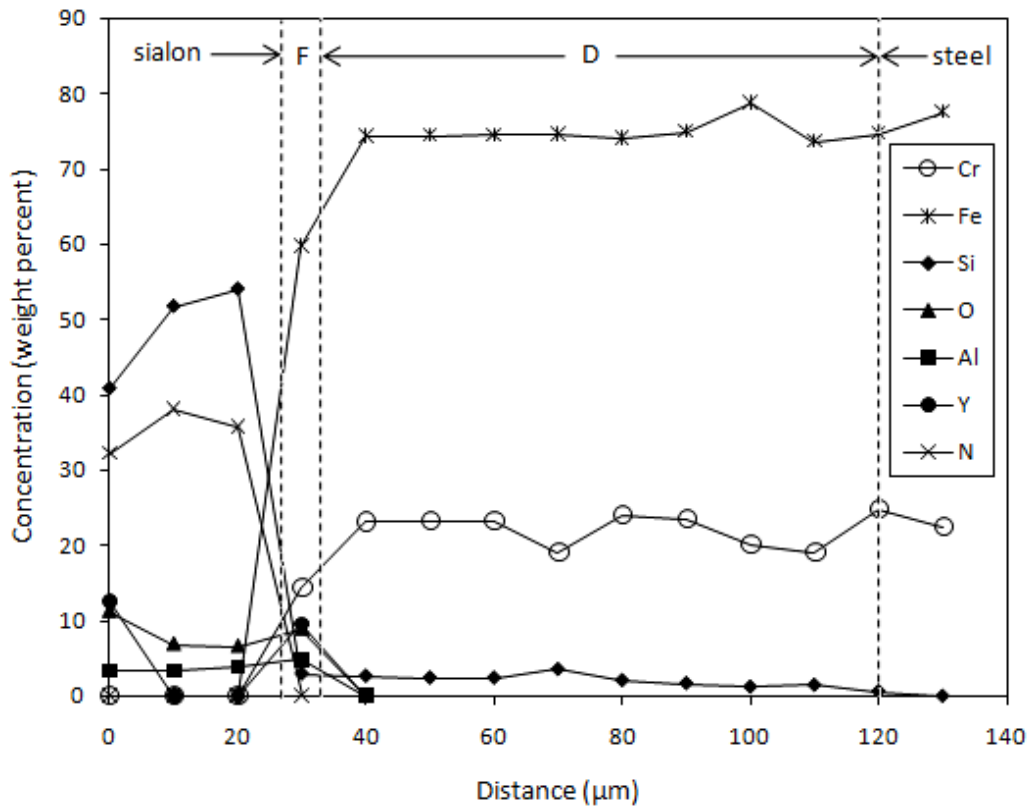


Figure 4.16 Concentration profile of elements across the sialon – as-received AISI 430 FSS joint; F=interface layer, D=diffusion layer

Elemental analysis was accomplished at the interface layer to study its phases. EDX analysis was conducted on the interface-layer matrix and the precipitates. The spots were determined randomly as it was explained in section 3.2.4.2. Map of the EDX analyses on the interface layer of sialon – as-received AISI 430 FSS joint is illustrated in Figure 4.17. The results of the analyses were tabulated in Table 4.1 and Table 4.2.

Table 4.1 shows that the interface-layer matrix consisted of mainly Fe, Cr and Si; nevertheless, other sialon's elements were also found in a few spots. Among the elements, Fe and Cr were more dominant than the silicon. The maximum concentrations for Fe and Cr are 80.13 and 24.84 weight percent, respectively. These were much higher than the maximum concentration of the silicon (*i.e.* 3.26 weight percent). The silicon concentration in the interface layer was lower than its concentration in the bulk sialon. This revealed that the layer was the decomposed-part of the sialon since this was originally part of the sialon.

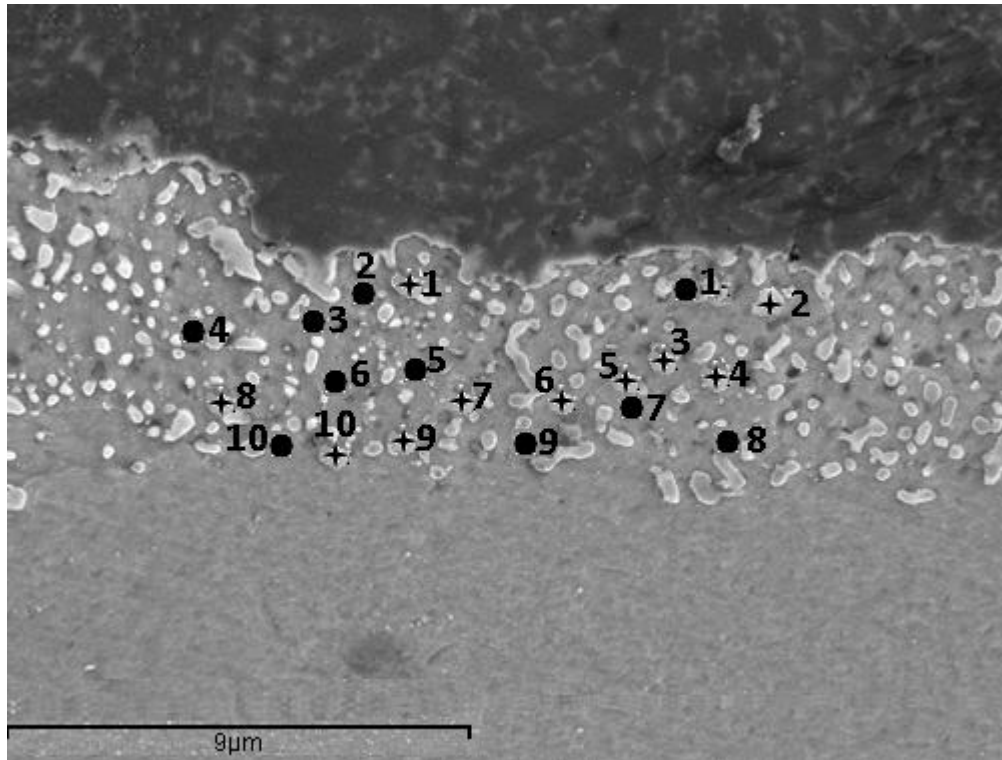


Figure 4.17 Map of EDX spot analysis at the interface layer of sialon – as-received 430 FSS joint; (●) = matrix, (+) = precipitates

Table 4.1 Concentration of elements of the interface-layer matrix in sialon – as received AISI 430 FSS joint (weight percent)

Spot number	Concentration (weight %)						
	Cr	Fe	Si	O	Al	Y	N
1	11.38	80.13	3.26	1.68	3.54	0	0
2	20.24	78.13	1.62	0	0	0	0
3	17.64	75.83	2.27	1.72	2.54	0	0
4	19.93	78.30	1.76	0	0	0	0
5	15.26	60.67	3.27	5.38	6.11	9.32	0
6	24.84	73.26	1.90	0	0	0	0
7	13.45	79.62	3.20	0	3.73	0	0
8	21.20	75.78	2.05	0.95	0	0	0
9	21.51	76.73	1.76	0	0	0	0
10	14.69	77.80	2.80	1.27	3.46	0	0

Same contrast of the interface-layer matrix in the sialon and the diffusion layer in the steel was displayed in the microstructure image of the layers. Furthermore, the compositions of elements in both parts were also similar. Steel's elements (*i.e.* Fe and Cr) are more dominant than the sialon's elements. Therefore, those reaction layers parts might have the same phase. It seemed that the steel had penetrated into the

sialon side across the initial contact plane (see Figure 4.15). Further characterization would be carried out to identify the phase on that area.

Table 4.2 Concentration of elements of the precipitates at the interface layer in sialon – as-received AISI 430 FSS joint

Spot number	Concentration (weight %)						
	Cr	Fe	Si	O	Al	Y	N
1	10.65	62.52	8.52	1.95	7.56	8.80	0
2	11.13	66.39	10.55	2.42	3.98	5.54	0
3	9.90	45.06	28.94	2.18	4.26	0	9.64
4	6.06	45.00	30.26	2.45	4.77	0	11.46
5	3.89	42.98	34.14	2.26	4.41	0	12.32
6	11.20	41.71	30.25	1.94	2.98	0	11.92
7	15.30	39.86	28.35	2.09	2.65	0	11.75
8	14.78	41.58	25.55	1.82	3.60	0	12.66
9	12.89	41.95	26.84	1.63	3.55	0	13.13
10	11.99	43.10	27.54	1.96	3.44	0	11.97

White precipitates were other species in the interface layer. Table 4.2 presents the EDX analyses on the precipitates. Several precipitates were selected randomly for the analysis as shown in Figure 4.17. The precipitates contained Fe and Cr in concentration of 66.39 weight percent and 15.3 weight percent respectively. Those were the maximum concentrations observed in the spots. Besides the steel's elements, the precipitates also comprised sialon's elements. Among the elements, silicon was found in higher concentration (*i.e.* 8.52 to 30.26 weight percent). Nitrogen concentration was also significant (*i.e.* 9.64 to 13.13 weight percent) where EDX was able to detect it. The presence of the elements from both materials implied that the precipitates were the reaction product of the sialon with the steel. Hence, the interface layer was the sialon-decomposed part and also the reaction front of the joined materials in the ceramics side.

The analysis disclosed that the precipitates were rich of Fe, Cr and Si. Nitrogen was also existed in relatively significant quantity. One could expect that the Fe and Si would form the iron silicides; whereas, N would tend to create nitrides when it met nitride formers such as Cr and Fe.

Further investigation on the phases of the layer was carried out using other characterization techniques. The later section of this chapter reports the

characterization works on the layer. The phases in the interface layer would be elaborated further based on the results of the investigations.

4.2.1.3 XRD

Elemental analysis on the reaction layer indicated that iron silicides or chromium nitrides might be formed in the precipitates. To scrutinize the phase, XRD examination was conducted on the joint. It has been reported in Chapter 3 that applying XRD examination on the cross-section of the joint was difficult due to the thin cross-section of the layer. Therefore the investigation was performed on the surface of the interface layer. To perform the XRD investigation on the layer, the joined sample was broken to expose the surface of the interface layer. The sialon at the steel was removed to ensure the clean surface of the layer. Microscopic observation on the cross section of the broken steel was carried out and it was found that the interface layer was still attached to steel. Subsequently the XRD test was attempted on the surface.

XRD pattern of the layer is shown in Figure 4.18. In the interface layer, strong peaks of α and FeSi_2 were detected. The ferrite peak should be from the interface layer since this contained Fe, Cr and Si. Both Cr and Si are ferrite formers that stabilize the ferrite. Thus, the silicon dissolved in the steel and formed the ferrite solid solution in the interface-layer matrix. This phase extended into the diffusion layer in the steel. The silicon diffused into this layer and dissolved in the same solid solution. The silicon diffusion diminished at the end of the layer. Hence, the ferrite phase was no longer existed and transformation to other phases (*i.e.* pearlite and martensite) occurred in the parent steel. This was disclosed since the diffusion layer consisted of similar elements with the interface-layer matrix. Those parts of the joint also displayed same contrast in the micrograph of the microstructure. This might imply that the joint parts had the same phase

Another peak which corresponds to FeSi_2 was also seen in the X-ray diffractogram. This peak should come from the precipitates since no other species existed in the layer. Although EDX and the literature study predicted that other

compounds might also be formed, yet only the FeSi_2 was confirmed by the XRD. To reveal the existence of the FeSi_2 in the interface layer, further assessment of the layer using XPS was carried out on the layer.

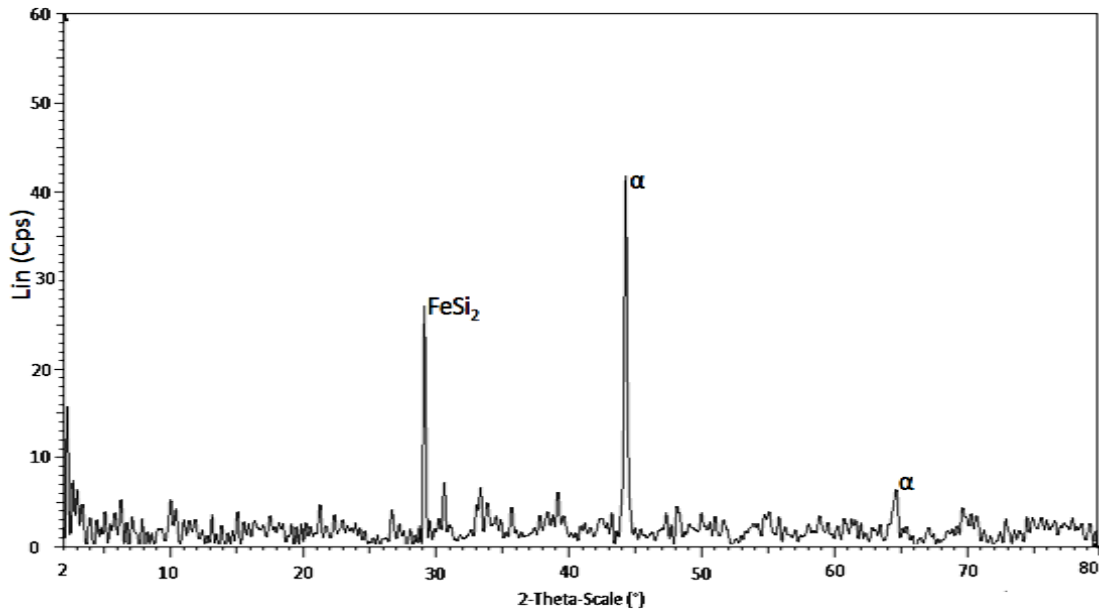


Figure 4.18 X-ray diffractogramme of the interface layer in sialon – as-received AISI 430 FSS joint

4.2.1.4 XPS

XPS analysis was performed on the surface of the interface layer. The analysis was focused on examining the existence of FeSi_2 as it had been shown by the XRD. For this purpose, Fe and Si were registered in the XPS examination to get the spectra. Figure 4.19 and Figure 4.20. present the XPS spectra for Fe and Si from the interface layer respectively. The red-colour curve is the raw data. Green curve in the spectra is the background selected for the peak fitting. In this case, smart background was used. The raw data was simulated and the result is given in the blue curve. The peaks were then fitted and resulted in the split peaks that are illustrated in yellow colour.

Figure 4.19 shows that four peaks of Fe were observed in the spectra. Those are at: 707.06 eV; 711.03 eV; 720.02 eV and 724.73 eV. The peaks at 710.99 eV and 724.89 eV were attributed to $\text{Fe}_{2p_{3/2}}$ from Fe_2O_3 [86-87]. The other two peaks at

707.06 eV and 720.02 eV could correspond to FeSi₂ [86, 88-90]. These peaks were also very close to the metallic Fe peak, which was at 706.75 eV and 719.95 eV [87]. However, the presence of plasmon loss at around 730 eV in the Fe spectra indicated the existence of FeSi₂ [86, 89]. It was suggested that the Fe_{2p} peak in the FeSi₂ shifted to higher binding energy (+0.2 eV) from the metallic Fe peak. Therefore, the existence of the metallic Fe could not be ignored with regard to the very small difference.

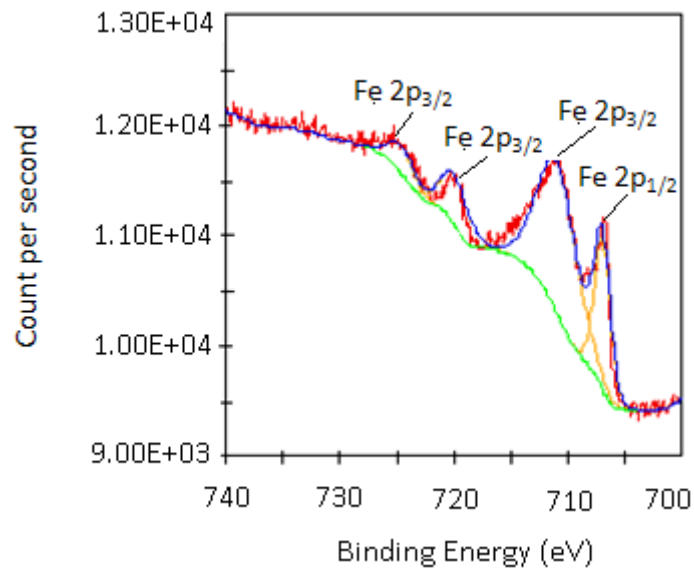


Figure 4.19 XPS spectra of Fe from the interface layer in sialon – as-received AISI 430 FSS joint

The spectra for Si (Figure 4.20) from the interface layer surface provide two peaks which attributed to SiO₂ and FeSi₂. The existence of the SiO₂ was represented by the peak of Si_{2p} at 102.96 eV. Another peak at 99.57 eV indicates the presence of FeSi₂ in the interface layer [86, 89-90].

The results of the XPS examination supported the existence of the FeSi₂ that had been found through XRD analysis. Therefore, it can be concluded that the precipitates in the interface layer of the joint consisted of the iron silicides. However, the analysis also suggested that the Fe was also in the form of Fe₂O₃. The Si spectra also revealed that SiO₂ was present in the layer.

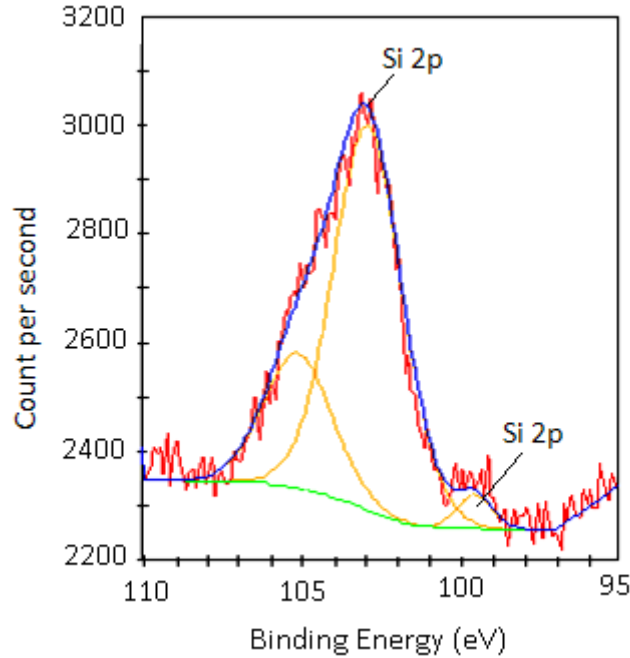


Figure 4.20 XPS spectra of silicon from the interface layer in sialon – as-received AISI 430 FSS joint

It was mentioned formerly that formation of oxides in the reaction layer of nitrogen-based ceramics joined with steel was possible. Insoluble oxides could be produced from the decomposition of silicon nitride ceramics [77-78]. Those were also possible compounds in the joint of alloy containing Cr and Ni with silicon nitride. Al_2O_3 , Cr_2O_3 , SiO_2 and NiO were reported as possible oxides to form in the joint [2]. Al_2O_3 was formed in the reaction of sialon – steel as a result of the recombination of Al^{3+} and O^{2-} that was liberated from the sialon decomposition [15].

In this work, Fe_2O_3 and SiO_2 were detected in the XPS examination. However, the XRD failed to identify the phases. It was probably due to their low volume fraction. The Fe_2O_3 might be formed due to the reaction of Fe^{3+} and O^{2-} in the interface layer. The steel diffused into the sialon-decomposed area and reacted with O^{2-} to produce the Fe_2O_3 . On the other side, SiO_2 was possibly created from the recombination of Si^{4+} and O^{2-} . The process was similar with the formation of Al_2O_3 that was suggested by Vluegels *et al.* [15]. Si and O_2 were released due to the decomposition of the sialon. The silicon dissolved in the steel in the interface-layer matrix and the diffusion

layer. Subsequently, part of the silicon that remained in the interface layer reacted with O^{2-} to form the SiO_2 .

4.2.1.5 Hardness Test across the Joint

Mechanical properties of the layers may have important role in achieving the joint. This is due to the different thermal expansion coefficient of the joined materials which leads to the excessive residual stress. The stress is generated during the cooling stage of the joining process. Ductile layer is expected in the joint to absorb the residual stress so that crack in the ceramics can be prevented. In this research, hardness test was carried out across the joint to study the mechanical properties of the reaction layers.

Hardness across the joint is given in Figure 4.21. The hardness of sialon decreased sharply at the interface layer. The decreased of the sialon's hardness in this layer was due to the decomposition of the ceramics in this area. Previous discussion had proved that this area was the decomposed part of the sialon. Therefore, the decomposition of the sialon had decreased its hardness. Compared to the diffusion layer, the interface layer was harder. As a matter of fact, the interface-layer matrix and the diffusion layer should have same hardness since those consisted of ferrite. However, the precipitates in the layer which consisted silicides and oxides enhanced the hardness.

The diffusion layer in the steel was the lowest-hardness part. Phase identifications that were carried out on the layer revealed that this was ferrite zone. As a result, the hardness of this layer was lower than the mixture of ferrite and precipitates at the interface layer. Its hardness was also lower than the pearlite in the parent steel. In overall, the hardness of the reaction layers (*i.e.* interface and diffusion layers) were lower than that of original sialon and the parent steel. Therefore, these parts were more ductile compared to the parent joined-materials.

Martensite and pearlite were produced in the parent steel after the joining. This had been shown earlier in the optical micrograph of the joint. Hence, the hardness of the steel was very high when indentation was performed on the martensite phase.

Conversely, lower hardness was obtained when the indenter penetration was applied on the pearlite structure.

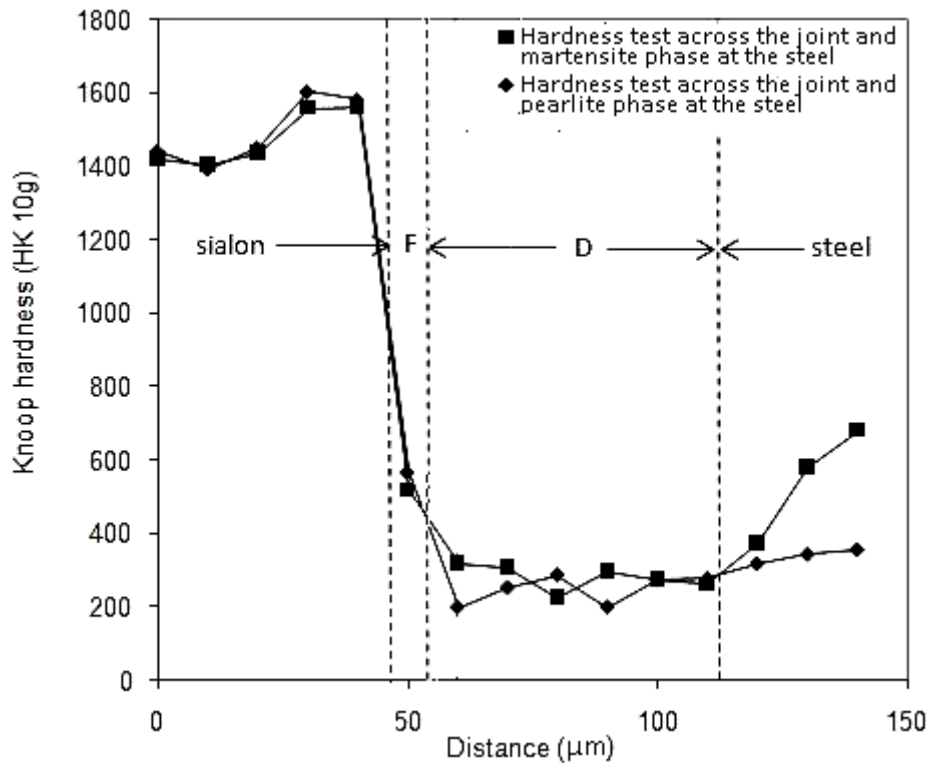


Figure 4.21 Hardness test across the joint of sialon – as-received AISI 430 FSS;
F=interface layer, D=diffusion layer

Low hardness of the diffusion layer showed its ductility. This was beneficial in achieving the joint. Especially in dealing with the residual stress that was generated during cooling stage in the diffusion bonding process. Crack at the ceramics due to this problem yielded to failure in the joining [5-6, 15, 17]. On the other side, intervention of the thermal expansion coefficient of the steel was not easy. In the current work, ferritic microstructure of the steel was changed to martensite and pearlitic during the joining. Martensite phase at the parent metal caused the steel to be more brittle. In this case, the layers would act as a bridge of the joined-material's properties. This was like the ductile metallic interlayer that was normally utilized to solve the problem of high residual stress at the joint of ceramics with metal.

4.2.2 Joining of Sialon with One-hour-nitrided AISI 430 FSS

Nitriding experiments discussed in section 4.1.1 disclosed that the treatment enhanced hardness of the surface of the AISI 430 FSS. Nitriding the steel for one hour was shown to improve the hardness up to approximately 0.35 mm below the surface. Surface hardness of the steel was increased and martensite phase was formed. It was believed that the hardness improvement and the martensite formation in the surface of the steel were due to the nitrogen diffusion into the steel. Therefore, the steel was diffusion bonded in nitrogen-pre-dissolved condition. Joining of the steel with the sialon was accomplished using the same technique and setting that were employed in the previous joining.

4.2.2.1 Microstructure of the Joint

Joining of the steel nitrided for one hour was successful. Good joint was achieved as illustrated in Figure 4.22 – Figure 4.24. Reaction layers were clearly appeared in the interface of the joint. Morphology of the layer was similar with the reaction layers formed in the sialon – as-received AISI 430 FSS joint. It consisted of rough-thin interface layer in the sialon side and diffusion layer in the steel side.

The presence of martensite and pearlite in the parent steel was obvious. This could be seen in Figure 4.22 and Figure 4.23. The phases were seen at the area near the diffusion layer. The pearlite structure extended into deeper area and diminished at the core of the steel. At this part, ferrite phase was appeared.

Microstructure of the interface layer can be observed in more detailed in Figure 4.24. Obviously, white precipitates appeared in the interface layer. These were observed throughout the interface layer which was the decomposed area of the sialon. The morphology of the interface-layer matrix shows same contrast with the diffusion layer. This might also lead to the same phase in the layers as it was found in the joint of sialon – as-received steel. Thus, this was the steel part that moved towards the decomposed-part of the sialon during the diffusion bonding. Elemental analysis on the joint was expected to give further information on the joint.

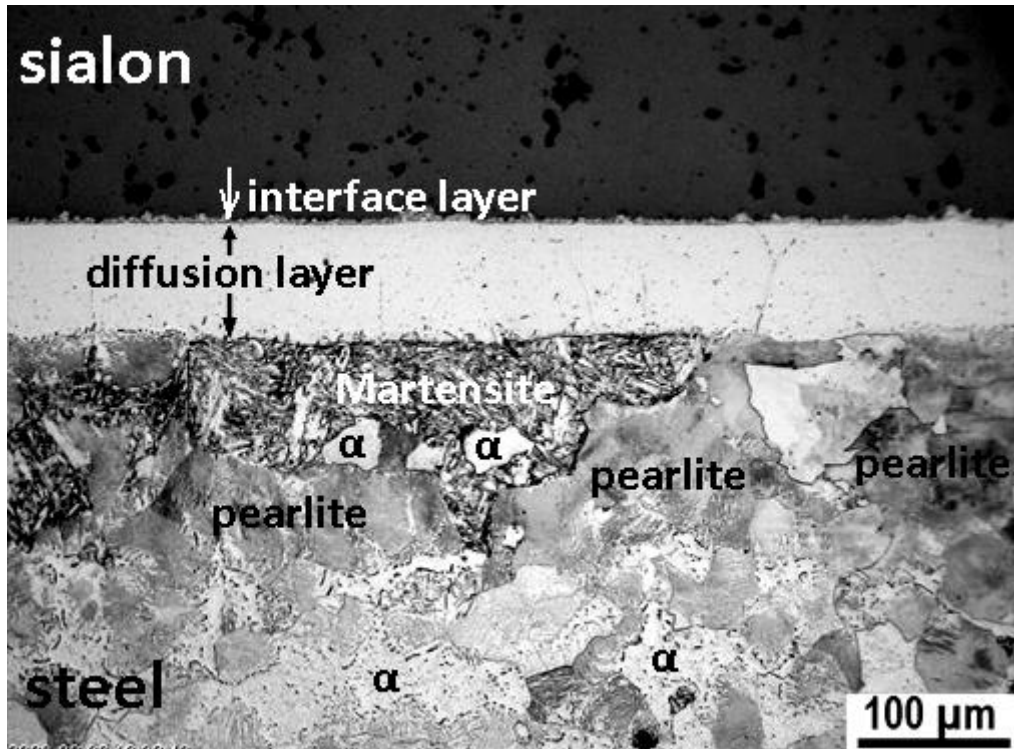


Figure 4.22 Optical micrograph of the cross section of sialon – one-hour-nitrided AISI 430 FSS joint

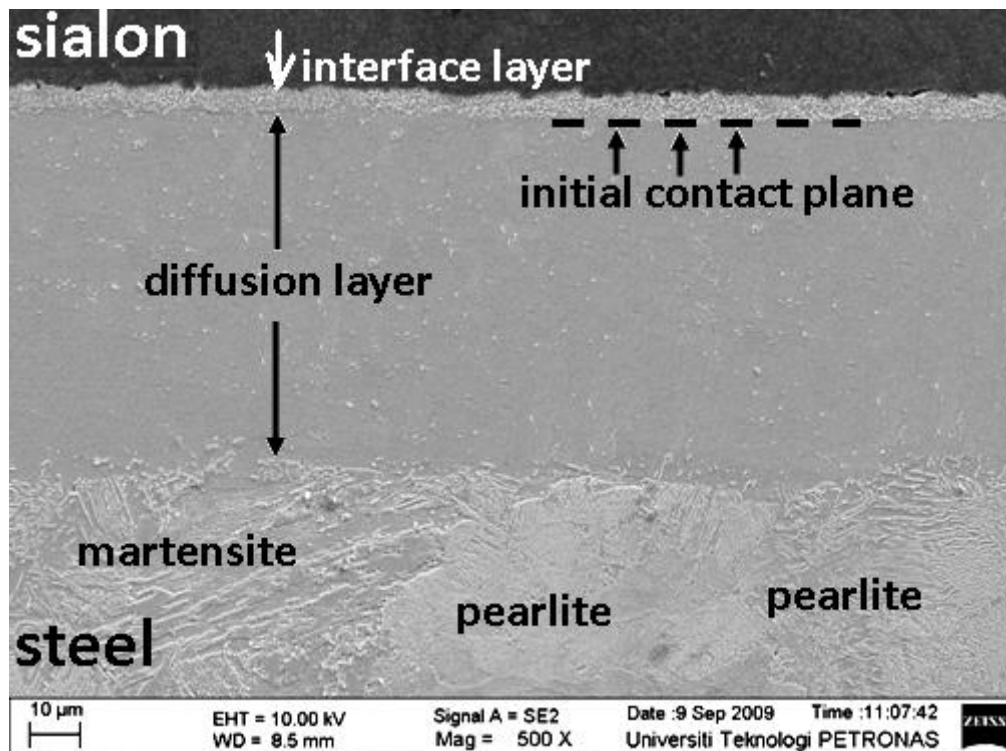


Figure 4.23 Scanning electron micrograph of the cross section of sialon – one-hour-nitrided AISI 430 FSS joint

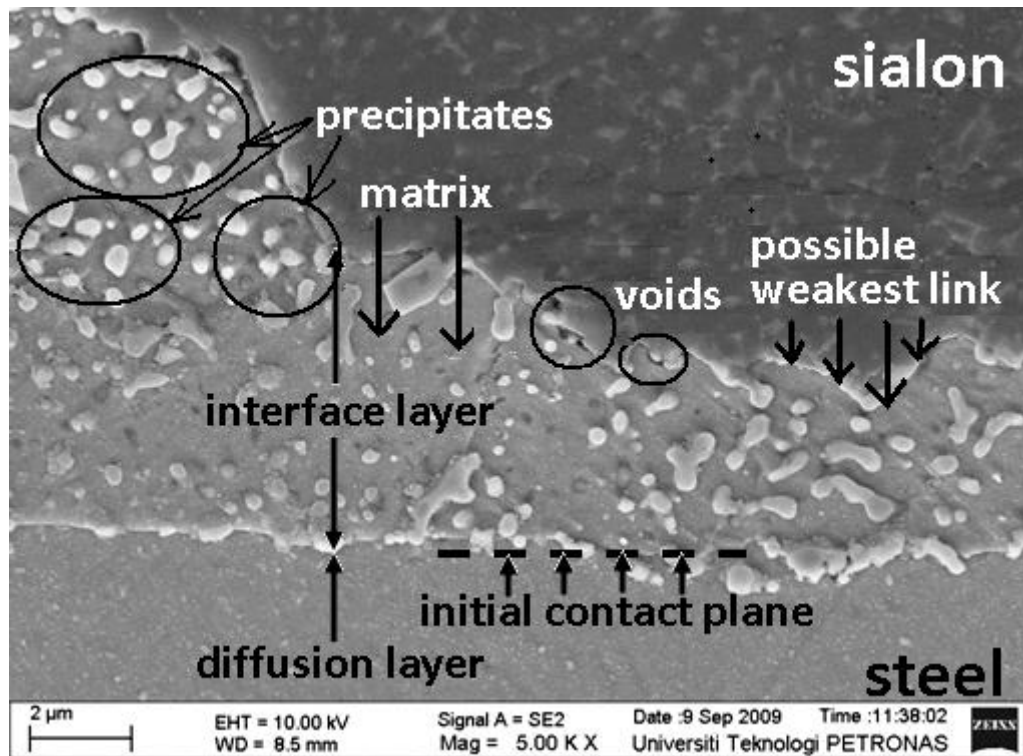


Figure 4.24 Scanning electron micrograph of the cross section of the interface layer in sialon – one-hour-nitrided AISI 430 FSS joint

The initial contact plane of sialon – steel in the joint was no longer appeared (Figure 4.24). This was caused by the reaction product of the materials that composed the joint. Therefore, the same phase was formed across the initial contact plane leading to the cohesive joint of the sialon with the steel. However, the border between the original sialon and the interface layer was clearly recognized in the microstructure of the interface layer shown in Figure 4.24. This part looked to turn into a new sialon–steel interface after the diffusion bonding. This was resulted due to penetration of the steel into the decomposed-part of sialon during the joining process. It could be expected that properties of the interface layer would be more similar to the steel properties as it was dominated by the steel phase. This has also been proven from the hardness test across the sialon – as-received AISI 430 FSS joint (Figure 4.21). On the other side, the original sialon remains very hard. Therefore this was the boundary of the two areas with extremely-different properties. Consequently this part could be the weakest zone of the joint. This part might become more critical as voids were also observed. The presence of the voids in this area might endanger the joint as this could initiate crack when the joint was subjected to working load during its service.

It was difficult to distinguish the joint of nitrided steel – sialon with as-received steel – sialon joint from the microstructure. The morphology of the joint as well as the parent metal was very similar. They also comprised similar phases. However, the interface layer and the diffusion layer in this joint were thinner than the layers in the sialon – as-received steel joint. The average thickness of the interface layer in this joint was 3.8 μm , whereas the thickness of the diffusion layer was 73.4 μm . These were smaller than the interface and the diffusion layers in the sialon – as-received steel joint which were 4.45 μm and 78.57 μm . This could be an early indication that the nitrided steel reduced the thickness of the interface layer as well as the diffusion layer. However, observation on the joining of the sialon with the longer-nitrided-steel might produce better information to reveal this prediction.

4.2.2.2 Elemental Analysis

EDX analysis on the overall joint depicted the diffusion elements from the sialon into the steel and *vice versa*. This was shown in Figure 4.25. The figure describes the similarity of the elements interdiffusion with the previous joining. For this joint, silicon diffused into the steel in approximately 70 μm from the initial contact of the sialon – steel. This was estimated from the figure. Alternatively, the length of the silicon-diffusion distance could be determined from the thickness of the diffusion layer. The average diffusion-layer thickness measured in the microstructure in this joint was 74.3 μm . This value was shorter than the thickness of the layer obtained in the sialon – as-received steel joint. This also means that the silicon diffused into shorter distance from the interface. It could be an early indication of shorter silicon-diffusion in the steel when the sialon was joined with the nitrided steel. Joining the sialon with longer-nitrided steel might produce more information to examine the prediction.

As also observed in joining of sialon – as-received steel, the interface layer was the reaction zone of the sialon and the steel in the ceramics side. This was revealed by the elements from both materials in this layer. It also disclosed that diffusion of Fe and Cr from the steel into the sialon also occurred in this joining. In this joint, the

average thickness of the layer was 3.8 μm . This was thinner than the layer in the joint of the sialon with the as-received steel.

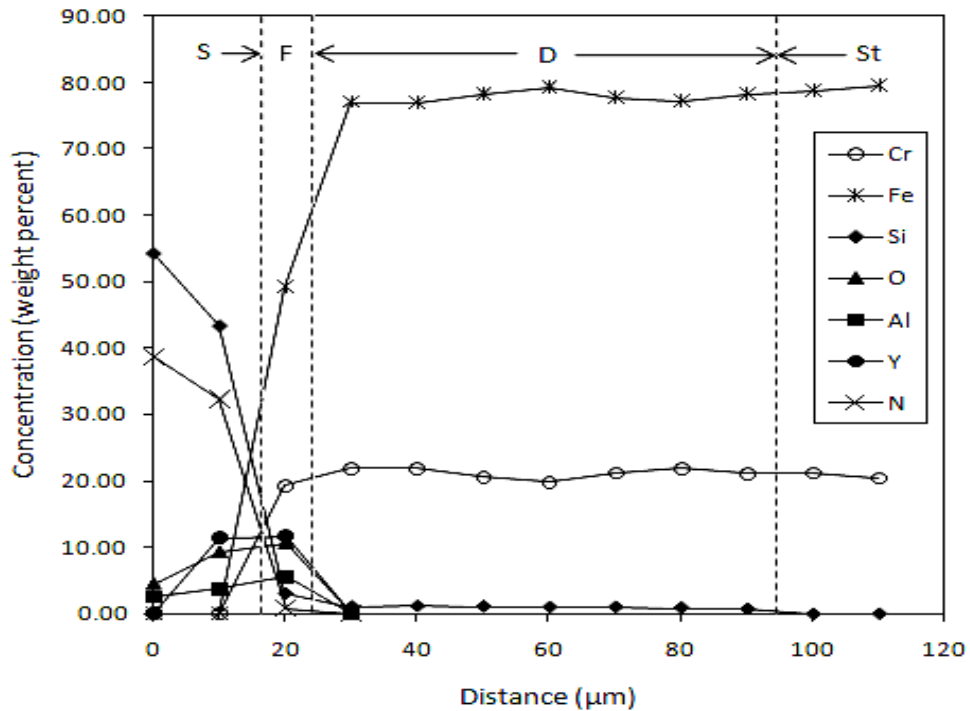


Figure 4.25 Concentration profile of elements across the sialon – one-hour-nitrided AISI 430 FSS joint; S=sialon, F=interface layer, D=diffusion layer, St=steel

Further analyses of elements in the interface layer and the precipitates were executed on the spots that selected randomly in the layer. The map of the spots in the interface-layer matrix and the precipitates for the EDX analyses is presented in Figure 4.26. The results of the analyses on the interface-layer matrix and the precipitates are presented in Table 4.3 and Table 4.4, respectively.

Matrix of the layer contained mainly Fe, Cr and Si (Table 4.3). Nevertheless other sialon's elements were also found in several spots. Fe was found in highest concentration than the other elements (*i.e.* 67.59 – 78.36 weight percent). Concentration of Cr was 14.90 – 24.86 weight percent; while Si was found in 1.47 – 1.96 weight percent. The existence of Fe and Cr disclosed the diffusion of the steel's elements into the sialon. These were shown in the results of the EDX-random-spot analyses on the interface-layer matrix (Table 4.3) and the precipitates (Table 4.4).

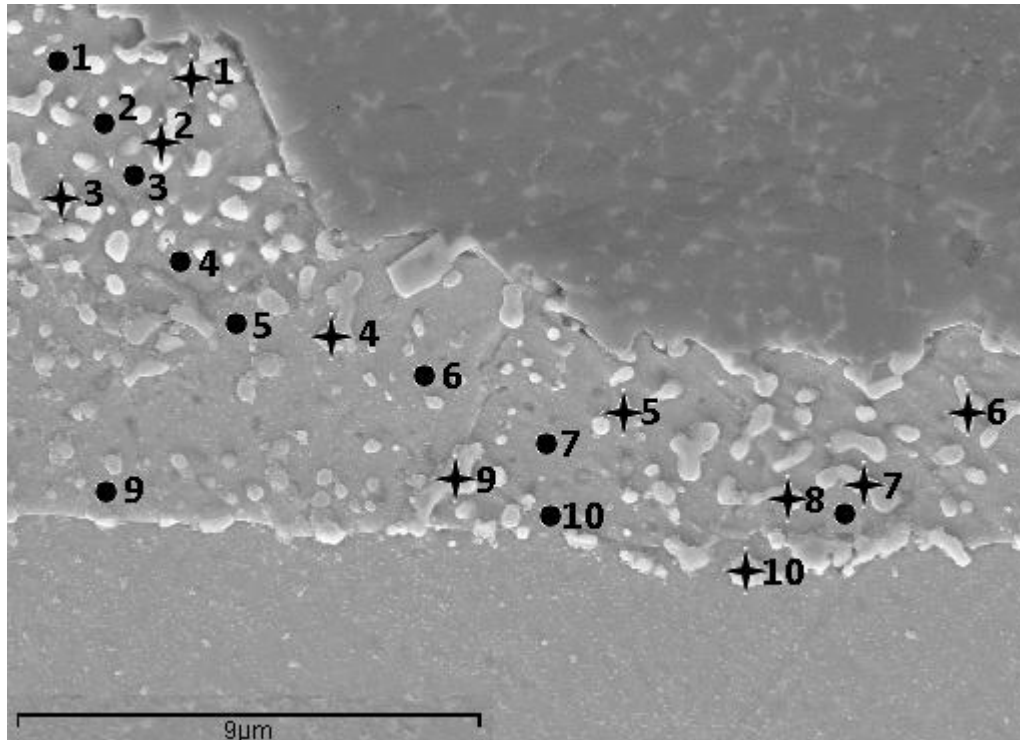


Figure 4.26 Map of EDX spot analysis at the interface layer of sialon – one-hour-nitrided AISI 430 FSS joint; (●) = matrix, (+) = precipitates

Table 4.3 Concentration of elements of the interface-layer matrix in sialon – one-hour-nitrided 430 FSS joint

Spot number	Concentration (weight %)						
	Cr	Fe	Si	O	Al	Y	N
1	21.86	76.18	1.96	0	0	0	0
2	21.60	76.92	1.47	0	0	0	0
3	20.88	77.53	1.60	0	0	0	0
4	24.86	72.60	1.60	0	1	0	0
5	14.90	76.16	1.62	2.96	1.53	2.84	0
6	21.18	77.25	1.57	0	0	0	0
7	22.17	76.32	1.52	0	0	0	0
8	19.94	78.36	1.70	0	0	0	0
9	17.89	67.59	1.84	5.32	2.56	4.79	0
10	21.53	76.94	1.53	0	0	0	0

Analysis on the interface layer in the previous joining concluded that silicon dissolved in the ferrite-iron solid solution in the interface-layer matrix. This was proven by the XRD examinations on the layer. The interface-layer matrix in the present joint had similar compositions of elements with the layer matrix obtained for the previous joining. Therefore, most probably the interface-layer matrix in the joint

also comprised the ferrite solid solution with silicon and other elements dissolved in it.

Table 4.4 Concentration of elements of the precipitates at the interface layer in sialon – one-hour-nitrided 430 FSS joint

Spot number	Concentration (weight %)						
	Cr	Fe	Si	O	Al	Y	N
1	9.83	53.45	5.33	12.36	6.44	12.58	0
2	18.48	53.97	2.79	9.11	5.72	9.95	0
3	17.01	58.01	2.37	7.66	5.33	9.62	0
4	12.93	59.93	2.71	9.93	4.83	9.67	0
5	16.04	57.24	2.70	9.75	5.36	8.90	0
6	15.72	28.90	3.87	19.00	10.14	22.38	0
7	10.09	67.12	2.11	8.38	4.11	8.20	0
8	16.94	38.86	4.71	15.32	5.61	18.55	0
9	14.63	52.19	3.32	11.44	5.94	12.48	0
10	14.36	45.26	2.40	13.88	8.09	15.99	0

It was recognized in section 4.2.1 that high concentration of Fe and Si in the precipitates in the joint of sialon – as-received AISI 430 FSS led to the formation of $FeSi_2$. Nitrides were also predicted based on the nitrogen content of the precipitates. Thus with lesser amount of silicon and nitrogen in the precipitates, it could be expected that silicides and nitrides might not present in the precipitates. In other words, nitrided steel might have suppressed the formation of the silicides and the nitrides in the interface of the joint. Further characterization was carried out to scrutinize the unavailability of the compound. Later part of this section will report the results of the work.

The average thickness of the interface layer and the diffusion layer for this joining condition were 3.8 μm and 74.3 μm , respectively. It has been mentioned in the previous section that these were smaller than the thickness of the interface and the diffusion layers in the sialon – as-received steel joint. In that joint, the thickness of the interface and the diffusion layer were 4.45 μm and 78.57 μm , respectively. Since the interface layer represented the decomposed part of the sialon and the reaction front of the joined materials, thus thinner interface layers divulged less decomposed sialon and also less reactivity of the materials. A few workers [77-80] referred to the thickness of the layer to justify the reactivity of the joined materials.

Former discussions established that the interface layer was the sialon-decomposed part. This was also the reaction front of the sialon and the steel in the sialon side. The thickness of the interface layer indicated the sialon part that was consumed for the reaction of the ceramics with the steel to produce the joint. In the steel, the thickness of the diffusion layer represented the length of silicon-diffusion distance. Oliveira *et al.* [77-78] found that in the joint of Si_3N_4 with steel, the thickness of the interface layer correlated well with the thickness of the diffusion layer. Thinner reaction layers in the present joint could be a hint of the less reactivity of the sialon with nitrated steel than with the steel in as-received condition. Study on the joining of the sialon with the longer-nitrated steel might also be required to provide better description on this phenomenon.

4.2.2.3 XRD

XRD pattern from the interface layer surface of the sialon – one-hour-nitrated steel joint is given in Figure 4.27. Apparently only α peak was found in the layer. No other phase was observed. Ferrite phase in the pattern emerged from the matrix of the layer which consisted of Fe, Cr and low-concentration Si. The diffusion layer should also comprise the ferrite phase as it had similar composition of elements. As it was expected, silicide was not present in the interface layer. Therefore the nitrated steel might have hindered the precipitation of silicide in the joint interface.

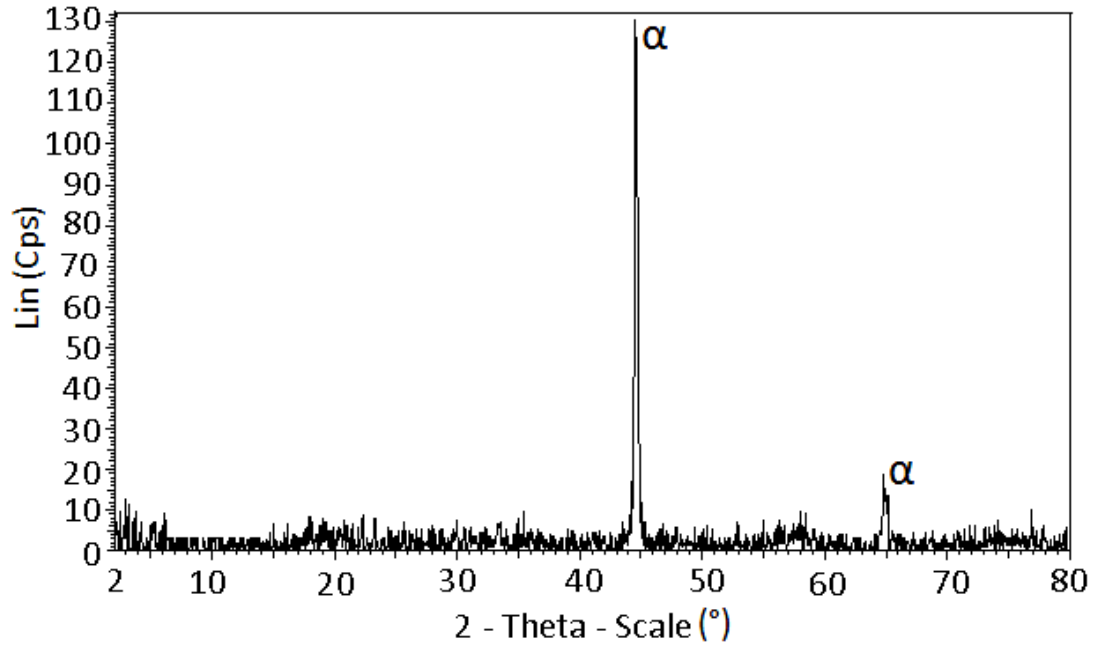


Figure 4.27 X-ray diffractogramme of the interface layer in sialon – one-hour-nitrided 430 FSS joint

4.2.2.4 XPS

To study the FeSi_2 , XPS analysis was carried out on the surface of the steel from the broken sample. XPS spectra for Fe and Si are given in Figure 4.28 and Figure 4.29, respectively. The spectra were similar with spectra obtained in the previous joining. Four peaks of Fe_{2p} were produced in the XPS spectra. However, in the present joint, the spectra did not clearly indicate the existence of plasmon loss at around 730 eV which was the sign of FeSi_2 compound. Therefore, two peaks at 706.92 eV and 719.58 eV were attributed to metallic Fe [87] rather than the FeSi_2 . According to the same reference, the other two peaks (*i.e.* at 710.98 eV and 724.3 eV) represented the Fe in the form of Fe_2O_3 .

Symmetrical spectrum of Si from the interface layer shown in Figure 4.29 characterized a single chemical state of the Si_{2p} . The only produced peak was at 102.95 eV which corresponded to Si_{2p} from SiO_2 [85, 88-89].

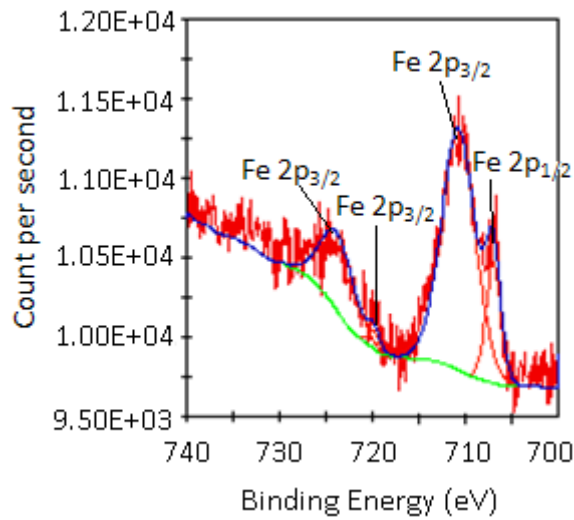


Figure 4.28 XPS spectra of Fe from the interface layer in sialon – one-hour-nitrided AISI 430 FSS joint

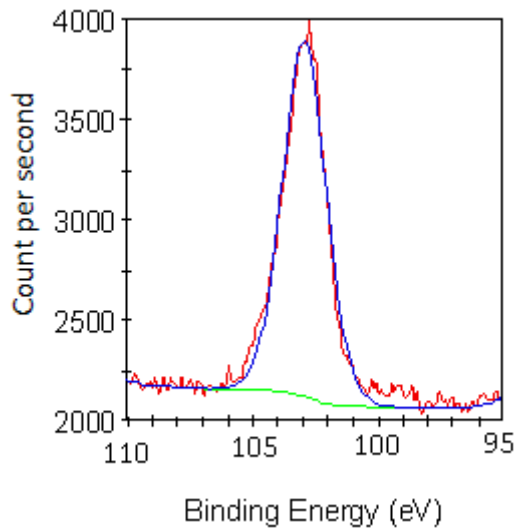


Figure 4.29 XPS spectra of silicon from the interface layer in sialon – one-hour-nitrided AISI 430 FSS joint

The XPS results established the absence of the silicides in the layer. The analysis showed Fe in the form of Fe_2O_3 and Si in the form of SiO_2 . Yet, the oxides were not detected by the XRD. These oxides were also found in the XPS examination of the interface layer in the joint of sialon – as-received steel. Thus, in this joint, Fe^{3+} reacted with O^{2-} to form the Fe_2O_3 . Recombination of Si^{4+} and O^{2-} which were released from the decomposed sialon occurred to produce the SiO_2 in the precipitates.

Characterizations on the interface layer (EDX, XRD and XPS) demonstrated a coherent result on the existence of the FeSi_2 . The iron silicide was found in the joint of sialon – as-received steel. Nevertheless, it was not formed in the interface layer of the sialon – one-hour-nitrided steel joint. In the joint of sialon – nitrided steel, the absence of the iron silicides was proven by the XRD and XPS. This divulged that nitrided steel had suppressed the formation of the silicide in the joint.

4.2.2.5 Hardness Test across the Joint

Figure 4.30 shows the hardness of the cross section of the joint. The diffusion layer was the area with the lowest hardness. This was due to the same reason for the hardness of the layer in the previous joining condition. The layer consisted of ferrite phase which was soft and ductile. Consequently the hardness of the layer was lower than the hardness of pearlite and martensite in the parent steel. In the interface layer, the precipitates which consisted of oxides contributed the hardness enhancement on the layer. Therefore, it appeared in Figure 4.30 that the hardness of the layer was slightly higher than the diffusion layer.

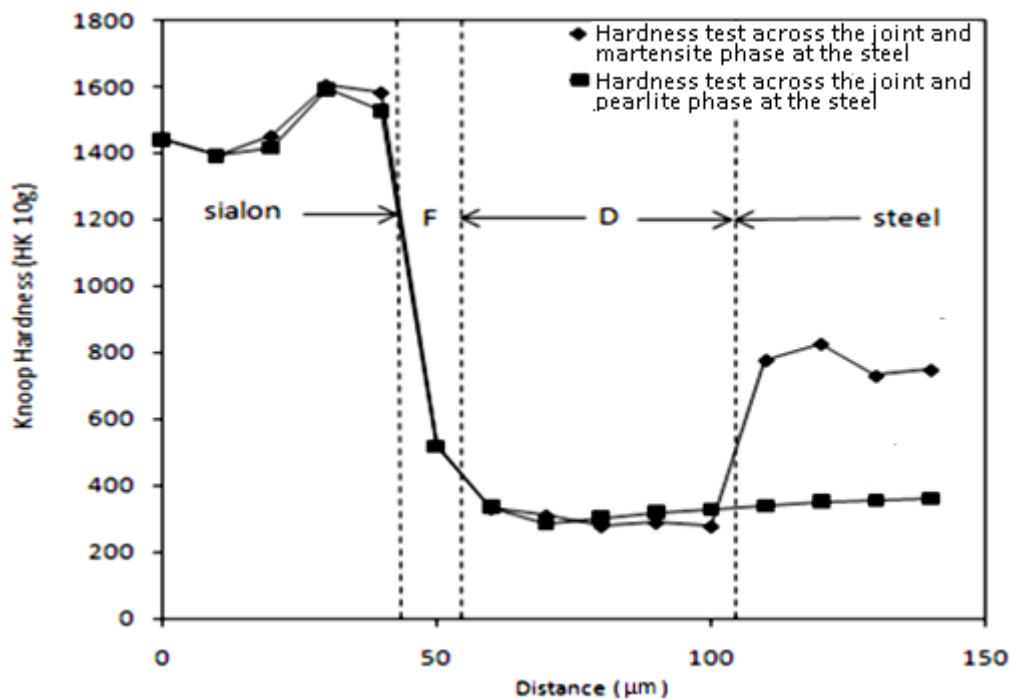


Figure 4.30 Hardness test across the joint of sialon – one-hour-nitrided AISI 430 FSS joint; F=interface layer, D=diffusion layer

4.2.3 Joining of Sialon with Four-hours-nitrided AISI 430 FSS

Nitriding the AISI 430 FSS for four hours improved the hardness of the whole cross section of the sample. Martensite transformation was also exhibited throughout the steel after the nitriding. This had been reported and discussed in section 4.1.1. Since there was a correlation between the hardness improvement and the martensite formation in the steel, it was believed that nitriding for four hours had dissolved the nitrogen throughout the steel. The four-hours-nitrided steel was subsequently joined with the sialon. The joint of the sialon with the steel was studied and compared with the previous joining condition.

4.2.3.1 Microstructure of the Joint

Sialon – four-hours-nitrided AISI 430 FSS joint can be seen from the microstructure displayed in Figure 4.31 to Figure 4.33. Morphology of the present joint and the previous joints were alike. Figure 4.32 and Figure 4.33 illustrate the interface and the diffusion layers in the joint which were also produced in the previous joining.

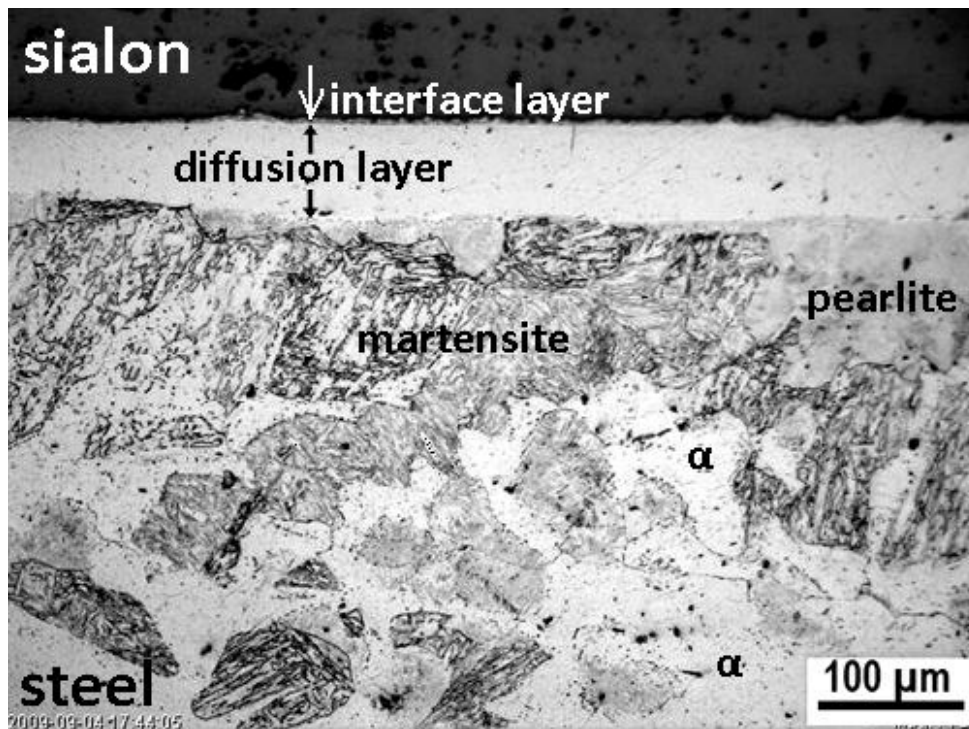


Figure 4.31 Optical micrograph of the cross section of sialon – four-hours-nitrided AISI 430 FSS joint

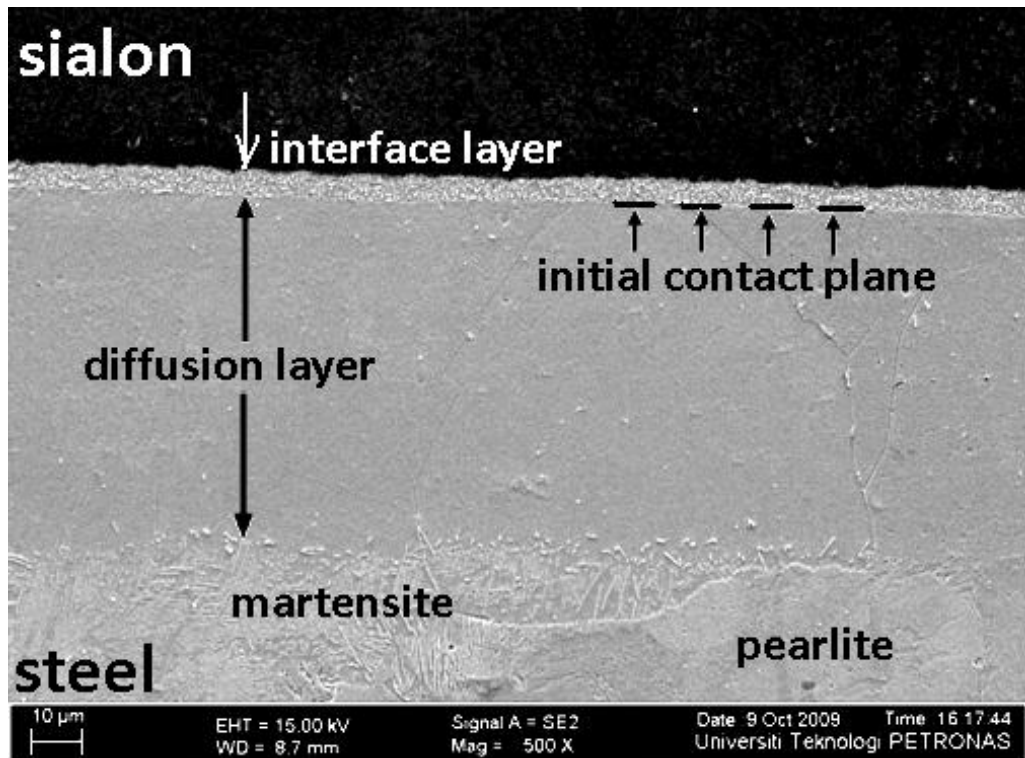


Figure 4.32 Scanning electron micrograph of the cross section of sialon – four-hours-nitrided AISI 430 FSS joint

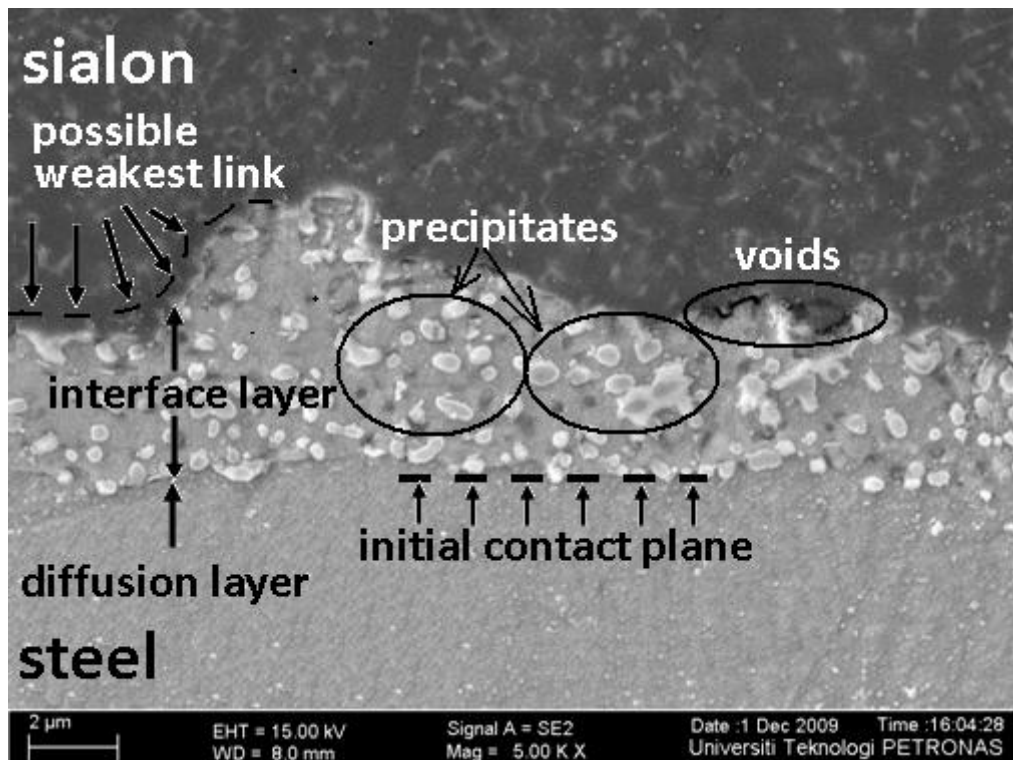


Figure 4.33 Scanning electron micrograph of the cross section of the interface layer in sialon – four-hours-nitrided AISI 430 FSS joint

Microstructure of the diffusion layer show that the layer consists of a single phase. This is illustrated in Figure 4.31 to Figure 4.33. Overall region of the diffusion layer comprises area with same contrast. No grain boundary was shown in the microstructure of the diffusion layer. Therefore, a single-phase in the diffusion layer is indicated. White precipitates were seen throughout the interface layer. It was clearly seen in the detail of the interface layer presented in Figure 4.33. Optical micrograph of the joint given in Figure 4.31 illustrates more martensite in the parent steel adjacent to the diffusion layer. The more martensite in the steel after the joining could be expected due to the longer nitriding of the steel prior to the joining. Figure 4.31 also illustrates the presence of pearlite in the area near the diffusion layer.

The boundary between the original sialon and the interface layer was noted. This could become the weakest part at the joint was. The original sialon and the interface layer should own very different properties. This has been observed in the two previous joining conditions. Therefore, the boundary between the original sialon and the interface layer might also become the most critical part. Voids were also seen in this borderline. This could worsen the part as the weakest link in the joint.

4.2.3.2 Elemental Analysis

Results of EDX analysis across the joint (Figure 4.34) outlined the sialon decomposition and the elements interdiffusion at the joint. Elemental analysis of the overall joint in this joining denoted the similarity with the two previous joining conditions. However, silicon diffused into the steel shorter than the two former joining conditions. In this joint, the silicon diffusion into the steel is approximately 55 μm from the initial contact plane. This was estimated from Figure 4.34. More precise thickness of the layer was obtained from the measurement. The average thickness of the diffusion layer and the interface layer measured in the microstructure was 59.6 μm and 3.4 μm , respectively. In the interface layer, change of the sialon's elements composition depicted the decomposition of the sialon. Diffusion of the steel's elements into the sialon was recognized from the existence of Fe and Cr in this area.

Elements in the interface layer were scrutinized at the interface-layer matrix and the precipitates. A number of spots were determined randomly throughout the cross section of the layer. It was expected that the spots analyses could represent the precipitates and the interface-layer matrix in the overall observed area. The spots for the EDX analysis on the precipitates and the interface-layer matrix of the sialon – four-hours-nitrided AISI 430 FSS joint are shown in Figure 4.35.

The output of EDX analysis on the interface-layer matrix and the precipitates are tabulated in Table 4.5 and Table 4.6, respectively. The sialon’s elements were distributed into the interface-layer matrix and the precipitates (Table 4.5). Therefore, as established for the previous joining, this layer was the decomposed sialon. These were also exhibited in the present joint. However, only silicon was found in the interface-layer matrix (Table 4.5). The element was identified in the spots with smaller quantity (*i.e.* 1.18 – 1.96 weight percent) than the Fe and Cr. The silicon should have diffused into the iron to form ferrite solid solution. This considered the investigation that was conducted for the previous joining.

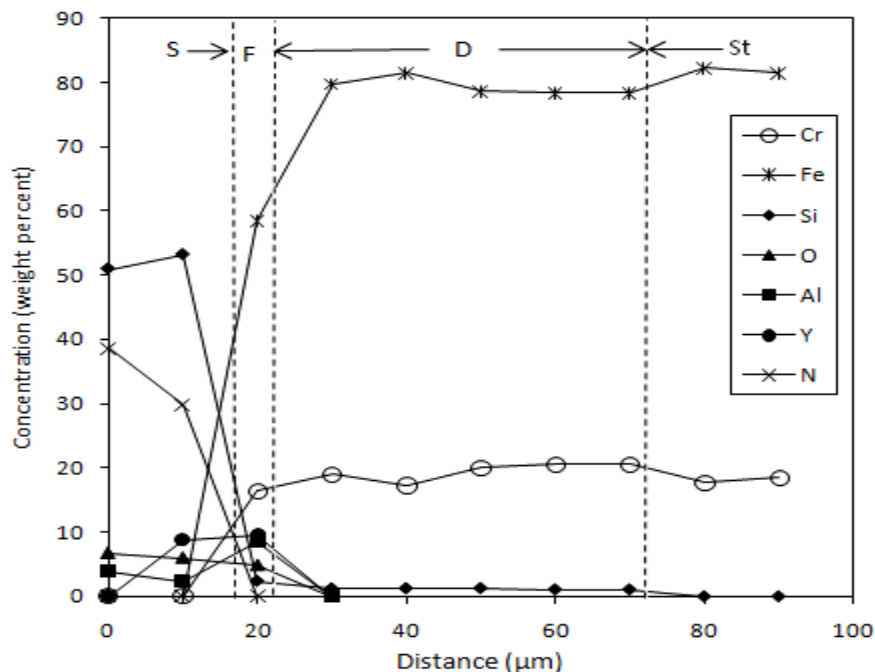


Figure 4.34 Concentration profile of elements across the sialon – four-hours-nitrided AISI 430 FSS joint; S=sialon, F=interface layer, D=diffusion layer; St=steel

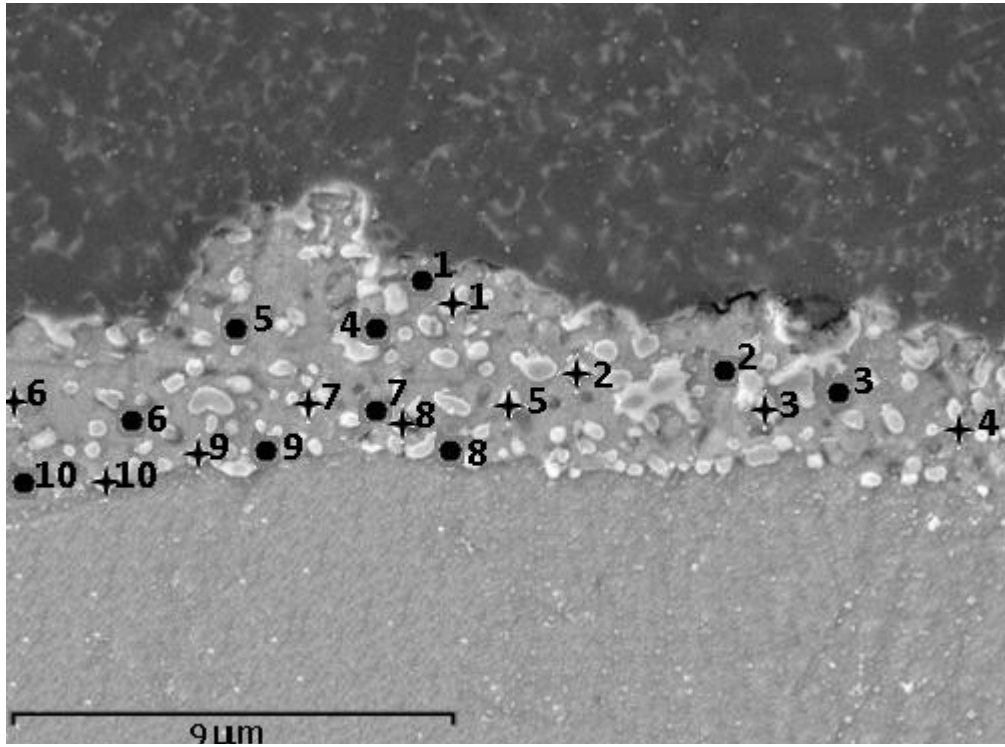


Figure 4.35 Map of EDX spot analysis at the interface layer of sialon – four-hours-nitrided AISI 430 FSS joint; (●) = matrix, (+) = precipitates

Table 4.5 Concentration of elements of the interface-layer matrix in sialon – four-hours-nitrided AISI 430 FSS joint

Spot number	Concentration (weight %)						
	Cr	Fe	Si	O	Al	Y	N
1	17.91	80.51	1.57	0	0	0	0
2	23.81	73.74	1.86	0	1	0	0
3	20.56	77.92	1.52	0	0	0	0
4	19.42	78.98	1.60	0	0	0	0
5	17.91	80.36	1.75	0	0	0	0
6	22.44	76.37	1.19	0	0	0	0
7	20.51	77.96	1.52	0	0	0	0
8	21.65	77.15	1.19	0	0	0	0
9	17.75	80.51	1.74	0	0	0	0
10	20.26	78.15	1.60	0	0	0	0

Table 4.6 Concentration of elements of the precipitates at the interface layer in sialon – four-hours-nitrided AISI 430 FSS joint

Spot number	Concentration (weight %)						
	Cr	Fe	Si	O	Al	Y	N
1	15.37	36.55	2.36	16.39	9.51	19.79	0
2	12.44	52.85	2.64	12.08	7.19	12.79	0
3	16.30	49.73	2.72	10.55	7.00	13.69	0
4	12.67	72.40	2.26	4.25	3.36	5.07	0
5	14.60	62.44	1.85	7.96	4.90	8.25	0
6	14.60	62.44	1.85	7.96	4.90	8.25	0
7	16.01	54.63	2.22	10.40	5.86	10.88	0
8	19.76	52.21	2.05	9.21	5.06	11.69	0
9	23.65	74.01	1.64	0	0.70	0	0
10	14.76	79.52	1.85	2.68	1.18	0	0

The precipitates were no longer rich of Si as it was found in the joint of the sialon – as-received steel. Nitrogen was not discovered either (Table 4.6). Its concentration could be too small to be detected by EDX. The chemical compositions of the precipitates was similar with the condition in the joint of sialon – steel nitrided for one hour joint. Therefore, most probably the precipitates did not contain silicides or nitrides. This divulged that joining of the sialon with the nitrided steels (*i.e.* for one and four hours) produced consistent results. Both joining might have suppressed the formation of silicides in the joint.

Analysis on the joint of the sialon – one-hour-nitrided AISI 430 FSS indicated that the reaction layers were thinner than the layers in the sialon – as-received AISI 430 FSS joint. Therefore, it shows that the nitrided steel had decreased the sialon decomposition as well as the sialon – steel reactivity. Thickness of the layers in the presents joint supported this idea. The interface layer and the diffusion layer in this joint were thinner than the layers produced by the two former joining. The four-hours-nitrided AISI 430 FSS – sialon joint produced the average thickness of 3.4 μm and 59.6 μm for the interface layer and the diffusion layer, respectively. This was smaller than the thickness of the layers in one-hour-nitrided AISI 430 FSS – sialon joint (*i.e.* 73.4 μm of the diffusion layer and 3.8 μm of the interface layer). Obviously these were also thinner than those produced in the joint of the sialon – as-received AISI 430

FSS joint, which were 78.57 μm and 4.45 μm for the diffusion layer and the interface layer, respectively. This observation disclosed that the nitrided steel had decreased the sialon decomposition in the joint of the sialon – AISI 430 FSS. Consequently, it reduced the reactivity of the sialon with the steel in the sialon side. The decrease of the diffusion layer thickness also concluded that the nitrided steels shortened the diffusion extent of the silicon into the steel.

4.2.3.3 XRD

Ferrite phase in the interface-layer matrix was revealed by α peaks in the XRD pattern of the layer (Figure 4.36). The peak emerged from the interface layer as it consisted of Fe, Cr and Si. With the same reason in estimating the phase in the layers for the previous joining, the diffusion layer should have the same phase.

With respect to the low silicon in the precipitates, it was unlikely that the iron silicides would exist. The X-ray diffractogramme of the layer revealed this. Phase identification using this technique proved the absence of FeSi_2 in the layer. This had also been proven for the joint of sialon – one-hour-nitrided steel. Therefore, it supported the indication that nitriding treatment on the steel prior to joining had suppressed the formation of iron silicide in the layer.

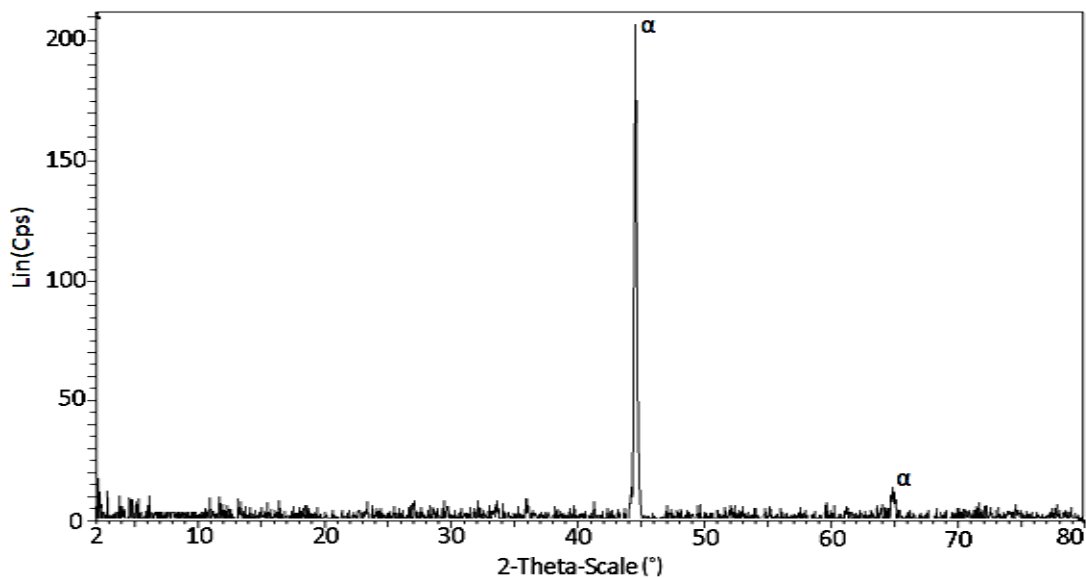


Figure 4.36 X-ray diffractogramme of the interface layer in sialon – four-hours-nitrided AISI 430 FSS joint

4.2.3.4 XPS

XPS spectra for Fe and Si from the interface layer were shown in Figure 4.37 and Figure 4.38, respectively. The XPS spectra provided four peaks of Fe_{2p}, namely: at 706.94 eV, 712.04 eV, 719.8 eV and 725.13 eV (Figure 4.37). Plasmon loss at around 730 eV (which indicates the FeSi₂ peak) did not present. Therefore, two peaks at 706.94 eV and 719.8 eV should correspond to metallic Fe [87, 89]. Based on the same references, Fe was also in oxide form (Fe₂O₃). This was represented by the other two peaks at 712.04 eV and 725.13 eV.

The Si spectrum in the Si XPS spectra (Figure 4.38) disclosed that the silicon was only in one chemical state (*i.e.* SiO₂). This was shown by the peak at 103.96 eV that was the only peak at the spectra. Therefore the XPS examination revealed that the FeSi₂ was not present in the layer.

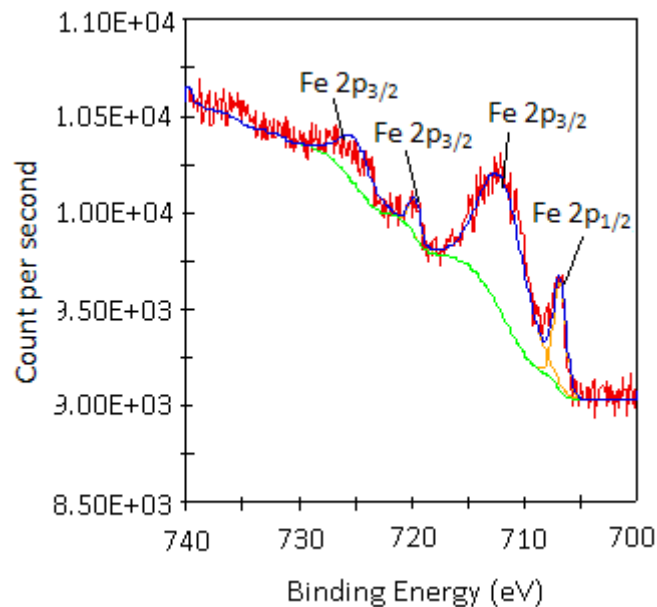


Figure 4.37 XPS spectra of Fe from the interface layer in sialon – four-hours-nitrided AISI 430 FSS joint

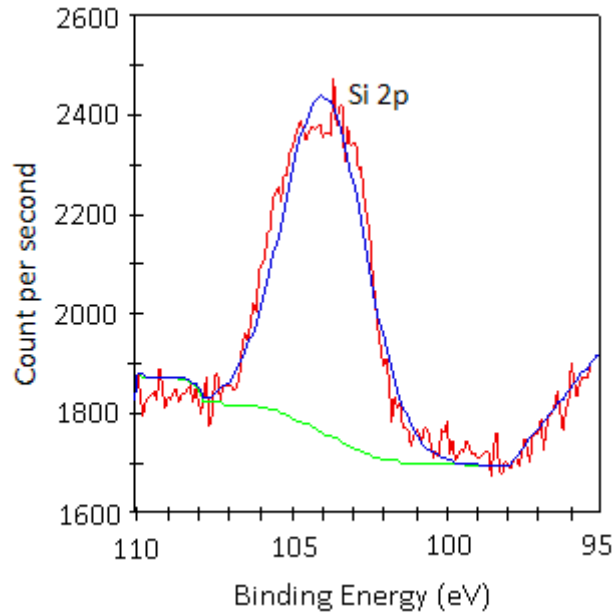


Figure 4.38 XPS spectra of Si from the interface layer in sialon – four-hours-nitrided AISI 430 FSS joint

4.2.3.5 Hardness Test across the Joint

Hardness of the cross section of the joint is illustrated in Figure 4.39. The diffusion layer was shown again as the lowest-hardness part of the joint. The interface layer was slightly harder than the diffusion layer due to the contribution of the hardness given by the precipitates. This layer was like the steel part that moved into the decomposed area of the sialon. Therefore its hardness should represent hardness of the steel. However, the precipitates which were a mixture of steel's and sialon's elements had increased the hardness slightly higher than the steel. Compared to the original sialon, lower hardness could be expected for it was the decomposed part of the sialon.

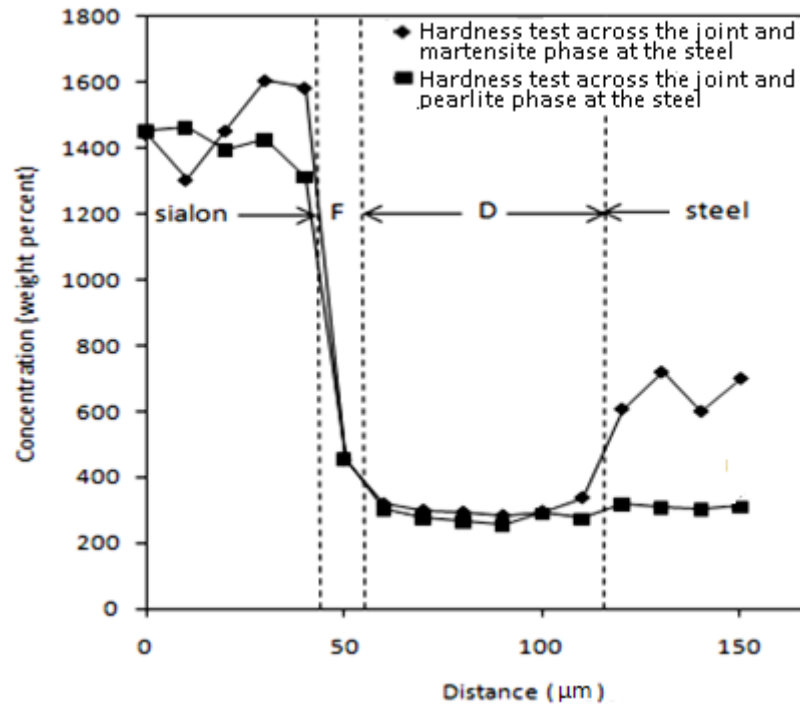


Figure 4.39 Hardness test across the sialon – four-hours-nitrided AISI 430 FSS joint;
 F=interface layer, D=diffusion layer

4.2.4 Discussion

Previous sections of this chapter presented the results of the sialon – as-received AISI 430 FSS joining. Interfacial joint of the materials was achieved in all joining conditions. Reactions of the joined materials were indicated. These had been identified and analyzed using several characterization techniques. This section discusses the overall results of the joining as well as the reaction layers in the joint.

4.2.4.1 Joining of Sialon – As-received Steel

Interfacial joint of sialon with as-received AISI 430 FSS was observed in the microstructure of the interface cross section. The joint was attained due to the reaction of the sialon with the steel.

Reaction layers in the joint comprised silicon-diffusion layer in the steel side and interface layer in the sialon side. Sialon decomposed and released silicon and nitrogen

that diffused into the steel. Fe and Cr from the steel diffused into the sialon-decomposed part. Interaction of the steel's elements in this part formed ferrite solid solution in the interface layer matrix. This was produced since Cr and Si are ferrite formers. Fe reacted with other sialon's elements to form precipitation of silicides and oxides in the form of white precipitates.

Matrix of the interface layer has same contrast with the steel part in the diffusion layer. Elemental analysis of the interface layer matrix also revealed that the elements of the interface layer matrix and the diffusion layer were similar. Analyses on the phase of these parts divulged that the diffusion layer and the interface layer matrix consisted of the same phase, *i.e.* α -Fe (Cr, Si). Thus, those parts were actually the same species. This species composed the joint of the sialon with the steel. Therefore, the same species was found across the initial contact plane. This made the initial sialon – steel contact plane disappeared and indicated cohesive joint at the sialon – steel interface.

Discussion on the preceding paragraph explained that during the diffusion bonding process, steel penetrated into the sialon and reacted with the sialon's element. This reaction also occurred in the diffusion layer. The steel moved across the joint and shifted the interfacial contact deeper into the sialon part. Hence, the border between the sialon and the original part was just like new steel – sialon interface. This area could possibly become the weakest part of the joint as this was the boundary between the original sialon and steel which have very-different properties.

Microstructure of the parent steel changed from ferritic to pearlitic and martensitic structure. The pearlite phase is possibly the nitrogen pearlite. Previous works had observed the similar phase in the interaction of silicon nitride – Fe-Cr alloy [13] and in sialon – steel-composite joint [82]. Those works predicted that the structure was nitrogen pearlite. Section 2.3 describes that besides stimulating martensite formation, nitrogen may also precipitate into nitrides. This was observed in nitriding of 17Cr-1Ni-0.5C martensitic stainless steel at 1050°C for one hour under 98.07 kPa of nitrogen [48]. Calculated vertical section phase diagram of Fe-24%Cr – (0-2.5)%N system given Figure 2.7 in section 2.3 explains that nitrogen pearlite (α +Cr₂N) is formed when the alloy is cooled down to below 1300K [49]. It suggests the possibility

of the pearlitic transformation (*i.e.* $\alpha + Cr_2N$) in the region of 1.0 – 2.5% N. Thus, during the diffusion bonding, nitrogen diffused into the steel. It produced Fe-Cr – N alloy system. Upon slow cooling in the furnace, nitrogen pearlite was possibly formed as suggested by Figure 2.7. This was seen in the area close to the diffusion layer. It seemed that the nitrogen diffusion is limited into this area, therefore the pearlite structure diminished in the core of the parent steel.

The formation of the martensite in the parent steel during the joining also seemed to be affected by the existence of the nitrogen. The results of nitriding experiment reported in section 4.2 divulged that nitrogen stimulated the formation of martensite in heat treatment of the AISI 430 FSS. This has also been recognized in other nitriding works [49-50]. Hence, the martensite formation in the parent steel during the joining could be the sign that nitrogen had diffused into the area.

Decomposition of the sialon occurred in the interface of the joint according to reactions 2.8 and 2.9 presented in section 2.6.1. Si_3N_4 decomposed through the gas-phase reaction (reaction 2.8) at above 636°C. Nitrogen dissolved in the steel according to reaction 2.9 at above 1033°C. In the current work, decomposition of the sialon also happened in the interface layer according to the same reactions.

Nitrogen that was released from the ceramics decomposition was distributed in several manners. This was noticed by previous works [6-7]. At the edge of the joined sample, close to the atmosphere, molecular nitrogen would be released to the surrounding atmosphere. Around the middle of the joint, nitrogen could not be liberated from the interface. Therefore it could be trapped in the interface and produced porosities. The porosities were observed in the microstructure of the joint. The nitrogen could also dissolve in the steel or precipitated as nitride when it met metallic nitride formers such as Fe or Cr [77-78]. In this work, chromium nitride was possibly formed in the joint of the sialon with the as-received steel as nitrogen was detected in relatively significant concentration in the precipitates which also contained the nitride formers (*i.e.* Fe and Cr). The nitrogen might also diffuse into the parent steel as indicated by the martensite phase.

The liberated-silicon diffused into the steel and formed the silicon-diffusion layer. The elements in the diffusion layer are Fe and Cr from the steel and silicon from the sialon. In this layer, the silicon content is 0.94 – 1.57 weight percent. At the reaction front in the sialon side, the silicon is in 1.76 – 3.27 weight percent concentration. The element dissolved in Fe and Cr which transferred towards the interface layer. Concentrations of Fe and Cr in the layer are 60.67 – 80.13 weight percent and 11.38 – 24.64 weight percent, respectively. It implied the similar element compositions of the interface-layer matrix and the diffusion layer. The transfer of Fe and Cr in significant amount into the sialon made the interface-layer matrix and the diffusion layer to have same contrast in the micrograph. Therefore, the microstructure depicted a steel-like phase in the interface-layer matrix.

Similarity of chemical composition and contrast between the interface-layer matrix and the diffusion layer indicated that the interface-layer matrix and the diffusion layer might own the same phase. XRD revealed that the interface-layer matrix and the diffusion layer consisted of the same phase, *i.e.* α -Fe (Cr, Si). Thus, in the diffusion layer, Si and Cr dissolved in the steel in the form of α -Fe (Cr, Si) solid solution. The presence of Si and Cr in the interface and the diffusion layers enhanced the ferrite formation since they are both ferrite formers [77-78]. Phase diagram of Fe – Si system (Figure 2.11) illustrates the maximum solubility of 10.9 weight percent (13.4 atomic percent) of Si in the α -Fe (Si). Heikinheimo *et al.* [6] discovered the same phase with maximum 12 atomic percent of Si in the interface of Si_3N_4 and iron. In the present work, silicon in the interface-layer matrix and in the diffusion layer had formed ferrite phase with maximum Si content of 3.58 weight percent (7.71 atomic percent). This was in a good agreement with the α -Fe (Si) solid solution in the phase diagram of Fe – Si.

Solubility of silicon in iron (18 atomic % at 1200°C) is much higher than the solubility of nitrogen (0.089 atomic % at 1200°C) as reported by Vleugels *et al.* [15]. Thus it seemed that the diffusion of silicon had pushed the nitrogen from the steel adjacent to the interface towards the parent steel. It created a silicon diffusion zone in the diffusion layer.

The nitrogen moved from the steel adjacent to the interface into the parent steel. Beyond the silicon-diffusion layer, it promoted the formation of martensite when the samples were cooled to room temperature. Mechanism of the martensite formation in nitrogen influence was well established in nitriding works of the stainless steel. It has been explained in section 2.3; *i.e.* nitrogen interstitially diffused into the austenite when the stainless steel was heat treated under nitrogenous atmosphere at 1200°C. This was trapped in the lattice when the steel was cooled even in a slow rate [17]. Therefore, nitrided ferritic stainless steel exhibited martensite at the steel surface. The depth of the martensite case depended on the length of the nitriding. At the end of the nitrogen diffusion extent, ferrite was also formed when the austenite in the steel was slowly cooled from the temperature of 1100°C.

The above discussion describes that reaction of the steel and the sialon occurred in diffusion layer and interface-layer matrix. Interaction of the elements in the layer produced α -Fe (Cr, Si) solid solution. Reaction of the materials in the sialon side took place when the sialon decomposed and Fe and Cr from the steel moved towards the sialon and filled up the sialon-decomposed area. Besides the α -Fe (Cr, Si), reaction of the elements in this layer produced precipitates that contained the elements from the steel and the sialon. This was disclosed by the findings of both materials' elements in the precipitates.

In this joint, the precipitates were rich of Fe (*i.e.* maximum concentration of 66.39 weight percent) and Si (*i.e.* maximum concentration of 34.14 weight percent). Cr and N were also found in many spots with maximum concentration of 15.3 and 13.13 weight percent, respectively. Other elements of the sialon (Al and O) were also present in lower concentration. Therefore the precipitates were the reaction products of the steel and the sialon. With the high Fe and Si in the precipitates, the formation of Fe-Si compound could be expected; whereas chromium nitrides might also present due to the existence of Cr and N. Nevertheless, the presence of O in the precipitates might also stimulate the oxides formation.

The precipitates had been observed in the reaction zone of silicon nitride with iron or iron alloy. Section 2.6.2 discusses the phases in the reaction layer of silicon nitride and sialon with various kinds of steels. The findings of the phases in the previous

works are cited again in this section to help analyzing the results. Heikinheimo *et al.* [6] claimed that no new compound or silicide was formed in the reaction of Si_3N_4 with iron. Instead of the silicides or nitrides, they observed the precipitates as the silicon-enriched sintering additives. Two other works also found the same things [78-79]. Those work justified their findings through the elemental analysis on the reaction zone. No other characterization techniques were utilized to prove the phase in the precipitates. Despite their claim that no new compound was produced in the joint, Polanco *et al.* [10] recognized the presence of silicides (*i.e.* Mo_3Si , Fe_xSi_y), nitrides (Cr_2N) with $\alpha\text{-Fe}$ in the reaction front of Si_3N_4 – AISI 316L SS. Those were confirmed using the GIA-XRD examination that was attempted on the surface of the interface layer. The work divulged that characterization technique such as XRD on the surface of the interface layer might be helpful to identify the phase rather than only rely on the elemental analysis.

Reaction between sialon with iron alloy was investigated by Vleugels *et al.* [15]. This was conducted by contacting the materials with relatively low pressure (*i.e.* 2.5 MPa) at 1200°C. The precipitates were claimed to be Al_2O_3 . Besides using the EDX analysis results, the work also confirmed the presence of the Al_2O_3 using Raman spectroscopy on the cross section of the reaction zone. The Al_2O_3 was formed from the recombination of Al and O which were initially released through the dissociation of the sialon. Thus, reaction of the steel with the sialon in that work only produced ferrite solid solution in the interface-layer matrix and in the silicon-diffusion layer.

The joint of sialon with 9% Cr ferritic stainless steel was achieved with 20 MPa diffusion bonding pressure [5, 17]. The work found that the reaction layer in the joint consisted of $\alpha\text{-Fe}$ (Cr) solid solution matrix and also the precipitates. EDX analysis revealed the elements of the steel and the sialon in the precipitates. However, only typical face-centered-cubic (FCC) CrN was concluded through the diffraction pattern produced by the TEM. The work predicted another compound of intermetallic based of $((\text{Fe,Cr})_2(\text{Si,Al}))$. XRD was not attempted to identify the phase in this work. Further work in the joining of sialon to steel composite steel [82] observed the precipitations of Cr_2N in the form of nitrogen pearlite.

The above discussion revealed that different kind of reaction products were identified in the interface of the Si_3N_4 – steel and sialon – steel joints. Polanco *et al.* [10] reported that the discrepancy could be due to different kind of steels that may influence the kinetics and also the fact that the use of different sintering additives affected the reactivity of the Si_3N_4 -steels [80]. The authors of the works also agreed that the characterization method was important in identifying the phases.

The aforementioned studies employed different techniques of phase identifications. Polanco *et al.* [10] claimed that GIA-XRD was very effective to detect the phase at the thin interface layer. Raman spectroscopy was employed to confirm the phase in the reaction layer [15]. Several works [6-7, 77-78] estimated the phase based on elemental analysis obtained by Electron Probe Micro Analysis (EPMA). Other researchers utilized the TEM to estimate the reaction product [17, 81]. Relying only on the EDX analysis results brought to the difficulties in accessing the phase in the reaction layer [5, 82]. Thus, characterization technique was also important in identifying the phase in the reaction layer of the joint.

In the present work, XRD and XPS were employed to identify the phase in the surface layer. XPS was very effective characterization for the upper surface of the layer, thus it could possibly detect the phase in the very thin interface layer. FeSi_2 in the precipitates was revealed by the employed techniques. This was also supported by the significant amount of Fe and Si given by the EDX analysis in the precipitates. Cr and N were also found in the precipitates leading to the expectation of the Cr_xN_y . However, the presence of oxides might also be possible due to the existence of oxygen in the precipitates. The presence of the oxides was not disclosed by the XRD examination. Nonetheless, XPS spectra of Fe and Si from the interface layer surface showed the elements in the state of oxides (*i.e.* Fe_2O_3 and SiO_2). Thus, besides the reaction of the Fe and Si to form the α -Fe (Cr, Si), recombination of the sialon's elements to form oxides were also observed.

XRD examinations on the interface layer surface in the sialon – as-received AISI 430 FSS joint detected the presence of α . As it was expected, the α peak was obtained from the interface-layer matrix. Other than the ferrite solid solution, FeSi_2 was also shown in the XRD pattern. The silicide was believed to be from the precipitates since

no other species existed in the layer. Since the FeSi_2 was also confirmed from the XPS spectra of Fe and Si from the layer surface, thus the results of EDX analysis, XRD and XPS on the FeSi_2 existence were coherent. However, the XPS spectra also informed the existence of Fe_2O_3 and SiO_2 from the layer. The oxides could not be identified by the XRD. Small volume fraction could possibly be the reason for the difficulties to identify the phases using XRD. It could also be due to the very small thickness of the interface layer. As it was stated previously in section 3.2, the XPS was very effective technique to identify the chemical state of elements in the thin layer. Hence, the precipitates in the interface layer were iron silicides and mixed of oxides.

The FeSi_2 might be produced from the silicon in the interface layer that did not completely dissolve in the steel. Nitrogen pressure was built up in the interface due to the dissociation of the sialon. This reduced solubility of the silicon in the steel [6]. When the silicon exceeded its solubility in the Fe, it formed FeSi_2 in the precipitates.

Formerly, the Fe_3Si was also found in the reaction layer of silicon nitride – 253MA steel joint [2]. It was suggested that the diffused Fe into the sialon decomposed area could react with Si to form the silicides. Nonetheless, other elements in the precipitates could also produce different compound as suggested by the previous discussion. Since Al, O and N also existed in the precipitates; oxides, nitrides or precipitation of the sintering additives might also be formed. In this work, Fe also reacted with O to form the Fe_2O_3 . Recombinations of Si and O from the dissociated sialon also occurred and formed the SiO_2 in the interface layer.

As it was discussed previously, reactivity study of sialon with steel under low contact pressure produced Al_2O_3 as a result of the Al and O recombination. Later studies on the joining of the sialon with 9% Cr ferritic stainless steel and steel composite failed to identify the new compound in the reaction layer though it was clearly indicated in the microstructure. Through the characterizations technique employed in the present work, the presence of iron silicides and mixed of oxides were revealed. Different materials, experiment setting and characterization method used in this work might be the reason for the above dissimilarity. For studying the reactivity, the previous works employed relatively low pressure to make a contact between the

materials (*i.e.* 2.5 – 5 MPa). This pressure was sufficient to produce the reaction between the contacted materials. With this condition it was shown that no iron silicide or other new compound was formed. Fe or Si was not present at the precipitates. In the present work, joining was carried out at higher uniaxial pressure (*i.e.* 20 MPa). The same diffusion bonding pressure was also used by the previous sialon – ferritic stainless steel joining [5, 17, 82]. In these setting, Fe and Si was obviously found at the precipitates which subsequently revealed as the FeSi₂ using XRD and XPS in the current work. Reaction of the Fe and Si powder in a hot isostatic press was investigated [91]. β -FeSi₂ was produced by the reaction. The formation of FeSi₂ was enhanced with the increased of pressure. Thus, it suggested that higher pressure applied in the work possibly facilitated the formation of the silicide.

Besides rich of Fe, the precipitates in the joint of the sialon with the as-received steel also contained significant amount of nitrogen so that it could be detected by the EDX. It was established earlier in this section that nitrogen could be released through the pores in the interface, freed to the atmosphere at the edge of the joint or permeated into the steel. Around the middle of the joint, nitrogen would be trapped in the pores or dissolved in the Fe (Cr, Si) in the layer matrix. The dissolution of nitrogen in the Fe (Si) solid solution in γ under 10⁵ Pa N₂ gas was reported to be negligible (*i.e.* 10⁻³ atomic percent at 1100°C) [6]. It could be higher in α solid solution [17]. Thus the undissolved nitrogen could also precipitate in the interface layer.

The elemental analysis revealed that chromium was also observed in the precipitates which contained the nitrogen. This brought to an expectation of the nitrides formation. Besides the dissolution into the solid solution, nitrogen might also be incorporated in steel through the precipitation of chromium nitrides (*i.e.* CrN or Cr₂N) [40]. This occurred when the steel was exposed in nitrogen gas. Thus, despite the failure to detect it by XRD, CrN or Cr₂N might exist in the precipitates in the interface layer of the joint.

The above discussion describes the sialon decomposition and the interdiffusion of elements across the joint. Silicon and nitrogen were liberated from the sialon. The silicon diffused into the steel and formed the diffusion layer. The nitrogen diffused across the reaction layers and brought to martensite formation in the parent steel. Fe

and Cr from the steel moved into the interface layer which was the decomposition part of the sialon. The elements distributed into the interface-layer matrix and the precipitates. The precipitates were the results of the sialon – steel reaction and recombination of the dissociated-sialon's elements.

4.2.4.2 Joining of Sialon – Nitrided Steel

Observation on the microstructure of the cross section of the sialon – nitrided steel joint illustrates that the joint was attained. Interfacial joint was seen in the interface of the sialon with the steel in one-hour and four-hours-nitrided conditions. Morphology of the joint (*i.e.* interface and diffusion layers) was similar with the joint of sialon – as-received steel AISI 430 FSS. The reaction layers contained the interface layer with the presence of the precipitates, and the diffusion layer in the steel side.

Formation of the interface layer can be explained similar to the mechanism of its formation in the sialon – as-received 430 FSS. Penetration of the steel's elements into the sialon-decomposed part occurred during the joining process. The existence of the steel material in the interface layer matrix was also revealed by the EDX analyses on the interface layer matrix. The analyses depicted the domination of Fe and Cr in the matrix of the layer. The materials move towards the sialon and created a new interface of sialon with steel. This new sialon – steel boundary was obviously seen in the microstructure of the interface layer. Penetration of the steel into the sialon shifted interface of the original sialon with the steel. Hardness test on the joint revealed the extreme hardness difference between the sialon and the interface layer. Therefore, the border between the original sialon and the interface layer in the joint might turn into the weakest part of the joint. This could be predicted as this part was the boundary between two areas with extremely-different properties.

Voids were observed in the boundary between the interface layer and the sialon. This was especially seen in the joint of sialon with nitrided AISI 430 FSS. The presence of the voids made this part to be more critical. Pores in the interface of ceramic – metal joint were frequently seen. These were observed to be from the trapped nitrogen [6, 9-10, 14]. Mechanism of the pores formation due to the trapped

nitrogen has been discussed in section 4.2.4.1. Nitrogen that could not escape from the joint or permeate into the steel may be trapped and created the pores. In the diffusion bonding of sialon with nitrided steel, the steel was joined in nitrogen-pre-dissolved condition. During the diffusion bonding process, nitrogen was released from the sialon. However, solubility of the nitrogen in the steel was suppressed by the existence of the nitrogen in the steel that was added from the nitriding treatment. Therefore, more nitrogen could be trapped in the interface of the joint when it could not be released to the atmosphere. Consequently, more voids would be produced. In the present work, more voids were found at the joint of sialon – nitrided AISI 430 FSS (see Figure 4.24 and Figure 4.33). Nonetheless, in the present work, the voids could also be due to the drastic changes of the ductility between the original sialon and the interface layer. Hardness test across the joint revealed the high hardness at the original sialon after the joining. The hardness test at the interface layer depicted significantly-lower hardness at the interface layer. This could be expected since the interface layer matrix contained ferrite solid solution.

Severe changes of the ductility between the original sialon and the interface layer might yield voids at their border. It could be predicted since the voids took place at the boundary of the original sialon and the steel phase in the interface layer. Thus, the voids were present at the point of drastic transition from a hard-and-brittle sialon to the more-ductile steel phase in the interface layer.

The voids formation could be initiated when residual stress occurred due to the different thermal expansion between the sialon and the steel. This might cause crack at the ceramics though the materials could be bonded. However, when the ceramics did not crack, the residual stress would take effect on the boundary of the original sialon with the interface layer. Drastic change of ductility from the sialon to the interface layer may lead to voids formation as illustrated in the microstructure of the interface layer (Figure 4.24 and Figure 4.33). The voids could become crack initiation at the ceramics when the joint is carrying working load. Hence, the border between the original sialon and the interface layer could become the weakest part of the joint.

As it was also observed in the joint of sialon – as-received AISI 430 FSS, the interface-layer matrix and the diffusion layer in the joint of sialon – one-hour-nitrided

and four-hours-nitrided AISI 430 FSS comprised mainly Fe and Cr from the steel and Si from the dissociated sialon. XRD then revealed α -Fe (Cr,Si) solid solution in the interface-layer matrix and the diffusion layer in the sialon – nitrided AISI 430 FSS. The solid solution was also observed in the interface-layer matrix and the diffusion layer for the joint of sialon – as-received AISI 430 FSS. However, silicon content of the layers in the joint of the sialon – nitrided AISI 430 FSS was less than in the joint of sialon – as-received AISI 430 FSS. In these parts, maximum concentrations of silicon for the sialon – one-hour-nitrided and sialon – four-hours-nitrided steels were 1.9 and 1.86 weight percents respectively (Table 4.3 and Table 4.5). This was less than in the joint of sialon – as-received steel, *i.e.* 3.26 weight percent of maximum concentration.

While the precipitates in the joint of sialon – as-received AISI 430 FSS were rich of Fe, Cr, Si and N; the amount of silicon in the precipitates of the sialon – nitrided AISI 430 FSS joint was insignificant. Maximum silicon concentration in the precipitates for the sialon – one-hour-nitrided AISI 430 FSS joint was 5.33 weight percent (Table 4.4) and in the joint of sialon – four-hour-nitrided steel was 2.72 weight percent (Table 4.6). In the same part, maximum concentration of silicon for the sialon – as-received AISI 430 FSS joint was significantly higher (*i.e.* 34.14 weight percent). This was shown in Table 4.2.

In the joint of sialon – nitrided steels, nitrogen was even not found. This showed that should nitrogen exist in the precipitates; its concentration was too low that EDX was unable to detect it. Examination using XRD and XPS discovered the absence of iron silicide in the interface layer. The XRD could only detect α -Fe (Si) from the interface-layer matrix. XPS spectra of Fe and Si from the interface layer informed the Fe and Si in the form of oxide, *i.e.* Fe_2O_3 and SiO_2 . This situation was found both in joining of the sialon with the AISI 430 FSS nitrided for one and four hours. The absence of FeSi_2 in the precipitates was in accordance with the compositions of elements in the precipitates which showed insignificant concentration of silicon. Thus, this could be the evidence that nitrided steel had suppressed the formation of the iron silicide. In this case, nitriding for one hour on the steel was enough to suppress the silicide formation.

Suppression of the silicide in the interface layer might be due to the decrease of the sialon decomposition caused by the nitrided steel used in the joining. Decomposition of the sialon in joining with the steel liberated the silicon and nitrogen. The nitrogen diffused into the steel provided that there was enough solubility. The nitrided steel was in the nitrogen-pre-dissolved condition when it was joined with the sialon. Therefore, less nitrogen from the sialon could dissolve in the steel. This would decrease the dissociation of the sialon. The decrease of the sialon decomposition also reduced the silicon that was released from the sialon. Hence, less silicon was precipitated in the interface layer. It decreased the opportunity of the silicon to form the silicides.

The above technique was the analogy of the method proposed by Stoop [16] which suggested silicon addition into the steel to suppress its decomposition during the interaction with stainless steel. When the materials were in contact, the steel would be as the sink where the silicon went. High silicon in the steel would decrease the movement of the silicon into the steel. Thus decomposition of the sialon could be reduced.

Similar phenomenon was also noticed in the reaction front of Si_3N_4 and titanium. Suppressing of the metallic silicides using the nitrogen pre-dissolved metal was demonstrated in the joint of Si_3N_4 – titanium reaction [8]. Ti_5Si_3 was the reaction product of the joined materials. The silicide was formed due to the decomposition of the silicon nitride and reaction with Ti. The nitrogen released from the ceramics dissolved in the titanium; whereas the silicon reacted with the Ti to form the Ti_5Si_3 . Thin Ti foil accommodated less nitrogen. When the Ti was saturated with N, decomposition of the silicon nitride was hindered. Thus, no more Si was released to form the Ti_5Si_3 . Therefore, thinner titanium foil produced thin Ti_5Si_3 . Experiment to join the nitrogen-pre-dissolved titanium with the Si_3N_4 had been proved to suppress the growth of the Ti_5Si_3 layer in the interface of the ceramics – titanium foil interface. It was also found that the suppression of the Ti_5Si_3 improved the strength of the joint.

In relevant to the above idea, the present study found less silicon concentration in the precipitates in the sialon – nitrided-AISI 430 FSS joint. Nitrogen was even not detected by the EDX; probably due to its too low concentration. Consequently, less

liberated nitrogen yielded to the absence of nitrogen in the precipitates. It was presumed that the nitrogen did not precipitate as chromium nitrides in the interface layer. Thus, nitriding on the steel prior to the joining was also believed to hinder the nitrides precipitation in the layer.

Sections 1.1 and 2.6.2 described that nitriding on the 9% Cr-ferritic stainless steel prior to the diffusion bonding had been reported to improve the joint of the steel with the sialon [5, 17]. However, the reason was not clearly explained. The improvement of the joint strength could be due to the role of the reaction layers. Nonetheless, the work did not decisively find the phase in the reaction layers. It was only claimed that the reaction layers were ductile. This ductile layer contributed to the joint. Since the phases on the reaction layers were not known, the relation of the joint strength with the phases was not established.

The phase such as iron silicide was brittle so that its formation in the joint should be avoided [6]. Suppression of Ti_5Si_3 by using nitrogen-pre-solved Ti improved the strength of $Si_3N_4 - Ti$ joint [8]. The brittle phase of Mo_3Si was found to decrease the strength of AISI 316 austenitic stainless steel – Si_3N_4 joint [10]. Fast ceramics decomposition and the production of brittle phase in the joint should be prevented in the joint of ceramic – metal joint [14, 16]. This has been highlighted in section 1.1. It seemed that improvement of the joint strength in the joint of sialon – nitrided 9%-Cr ferritic stainless steel that was reported by Hussain *et al.* [5, 17] could be due to the absence of the silicides. The present study recognized that the use of nitrided steel in joining with sialon was beneficial since it reduced the sialon decomposition and subsequently suppressed the formation of $FeSi_2$ in the joint. It was also believed to prevent the formation of chromium nitrides in the joint.

Influence of the nitrided steel on decreasing the decomposition of the sialon could be studied from the thickness of the reaction layers in the joint. The interface layer in the joint has been noticed as the decomposed-part of the ceramics. Reaction of the sialon's and the steel's elements in this area yielded this part as the reaction front in the ceramics. In the steel side, the diffusion layer could also be considered as the reaction zone of the materials. This was presumed since Fe and Si had formed a solid

solution. Several workers [15, 77-78] utilized the layer thickness to justify the reactivity of the ceramics with the metal.

Average thickness of reaction layers in sialon – AISI 430 FSS joint is given in Figure 4.40. It was shown that the nitrated AISI 430 FSS decreased the thickness of the interface and the diffusion layers in the joint. Therefore it can also be disclosed that the nitriding reduce reactivity of sialon with the steel.

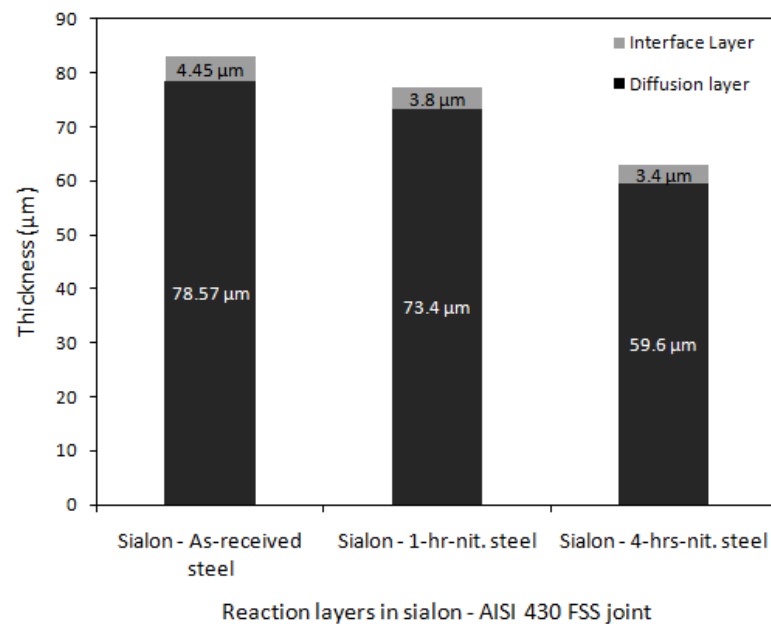


Figure 4.40 Average thickness of the interface layer and the diffusion layer in the sialon – AISI 430 FSS joint

Figure 4.40 divulged the decrease of the layer thickness was more significant when the sialon was joined with the longer-nitrated steel. In the former discussion, the interface layer was established as the sialon-decomposed part. This decomposed sialon would be consumed in the reaction with the steel. Thus, thinner interface layer might represent less decomposition of the sialon. This led to less silicon and nitrogen which were liberated from the sialon. Consequently, this resulted in shorter silicon-diffusion zone as illustrated in Figure 4.40. Since reaction of the sialon with the steel occurred in the layers, reduction of the layer thickness also disclosed less reactivity. Based on this argument, it can be concluded that nitriding hindered reactivity of AISI 430 FSS with sialon in diffusion bonding process.

The study has explored the benefit of the nitrided steel in the joint. The pre-treated steel prevented excessive decomposition of the sialon. This would be beneficial and therefore this was recommended by the previous works [8, 10]. This was also suggested by Stoop [16]. The workers also advised that brittle phase such as silicides should be avoided. Therefore, suppressing the FeSi_2 in the joint of the sialon – nitrided steel might improve the strength.

With regard to the reactivity (*i.e.* the reaction layer thickness), Stoop [16] found that the strength of Si_3N_4 – 316 austenitic stainless steel joint was directly related to the thickness of the porous zone in the ceramics (*i.e.* the interface layer in the present work). The researcher observed certain thickness of the porous zone that gave the strongest joint. This might also occur in the joining that was explored in the present work. Hence, study on the relation of the joint strength and the layer thickness is required to obtain the process setting that could produce strongest joint. Investigation on the relation of the joint strength with the joined-steel condition was also meaningful. This would also inform the optimum nitriding condition that could produce good joint. The study was beyond the scope of this work. Therefore, it was recommended for the continuation of the research.

4.2.4.3 Hardness of the Joint Section

In the present work hardness test was employed to estimate the mechanical properties of the reaction layers in the joint. Hardness test results across the joint of sialon – as-received AISI 430 FSS and sialon – nitrided AISI 430 FSS were similar. No change was observed on the hardness of the original sialon after the joining. This was expected for its stability in high temperature. However, hardness improvement was exhibited by the parent steel due to the martensite formation.

In between the original sialon and the steel, reaction layers in the joint of sialon – AISI 430 FSS formed two different-hardness areas. Both interface and diffusion layers had ferrite phase. Thus it should have same hardness. However, precipitates were also present in the interface layer. In the joint of sialon – as-received steel, the precipitates were estimated to be iron silicide, nitride and oxides; while in the joint of

sialon with nitrided steel, the precipitates contained only oxides. The phases in the precipitates enhanced the hardness of the interface layer. Therefore it was harder than the ferritic-phase diffusion layer, yet it was softer than the original sialon.

The diffusion layer in the steel was the lowest-hardness part. Phase identifications that were carried out on the layer revealed that this was ferrite-single-phase zone. As a result, the hardness of this layer was lower than the mixture of ferrite and precipitates at the interface layer. Its hardness was also lower than the pearlite in the parent steel. Assessment on the hardness across the joint proved that the diffusion layer possesses the lowest-hardness among the joint parts. This was in accordance with the mechanical properties of ferrite phase that was soft and ductile. Hardness of the interface layer was higher than the diffusion layer due to the presence of the precipitates. In overall, hardness of the reaction layers (*i.e.* interface and diffusion layers) were lower than the original sialon and the parent steel. Therefore, these parts were more ductile compared with the parent joined materials.

Different thermal expansion coefficient between ceramics and metal caused excessive residual stress at the joint. The stress was generated during the cooling stage in the joining process. Section 2.6.2 reported that despite good bonding, crack frequently occurred at the ceramics during the interaction of silicon nitride – steel [6-7] and sialon – steel [15]. This was due to the inability of the ceramics to accommodate the residual stress. In this case, martensite in the steel reduced the contraction of the steel during cooling [17]. As it was also suggested by the worker, the present work also agreed that the ductile layers in the interface of the joint helped in accommodating the stress and contribute the joint. This would act as the ductile metallic interlayer that was normally utilized to solve the problem of high residual stress at the joint of ceramics with metal.

4.3 Joining of Sialon with 7.5%-Cr FS

High-chromium ferritic steel was widely used in high-temperature applications. Therefore, the material was suitable to be combined with ceramics to serve the working environment. In this study, joining of 7.5%-Cr FS was attempted. The

joining method and condition of the previous experiments were employed to carry out the study.

4.3.1 Joining of Sialon with As-received 7.5%-Cr FS

For the first condition of the study, the sialon was joined with the as-received 7.5%-Cr FS. Detailed information of the steel was given in Chapter 3. Procedure of the joining was the same with the joining of the sialon with the AISI 430 FSS. Investigation on the microstructure of the joint, element diffusion and mechanical properties of the reaction layers were also performed in similar technique with the previous joining.

4.3.1.1 Microstructure of the Joint

Microstructure of the joint of sialon – as-received 7.5%-Cr FS is presented in Figure 4.41 and Figure 4.42. The figures show that interfacial joint was attained. Reaction layers were formed in the joint.

The morphology of the reaction layers were similar with the layers in the joint of the sialon –AISI 430 FSS. The interface layer was part of the reaction layer in the sialon; while in the steel side a diffusion layer was built. In the parent steel, the structure was fully martensitic. No other phase was indicated in the microstructure of the parent steel. This had been observed by Hussain *et al.* [5, 17] in the joint of the steel with sialon. It was noted that the martensite formation was due to nitrogen that diffused into the steel. This was also revealed by the results of the nitriding experiments given section 4.2.2 of this chapter.

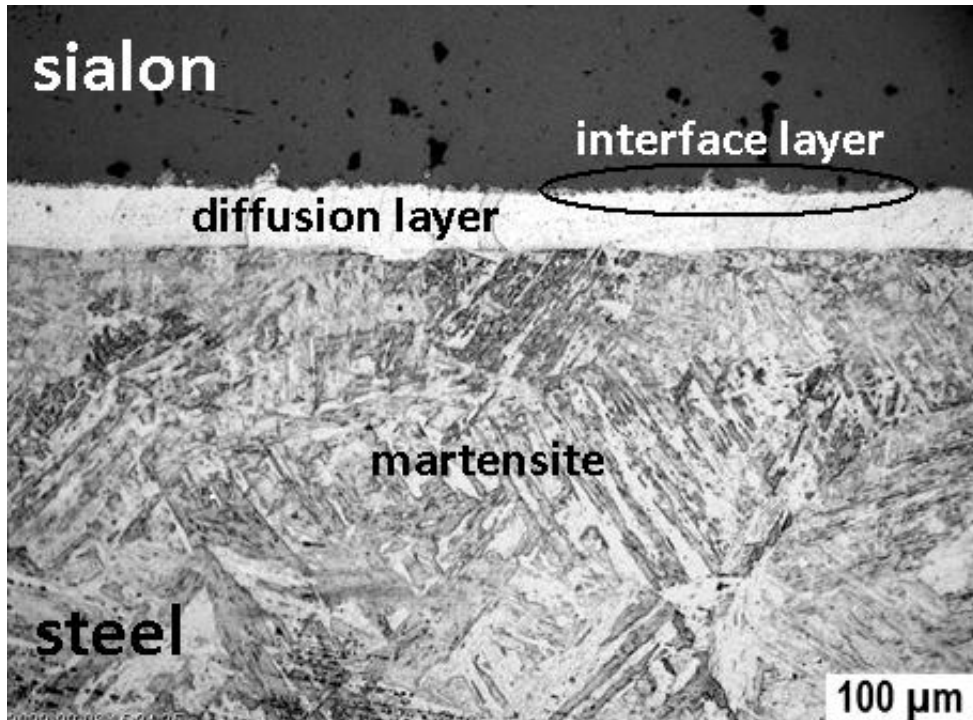


Figure 4.41 Optical micrograph of the cross section of sialon – as-received 7.5%-Cr FS joint

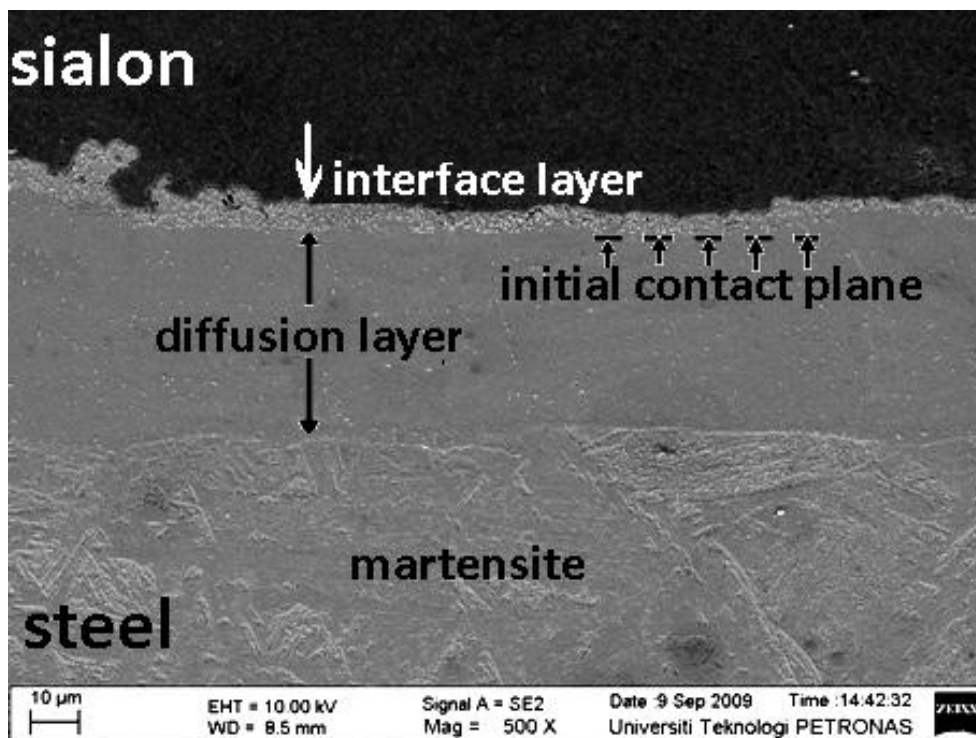


Figure 4.42 Scanning electron micrograph of the cross section of sialon – as-received 7.5%-Cr FS joint

Morphology of the interface layer is illustrated in Figure 4.43. Irregularity of the interface layer thickness was also observed. The average thickness of the interface layer was 3.64 μm . This was smaller than the thickness of the layer in the joint of sialon – as-received AISI 430 FSS (*i.e.* 4.45 μm). Precipitates in the interface layer brought to rough surface of the layer.

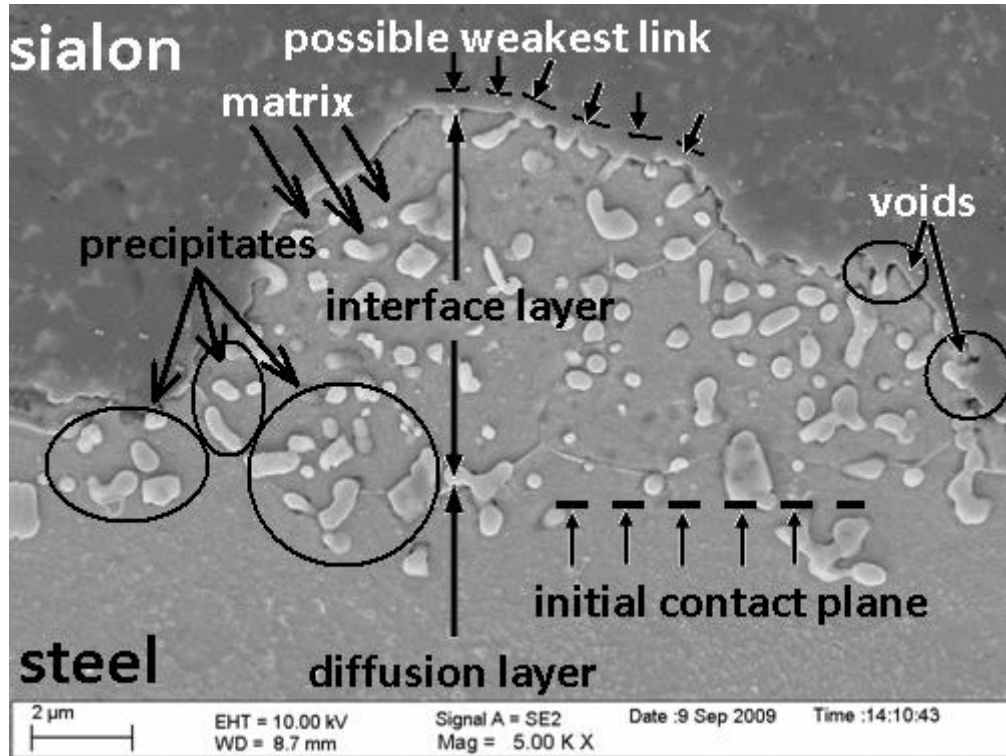


Figure 4.43 Scanning electron micrograph of the cross section of the interface layer in sialon – as-received 7.5%-Cr FS joint

The microstructure depicted that the diffusion layer in the steel contained a single phase. This could be estimated from the contrast of the layer in the micrograph. Furthermore, this characteristics was also owned by the layer in the former joining conditions. Measurement of the diffusion layer thickness showed the average value of 39.11 μm . This was significantly shorter than the thickness of the layer in the sialon – as-received AISI 430 FSS joint; *i.e.* 78.57 μm .

Figure 4.43 illustrates that the interface layer matrix and the diffusion layer have the same contrast. Analyses on these regions in the joint of sialon – AISI 430 FSS revealed that these area own the same phase, that is ferrite solid solution. Therefore, transfer of material from steel to sialon might have also occurred in the present

joining. The steel moved across the initial contact plane. It penetrated into the sialon side and formed the interface layer. This could be studied from the microstructure of the interface layer presented in Figure 4.43. Ferrite solid solution in the interface layer matrix is commonly soft and ductile, while the original sialon is very hard and brittle. Thus, the boundary between the original sialon and the interface layer is the transition area from the brittle sialon to the soft-and-ductile ferrite solid solution. Combined with the voids presence in this area, the border between the interface layer and the original sialon could turn into the weakest link in the joint.

4.3.1.2 Elemental Analysis

EDX analysis was executed in the joint as well as in the interface-layer matrix and the precipitates. The result of the analysis on the overall joint is given in Figure 4.44; whereas Table 4.7 and Table 4.8 provide output of the analysis on the interface layer.

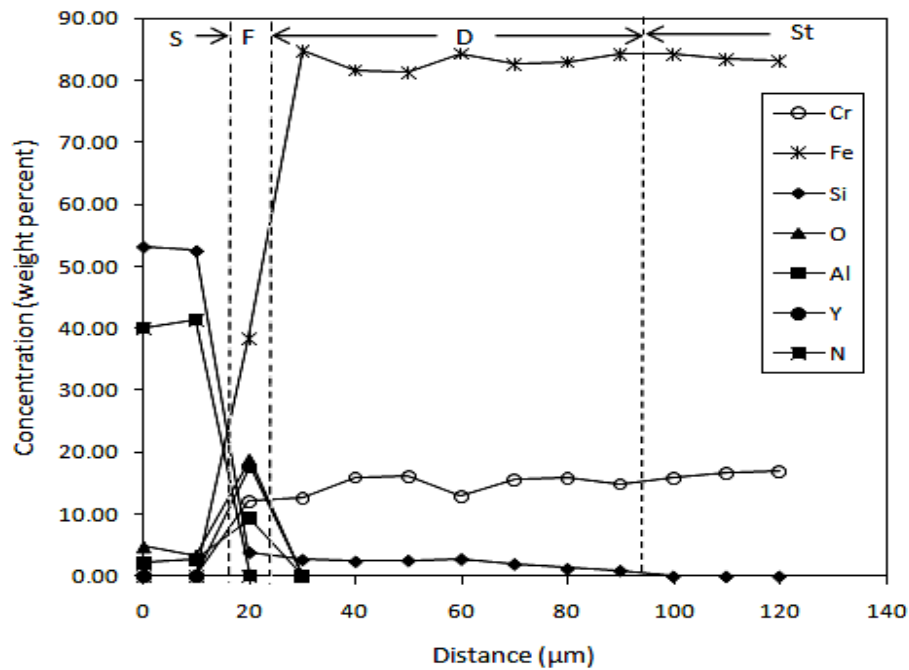


Figure 4.44 Concentration profile of elements across the sialon – as-received 7.5%-Cr FS joint; S=sialon, F=interface layer, D=diffusion layer St=steel

Figure 4.44 depicts the existence of silicon in the diffusion layer in the steel side. No other sialon's element was found to diffuse into the steel. Obviously the analysis also revealed the existence of Fe and Cr since this area was the steel part. Discussion

on the previous joining (section 4.3) established that this was the silicon-diffusion layer. The silicon-diffusion zone was estimated from the thickness of the diffusion layer. This was measured in the optical micrograph of the layer. As it was mentioned in the previous section, the average thickness of the layer was 39.11 μm . The result revealed that the silicon was liberated from the sialon and diffused into the steel. It reached 39.11 μm from the interface of the joint.

Random-spot elemental analyses were performed on the interface layer-matrix and the precipitates. Several spots were selected randomly in the interface layer. Those were selected from the area closest to the sialon and move towards the diffusion layer. It was also attempted to select the spots that distributed in the overall observed area. Figure 4.45 shows the map of the spots for the elemental analyses on the interface layer of the sialon – 7.5%-Cr FS joint. The EDX analyses on the interface layer provided the elements condition on the interface layer-matrix and also the precipitates. These are presented in Table 4.7 and Table 4.8, respectively.

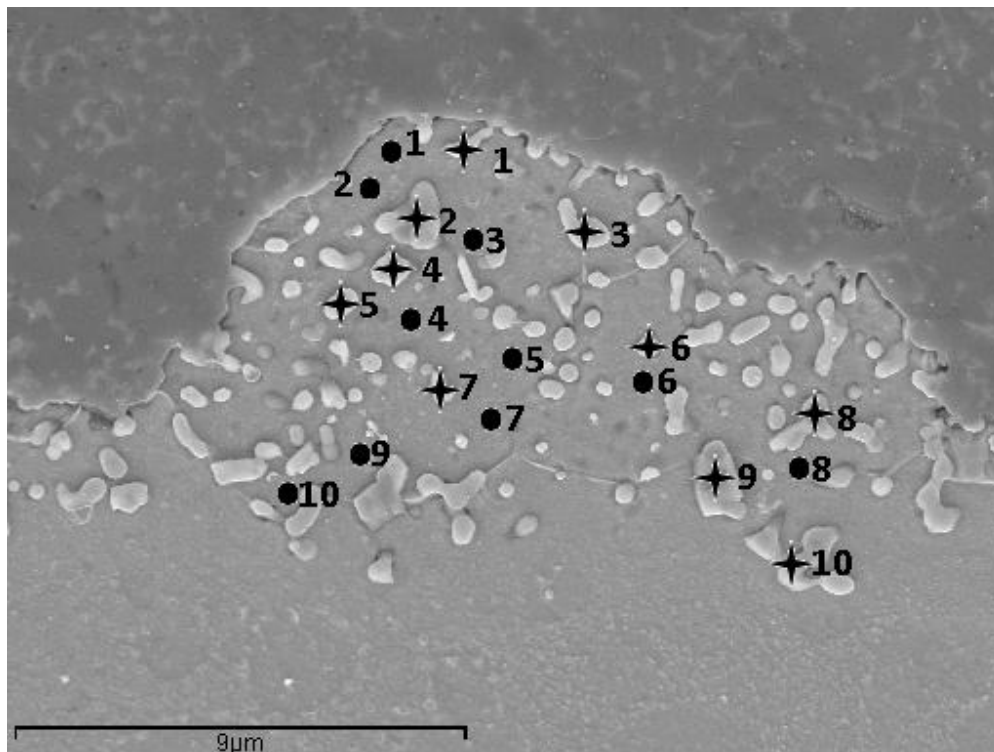


Figure 4.45 Map of EDX spot analysis at the interface layer of sialon – as-received 7.5%-Cr FS joint; (●) = matrix, (+) = precipitates

Fe and Cr diffused into the sialon as they were found in the interface-layer matrix as well as in the precipitates. Fe and Cr were identified in the matrix with highest concentration of 81.17 and 20.72 weight percent respectively (Table 4.7). The layer matrix contained silicon with the highest content of 3.64 weight percent.

Table 4.7 Concentration of elements of the interface-layer matrix in sialon – as-received 7.5%-Cr FS joint

Spot number	Concentration (weight %)						
	Cr	Fe	Si	O	Al	Y	N
1	20.50	76.45	3.05	0.00	0	0	0
2	17.76	78.00	3.00	1.24	0	0	0
3	19.08	77.67	2.53	0.73	0	0	0
4	19.51	77.97	2.51	0.00	0	0	0
5	10.93	69.05	2.74	3.44	6.78	7.05	0
6	19.79	77.51	2.70	0	0	0	0
7	0.51	81.17	3.64	3.14	6.64	4.89	0
8	19.97	77.28	2.18	0.57	0	0	0
9	11.89	41.33	25.71	2.04	5.71	0	13.32
10	20.72	75.85	2.69	0.74	0	0	0

Table 4.8 Concentration of elements of the precipitates at the interface layer in sialon – as-received 7.5%-Cr FS joint

Spot number	Concentration (weight %)						
	Cr	Fe	Si	O	Al	Y	N
1	15.24	81.24	3.52	0.00	0	0	0
2	7.18	75.56	3.31	2.76	6	6	0
3	17.99	78.44	2.94	0.63	0	0	0
4	6.93	83.52	3.46	1.85	4	0	0
5	17.62	60.78	14.26	1.14	0	0	6
6	0.72	48.47	29.71	2	5	0	14
7	8.56	48.44	26.64	2.30	3.30	0	11
8	5.42	49.04	27.37	2.33	5	0	11
9	7.43	48.37	26.35	2.81	4.31	0	10.72
10	7.75	48.79	26.61	2.41	4	0	10

In the precipitates, Fe and Cr were also detected in maximum concentrations of 83.52 and 17.99 weight percents, respectively (Table 4.8). A few precipitates contained low silicon. Nevertheless, in some other precipitates, higher silicon was found (*i.e.* 29.71 weight percent of maximum concentration). Nitrogen was also detected in these precipitates with 14 weight percent maximum concentration. Thus,

the precipitates were rich of Fe, Cr, Si and N. The elements composition of the precipitates was similar with the precipitates in the joint of sialon – as-received AISI 430 FSS. With this situation, similar reaction could be expected, *i.e.* the precipitates would consist of the FeSi_2 .

The above results revealed the diffusion of the elements in the joint of sialon – as-received 7.5%-Cr FS. The sialon dissociated with the same mechanism as discussed in section 2.6.1. It took place according to reactions 2.8 and 2.9. Silicon and nitrogen were released from the sialon due to its decomposition. Length of the silicon-diffusion zone in the steel was 39.11 μm . This was estimated from the measured thickness of the layer. Nitrogen was also believed to diffuse into the steel and helped to produce martensite phase. It was also trapped in the interface as indicated by porosities in the border of the sialon with the interface layer.

It seemed likely that not all of the silicon and the nitrogen could dissolve in the steel. This was divulged by the presence of the elements in the precipitates. In this species, reaction of silicon and nitrogen with Fe and Cr might take place. Subsequently, XRD and XPS examinations were employed to scrutinize the reaction products of the materials.

Thickness of the reaction layer in this joint was smaller than the thickness of the layers in the joint of sialon – as-received AISI 430 FSS. Average thickness of the interface layer and the diffusion layer in the current joint was 3.64 μm and 39.11 μm respectively. Compared to the thickness of the layers in the joint of sialon – as-received AISI 430 FSS, the layers in this joint was thinner. In the sialon – as-received AISI 430 FSS joint, the measured thickness of the interface layer and the diffusion layer were 4.45 μm and 78.57 μm , respectively. This disclosed that reactivity of the 7.5%-Cr FS with sialon was less than the reactivity of AISI 430 FSS with the ceramics. As shown in Figure 2.4 (section 2.3), Cr enhanced the reactivity of the steel with the sialon; while C decreased it. Therefore, the results in the present work agreed with the suggestion; *i.e.* lower Cr in the 7.5%-Cr FS yielded to less reactivity with the sialon than the AISI 430 FSS which contains 15.7% Cr.

4.3.1.3 XRD

Figure 4.46 shows the XRD pattern from the surface of the interface layer. The examinations gave two peaks of α -Fe (Si). As it was predicted from the elemental analysis, the α -Fe (Si) should originate from the interface-layer matrix. Another peak that revealed FeSi_2 was also found. This came from the precipitates as no other species were observed in the microstructure of the interface-layer matrix.

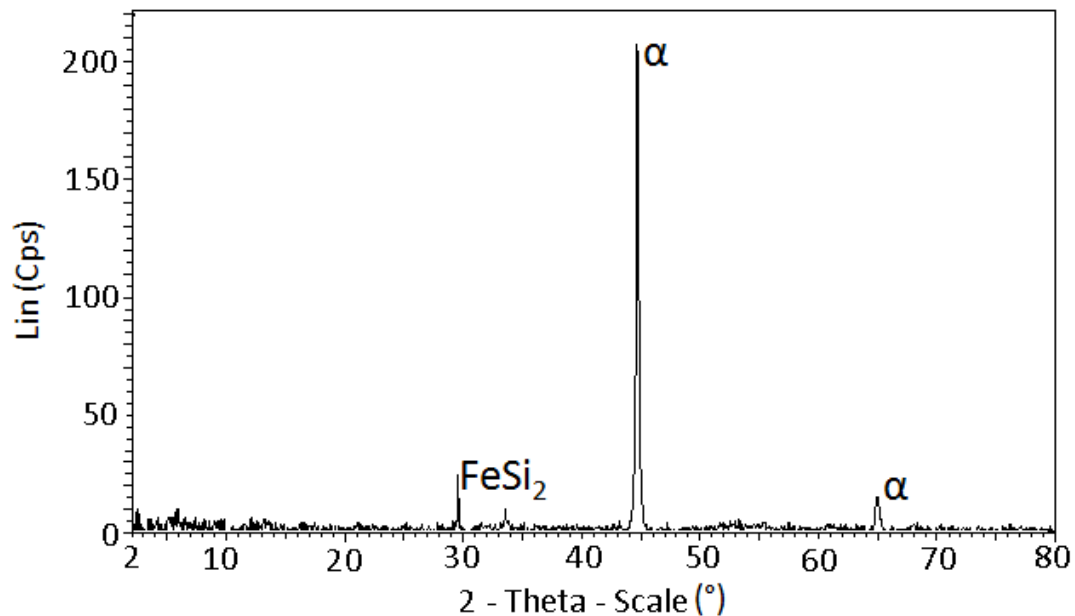


Figure 4.46 X-ray diffractogramme of the interface layer in sialon – as-received 7.5%-Cr FS joint

4.3.1.4 XPS

XPS spectra of Fe and Si from the interface layer are given in Figure 4.47 and Figure 4.48, respectively. Peak fitting of the Fe XPS spectra provided five peaks. Those were at 706.78 eV; 710.88 eV; 713.68 eV; 719.68 eV and 724.58 eV. The FeSi_2 was indicated by the peaks at 706.78 eV and 719.68 eV and the plasmon loss at around 730 eV. The plasmon loss was also seen in the XPS spectra of Fe in the joint of sialon – as-received AISI 430 FSS (Figure 4.19. Refer to the same references; the other two peaks at 710.88 eV and 724.58 eV were attributed to Fe_2O_3 .

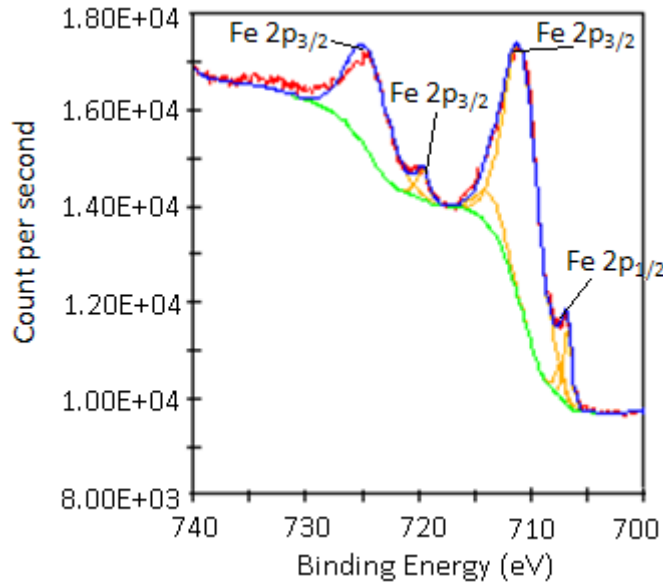


Figure 4.47 XPS spectra of Fe from the interface layer in sialon – as-received 7.5%-Cr FS joint

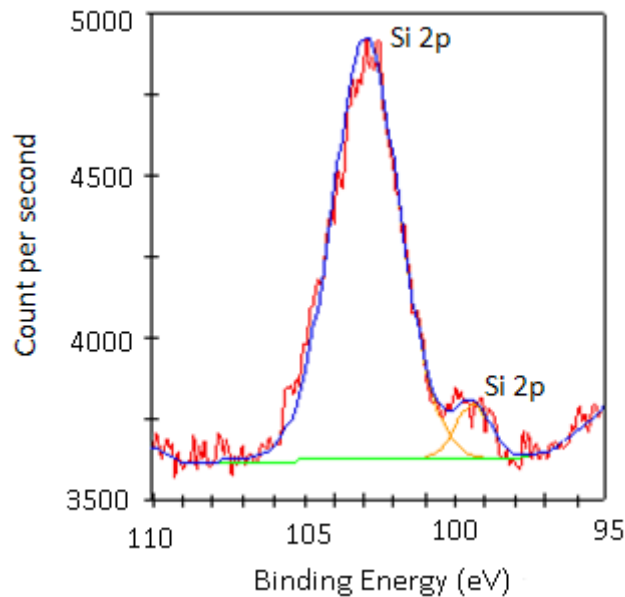


Figure 4.48 XPS spectra of Si from the interface layer in sialon – as-received 7.5%-Cr FS joint

In the Si spectra, two peaks were obtained (Figure 4.48). Those were at 102.98 eV and 99.58 eV. The peak at 102.98 eV represents the Si in the form of SiO_2 ; while another peak was attributed to FeSi_2 . This was according to the literatures that were referred previously [85, 88-89].

Results of the XPS analyses were inline with the XRD output that revealed the existence of FeSi_2 in the layer. Thus it was a strong indication that the iron silicide was formed at the precipitates in the interface layer. Nevertheless, besides the FeSi_2 , the XPS spectra of Fe and Si showed that the elements were also in oxide states, *i.e.* Fe_2O_3 and SiO_2 . Hence, besides the formation of FeSi_2 in the interface layer, Fe^{3+} also reacted with O^{2-} from the dissociated sialon to form the oxides. As suggested by the previous discussion, SiO_2 was the results of the recombination of Si^{4+} and O^{2-} . The aforementioned discussion exhibited similar condition with the AISI 430 FSS – sialon joint. Both joining produced the FeSi_2 and oxides precipitates in the interface layer. Therefore, this implied that outputs of the experiment were consistent with investigation on AISI 430 FSS – sialon joint. In the joining, of sialon – as-received AISI 430 FSS, the presence of FeSi_2 and oxides in the joint was also demonstrated.

4.3.1.5 Hardness Test across the Joint

Figure 4.49 displays hardness across the joint. Hardness of the parent steel reached HK 600. The high hardness in this part was due to the fully martensite phase. Diffusion layer in the steel owned the lowest hardness. This zone represented the ferrite phase which is soft and ductile.

The interface layer phase was a mixture of ferrite solid solution and precipitates. This layer was harder than the diffusion layer in the steel. Thus the precipitates in the layer made it as the hard layer in the joint. The hardness of the sialon was originally very high. It was not changed after the joining. The ductility of the reaction layers could be expected due to its low-hardness properties. Refer to the discussion for the previous joining (section 4.3) this might be beneficial in dealing with the residual stress in the joint.

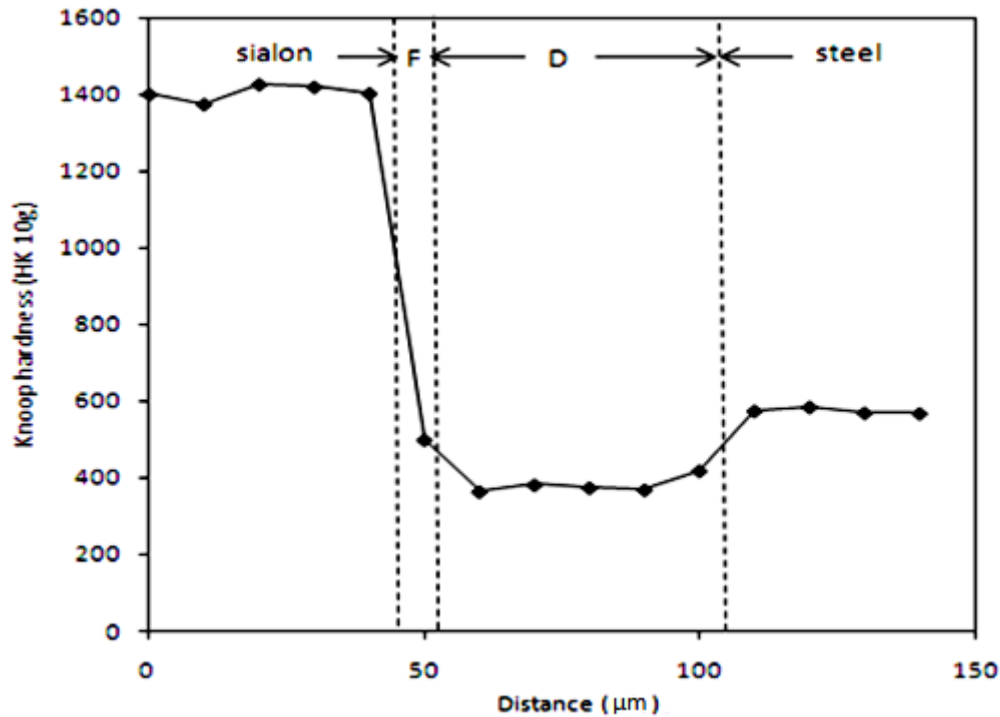


Figure 4.49 Hardness across the sialon – as-received 7.5%-Cr FS joint; F=interface layer, D=diffusion layer

4.3.2 Joining of Sialon with One-hour-nitrided 7.5%-Cr FS

Influence of solution nitriding on hardness and microstructure of 7.5%-Cr FS was reported in section 4.2.2. The diffusion of nitrogen into the steel was implied by the enhancement of the steel's hardness and the martensite formation. With this condition, nitrogen in the surface of the steel was expected. Joining of the sialon with the steel nitrided for one hour was attempted. Influence of the treatment on the joint was investigated and reported in this section.

4.3.2.1 Microstructure of the Joint

Figure 4.50 and Figure 4.51 present the microstructure of the overall joint of the sialon with the one-hour-nitrided 7.5%-Cr FS. As shown in the figures, interfacial joint was attained. The microstructure informed that the joint morphology was similar

with the sialon – as-received 7.5%-Cr FS joint. Reaction of the materials was shown by the interface layer (Figure 4.52) in the sialon and the diffusion layer in the steel.

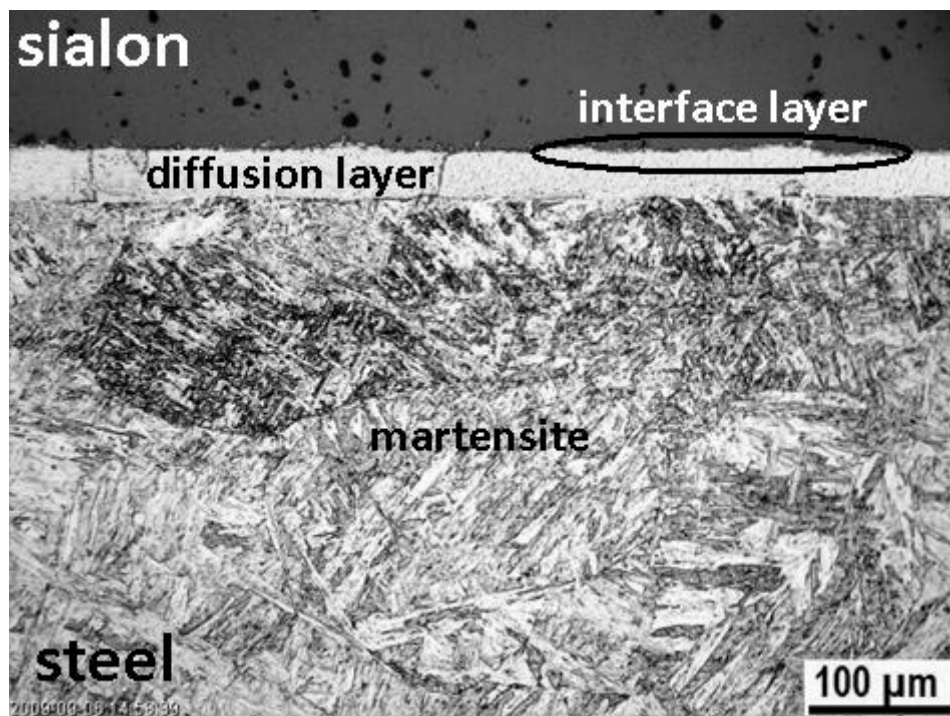


Figure 4.50 Optical micrograph of the cross section of sialon – one-hour-nitrided 7.5%-Cr FS joint

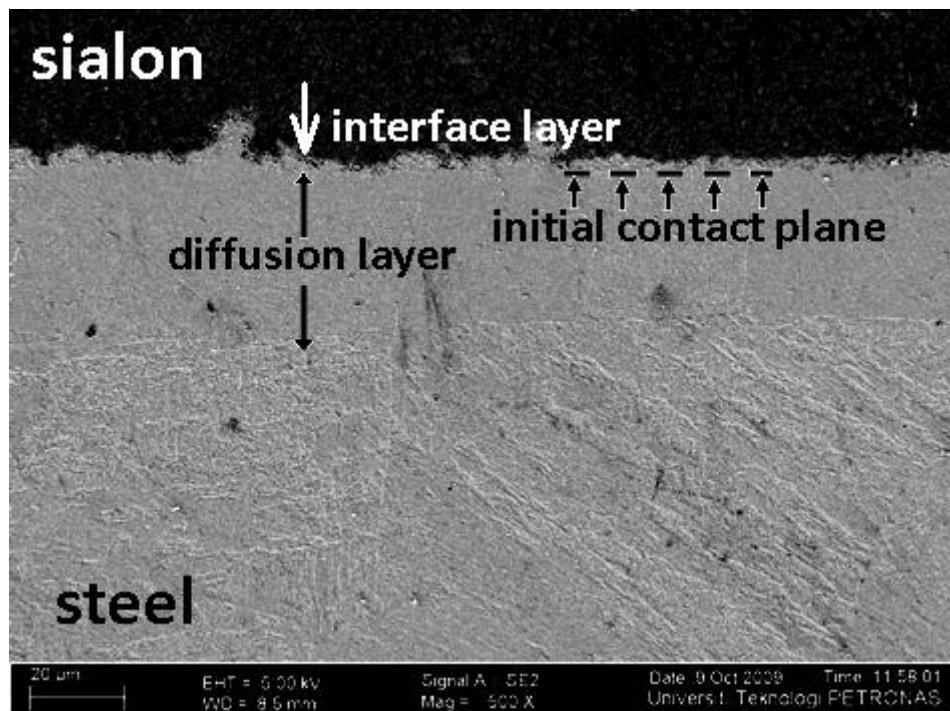


Figure 4.51 Scanning electron micrograph of the cross section of sialon – one-hour-nitrided 7.5%-Cr FS joint

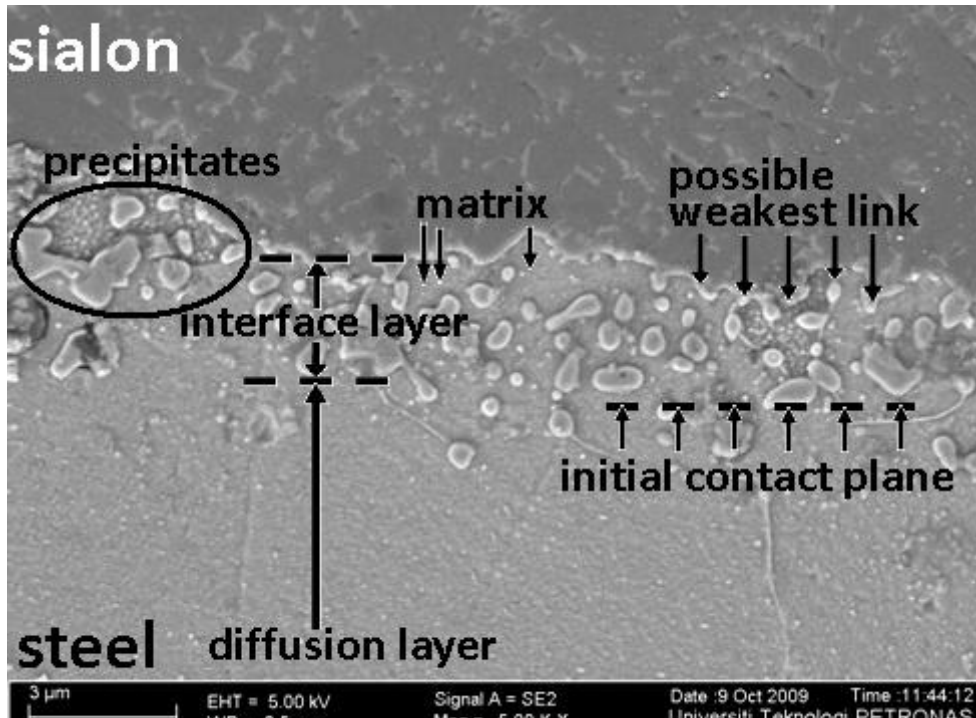


Figure 4.52 Scanning electron micrograph of the cross section of the interface layer in the sialon – one-hour-nitrided 7.5%-Cr FS joint

Transfer of steel into the sialon-decomposed part in the interface layer could be estimated from the similar contrast between the interface layer matrix and the diffusion layer. This could be seen in Figure 4.52. The border between the diffusion layer and the interface layer matrix was not clearly indicated. It looked like that the interface layer was part of the steel that moved towards the sialon part. Voids were not found in the observed area. However, the boundary between the original sialon and the interface layer could become the weakest link of the joint due to the extreme difference of the sialon's and the interface-layer's properties.

Similarity with the joint of sialon – as-received steel was also exhibited in the microstructure of the parent steel which consisted of martensite phase. Prior to the joining, the microstructure of the steel was also martensite as the result of the nitriding treatment. However, the optical micrograph shown in Figure 4.50 displayed denser martensite compared to the microstructure of the nitrided steel presented in section 4.1.2 (Figure 4.8). This might be due to the diffusion of the nitrogen into this area during the joining. It had been recognized that the nitrogen produced finer martensite and enhanced its hardness [17, 92].

Joining one-hour-nitrided 7.5%-Cr FS with sialon produced thinner reaction layers. For this joint, the average thickness of the interface and the diffusion layer was 2.8 μm and 35.4 μm respectively. The thickness of the layers in the joint of the sialon – as-received 7.5%-Cr FS was 3.64 μm for the interface layer and 39.11 μm for the diffusion layer. Thus, the use of one-hour-nitrided steel in the joining reduced the thickness of reaction layers.

4.3.2.2 Elemental Analysis

Compositions of elements across the joint are illustrated in Figure 4.53. It was difficult to determine the exact silicon-diffusion extent in the steel from the figure. However, compared to Figure 4.44, in this joint, silicon diffused into shorter distance from the interface. The more-accurate extent of the silicon diffusion was determined from the thickness of the diffusion layer in the microstructure of the joint. This had been shown in the former section. Based on the measurement of the diffusion layer thickness, 35.4 μm of the silicon diffusion distance was disclosed. This was shorter than in the joint of the sialon with the as-received 7.5%-Cr FS.

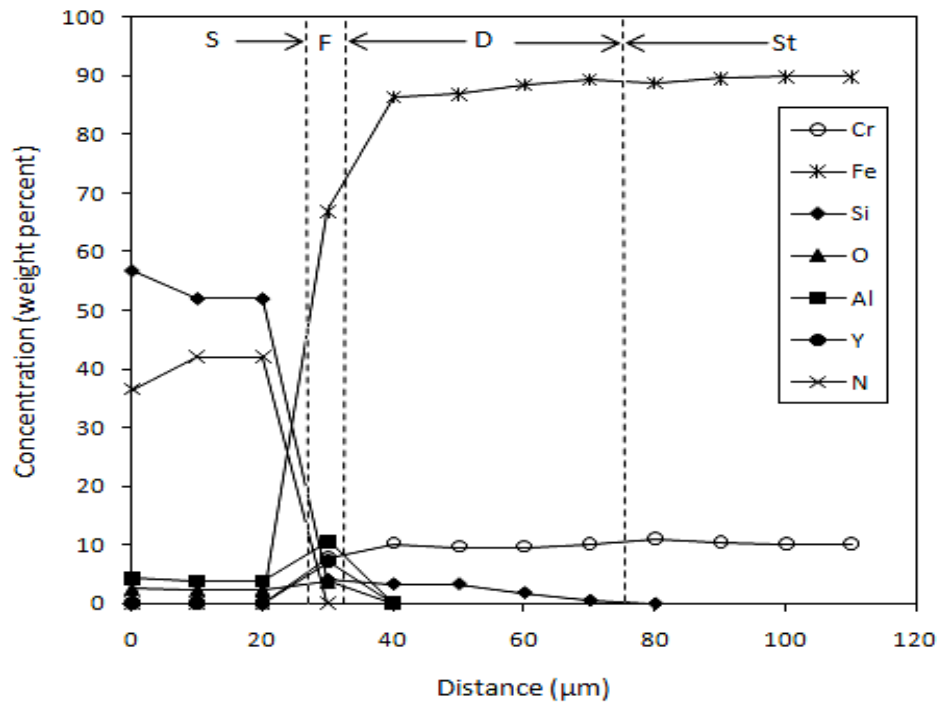


Figure 4.53 Concentration of elements across the sialon – one-hour-nitrided 7.5%-Cr FS joint; S=sialon, F=interface layer, D=diffusion layer, St=Steel

Several spots was chosen in the interface layer for the elemental analyses. Since the layer is very thin, the spots were selected along the layer in the observed area. However, the selection covers the spots from the area closest to the sialon towards the area near by the diffusion layer. The map of the spot is illustrated in Figure 4.54.

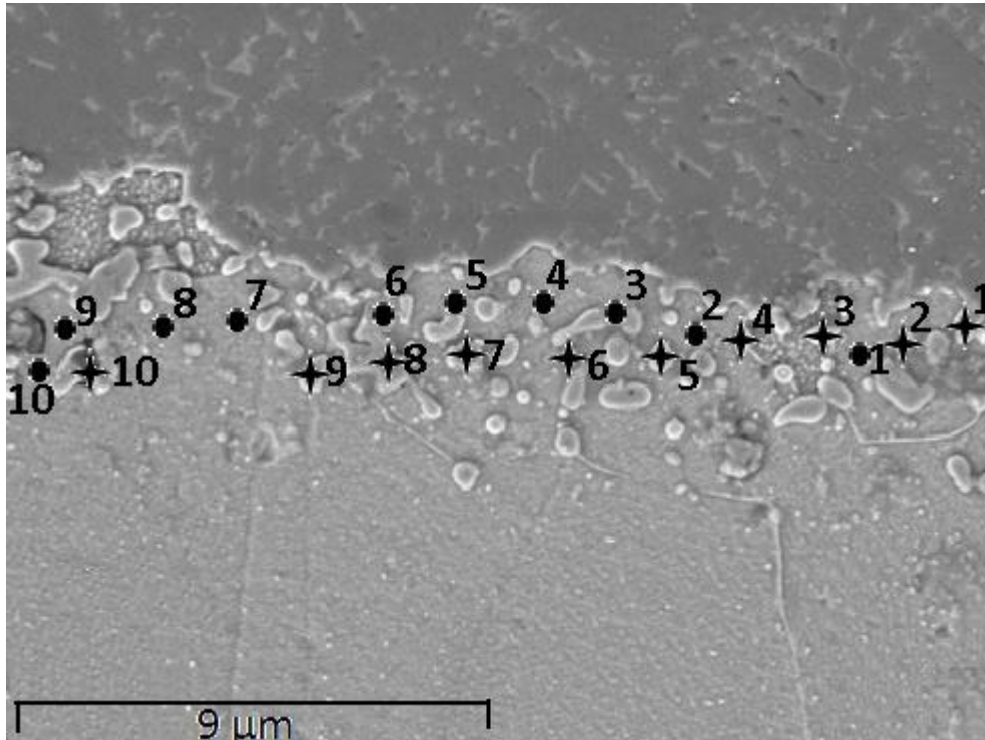


Figure 4.54 Map of EDX spot analysis at the interface layer of sialon – one-hour-nitrided 7.5%-Cr FS joint; (●) = matrix, (+) = precipitates

Composition of elements in the interface layer is given in Table 4.9 and Table 4.10. The interface-layer matrix contained Fe and Cr in the maximum concentrations of 82.26 and 9.69 weight percents. The matrix also comprised Si and O. Those were in 12.49 and 7.17 weight percent of maximum concentrations. Aluminium was also observed in the matrix with less quantity than the other elements. Since the element compositions of this part in this joint and the other previous joints were alike, the phase in this zone should also be ferrite solid solution. The XRD pattern from the layer surface proved this and will be displayed in the later section.

High concentration of Fe was also found in the precipitates (Table 4.10). Other elements, which are Si, Al, and O from the sialon and Cr from the steel, were also discovered in smaller quantity. Low concentration of Si in the precipitates in this

joining could be highlighted. In joining of the sialon with the 7.5%-Cr FS in as-received condition (section 4.3.1), the precipitates were rich of Fe, Cr, Si and N (Table 4.8). Further investigation subsequently found FeSi₂ in the precipitates. However, in the present joining, Si was found in all spots with low quantity. The amount of Si in the precipitates might not be sufficient to form FeSi₂. This had also been demonstrated in the joining of the sialon with the nitrided AISI 430 FSS. Therefore, the nitriding treatment might exhibit same effect on the FeSi₂ formation in the joint of sialon either with AISI 430 FSS or 7.5%-Cr FS. Further characterization on the layer was carried out to reveal this. The later section discusses the XRD and the XPS for this joint.

Table 4.9 Concentration of elements of the interface-layer matrix in sialon – one-hour-nitrided 7.5%-Cr FS joint

Spot number	Concentration (weight %)						
	Cr	Fe	Si	O	Al	Y	N
1	8.04	67.31	12.49	7.17	0.86	0	4.14
2	8.59	78.45	6.79	5.53	0.63	0	0
3	9.69	81.27	4.40	4.63	0	0	0
4	8.31	72.15	4.46	8.52	2.24	4.31	0
5	9.68	81.16	3.86	5.29	0	0	0
6	9.55	75.74	4.05	6.79	1.27	2.59	0
7	9.36	81.26	3.94	4.77	0.69	0	0
8	8.94	81.16	3.90	5.17	0.82	0	0
9	8.64	77.00	3.94	6.12	1.10	3.19	0
10	9.11	82.26	3.70	4.04	0.91	0	0

Table 4.10 Concentration of elements of the precipitates at the interface layer in sialon – one-hour-nitrided 7.5%-Cr FS joint

Spot number	Concentration (weight %)						
	Cr	Fe	Si	O	Al	Y	N
1	5.21	40.03	18.00	15.44	4.30	8.44	8.59
2	5.11	38.66	9.41	21.80	8.39	16.62	0
3	6.37	55.34	4.16	15.83	6.34	11.97	0
4	8.16	66.87	4.96	12.47	4.05	5.36	0
5	8.08	67.61	5.19	11.62	2.86	4.63	0
6	6.34	54.12	4.17	15.98	7.42	11.99	0
7	7.74	61.89	4.12	12.95	4.97	8.34	0
8	6.79	59.77	4.74	14.15	5.05	9.50	0
9	5.24	36.20	4.91	24.58	9.28	19.79	0
10	7.33	34.03	8.82	23.94	2.64	23.24	0

Nitrided steel decreases thickness of the interface layer in sialon – AISI 430 FSS joint. The interface layer was the decomposed-part of the sialon. It was also the reaction front of the joined materials in the sialon side. This was disclosed previously in section 4.2.1.3. The pre-treated steel also suppressed the diffusion of silicon into the steel. These influences were also indicated in the current joining. It has been mentioned in the former section (*i.e.* section 4.3.2.1) that the average thickness of the interface and the diffusion layer was 2.8 μm and 35.4 μm , respectively. These were thinner than the layers in the joint of the sialon with the steel in as-received condition. In the sialon – as-received 7.5%-Cr FS joint, thickness of the interface layer was 3.64 μm ; while thickness of the diffusion layer was 39.11 μm . Section 4.2.4 has established that the decrease of the diffusion layer thickness revealed reduction of reactivity of the joined materials. Therefore, the nitrided steel might also have restrained reactivity of the 7.5%-Cr FS with the sialon. This would be examined further on the joining of the sialon with the steel nitrided for four hours.

4.3.2.3 XRD

XRD examination that was applied on the surface of the interface layer produced only two peaks that represented the ferrite phase (Figure 4.55). This should have been obtained from the interface-layer matrix that comprised significantly high Fe and less quantity of Cr and Si. Hence, the interface-layer matrix in this joint was ferrite solid solution.

No other phase could be detected from the layer by this technique. FeSi_2 that was found in the interface layer of the joint of sialon – as-received 7.5%-Cr FS was not identified in the joint of the current joining condition. Therefore, as it was experienced in joining the sialon with the AISI 430 FSS, it seemed that the nitrided steel had hindered the formation of the iron silicides in the joint.

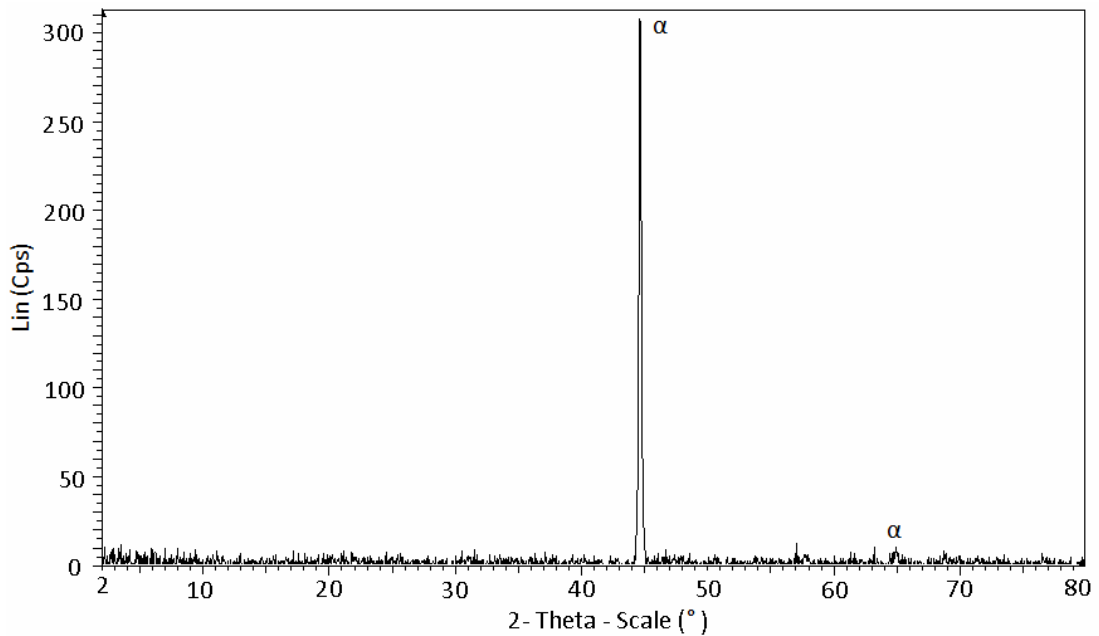


Figure 4.55 X-ray diffractogramme of the interface layer in sialon – one-hour-nitrided 7.5%-Cr FS joint

4.3.2.4 XPS

XPS spectra of Fe and Si from the interface-layer surface supported the information from the XRD examination. The XPS spectra of the elements are shown in Figure 4.56 and Figure 4.57. Plasmon loss as the indication of FeSi_2 peak at around 730 eV was not observed. The Fe was identified in the form of Fe_2O_3 . This was represented by two peaks at 710.33 eV and 723.51 eV. The other two peaks at 707.18 eV and 719.94 eV could be attributed to metallic Fe; while two other peaks at 708.71 eV and 712.84 eV are the satellite peaks. Based on this analysis, the FeSi_2 was not formed in the layer.

The absence of FeSi_2 was also revealed by the Si XPS spectra (Figure 4.57). The examination of the layer surface produced only one peak at 101.98 eV. This corresponds to Si in the form of SiO_2 [85, 88-89].

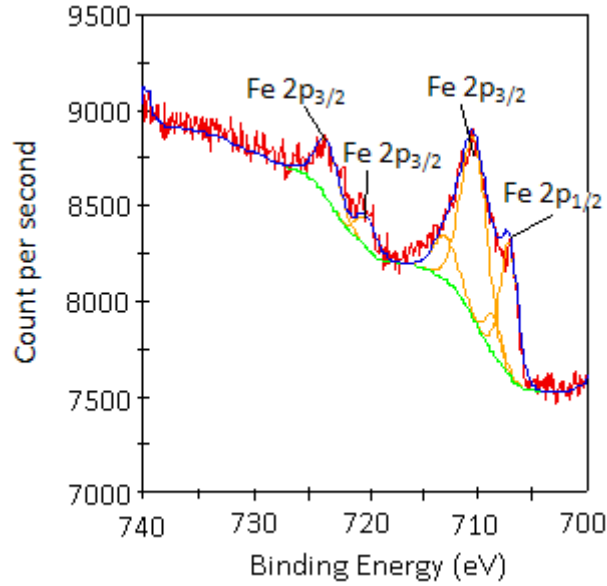


Figure 4.56 XPS spectra of Fe from the interface layer in sialon – one-hour-nitrided 7.5%-Cr FS joint

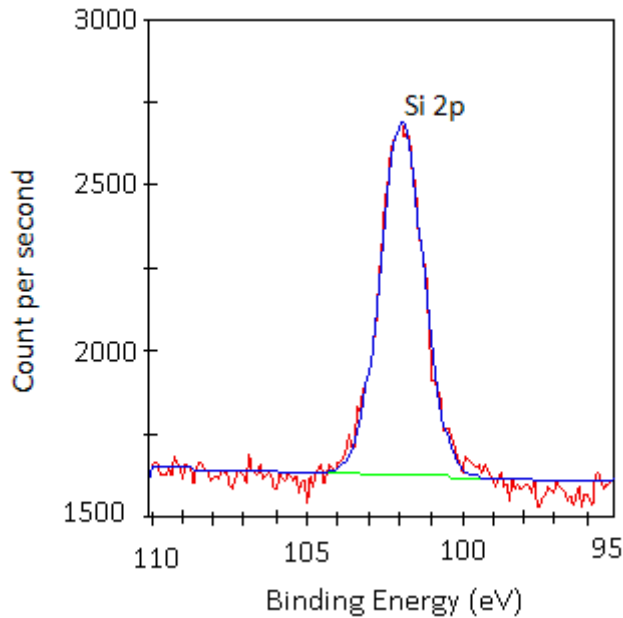


Figure 4.57 XPS spectra of Si from the interface layer in sialon – one-hour-nitrided 7.5%-Cr FS joint

Results of the analyses concluded that FeSi_2 was not formed in the interface layer. These were in accordance with the output of other characterization techniques (*i.e.* EDX and XRD) that were also attempted. The EDX analyses on the interface layer showed that the layer contained less Si. Therefore, composition of the elements were

insufficient to form the silicide. The presence of the silicide was neither detected by the XRD. Hence, it could be concluded that the formation of the iron silicide was hindered in the joint of the sialon – one-hour-nitrided 7.5%-Cr FS. This effect was noticed formerly in the joining of sialon with one-hour-nitrided AISI 430 FSS. This divulged that the experiments had produced a consistent finding, *i.e.* the nitriding suppressed formation of the iron silicide in the joint of the sialon with the steels.

4.3.2.5 Hardness Test across the Joint

Hardness of the reaction layers in the joint is presented in Figure 4.58. The reaction layers of the joint were the lowest-hardness part. Among the layers, the interface layer was harder than the diffusion layer. Hardness of the diffusion layer represented hardness of the ferrite phase which is soft and ductile. The interface layer was slightly harder than the diffusion layer since the phases of the layer were comprised of precipitates and ferrite matrix.

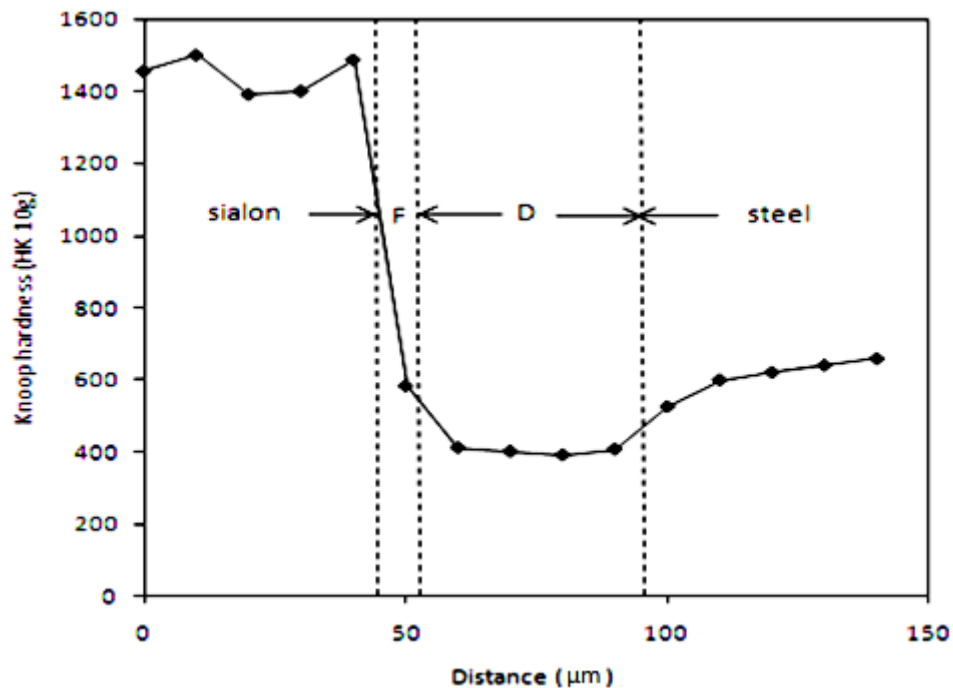


Figure 4.58 Hardness test across the sialon – one-hour-nitrided 7.5%-Cr FS joint;

F=interface layer, D=diffusion layer

4.3.3 Joining of Sialon with Four-hours-nitrided 7.5%-Cr FS

Longer nitriding time was expected to diffuse more nitrogen into the steel and increase the hardened-case depth. This was confirmed in the solution nitriding experiment results that were reported earlier in this chapter (section 4.1.2). The experiment results reported in that section revealed that nitriding for four hours should have diffused nitrogen throughout the steel sample. In this study, joining of the four-hours-nitrided 7.5%-Cr FS to sialon was conducted. The results were explored and compared with the other joining.

4.3.3.1 Microstructure of the Joint

Microstructure of the joint is presented in Figure 4.59 to Figure 4.61. Apparently, the reaction layers in the joint consisted of the interface and the diffusion layers (Figure 4.59 and Figure 4.60). In the parent steel, the existence of fine martensite was obvious. Figure 4.61 depicted that joining of sialon with 7.5%-Cr FS nitrided for four hours seemed to produce the sound joint. However, porosity was observed along the border between the interface layer and the original sialon.

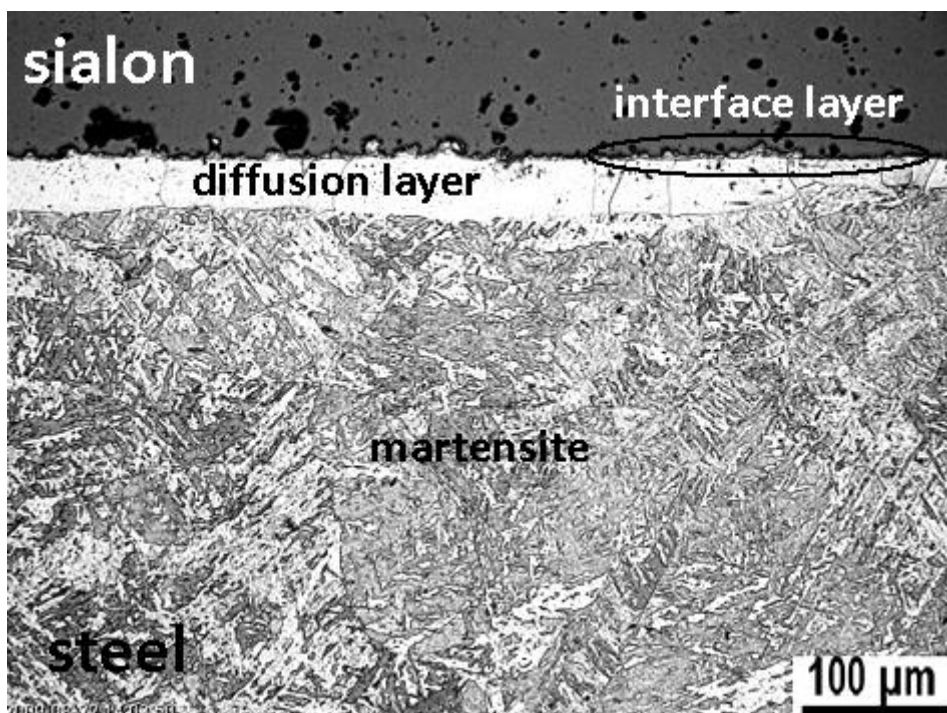


Figure 4.59 Optical micrograph of the cross section of sialon – four-hours-nitrided 7.5%-Cr FS joint

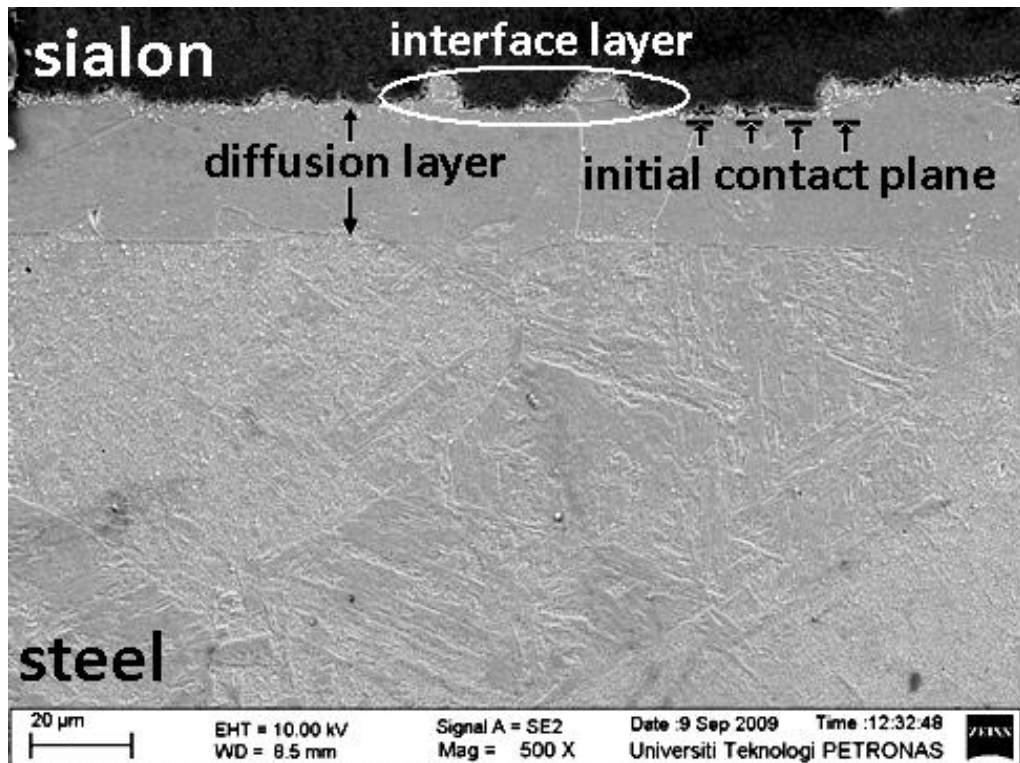


Figure 4.60 Scanning electron micrograph of the cross section of sialon – four-hours-nitrided 7.5%-Cr FS joint

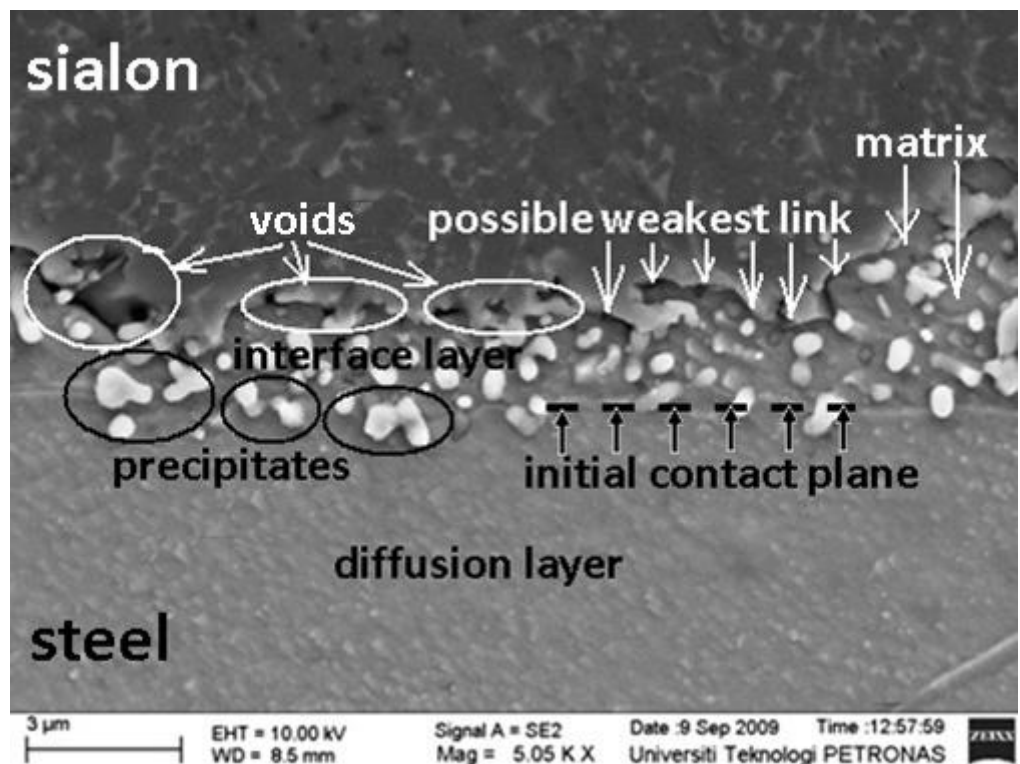


Figure 4.61 Scanning electron micrograph of the cross section of the interface layer in sialon – four-hours-nitrided 7.5%-Cr FS joint

The joint was formed at the location indicated as the initial contact plane (Figure 4.61). After the joining, the initial contact plane of the sialon and the steel was no longer appeared. Previous joining discussed in sections 4.3.1 and 4.3.2 revealed that diffusion layer at the steel side and matrix of the interface layer at the sialon side were the same species that composed the joint. Therefore, as it can be seen in Figure 4.61, microstructure of the sialon – steel interface shows that sound joint has been produced.

Average thickness of the diffusion layer in the joint was 29.4 μm ; while the thickness of the interface layer was 1.8 μm . White precipitates could be seen in the interface layer as shown in Figure 4.61. The interface and the diffusion layers in this joint were thinner than the thickness of the layers formed in the previous joints. It showed that longer-nitrided steel had more significant effect in decreasing the thickness of the interface and the diffusion layers. This might also imply that longer nitriding on the steel lessened its reactivity with the sialon. Further discussion on this effect will be presented in the later section.

The existence of voids in the boundary between sialon and interface layer in this joint were more apparent than in the joint of sialon – as received steel and sialon – one-hour-nitrided steel. Figure 4.61 shows that the voids were observed along the boundary between the sialon and the interface layer. Therefore, this region could become the weakest part of the joint. The voids could lead to crack initiation when the joint is subjected to stress.

4.3.3.2 Elemental analysis

Elemental analysis across the joint shown in Figure 4.62 explains the interdiffusion of elements in the joint. The figure noticed that silicon diffused shorter into the steel than in the joining of sialon with as-received (see Figure 4.44) and one-hour-nitrided steels (see Figure 4.53).

Thickness of the diffusion layer which represented depth of silicon diffusion into the steel was given in the previous section. It has been revealed that the nitrided steel produced shorter diffusion distance of the silicon into the steel in its joining with sialon. Increasing nitriding time on the steel was also recognized to form smaller silicon-diffusion extent. Thinner diffusion layer in the microstructure of the joint reflected this condition. This disclosed that longer-nitrided steel reduced its reactivity with sialon. This was possible since longer nitriding added more nitrogen into the steel. Thus, the steel had more nitrogen content when it was joined with the sialon. Higher nitrogen content in the steel more strongly restrained the diffusion of the silicon into the steel. Consequently, thinner diffusion layer was formed.

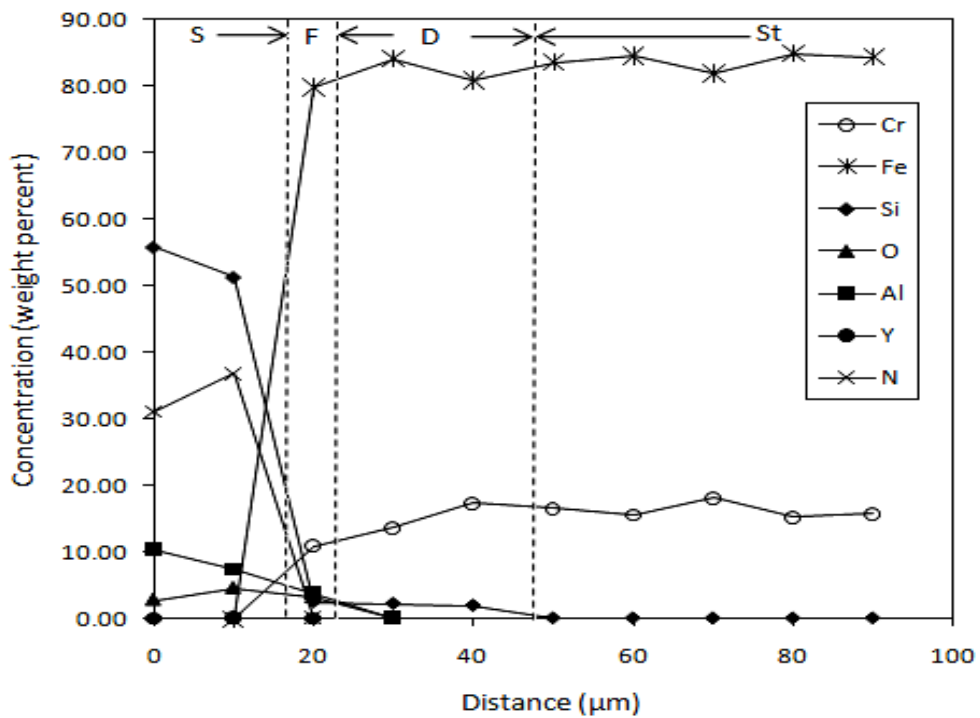


Figure 4.62 Concentration of elements across the joint of sialon – four-hours-nitrided 7.5%-Cr FS joint; S=sialon, F=interface layer, D=diffusion layer

The elements interdiffusion across the joint was similar with the condition in the joint of the sialon – 7.5%-Cr FS nitrided for one hour. The interface layer was formed in the sialon with the average thickness of 1.8 μm. The layer matrix was dominated by Fe and Cr (Table 4.11). Table 4.11 and Table 4.12 were obtained from the elemental analyses carried out at the matrix and the precipitates in the interface layer. The

analyses were carried out according to the spot map given in Figure 4.63. The spots were selected along the layer as the layer is a little bit thin.

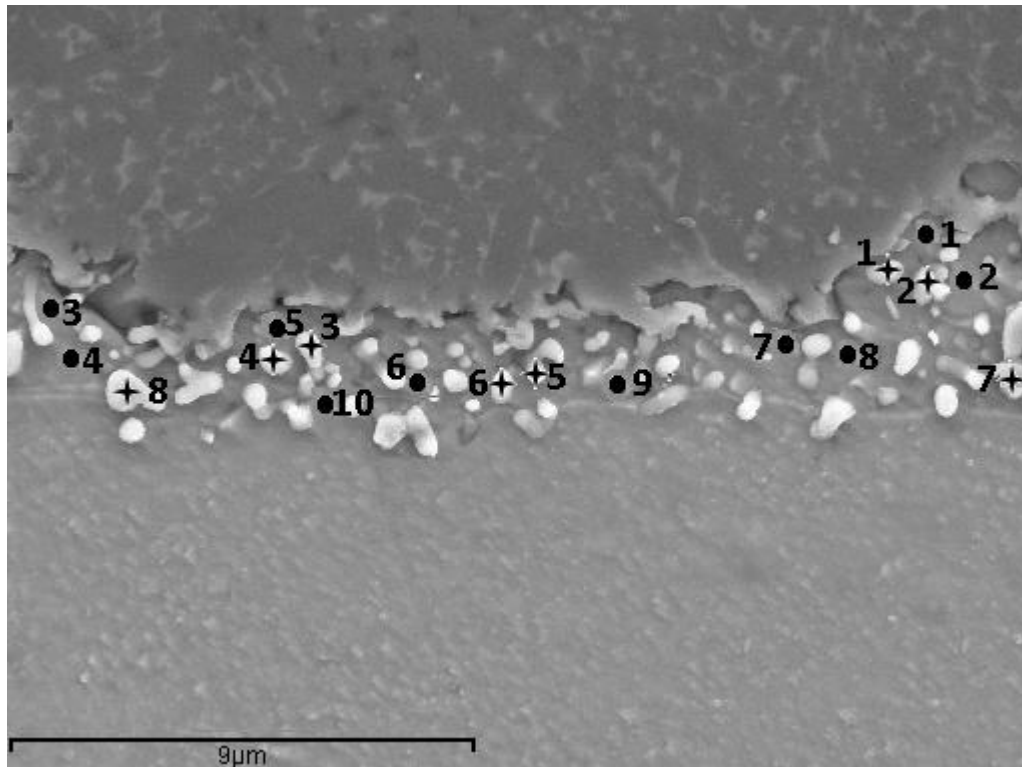


Figure 4.63 Map of EDX spot analysis at the interface layer of sialon – four-hours-nitrided 7.5%-Cr FS joint; (●) = matrix, (+) = precipitates

Table 4.11 Concentration of elements of the interface-layer matrix in sialon – four-hours-nitrided 7.5%-Cr FS joint

Spot number	Concentration (weight %)						
	Cr	Fe	Si	O	Al	Y	N
1	9.89	83.07	3.34	2.87	0.84	0	0
2	7.61	81.09	5.53	4.45	1.33	0	0
3	14.57	82.24	3.17	0	0	0	0
4	8.15	70.18	3.33	6.51	3.87	7.96	0
5	20.20	76.83	2.17	0.00	0.81	0	0
6	18.65	77.89	2.92	0.00	0.54	0	0
7	11.30	78.81	4.82	3.28	1.79	0	0
8	22.44	75.09	2.46	0	0	0	0
9	18.35	79.13	2.51	0	0	0	0
10	20.22	76.81	2.27	0	1	0	0

Table 4.12 Concentration of elements of the precipitates at the interface layer in sialon – four-hours-nitrided 7.5%-Cr FS joint

Spot number	Concentration (weight %)						
	Cr	Fe	Si	O	Al	Y	N
1	7.51	35.54	5.73	22.05	9.65	19.53	0
2	13.97	41.19	2.71	17.94	5.06	8.76	10.38
3	4.44	65.98	4.38	10.33	5.75	9.11	0
4	15.74	80.08	4.18	0	0	0	0
5	19.32	76.86	2.78	0	1.05	0	0
6	18.69	79.06	2.25	0	0	0	0
7	21.86	73.95	4.20	0	0	0	0
8	18.25	79.10	2.65	0	0	0	0

In the interface layer matrix, Fe was found in the spot in the concentration of 70.18 to 83.07 weight percent (Table 4.11). Cr was detected in concentrations of 7.61 to 22.44 weight percent. Sialon's elements were found in small quantity and might dissolve in the iron solid solution. These should form ferrite phase as it was suggested by the analysis for the other joining.

All precipitates in the interface layer contained Fe, Cr and Si (Table 4.12). Fe was found in the range of concentration of 33.08 to 76.8 weight percent. This was the highest-concentration element in the precipitates. Concentration of Cr was much lower than the Fe (*i.e.* 4.21 to 20.15 weight percent). The precipitates also comprised sialon's elements; however, only Si was discovered in all spots of EDX analysis. This was found in the range of 3.16 to 5.33 weight percent.

The elements composition in the interface-layer matrix and the precipitates described similar condition with the joint of the sialon with the steel nitrided for one hour. In this joint, besides the domination of Fe, the layer also consisted of Si in small quantity. In the joint of the sialon and the steel in as-received condition, the Si was observed in relatively high concentration. It was then revealed that the composition of Fe and Si in the precipitates had formed FeSi₂. With little quantity of Si in the precipitates, it could be expected that the silicides might not be formed in the present joint. This condition was formerly faced in the joint of the sialon with the steel nitrided for one hour.

It was reported in section 4.2.4.2 that growth of interface layer in the joint followed the same trend with development of the diffusion layer; *i.e.* joining of the sialon with longer-nitrided steel decreased more significantly thickness of the layer. The previous section (*i.e.* section 4.3.3.1) had given the average thickness of the interface layer of the joint. Obviously, in this joint thickness of the interface layer was smaller than the layer produced in the joint of sialon with as-received and one-hour-nitrided 7.5%-Cr FS. The decrease of the interface layer delineated suppression of the sialon decomposition and also reactivity of the steel with the sialon. The analysis on this joint confirmed that nitrided steel had hampered reactivity of the sialon with the steel. Longer nitriding on the steel prior to joining with sialon signified its hindering effect on the reactivity with the ceramics.

4.3.3.3 XRD

XRD pattern obtained from the surface of the interface layer is displayed in Figure 4.64. The pattern produced several peaks that represented the phases in the layer. Ferrite solid solution was indicated through the existence of α peak. Previous analysis had suggested that this was from the interface-layer matrix which comprised of the ferrite former elements. Other peaks which represented sialon phase were also observed. The peaks emerged from sialon in the steel that was not properly cleaned during sample preparation for the XRD examination. No other new phase or compound was discovered from the layer by this technique. The FeSi_2 peak which was identified in the joint of sialon – as-received 7.5%-Cr FS was not found in this joint. The XRD result agreed with the elemental analysis on the interface layer which found a low concentration of Si. The outcome was also consistent with the previous joining, where nitrided steel in the joining hindered formation of the silicides

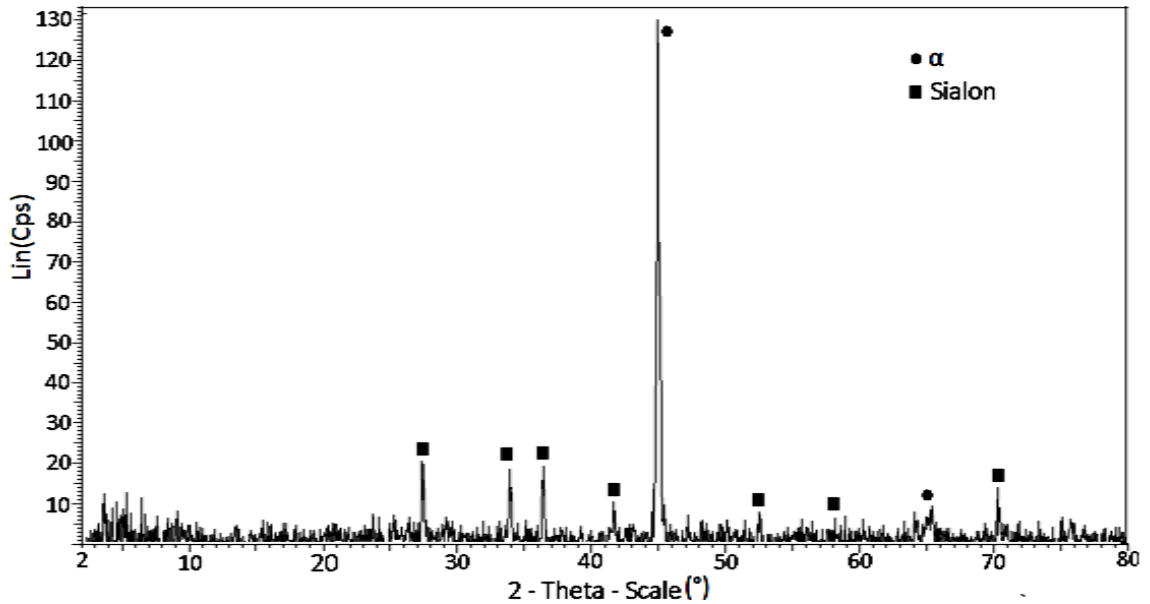


Figure 4.64 X-ray diffractogramme of the interface layer in sialon – four-hours-nitrided 7.5%-Cr FS joint

4.3.3.4 XPS

XPS spectra of Fe and Si from the layer are shown in Figure 4.65 and Figure 4.66, respectively. In the Fe XPS spectra, four peaks of Fe_{2p} can be seen from the fitted spectra. Plasmon loss that indicates $FeSi_2$ did not appear in the spectra. Thus, two peaks at 706 eV and 719 eV correspond to Fe_{2p} in metallic form; while the other peaks at 711.29 eV and 724.48 eV were attributed to the Fe_{2p} in the form of Fe_2O_3 .

Si in the interface layer was in the form of SiO_2 (Figure 4.66). This was suggested by the XPS spectra of the elements from the layer surface. XPS examination on the surface of the interface layer produced only one peak of Si_{2p} at 103.83 eV which corresponds to the Si in the form of the SiO_2 .

The XPS results revealed that Fe was found in the form of oxide and metallic element, while the Si was identified in the form of oxide. The examination did not identify the iron silicide which was found in the interface layer of the sialon – as-received steel. This output was in accordance with the EDX and the XRD results. Elemental analysis on the layer identified the Si in low content. Thus, its composition

might be insufficient to form the iron silicide. This was then confirmed with the XRD results that only found ferrite phase in the layer.

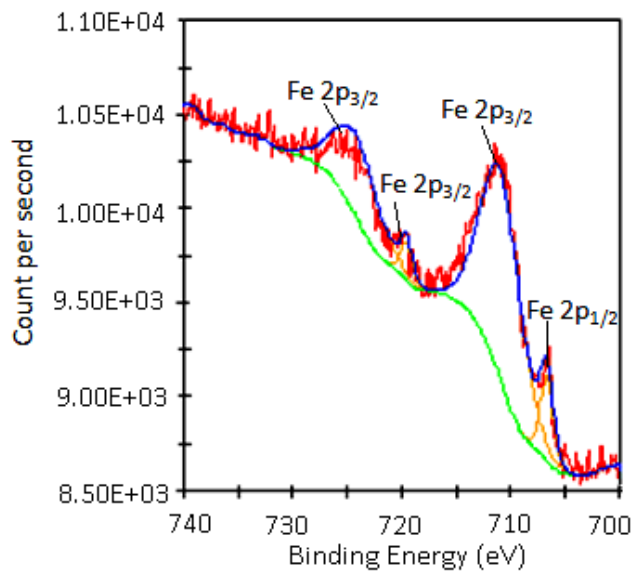


Figure 4.65 XPS spectra of Fe from the interface layer in sialon – four-hours-nitrided 7.5%-Cr FS joint

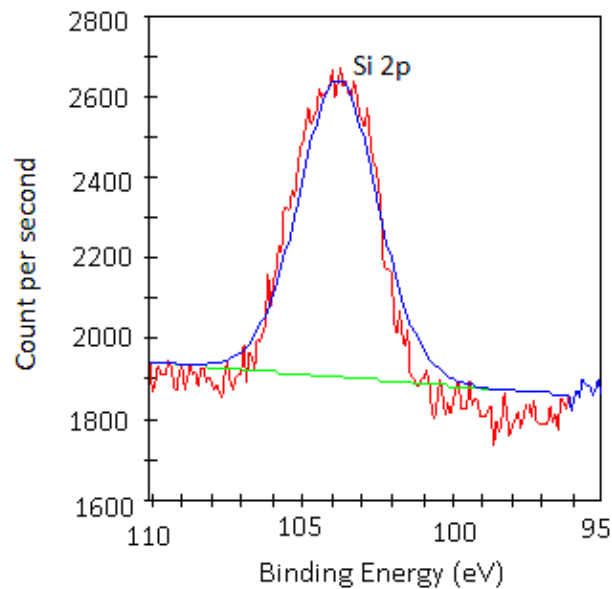


Figure 4.66 XPS spectra of Si from the interface layer in sialon – four-hours-nitrided 7.5%-Cr FS joint

The XPS results supported analysis of the layer using EDX and XRD. This assessment revealed that reaction product of the sialon with the four-hours-nitrided

7.5%-Cr FS was ferrite solid solution in the interface-layer matrix and the diffusion layer. Reaction of the materials also produced precipitates in the layer. Investigations on the interface layer using XPS found iron oxide (Fe_2O_3) and silicon oxide (SiO_2) in the precipitates.

4.3.3.5 Hardness Test across the Joint

Hardness test across the joint of sialon with 7.5%-Cr FS nitrided for four hours is given in Figure 4.67. Hardness of the diffusion layer was lower than the other parts of the joint. This represents hardness of ferrite in the diffusion layer. The hardness of the interface layer was slightly higher than the diffusion layer due to the presence of the precipitates.

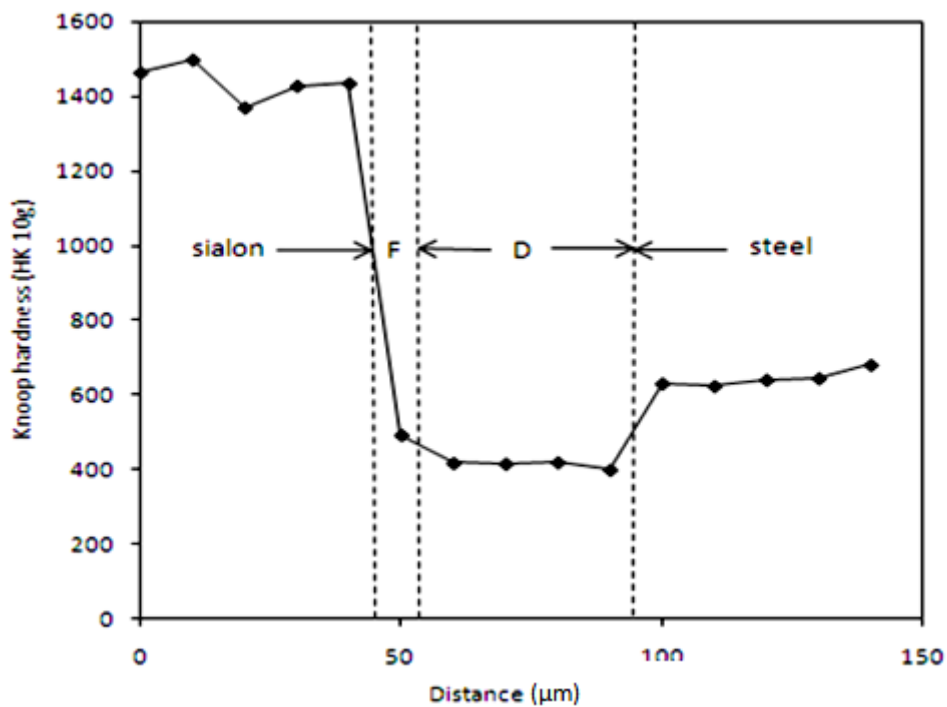


Figure 4.67 Hardness test across the sialon – four-hours-nitrided 7.5%-Cr FS joint;

F=interface layer, D=diffusion layer

4.3.4 Discussion on the Joining of Sialon with 7.5%-Cr FS

Experiments on the joining of sialon with 7.5%-Cr FS revealed that cohesive joint could be achieved using diffusion bonding process. This could be attained in the joining of the sialon with the steel in as-received as well as in nitrided conditions. Reaction between the steel and the sialon was indicated in the joint by the formation of the reaction layers in the joint. Analysis on the joint as well the reaction layers in the joining of the sialon with as-received and nitrided 7.5%-Cr FS is discussed in the following part.

4.3.4.1 Joining of Sialon – As-received 7.5%-Cr FS

Despite little porosities in the border between the interface layer and the original sialon, no crack occurred at the joint of sialon – as-received 7.5%-Cr FS. As also found in the joining of the sialon with the AISI 430 FSS, this joining produced two reaction layers in the joint. The diffusion of the elements from the steel to sialon and *vice versa* was clearly recognized from the elemental analysis of the joint. Diffusion of the steel's elements was known from the existence of Fe and Cr in the interface layer; whereas, silicon was found in the diffusion layer in the steel. Decomposition of the sialon in this joining occurred according to the reaction 2.8. This decomposition took place in the interface layer. The steel's elements diffused into this area. This made the background of the layer to be the steel-like phase.

EDX analyses revealed that the interface layer was dominated by Fe and Cr which were from the steel. Silicon was present in this layer due to the sialon decomposition. The silicon dissolved in the ferrite solid solution in the interface layer matrix as it was revealed by the XRD examination. Dissolution of Si in ferrite solid solution also took place in the diffusion layer at the steel side. Hence, ferrite solid solution had composed the sialon – steel joint. This made the sialon's part (*i.e.* interface layer matrix) and the steel's part (*i.e.* diffusion layer) to be one region; therefore cohesive joint had been produced. This was also indicated by the initial sialon – steel contact plane which disappeared after the joining.

It looked like that transfer of steel part into the sialon took place during the diffusion bonding. It was indicated by the steel-like phase in the matrix of the interface layer. This seemed to shift the sialon – steel contact plane further into the sialon side. Therefore, the boundary between the sialon and the interface layer looked to turn into the new sialon – steel interface. In this region, very-different properties could be expected from the original sialon and the interface layer as sialon is very hard, while ferrite is soft and ductile. The extreme properties difference of the sialon and the interface layer were proven by the hardness test across the joint. The severe properties difference in the sialon and the interface could lead the boundary of these areas to become the weakest part of the joint. This was also noted in the joint of sialon – AISI 430 FSS.

Voids were also formed at the border of the original-sialon – interface-layer. Many workers believed that pores in the reaction layer were created due to the trapped nitrogen [6, 9-10, 12]. Since the voids formation also occurred in the sialon – AISI 430 FSS joint, mechanism of the pores formation has also been explained for the joining of sialon with AISI 430 FSS in section 4.2.4.1. It was explained that the pores might be due to nitrogen which could not escape from the joint.

Compared to the joint of sialon – as-received AISI 430 FSS, more voids were found in the joint of sialon – 7.5%-Cr FS. This was possibly because of the lower Cr content in the 7.5%-Cr FS. Reactivity of nitrogen ceramics (*e.g.* Si_3N_4 , Sialon) was governed by solubility of nitrogen in the steel. Solubility of nitrogen in the steel was restrained by Si and enhanced by Cr. Therefore, with less Cr in the steel, less nitrogen could dissolve in the steel. This yielded more nitrogen which should be removed through the joint. Nitrogen which could not escape from the joint was trapped in the interface and created the porosities.

Taking into account the highly-different properties of the sialon and the interface layer, another mechanism could be proposed. This mechanism has been discussed to explain the voids formation at the interface-layer – original-sialon boundary in sialon – nitrided-AISI 430 FSS joint (section 4.2.4.2). Different properties of interface layer and the original sialon might be responsible for the voids formation in the interface layer – sialon border. The voids formation also related to residual stress that was

generated during cooling stage in the diffusion bonding process. Though the interfacial bond was formed, ceramics would crack if it could not hold the stress. Nevertheless, the joint could be maintained when it could absorb the residual stress. In this case, the effect of the residual stress would be carried by the interface of the sialon – steel (*i.e.* the boundary between the original sialon and the interface layer), since a single part was formed on the joint, which should be capable of holding the effect of the residual stress. Simulation of the residual stress at the joint of sialon – AISI 316 stainless steel using ANSYS software was conducted by Abed *et al.* [4]. The work disclosed that the nature of the stress at the joint was compressive at the free ends and rising tensile toward the centre of the joint section. Therefore, the joint would have to hold the tensile stress at the centre cross section. Due to the extremely-different ductility of the ceramics and the interface layer, the original-sialon – interface-layer boundary would be subjected to the tensile stress. This would produce voids at this part. Hence, this region could become the weakest part of the joint.

Increasing Cr content in the steel increased the reactivity of the ceramics with the alloy. This was also reported in the work which investigated the reactivity of sialon with Fe-Cr alloy [15]. Oliveira *et al.* [78] also supported these claims. With regard to this suggestion, lower Cr content in the 7.5%-Cr FS (compared to the AISI 430 FSS) should have reduced the reactivity of the steel with the sialon. The reactivity of the sialon with the steel could be evaluated based on the thickness of the interface layer or the diffusion layer [15, 77-78]. The thickness of the reaction layer and the diffusion layer in the joint of sialon – 7.5%-Cr FS was approximately 3 μm and 40 μm respectively. This was shorter than the thickness of the layers in the sialon – as-received 430 FSS joint (*i.e.* approximately 5 μm and 60 μm respectively). Therefore, it seemed that 7.5%-Cr FS owned less reactivity with sialon than AISI 430 FSS.

The reaction of the steel and the sialon produced the precipitates in the interface layer. The precipitates in this joining are rich of Fe and Cr from the steel, and Si and N from the sialon. This elemental condition was also found in the joint of the sialon – as-received AISI 430 FSS.

The elements composition in the precipitates led to the prediction of the metallic silicides and nitrides. However, only Fe-Si compound was confirmed through XRD

and XPS examinations. FeSi_2 was the only compound which was detected by the XRD. The technique was not able to detect the chromium nitride even though the EDX analysis in the precipitates found high Cr and N. The FeSi_2 was also revealed by the XPS examination in the surface of the interface layer. Besides FeSi_2 , XPS also found Fe and Si in the form of Fe_2O_3 and SiO_2 . These compounds were also discovered in the joint of sialon with AISI 430 FSS in as-received condition.

The above discussion revealed that the distributions of elements in the joint were similar with the condition in the joint of sialon – as-received 430 FSS that was discussed previously. Despite its less reactivity with sialon; the lower Cr content in the steel did not seem to give significant effect on the reaction products of the materials. Therefore, same explanation could be proposed for the reaction of the steel with the sialon. Decomposition of sialon in contact with 7.5%-Cr FS liberated Si and N. At the same time Fe and Cr from the steel transferred into the sialon-decomposed area. Nitrogen was first dissociated through gas phase. This molecular nitrogen was trapped in the interface and produced the porosities. The nitrogen also diffused into the parent steel as indicated by the martensite formation in this area. Reaction of Si with Fe and Cr in this area produced $\alpha\text{-Fe}(\text{Cr}, \text{Si})$ in the interface-layer matrix. This reaction also occurred in the steel and built the silicon-diffusion layer in the steel. Cr and Si stabilized the ferrite solid solution in those areas as both elements are ferrite formers. Fast decomposition rate of the sialon released silicon that could not completely dissolve in the steel. The silicon reacted with Fe and formed the FeSi_2 in the precipitates in the layer. The interaction of Fe and O in this part also created iron oxide (Fe_2O_3). Oxide of silicon was also formed in the precipitates as the product of Si and O recombination.

Possibility of Fe – Si compound formation in the Fe – Si system was discussed in section 2.6.2. The section also explored the works which found Fe – Si compound through their characterization on the interface layer of the Si_3N_4 – steel joint. A few of them judged that no new compound was formed in the interface layer. However, several others suggested that metallic silicide and nitride were produced in the layer.

In the reaction of the sialon – steel, recombination of Al and O was claimed to be in the precipitates [15]. Nevertheless, another work predicted the compound of Fe – Si

in the interface of the sialon – 9%-Cr ferritic stainless steel joint [5, 17]. The present study has shown that FeSi_2 was strongly indicated in the joining of the sialon with the two kinds of steel, *i.e.* 7.5%-Cr FS and AISI 430 FSS. Besides the iron silicide, Fe_2O_3 and SiO_2 possibly were also formed in the precipitates as they were shown by the XPS spectra. The oxides might be formed due to the reaction of Fe and O from the dissociated sialon; while the SiO_2 was the results of the sialon's elements recombination.

4.3.4.2 Joining of Sialon – Nitrided 7.5%-Cr FS

Morphology of the reaction layers in sialon – nitrided-7.5%-Cr FS joint was similar with the morphology of sialon – as-received 7.5%-Cr FS joint. The reaction layers contained silicon diffusion layer in the steel and interface layer in sialon. The interface layer was the region where the sialon decomposed during the diffusion bonding. Diffusion of steel's element produced ferrite solid solution in the interface layer matrix. Reaction of Fe and Cr with other sialon's elements formed oxides precipitation. EDX analyses in the interface layer identified that content of Fe and Cr was dominant either in the precipitates or the layer matrix. This revealed that the steel transferred into the decomposed-part of the sialon. The steel moved across the initial sialon – steel contact plane. Therefore the interface of the steel and the original sialon shifted to the boundary between the interface layer and the original sialon.

The boundary between sialon and interface layer could be the weakest region of the joint. This was due to properties of the original sialon and the interface layer which were highly different. Voids at the border between original sialon and interface layer in the sialon – nitrided 7.5%-FS were more apparent than in the joint of sialon – as-received 7.5%-Cr FS. The voids were observed along the interface of the original sialon and the interface layer. The presence of voids in this part could also make the sialon-interface layer boundary become the most-critical part.

As also explained in the previous joining, many researchers agreed that voids in the interface layer might be due to the trapped nitrogen. The nitrogen was produced from the decomposition of sialon during the joining process. With sufficient solubility

of nitrogen in the steel, more nitrogen could be accommodated. Nitrogen that did not dissolve in the steel would escape from the joint through the opening at the edge of the joint. The rest of nitrogen would be trapped in the joint and created pores at the reaction layer in the ceramics. Degassing experiment proved that pores at the reaction layer in Si_3N_4 – AISI 316 stainless steel joint was filled with molecular nitrogen [12].

For the joint of sialon – nitrided steel, the steel had contained nitrogen prior to the joining. Nitrogen in the steel decreased the solubility of nitrogen released from the sialon decomposition. Thus, less nitrogen could dissolve in the steel. Consequently, more nitrogen concentrated in the joint. This could potentially produced pores.

In the present work, voids were formed along the boundary between the original sialon and the interface layer. Therefore, voids along the sialon – interface-layer border might also be due to the big difference between the sialon's and interface-layer's properties. The extreme difference of the properties from both regions was revealed by the result of the hardness test. As it was expected, the original sialon owned significantly higher hardness than the interface layer. Big gap of ductility between the sialon and the interface layer could make the boundary between them to be the most-critical part for failure. The sialon and the interface layer should also have different coefficient thermal expansion. Those extremely-different properties led the joint section to be in state of stress when cooled from the joining temperature [11]. The residual stress induced voids in the boundary between the sialon and the interface layer. The voids in the sialon – interface-layer boundary were the points of stress concentration and could become the point of crack initiation. This may weaken the joint. Therefore the sialon – interface-layer boundary might become the weakest part of the joint.

Suppression of FeSi_2 in the interface layer was exhibited in the joint of sialon with AISI 430 FSS in nitrided conditions. This phenomenon was also demonstrated in the joint of sialon with nitrided 7.5%-Cr FS. This was observed in the joint of the ceramics with the steel nitrided for one and four hours. FeSi_2 was identified in the interface layer of the sialon – as-received 7.5%-Cr FS joint. However, it was not found in the sialon – nitrided 7.5%-Cr FS joint. In the interface-layer matrix, reaction

of the nitrided 7.5%-Cr FS and the sialon produced ferrite solid solution. This reaction was extended into the steel side and formed the silicon-diffusion layer.

Precipitates as the reaction products of the materials in the interface layer contained less Si and N than in the reaction of the sialon with the as-received 7.5%-Cr FS. This had been identified in the joint of the sialon with one-hour-nitrided 7.5%-Cr FS. Further characterization on the interface layer surface using XRD and XPS disclosed the absence of the FeSi_2 . The XPS found Fe and Si as oxides (*i.e.* Fe_2O_3 and SiO_2) in the layer. Thus, nitriding as short as one hour had suppressed the formation of the metallic silicides in the joint interface.

Since similar reactions products were shown in the joint of sialon with the nitrided AISI 430 FSS, the reactions of the sialon with the nitrided 7.5%-Cr FS might take place through the same mechanism. The solution nitriding applied on the steel had made the steel to be in a nitrogen-pre-solved condition. Nitrogen in the steel reduced the decomposition of the sialon. Thus, less sialon was decomposed. The silicon dissolved in the iron in the interface layer as well as in the diffusion layer in the steel. Less fraction of the silicon precipitated in the layer. This was insufficient to form the silicides with the iron. Instead of forming silicides, Fe reacted with O_2 and formed Fe_2O_3 in the precipitates; while the silicon recombined with oxygen and produced SiO_2 . Formation of the oxides might be possible considering relatively-high concentration of oxygen in the precipitates. These compounds were not identified by the XRD, yet it was detected through the XPS examinations. Formation of the insoluble oxides in the interface layer was also suggested by a few workers in this area [2, 13]. Similar mechanism was observed in the joint of Ti with Si_3N_4 . This has been discussed in sections 1.1 and 4.3.4.2. In this joint, formation of Ti_5Si_3 was suppressed when the dissolved nitrogen reached certain amount [8]. Therefore adding nitrogen into the metal prior to joining restrained the growth of the metallic silicides in the interface.

The similarity of reaction products in sialon – nitrided 7.5%-Cr FS and sialon – nitrided AISI 430 FSS joints disclosed the consistency of the experiments results. The suppression of Fe-Si compound in the interface layer of the joint was performed by the nitrided steel. Section 4.2.4.2 disclosed that the suppression was achieved through

decreasing the dissociation of the sialon due to the nitrogen in the steel. Thus, it hindered the formation of iron silicide. In this case, the experiments outcome suggested that nitriding for one hour was sufficient to prevent Fe-Si compound formation in the joint interface.

Benefit of the FeSi_2 suppression has been established previously in section 4.2.4.2. The section also addressed that fast decomposition of the ceramics and production of the brittle phase should be prevented in the joint. As metallic silicides is commonly a brittle phase, it also has to be avoided. For this purpose, nitrided-7.5%-Cr FS hindered the decomposition of the sialon and avoid the formation of the metallic silicides in the joint. Considering that metallic silicide is brittle, suppression of the compound formation in the joint by the nitrided steel could be expected to produce stronger joint. Study of the mechanical strength of the joint may be able to prove this. Evaluation of the joint strength is beyond the scope of this work. Hence, it is recommended for the further work in this area.

Nitrided steel in the present joint was also proven to prevent the growth of the interface layer and the diffusion layer. The reduction of the layers' thickness was demonstrated in the joint of sialon – 7.5%-Cr FS nitrided for one and four hours. Average thickness of the layers in the joint of sialon – 7.5%-Cr FS is displayed in Figure 4.68.

Figure 4.68 illustrates that thickness of the interface layer and the diffusion layer decreased when the sialon was joined with the nitrided steel. The decrease of the layers' thickness was more significant in the joint of the sialon with longer-nitrided steel. Thus it evidenced that the nitrided steel suppressed the growth of the reaction layers thickness in the sialon – 7.5%-Cr FS joint. This also reflected that the nitrided steel lessened the decomposition of sialon and silicon diffusion in the steel side. The mechanism of this phenomenon is similar with the joint of sialon – AISI 430 FSS. Nitrogen in the steel (that is added into the steel through the solution nitriding process) hampered the decomposition of the sialon. This produced thinner decomposition part of the sialon (*i.e.* the interface layer). It also produced less decomposed sialon that was consumed by the sialon – steel reaction in the joint. Therefore, silicon diffused shorter into the steel and built a thinner diffusion layer.

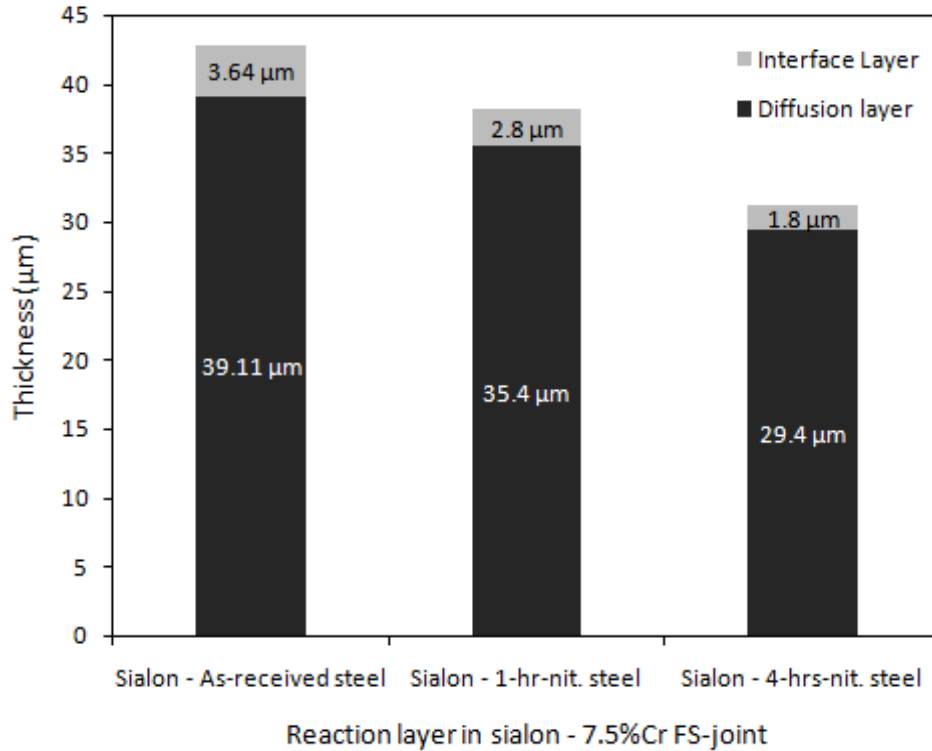


Figure 4.68 Average thickness of interface layer and diffusion layer in sialon – 7.5%-Cr FS joint

Formation of the thin reaction layers in the steel –sialon joint was found earlier in the sialon – AISI 430 FSS joint. It was explored and discussed in section 4.3.4.2. Reduction of the reaction layers caused by the nitrated steel in the joint of sialon – AISI 430 FSS and sialon – 7.5%-Cr FS were in a similar trend. The former joint also illustrated that thickness of the reaction layers decreased when the sialon was joined with the nitrated steel. The reduction was more significant when the ceramics was joined with the longer-nitrated steel. In all joining conditions, the interface and the diffusion layers in the sialon – AISI 430 FSS joint were thicker than the layers in the joint of sialon – 7.5%-Cr FS. As explained in section 4.3.1.2, this was due to higher Cr content in AISI 430 FSS which enhanced reactivity of the joined materials. The discussions in this paragraph highlights that in this work, the role of the nitrated steel to dwindle the growth of the interface and the diffusion layers was exhibited in the joint of sialon with both 7.5%-Cr FS and AISI 430 FSS. Therefore, this phenomenon could possibly be generalized for the joining of sialon with chromium steel.

Ruiz *et al.* [11] suggested that reaction layer in ceramic – metal joint affected the joint strength in a number of factors, namely: mechanical properties of the layer, its thickness and morphology, and the strength of the interfacial bond. However, thickness of the reaction layer played a dominant effect. The joint was produced by the interdiffusion of elements and reaction that produced interfacial bond. This was indicated by formation of reaction layers in the joint. Too-thin reaction layers might indicate that the reaction was not sufficient to produce the interfacial bond. However, excessive growth of the layer may decrease the joint strength. This was due to the reaction products in the layers which mostly are brittle phase. Hence, there would be an optimum layer thickness that provided maximum joint strength. Several works observed an optimum reaction layer thickness that gave maximum joint strength [75-76]. It was noted that initially the joint strength of ceramic – metal increased with the increasing reaction layer thickness. Subsequently, the joint strength diminished when excessive growth of the layer occurred.

In the present work, nitrided steel decreased the thickness of the reaction layer. The decrease of the layer was more obvious in the joint of sialon with longer-nitrided steel. The nitrided steel also avoided the brittle-silicide formation. This agreed well with the phenomenon discussed in the previous paragraph. Despite the benefit that could be gained from the iron-silicide suppression, too thin reaction layers produced in the joint of sialon – four-hours-nitrided 7.5%-Cr FS divulged poor reactivity of materials. According to the discussion in the preceding paragraph, this could produce insufficient reaction to produce strong interfacial bond. With this reason, too long nitriding on the steel might not be recommended for the joining with sialon.

4.3.4.3 Hardness of the Joint Section

Hardness test on the joint cross section predicted mechanical properties of the reaction layers in the joint. Hardness of the joint section in sialon – 7.5%-Cr FS joint is similar with the hardness of the sialon – AISI 430 FSS joint section. Since the joint section consists of three parts (*i.e.* original sialon, interface layer, diffusion layer and parent steel), four hardness levels was indicated in the joint.

The original sialon shows highest hardness. This could be expected since the ceramics is originally hard and stable at high temperature. Thus, its high hardness was maintained during the joining. However, decomposition of the sialon due to reaction with steel had decreased its hardness. This was shown by the hardness of the interface layer. The decomposed part of the sialon (*i.e.* the interface layer) transformed to ferritic structure with iron silicide and oxides precipitates. Thus, it was just like a sialon – steel composite.

Hardness of the interface layer should be the combination of ferrite solid solution in the matrix and iron silicide and/or oxides in the precipitates. Ferrite solid solution is the only phase in the diffusion layer. Thus, hardness of the interface-layer matrix and the diffusion layer should be the same, since it contains the same phase. Hardness test for the sialon – 7.5%-Cr FS joint section shows that the interface layer is harder than the diffusion layer. Hence, it reveals that the precipitates increase hardness of the layer.

Microstructure of the parent steel of 7.5%-Cr FS after the diffusion bonding is fully martensitic. With this structure, high hardness in this part could be expected. This was also revealed in the hardness test results across the joint. Morphology of the joint section of sialon – as-received 7.5%-Cr FS and sialon – nitrided 7.5%-Cr FS was similar. Reaction layers in those joints comprise the diffusion and the interface layer. Section 4.3.4.2 established that reaction layers in the joints differed only in their thickness. Therefore, the above discussion represented hardness condition of the joint section for all joining conditions (*i.e.* sialon – as received 7.5%-Cr FS and sialon – nitrided 7.5%-Cr FS).

Similar with the joint section of sialon – AISI 430 FSS joint, hardness of the reaction layers is lower than the original sialon and the parent steel. The lower hardness indicates that the layers are more ductile than the original sialon and the parent steel which consists of martensite phase. Thus, as it was also observed in the joint of sialon – AISI 430 FSS, this layer could act as a bridge between the two brittle parts. In one side, this might be beneficial in dealing with the residual stress at the joint. The ductile layers in the joint could absorb the residual stress to avoid crack at

the join. However, the drastic change in ductility might also lead to voids formation in the boundary between the original sialon and the interface layer.

CHAPTER 5

CONCLUSIONS AND RECOMMENDATIONS

5.1 Conclusions

The experimental study that was accomplished in this research generated several main conclusions. Those are as follows:

1. Sialon – AISI 430 FSS and sialon – 7.5%-Cr FS joints were achieved by the diffusion bonding process carried out at 1200°C for one hour in a hot press machine. Heating the properly-contacted sialon and steel surface for one hour during the diffusion bonding induced the sialon decomposition and elements interdiffusion. Reaction of the elements built reaction layers both in the sialon and the steel sides in the joint interface. The reaction layers produced interfacial joints of the materials.
2. Diffusion bonding produced cohesive sialon – steel joint by creating reaction-product layers in the interface. As the results of the sialon – steel interaction, a ferrite-solid-solution bridge was built in the sialon and the steel in the joint interface. The ferrite-solid-solution bridge in the sialon – steel interface produced the cohesive joint. The solid solution composed of the sialon's and the steel's elements. The interfacial joint was produced through decomposition of sialon and elements interdiffusion. Heating the mating sialon and steel surfaces at 1200°C for one hour decomposed the sialon which liberated Si and N. It also facilitated the diffusion of elements between the sialon and the steel. Silicon and nitrogen diffused into the steel which has lower Si and N concentrations. Conversely, Fe and Cr from the steel also diffused into the sialon which had lower content of the elements. Reaction product layers were

formed in the sialon and the steel side. Formation of the reaction layers in the sialon – steel interface produced the joint.

3. Decomposition of sialon and elements interdiffusion in the diffusion bonding yielded diffusion layer in the steel and interface layer in the sialon. Microstructure of the joint cross section showed that part of the reaction layers in the sialon (*i.e.* interface-layer matrix) and in the steel sides (*i.e.* diffusion layer) had the same contrast. EDX analyses disclosed that those parts composed of sialon's and steel's elements in similar composition. XRD and XPS examinations subsequently found the same phase, *i.e.* α -Fe (Cr, Si) on those regions. Thus, the interface-layer matrix and the diffusion layer were the same species that composed the sialon – steel joints. Therefore, the initial sialon – steel contact plane was no longer appeared. This indicated that sound joint between the sialon and the steel was formed by reaction of the materials. Besides ferrite solid solution, precipitation of silicides and oxides were formed in the interface layer of sialon – as-received steel; while in the sialon – nitrided steel, the precipitates contained only oxides. Thus, Fe and Cr also reacted with other sialon's elements in the interface layer to produce white precipitates which comprised oxides and silicides. The diffusion layer was ductile since it comprised ferrite solid solution. Hardness test across the joint revealed that the diffusion layer owned lower hardness than the steel. The interface layer was slightly harder than the diffusion layer due to the presence of the precipitates. However, its hardness was lower than the original sialon. Therefore, in overall, the ductility of the reaction layers (*i.e.* interface and diffusion layers) was in between the sialon and the parent steel. Thus, the ductile reaction layers in the joint were bridging the hard-and-brittle sialon and martensitic parent steel. The layers could be advantageous for accommodating the residual stress that was generated during cooling and contributed the strength to the joint. Reactivity of the sialon – AISI 430 FSS was better than that of the sialon – 7.5%-Cr FS since the AISI 430 FSS has higher Cr content. The better-reactivity of the sialon with the AISI 430 FSS was depicted by formation of thicker reaction layers in the joint.

4. The work attempted the diffusion bonding of sialon with nitrided steels. Nitriding was applied on the steels so that the steels were diffusion bonded in nitrogen-pre-dissolved condition. Addition of nitrogen into the steels was indicated by martensite formation and hardness improvement on the steel. Nitrogen added into the steel through the nitriding decreased the sialon decomposition. It also restrained the solubility of nitrogen in the steel during the diffusion-bonding process. Thus, the nitrided steel reduced reactivity of the sialon with the steel. It was depicted by the thinner reaction layers that were developed in sialon – nitrided steels joint than in sialon – as-received steel. Reduction of the sialon decomposition suppressed the formation of FeSi_2 in the interface layer. The FeSi_2 was revealed by XRD and XPS examinations on the interface layer of sialon – as-received steel joint. Nevertheless, it was not identified in the interface layer of sialon – nitrided steel joint. The suppression of FeSi_2 formation in the joint could be beneficial as the silicide is brittle. Thus, preventing its formation might be able to improve the joint strength.

5.2 Contributions

The overall research provides several contributions on the area of the ceramic-metal joining. Those are as follows:

1. This work has successfully joined sialon and AISI 430 FSS using the diffusion bonding process. AISI 430 FSS has a good corrosion resistance as commonly owned by other stainless steel. This material is also used for high temperature applications. Thus it is suitable to be combined with sialon to serve corrosive and high temperature applications. Since the AISI 430 FSS is readily available in the market, the joining with sialon has a good prospect to be developed to expand the sialon's utilization.
2. The work has identified FeSi_2 in the reaction layer of the sialon and AISI 430 FSS. The silicide was also characterized at the reaction layers of the sialon and 7.5%-Cr FS. Although previous similar works predicted the presence of the

silicide, yet the characterization performed in that study failed to prove it. It also failed to identify the exact compound of the silicide.

3. The work provided evidence of hindering-effect of nitrided steel on sialon decomposition. Influence of the nitrided steel prior on suppressing silicide formation was also observed.

5.3 Recommendations

The overall activities carried out in this project identify several recommendations for further exploration of the area. Those are as follows:

1. The joining of the sialon with AISI 430 FSS and 7.5%-Cr FS using diffusion bonding process was possible. The role of the ductile reaction layers in avoiding crack at the ceramics was implied. However, the present work did not scrutinize the joint strength produced by the joining process of the materials. Thus, further work on accessing the joint strength is recommended.
2. Nitrided steel could be beneficial to produce the joint by suppressing the brittle FeSi_2 in the interface. This possibly reduced the brittleness of the interface layer. Nevertheless, the reactivity of the materials that contributed to the joint formation might be impeded by the pre-treated steel. Thus, there might be an optimum condition that provides the best condition for the joint. Further study on the influence of the nitrided steel on the strength of its joint with sialon would be useful. The study would be more meaningful if it could provide the optimum nitriding condition which gives highest joint strength. Those are beyond the scope of the present study. Therefore, the investigations are recommended for the continuation of the research.
3. Prevention of brittle silicide could improve the joint strength as it was also agreed by previous works. However, the absence of the silicide in the sialon – steel interface might also be detrimental as this makes large properties distribution between the sialon and the steel in the interface layer. The extreme properties difference between the sialon and the interface layer might induce

voids in their border and could lead to crack initiation. These voids were observed in the border between the original sialon and the interface layer through the scanning electron micrograph of the interface-layer. Investigation on the influence of the silicide on voids formation in the joint interface is suggested for further study.

4. Previous study suggested that joining sialon with austenitic stainless steel produced crack at the ceramics. The present research found that joining sialon with ferritic steel and ferritic stainless steel was successful. Investigation on the joining the sialon with other types of stainless steels, *i.e.* martensitic and duplex, is valuable for future works.

AWARDS AND PUBLICATIONS

Conferences:

1. “Microstructure and hardness of 9% Cr ferritic stainless steel nitrided at high temperature,” *Proceeding of the 6th International Materials Technology Conference & Exhibition*, Kuala Lumpur, Malaysia, 26 – 27 August, 2008.
2. “Solution nitriding of AISI 430 ferritic stainless steel,” *Proceedings of International Conference on Materials and Metallurgical Technology*, Surabaya, Indonesia, 24 – 25 June 2009.
3. “Interface and interphases study of 7.5%-Cr ferritic steel/sialon joint using scanning electron microscopy with EDAX spectroscopy,” *Proceedings of 19th Scientific Conference of the Electron Microscopy Society of Malaysia*, Langkawi, Malaysia, 8 – 10 December 2010.

Journal Publications:

1. “Interface layer of the diffusion-bonded sialon with high-chromium steel”, *Journal of Applied Sciences* v 11(3) 2011.
2. “Suppression of iron-silicide formation in the joint of sialon – 7.5%-Cr ferritic steel,” accepted for publication (article in press) in *Journal of Defect and Diffusion Forum*, by Trans Tech. Publications, Switzerland.

Awards:

1. Gold Medal in 24th *UTP-Engineering Design Exhibition (EDX)*, UTP, 21 – 22 October 2009.
2. Gold medal and Brussel Innova Special Award in *INNOVA BRUSSEL 2009 – The Belgian and International Trade Fair for Technological Innovation (Innova Eureka Competition)*, Belgium, 19 – 21 November 2009.
3. Silver medal in 21st *International Invention, Innovation & Technology Exhibition (ITEX) 2010*, Kuala Lumpur, 14 – 16 May 2010.

Patent Filing:

1. “A Method of Joining an Engineering Ceramics to Metal”, Patent filing no: PI 2010001428

REFERENCES

- [1] J. L. Ruiz and R. A. L. Drew, "Joining of silicon nitride with a titanium foil interlayer," *Materials Science and Engineering A*, vol. 352, pp. 169-178, 2003.
- [2] A. Krajewski, "Joining of Si₃N₄ to wear-resistant steel by direct diffusion bonding," *Journal of Materials Processing Technology*, vol. 54, pp. 103-108, 1995.
- [3] J. A. Fernie, R. A. L. Drew, and K. M. Knowles, "Joining of Engineering Ceramics," *International Materials Reviews*, vol. 54, pp. 283-331, 2009.
- [4] A. Abed, P. Hussain, I. S. Jalham, and A. Hendry, "Joining of sialon ceramics by a stainless steel interlayer," *Journal of the European Ceramic Society*, vol. 21, pp. 2803-2809, 2001.
- [5] P. Hussain and A. Isnin, "Joining of austenitic stainless steel and ferritic stainless steel to sialon," *Journal of Materials Processing Technology*, vol. 113, pp. 222 – 227, 2001.
- [6] E. Heikinkeimo, I. Isomaki, A. A. Kodentsov, and F. J. J. v. Loo, "Chemical interaction between Fe and silicon nitride ceramic," *Journal of European Ceramic Society*, vol. 17, pp. 25 – 31 1997.
- [7] M. Kalin, J. Vižintin, J. Vleugels, and O. V. D. Biest, "Chemical reactivity of silicon nitride with steel and oxidized steel between 500 and 1200°C," *Materials Science and Engineering A*, vol. 281, pp. 28-36, 2000.
- [8] M. Maeda, R. Oomoto, M. Naka, and T. Shibayanagi, "Interfacial reaction between titanium and silicon nitride during solid state diffusion bonding," *Trans. JWRI*, vol. 30, 2001.
- [9] M. I. Osendi, A. D. Pablos, and P. Miranzo, "Microstructure and mechanical strength of Si₃N₄/Ni solid state bonded interfaces," *Materials Science and Engineering A*, vol. 308, pp. 53-59, 2001.

- [10] R. Polanco, A. D. Pablos, and M. I. Osendi, "Metal–ceramic interfaces: joining silicon nitride–stainless steel," *Applied Surface Science*, vol. 238, pp. 506–512, 2004.
- [11] J. L. Ruiz, A. L. P. J., and A. L. Drew, "Self-joining of Si₃N₄ using metal interlayers," *Metallurgical and Materials Transactions A*, vol. 37A, 2006.
- [12] B. T. J. Stoop and G. d. Ouden, "Diffusion bonding of silicon nitride to austenitic stainless steel with metallic interlayers," *Metallurgical Transactions A*, vol. 26A, 1995.
- [13] S. D. Peteves, M. Paulasto, G. Ceccone, and V. Stamos, "The reactive route to ceramic joining: fabrication, interfacial chemistry and joint properties," *Acta Mater*, vol. 46, pp. 2407-2414, 1998.
- [14] B. T. J. Stoop and G. d. Ouden, "Diffusion bonding of silicon nitride to austenitic stainless steel without interlayers," *Metallurgical Transactions A*, vol. 24A, 1993.
- [15] J. Vleugels, L. Vandeperre, and O. V. D. Biest, "Influence of alloying elements on the chemical reactivity between Si-Al-O-N ceramics and iron-based alloys," *Journal of Materials Research*, vol. 11, 1996.
- [16] B. T. J. Stoop, "Diffusion bonding of silicon nitride to austenitic stainless steel," PhD Dissertation, Department of Materials Science and Engineering, Delft University of Technology, Delft, 1992.
- [17] P. Hussain, "Diffusion bonding of sialon and stainless steel," Ph.D Dissertation, Mechanical Engineering Department, University of Strathclyde, Glasgow, UK, 1997.
- [18] R. Riedel and I.-W. Chen, Eds., *Materials and Properties* (Ceramics Science and Technology). Weinheim: Wiley-VCH Verlag, p. 68, 2010.
- [19] M. S. M. Noaman, Z. Lences, M. Vitkovič, Z. Gabrišová, and M. Palou, "Comparison of two β-SiAlON ceramics prepared from synthetic and natural raw materials," *Acta Chimica Slovaca*, vol. 2, pp. 3-13, 2009.
- [20] D. Q. Peng, T. H. Kim, J. H. Chung, and J. K. Park, "Development of nitride-layer of AISI 304 austenitic stainless steel during high-temperature ammonia gas-nitriding," *Applied Surface Science*, vol. 256, pp. 7522–7529, 2010.

- [21] X. Yi, K. Watanabe, and T. Akiyama, "Fabrication of dense β -SiAlON by a combination of combustion synthesis (CS) and spark plasma sintering (SPS)," *Intermetallics*, vol. 18, pp. 536–541, 2010.
- [22] S. Hampshire, "Silicon nitride ceramics – review of structure, processing and properties," *Journal of Achievements in Materials and Manufacturing Engineering*, vol. 24, pp. 43-50, 2007.
- [23] A. Rosenflanz, "Silicon nitride and sialon ceramic," *Current Opinion in Solid State and Materials Science*, vol. 4, pp. 453-459, 1999.
- [24] G. Z. Cao and R. Metselaar 1991, " α' -Sialon ceramics: a review " *Chemistry of Materials*, , vol. 3, pp. 242-252, 1991.
- [25] Z. Shen and M. Nygren, "Implications of kinetically promoted formation of metastable α -sialon phases," *Journal of the European Ceramic Society*, vol. 21, pp. 611-615, 2001.
- [26] I. Zalite, N. Zilinska, and G. Kladler, "SiAlON ceramics from nanopowders," *Journal of the European Ceramic Society*, vol. 28, pp. 901–905, 2008.
- [27] F. Ye, M. J. Hoffmann, S. Holzer, Y. Zhou, and M. Iwasa, "Effect of the amount of additives and post-heat treatment on the microstructure and mechanical properties of yttrium– α -sialon ceramics," *Journal of American Ceramic Society*, vol. 86, pp. 2136–2142, 2003.
- [28] J. R. Davis, *ASM Handbook*: ASM International, p. 152, 2001.
- [29] D. T. Llewellyn and R. C. Hudd, *Steels: metallurgy and applications*. Oxford: Butterworth-Heinemann, 2000.
- [30] "Binary Alloy Phase Diagram," in *ASM Handbook*. vol. 3, 10 ed Metals Park, OH: American Society for Metals, 1993.
- [31] G. E. Totten, *Steel Heat Treatment Handbook*, 2 ed.: Taylor and Francis, 2006.
- [32] R. B. Frandsen, T. Christiansen, and M. A. J. Somers, "Simultaneous surface engineering and bulk hardening of precipitation hardening stainless steel," *Surface & Coatings Technology*, vol. 200, pp. 5160 – 5169, 2006.
- [33] M. Keddam, B. Bouarour, R. Kouba, and R. Chegroune, "Growth kinetics of the compound layers: effect of the nitriding potential," *Physics Procedia*, vol. 2, pp. 1399–1403, 2009.

- [34] P. Kochmanski and J. Nowacki, "Influence of initial heat treatment of 17-4 PH stainless steel on gas nitriding kinetics," *Surface & Coatings Technology*, vol. 202, pp. 4834-4838, 2008.
- [35] P. Kochmański and J. Nowacki, "Activated gas nitriding of 17-4 PH stainless steel," *Surface & Coatings Technology*, vol. 200, pp. 6558–6562, 2006.
- [36] J. Ratajski, "Relation between phase composition of compound zone and growth kinetics of diffusion zone during nitriding of steel," *Surface & Coatings Technology*, vol. 203, pp. 2300-2306, 2009.
- [37] S. D. d. Souza, M. Kapp, M. Olzon-Dionysio, and M. Campos, "Influence of gas nitriding pressure on the surface properties of ASTM F138 stainless steel," *Surface & Coatings Technology*, vol. 204, pp. 2976–2980, 2010.
- [38] J. Baranowska and B. Arnold, "Corrosion resistance of nitrided layers on austenitic steel," *Surface & Coatings Technology*, vol. 200, pp. 6623–6628, 2006.
- [39] H. Berns and S. Siebert, "High nitrogen austenitic cases in stainless steels," *ISIJ International*, vol. 36, pp. 927-931, 1996.
- [40] A. P. Tschiptschin, "Powder metallurgy aspects of high nitrogen steels," in *High Nitrogen Steels and Stainless Steels: Manufacturing, Properties and Applications*, U. K. Mudali and B. Raj, Eds., ed Pangbourne, UK: Alpha Science International Ltd, 2002.
- [41] H. Berns and A. Kühn, "Reduction in wear of sewage pump through solution nitriding," *Wear*, vol. 256, pp. 16-20, 2004.
- [42] A. P. Tschiptschin, C. M. Garzon, and L. D. M., "The effect of nitrogen on the scratch resistance of austenitic stainless steels," *Tribology International* vol. 39, pp. 167–174, 2006.
- [43] T. Nakanishi, T. Tsuchiyama, H. Mitsuyasu, Y. Iwamoto, and S. Takaki, "Effect of partial solution nitriding on mechanical properties and corrosion resistance in a type 316L austenitic stainless steel plate," *Materials Science and Engineering*, vol. A, pp. 186-194, 2007.
- [44] S. Frèchard, A. Lichtenberger, F. Rondot, N. Faderl, Redjamia, and M. Adoum, "A new consecutive model for nitrogen austenitic stainless steel," presented at the 4th European LS – DYNA Users Conference, Ulm – Germany, 2000.

- [45] J. F. d. Santos, C. M. Garzón, and A. P. Tschiptschin, "Improvement of the cavitation erosion resistance of an AISI 304L austenitic stainless steel by high temperature gas nitriding," *Materials Science and Engineering* vol. A, pp. 378–386, 2004.
- [46] T. Tsuchiyama, T. Fukumaru, M. Egashira, and S. Takaki, "Calculation of nitrogen absorption into austenitic stainless steel plate and wire," *ISIJ International*, vol. 44, pp. 1121-1123, 2004.
- [47] C. M. Garzon and A. P. Tschiptschin, "Growth kinetics of martensitic layers during high temperature gas nitriding of a ferritic – martensitic stainless steel," *Materials Science and Technology*, vol. 20, 2004.
- [48] H. W. Lee, J. H. Kong, D. J. Lee, H. Y. On, and J. H. Sung, "A study on high temperature gas nitriding and tempering heat treatment in 17Cr-1Ni-0.5C steel," *Materials and Design*, vol. 30, pp. 1691-1696, 2009.
- [49] H. Mitsui and S. Kurihana, "Solution nitriding treatment of Fe–Cr alloys under pressurized nitrogen gas," *ISIJ International*, vol. 47, pp. 479–485, 2007.
- [50] J. H. Sung, J. H. Kong, D. K. Yoo, H. Y. On, D. J. Lee, and H. W. Lee, "Phase changes of the AISI 430 ferritic stainless steels after high-temperature gas nitriding and tempering heat treatment," *Material Science Engineering A*, 2008.
- [51] C. M. Garzon and A. P. Tschiptschin, "New high temperature gas nitriding cycle that enhances the wear resistance of duplex stainless steels," *Journal of Materials Science* vol. 39, pp. 7101 – 7105 2004.
- [52] H. J. Lee, C. S. Lee, and Y. W. Chang, "Role of nitrogen in the cyclic deformation behavior of duplex stainless steels," *Metallurgical and Materials Transactions A*, vol. 36A, 2005.
- [53] A. Toro and A. P. Tschiptschin, "Chemical characterization of a high nitrogen stainless steel by optimized electron probe microanalysis," *Scripta Materialia*, vol. 63, pp. 803–806, 2010.
- [54] D. L'opez, N. A. Falleiros, and A. P. Tschiptschin, "Corrosion–erosion behaviour of austenitic and martensitic high nitrogen stainless steels," *Wear*, vol. 263, pp. 347-354, 2007.

- [55] M. G. Nicholas, *Joining process: introduction to brazing and diffusion bonding*: Kluwer Academic Publisher, 1998.
- [56] M. Powers, S. Sen, T. Nguyentat, O. M. Knio, and T. P. Weihs, "Bonding Processes," in *Materials Processing Handbook*, J. R. Groza and J. F. Shackelford, Eds., ed Boca Raton: Taylor & Francis Group, 2007, pp. 21.1-21.26.
- [57] A. Lupulescu and J. Colinge, "Diffusion-based Process," in *Materials Processing Handbook*, J. R. Groza and J. F. Shackelford, Eds., ed Boca Raton: Taylor & Francis Group, 2007, pp. 18.1 - 18.21.
- [58] J. William D Callister, *Materials Science and Engineering: An Introduction*, Seventh ed. New York: John Wiley & Sons, Inc., 2007.
- [59] Z. Yong, F. Di, H. Zhi-Yong, and C. Xi-Chun, "Progress in joining ceramics to metals," *Journal of Iron and Steel Research, International*, vol. 13, pp. 1-5, 2006.
- [60] A. P. Tomsia, "Ceramic/metal joining for structures and materials," *Journal De Physique IV*, vol. 3, 1993.
- [61] Y. Liang and S. P. Dutta, "Application trend in advanced ceramic technologies," *Technovation*, vol. 21, pp. 61-65, 2001.
- [62] M. d. Nascimento, A. E. Martinelli, and J. A. Buschinelli, "Review article: recent advances in metal-ceramic brazing," *Cerâmica*, vol. 49, pp. 178-198, 2003.
- [63] S. Dahmsa, F. Gemsea, U. Baslera, H.-P. Martin, and A. Triebert, "Diffusion joining of silicon nitride ceramics," *Estonian Journal of Engineering*, vol. 15, pp. 301-308, 2009.
- [64] M. Powers, S. Sen, T. Nguyentat, O. M. Knio, and T. P. Weihs, *Materials Processing Handbook*: Taylor Francis Group LLC, 2007.
- [65] G. Blugan, J. Janczak-Rusch, and J. Kuebler, "Properties and fractography of Si₃N₄/TiN ceramic joined to steel with active single layer and double layer braze filler alloys," *Acta Materialia*, vol. 52, pp. 4579 - 4588, 2004.
- [66] M. L. Hattali, S. Valette, F. Ropital, G. Stremsoerfer, N. Mesrati, and D. Tréheux, "Study of SiC–nickel alloy bonding for high temperature applications," *Journal of the European Ceramic Society*, vol. 29, pp. 813-81, 2009.

- [67] D. Travessa, M. Ferrante, and G. d. Ouden, "Diffusion bonding of aluminium oxide to stainless steel using stress relief interlayers," *Materials Science and Engineering A*, vol. 337, pp. 287-296, 2002.
- [68] S. Das, A. N. Tiwari, and A. R. Kulkarni, "Thermo-compression bonding of alumina ceramics to metal," *Journal of Materials Science*, vol. 39, pp. 3345 – 3355, 2004.
- [69] G. G. Sozhamannan and S. B. Prabu, "An experimental investigation of the interface characteristics of aluminium/silicon carbide," *Journal of Alloys and Compounds*, vol. 503, pp. 92–95, 2010.
- [70] X. Shen, L. Yajiang, W. Juan, H. Wanqun, and Y. Fusheng, "Diffusion bonding of Al₂O₃-TiC composite ceramic and W18Cr4V high speed steel in vacuum," *Vacuum*, vol. 84, pp. 378–381, 2010.
- [71] W. M. Tang, Z. X. Zheng, H. F. Ding, and Z. H. Jin, "A study of the solid state reaction between silicon carbide and iron," *Materials Chemistry and Physics*, vol. 74, pp. 258-264, 2002.
- [72] M. Paulasto, J. K. Kivilahti, and F. J. J. v. Loo, "Interfacial reactions in Ti/Si₃N₄ and TiN/Si diffusion couples," *Journal of Applied Physics*, vol. 77, 1995.
- [73] F. Deschaux-Beaume, N. Frety, and C. Colin, "Diffusion bonding of Si₃N₄-TiN composite with nickel-based interlayers," *Metallurgical and Materials Transactions A*, vol. 34A, 2003.
- [74] J. L. Ruiz, E. B. Becerril, and J. G. F. Lopez, "Joining and characterization of silicon nitride (Si₃N₄) to titanium (Ti) using a Cu-foil and Cu-Zn braze alloy," *Revista Mexicana De Fisica*, vol. S55, pp. 25-29, 2009.
- [75] E. Martinelli and R. A. L. Drew, "Microstructure and mechanical strength of diffusion-bonded silicon nitride-molybdenum joints," *Journal of the European Ceramic Society*, vol. 19, pp. 2173-2181, 1999.
- [76] A. K. Jadoon, B. Ralph, and P. R. Hornsby, "Metal to ceramic joining via a metallic interlayer bonding technique," *Journal of Materials Processing Technology*, vol. 152, pp. 257-265, 2004.
- [77] F. J. Oliveira, R. F. Silva, and J. M. Vieira, "Thermochemistry of contacts between silicon nitride ceramics and steels," *Acta Materialia*, vol. 48, pp. 4659–4665, 2000.

- [78] F. J. Oliveira, R. F. Silva, and J. M. Vieira, "Chemical interaction silicon nitride ceramics and iron alloys," *Boletín de la Sociedad Española Cerámica y Vidrio*, vol. 39, pp. 711-715, 2000.
- [79] M. Kalin and J. Vižintin, "Influence of mechanical pressure and temperature on chemical interaction between steel and silicon nitride ceramics," *Journal of Material Research*, vol. 15, 2000.
- [80] F. J. Oliveira, R. F. Silva, and J. M. Vieira, "The reaction rate at Si₃N₄/steel interfaces as a function of sintering aids," *Journal of the European Ceramic Society*, vol. 22, pp. 2561–2570, 2002.
- [81] P. Poza, P. Miranzo, and M. I. Osendi, "Transmission electron microscopy study on silicon nitride/stainless steel bonded interfaces," *Thin Solid Films*, vol. 517, pp. 779–781, 2008.
- [82] P. Hussain and O. Mamat, "Interdiffusion and interreaction of steel - composite - sialon joint," *Journal of Mechanical Engineering*, vol. 5, pp. 73 – 80, 2008.
- [83] D. K. Yoo, D. W. Joo, I. Kim, C. Y. Kang, and J. H. Sung, "Nitrogen permeation treatment of duplex and austenitic stainless steels," *Journal of the Korean Society for Heat Treatment*, vol. 15, pp. 57 – 64, 2002.
- [84] "Metallography and Microstructures," in *ASM Handbook*. vol. 9, G. F. V. Voort, Ed., ed: ASM International, 2004.
- [85] F. Esaka, H. Yamamoto, N. Matsubayashi, Y. Yamada, M. Sasase, K. Yamaguchi, S. Shamoto, M. Magara, and T. Kimura, "X-ray photoelectron and X-ray absorption spectroscopic study on β-FeSi₂ thin films fabricated by ion beam sputter deposition," *Applied Surface Science*, vol. 256, pp. 3155–3159, 2010.
- [86] T. Saito, H. Yamamoto, M. Sasase, T. Nakanoya, K. Yamaguchi, M. Haraguchi, and K. Hojou, "Surface chemical states and oxidation resistivity of 'ecologically friendly' semiconductor (β-FeSi₂) thin films," *Thin Solid Films*, vol. 415, pp. 138-142, 2002.
- [87] C. D. Wagner, W. M. Riggs, L. E. Davis, J. F. Moulder, and G. E. Muilenberg, *Handbook of X-ray photoelectron spectroscopy*. Minnesota, USA: Perki-Elmer Corporation, 1979.

- [88] H. Qi, C. Qian, and J. Liu, "Synthesis of uniform double-walled carbon nano tubes using iron disilicide as catalyst," *Nano Letters*, vol. 7, pp. 2417-2421, 2007.
- [89] K. Rührschopf, D. Borgmann, and G. Wedler, "Growth of Fe on Si (100) at room temperature and formation of iron silicide," *Thin Solid Films*, vol. 280, pp. 171-177, 1996.
- [90] X. Gao, D. Qi, S. C. Tan, A. T. S. Wee, X. Yu, and H. O. Moser, "Thickness dependence of X-ray absorption and photoemission in Fe thin films on Si(0 0 1)," *Journal of Electron Spectroscopy and Related Phenomena*, vol. 151, pp. 199–203, 2006.
- [91] S. Ito, Y. Takahashi, and Takashi, "Solid state reactions in Fe–Si system under HIPping pressure," *Solid State Ionics*, vol. 141-142, pp. 433-438, 2001.
- [92] F. Bahrami, "Microstructure, strength and fatigue behaviour of nitrogen alloyed martensitic and austenitic stainless steel," PhD Dissertation, Mechanical Engineering Department, University of Strathclyde Glasgow, UK, 1993.